Universidade do Minho
Escola de Medicina

Ana Maria Franco Aveiro Marote

Unveiling the potential of iPSCs-derived mesenchymal stem cells for the development of cell-free therapies for Parkinson's disease

março de 2020

Unveiling the potential of iPSCs-derived mesenchymal stem cells for the development of cell-free therapies for Parkinson's disease

Ana Maria Franco Aveiro Marote

UMinho | 2020

Universidade do Minho
Escola de Medicina

Ana Maria Franco Aveiro Marote

Unveiling the potential of iPSCs-derived mesenchymal stem cells for the development of cell-free therapies for Parkinson's disease

Tese de Doutoramento em Ciências da Saúde

Trabalho efetuado sob a orientação do
Doutor António José Braga Osório Gomes Salgado
e da
Doutora Luísa Alexandra Meireles Pinto

Março de 2020

Acknowledgments/Agradecimentos

Reaching the end of this journey would not be possible without the important contribution of several people and institutions, to whom I would like to express my deep gratitude. • Firstly, to my supervisor, António Salgado, for challenging me to work with iPSCs and providing all the means for that, for trusting in my work and giving me the freedom of thought that allowed me to grow so much. To my supervisor at Bn'ML, Luísa Pinto, for all her support, guidance and help in the *in vivo* experiment. To Laurent Roybon, for accepting me in his lab, providing me all the opportunities to learn about iPSCs and for all his support • To Professors Jorge Pedrosa, Jorge Correia Pinto, Nuno Sousa and João Bessa for all their institutional support from the School of Medicine, ICVS and NeRD. • To our external collaborators: at the clinics - Dr. Miguel Gago, Dr. Margarida Rodrigues and Enf.ª Ana Monteiro; at the IBB - Ana Fernandes-Platzgummer and Cláudia Lobato da Silva; and at IPO - Dr. Manuel Teixeira and Joana Vieira, for all their availability. • To all the members of "Tó team". Specially to: Bárbara, the best partner I could have during these four years, for always making everyone around happy and for, together with Verónica, being part of the best surgery team ever; Eduardo Gomes, for being always available to help and for all his support in this work; Sandra, for all her help in the long nights at the animal facility; Inês, for the friendship and for being such a good partner at the cell culture; Rita, my desk neighbor and confident, for all the moments shared along these years; Nuno Silva and Susana, for all their relevant scientific discussions; Fábio, for establishing important collaborations and methodologies for the development of this project. Also to all the people that temporarily joined the team to work with me, specially to Hugo, Caroline, Miguel and Diogo for their help and for proving that *teaching is learning twice*. • To all NeRD members. Specially to: Carina, for the assistance and guidance in the last months; Patrícia, for the help in addressing how (un)happy the animals were and for all the fast lunches shared along the years; Cláudia Miranda, for all the support in flow cytometry and also for the friendship; Sara Silva, for her "molecular" help; Eduardo Campos, for the friendship and all joyful moments. Also, to my dear friends Jorge Silva and Joana Correia, for all the after-work moments and for listening to my worries and successes. • To all the people that made my stay in Lund so pleasant. My CSC lab mates, specially: Yuriy for all his support; Ulla, for being always around, even at non-conventional working hours; and Anna, my beloved Spanish sister. To all A10 members, for all the after hours drinks, all the *Fika.* To all the Portuguese that welcomed me so well during this time, specially to the lovely family Maria, João and Afonso.

A toda a minha família, por todos os valores transmitidos ao longo da minha vida e por saber que, mesmo estando longe, posso sempre contar convosco. Em especial aos meus pais, por me deixarem seguir o meu caminho e porque sem o vosso esforço e dedicação, tudo isto não seria possível. À Júlia, por todo o apoio durante os dias de escrita. Ao Pedro, por ter estado sempre ao meu lado nos dias bons e nos dias maus, por toda a compreensão e por todo o amor que fizeram com que este caminho se tornasse mais fácil. Por fim, gostaria de dedicar este trabalho à minha avó, que certamente olhou por mim ao longo destes anos.

The work presented in this thesis was performed at the Life and Health Sciences Research Institute (ICVS) and at the Bn'ML – Behavioral & Molecular Lab, at the School of Medicine, University of Minho. Financial support was provided by Portuguese Foundation for Science and Technology (FCT): Doctoral fellowship (PDE/BDE/113598/2015) to A. Marote; IF Development Grants to A. J. Salgado (IF/00111/2013) and L. Pinto (IF/01079/2014). This work was also funded by FEDER, through the Competitiveness Internationalization Operational Programme (POCI), and by National funds, through the FTC, under the scope of the projects POCI-01-0145-FEDER-007038; POCI-01-0145-FEDER-029751 and POCI-01-0145-FEDER-032619. This project has also been developed under the scope of the project NORTE-01-0145-FEDER-000023, supported by the Northern Portugal Regional Operational Programme (NORTE 2020), under the Portugal 2020 Partnership Agreement, through the European Regional Development Fund (FEDER). Part of the work was also developed at Department of Experimental Medical Science at Lund University and financially supported by the Strategic Research Environment MultiPark–multidisciplinary research on Parkinson's disease and Crafoord Foundation Sweden.

STATEMENT OF INTEGRITY

I hereby declare having conducted this academic work with integrity. I confirm that I have not used plagiarism or any form of undue use of information or falsification of results along the process leading to its elaboration.

I further declare that I have fully acknowledged the Code of Ethical Conduct of the University of Minho.

Ana Nanote

Ana Maria Franco Aveiro Marote

Desvendando o potencial das células estaminais mesenquimatosas derivadas de iPSCs para o desenvolvimento de terapias livres de células para a doença de Parkinson

Resumo

A doença de Parkinson (DP) é a segunda doença neurodegenerativa mais comum mundialmente, caracterizada principalmente pela perda de neurónios dopaminérgicos na substancia nigra *pars compacta* (SNc), levando a uma desnervação do sistema nigroestriatal. A neurodegeneração na SNc e noutras áreas dopaminérgicas e não dopaminérgicas são clinicamente traduzidas em lentidão dos movimentos, rigidez e tremor em repouso, bem como manifestações não-motoras, como a depressão. Devido à sua complexidade e causa desconhecida, terapias modificadoras da doença, capazes de abrandar, interromper ou reverter a neurodegeneração inerente à DP, constituem uma necessidade não atendida na área. As células estaminais mesenquimatosas (MSCs) são uma população adulta de células estaminais que tem sido sugerida como uma abordagem terapêutica promissora para a DP, particularmente devido à libertação de fatores solúveis e vesículas, coletivamente designados como *secretoma.* Apesar da crescente evidência do potencial neuroprotetor do secretoma das MSCs, MSCs derivadas de tecidos, tais como a comumente utilizada medula óssea (BM-MSCs), têm uma capacidade proliferativa limitada e estão sujeitas a variabilidade do dador, dificultando assim a recolha de volumes de secretoma significativos para uma aplicação clínica abrangente. O principal objetivo desta tese é avaliar o potencial terapêutico do secretoma recolhido de uma fonte MSCs emergente e clinicamente adequada – as células estaminais pluripotentes induzidas (iPSCs). Para isso, gerámos iPSCs de sujeitos saudáveis e de pacientes com DP, através da reprogramação de fibroblastos e células mononucleares do sangue periférico. Posteriormente, as iPSCs obtidas de sujeitos saudáveis foram diferenciadas em MSCs (iMSCs) e o seu secretoma foi recolhido e comparado com o secretoma das BM-MSCs. Tanto o secretoma das BM-MSCs como o das iMSCs atenuaram os défices motores e a degeneração nigrostriatal num modelo de DP de rato baseado na exposição a 6-OHDA, apesar de não protegerem de maneira significativa neurónios dopaminergicos derivados de células estaminais embrionárias de murganho do mesmo insulto tóxico *in vitro*. A semelhança entre as duas fontes foi também revelada numa análise proteómica direcionada do secretoma das duas fontes, mostrando um perfil de secreção comparável de citocinas e fatores de crescimento, que podem mediar os seus efeitos neuroprotetores *in vivo*. Deste modo, o nosso estudo demonstra o potencial terapêutico do secretoma das iMSCs no contexto da DP, abrindo caminho para o uso desta fonte de MSCs emergente em testes clínicos subsequentes.

Palavras-chave: células estaminais pluripotentes induzidas, células estaminais mesenquimatosas, doença de Parkinson, neuroprotecção, secretoma

Unveiling the potential of iPSCs-derived mesenchymal stem cells for the development of cell-free therapies for Parkinson's disease

Abstract

Parkinson's disease (PD) is the second most common neurodegenerative disease worldwide, mainly characterized by the loss of dopaminergic neurons from the substantia nigra *pars compacta* (SNc) leading to the denervation of the nigrostriatal tract. Neurodegeneration at the SNc and other dopaminergic and non-dopaminergic areas are clinically translated into slowness of movement, rigidity and tremor at rest, as well as nonmotor manifestations, such as depression. Due to its complexity and unknown etiology, disease-modifying therapies, able to slow, halt or reverse PD underlying neurodegeneration, are a large unmet need in the field. Mesenchymal stem cells (MSCs) are a population of adult of stem cells that has been put forward as a promising therapeutic approach for PD, particularly due to the release of soluble factors and vesicles, collectively known as *secretome*. Despite the growing evidence of the neuroprotective potential of MSCs secretome, tissue-derived MSCs, such as the commonly used bone marrow-derived MSCs (BM-MSCs), have limited proliferative capacity and are subjected to donor variability, thereby hindering the collection of significant volumes of secretome for a widespread clinical application. The main goal of this thesis was to address the therapeutic potential of the secretome collected from an emerging and clinically appropriate source of MSCs – induced pluripotent stem cells (iPSCs). For that, we have firstly generated iPSCs from heathy subjects and PD patients, through the reprograming of fibroblasts and peripheral blood mononuclear cells. Subsequently, iPSCs obtained from healthy subjects were differentiated into MSCs (iMSCs) and their secretome was collected and compared to BM-MSCs secretome. Both BM-MSCs and iMSCs secretome were able to attenuate motor deficits and nigrostriatal degeneration in a rat model of PD based on 6-OHDA exposure, although they did not significantly protect mouse embryonic stem cells (mESCs)-derived dopaminergic neurons from the same toxic insult *in vitro*. The similarity between both sources was further revealed in a targeted proteomic analysis of the secretome from both sources, showing a comparable secretion profile of neuroregulatory cytokines and growth factors, which might mediate their neuroprotective effects *in vivo.* Therefore, our study demonstrates the therapeutic potential of iMSCs secretome in the context of PD, paving the way for the use of this emerging MSC source in subsequent clinical testing.

Keywords: Induced Pluripotent stem Cells, Mesenchymal Stem Cells, Neuroprotection, Parkinson´s Disease, Secretome

Contents

CHAPTER 2

CHAPTER 3

CHAPTER 4

Abbreviations list

#

2D – two-dimensional

3D – tridimensional

6-OHDA – 6-hydroxydopamine

A

AAV - Adeno-associated virus

AFP – alpha Fetoprotein

ANOVA – Analysis of Variance

ASCs – Adipose tissue derived Mesenchymal Stem Cells

B

BDNF – Brain-derived Neurotrophic Factor

BM – Bone Marrow

BSA – Bovine Serum Albumin

C

Ca^{2+} – Calcium

CD – Cluster of differentiation

CM – Conditioned Medium

cm – centimeter

D

DA – dopamine

DAB – diaminobenzidine tetrahydrochloride

DAPI – 4′,6-diamidino-2-phenylindole

DAT – dopamine transporter

DMEM – Dulbecco's Modified Eagle Medium

DNA – Deoxyribonucleic acid

E

EBs – Embryoid Bodies

ECM – Extracellular Matrix

EPM – Elevated plus maze

ER – Endoplasmic Reticulum

ESCs – Embryonic Stem Cells

F

FBS – Fetal Bovine Serum

FGF – Fibroblast Growth Factor

G

G-CSF – Granulocyte-Colony Stimulating Factor

GDNF – Glial-Derived Neurotrophic Factor

GFP – Green Fluorescent Protein

H

HB-EGF – Heparin-Binding Epidermal growth factor-like Growth Factor

HEPES – 4-(2-hydroxyethyl)-1-piperazineethanesulfonic acid

hNPCs – human Neural Progenitor Cells

HPLC – high-performance liquid chromatography

I

IGF-I – Insulin-like growth factor type I

IL – Interleukin

iPSCs – induced Pluripotent Stem Cells

L

LRRK2 – Leucine Rich Repeat Kinase 2

M

MAP2 – Microtubule Associated Protein-2

MCP-1 – Monocyte Chemoattractant Protein 1

MDS – Movement Disorder Society

MEF – Mouse Embryonic Fibroblasts

MEM – Minimal Essential Medium

mESCs – mouse Embryonic Stem Cells

MFB – Medial Forebrain Bundle

min – minutes

MMPs – Matrix Metalloproteinases

MPTP – 1-methyl-4-phenyl-1,2,3,6-tetrahydropyridine

MSCs – Mesenchymal stem cells

MTS – 3-(4,5-dimethylthiazol-2-yl)-5-(3-carboxymethoxyphenyl)-2-(4-sulfophenyl)-2H-tetrazolium)

N

NGF – Nerve Growth Factor

P

PBMCs – Peripheral Blood Mononuclear Cells

PBS – Phosphate Buffered Saline

PD – Parkinson's disease

PFA – Paraformaldehyde

PINK1 – Phosphatase and tensin homolog induced novel kinase 1

R

RNA – Ribonucleic acid

ROS – Reactive Oxygen Species

RT – Room Temperature

S

SAG – Smoothened Agonist

SCT – Sucrose Consumption Test

SDT – Sweet Drive Test

SEM – Standard Error of Mean

Shh – Sonic hedgehog

SMA – Smooth Muscle Actin

SNc – Substantia nigra pars compacta

T

TGF – Transforming Growth Factor

TH – Tyrosine Hydroxylase

V

VEGF – Vascular Endothelial Growth Factor

Figures list

CHAPTER 1

INTRODUCTION

CHAPTER 2

GENERATION OF PATIENT-DERIVED INDUCED PLURIPOTENT STEM CELLS

CHAPTER 3

GENERATION OF AN *IN VITRO* MODEL OF PARKINSON'S DISEASE

CHAPTER 4

INDUCED PLURIPOTENT STEM CELL-DERIVED MESENCHYMAL STEM CELLS: AN UNLIMITED SOURCE OF NEUROPROTECTIVE FACTORS WITH THERAPEUTIC POTENTIAL FOR PARKINSON'S DISEASE

CHAPTER 5

GENERAL DISCUSSION AND CONCLUSIONS

Tables list

CHAPTER 1

INTRODUCTION

CHAPTER 2

GENERATION OF PATIENT-DERIVED INDUCED PLURIPOTENT STEM CELLS

Thesis aims and layout

The main aim of this thesis was to address the therapeutic potential of the secretome collected from induced pluripotent stem cells (iPSCs)-derived mesenchymal stem cells (iMSCs) in the context of Parkinson's disease (PD). For that, we have established the following specific aims:

- Generation of iPSCs from healthy subjects and PD patients, in view of providing an inexhaustible source of iMSCs and establishing a cell library for further disease modeling studies, respectively;
- Generation of a time- and cost- effective 3D *in vitro* model of PD for assessing the neuroprotective potential of iMSCs secretome;
- Generation of iMSCs under chemically-defined culture conditions;
- Comparison of the neuroprotective potential of the secretome from iMSCs and the gold standard tissue-derived MSCs - bone marrow-derived MSCs (BM-MSCs) - using both *in vitro* and *in vivo* PD experimental models;
- Characterization of iMSCs and BM-MSCs secretome composition.

Before addressing these aims, we provide an overview about PD, describing the current understanding of this neurodegenerative disease from the clinical to the molecular level. Moreover, we describe the existing experimental models of PD, as well as the available symptomatic therapy and innovative disease-modifying therapeutic approaches currently being developed. – **Chapter 1**

Then, we present the generation of 11 lines of iPSCs, comprising both healthy and PD patient derived cells reprogrammed from fibroblasts and peripheral blood mononuclear cells using the non-integrating Sendai virus technology. – **Chapter 2**

Next, we describe the generation of an *in vitro* model of PD, which is based on the differentiation of mouse embryonic stem cells into dopaminergic neurons and subsequent transfer to a collagen hydrogel to provide a 3D culture platform, wherein they are exposed to 6-OHDA to mimic the dopaminergic cell death underlying PD. – **Chapter 3**

Later, in line with main aim of this thesis, we describe the generation of iMSCs from three healthy iPSCs donors and compare the effects of their secretome with the secretome from their tissue-derived counterparts (BM-MSCs) at the cellular and behavioral level. Additionally, we assess the secretome profile from both sources, regarding specific neuroregulatory molecules. – **Chapter 4**

Finally, we discuss the advantages and limitations of the generated stem cell-based tools and their application in PD research field. – **Chapter 5**

CHAPTER 1

INTRODUCTION

Part of this chapter is based on the following publication:

Marote A, Teixeira FG, Mendes-Pinheiro B, & Salgado AJ. (2016). MSCs-Derived Exosomes: Cell-Secreted Nanovesicles with Regenerative Potential. *Frontiers in Pharmacology*, 7(231). doi:10.3389/fphar.2016.00231

Chapter 1 | Introduction

Abstract

Parkinson's disease (PD) is the most common movement disorder and the second most common neurodegenerative disease worldwide. Motor parkinsonism, defined by bradykinesia in combination with either rest tremor, rigidity, or both, is the core feature that clinically characterizes PD. Nevertheless, a growing amount of evidence has spurred the occurrence of nonmotor symptoms in combination with motor manifestations or even before their appearance – referred to as prodromal PD. Loss of dopaminergic neurons in the nigrostriatal system, as well as the presence of widespread Lewy body pathology, are the definitive post-mortem pathological findings of PD. Nonetheless, nonmotor manifestations point out the involvement of non-dopaminergic systems in PD pathology, thereby contributing for the classification of PD as a heterogeneous and multi-factorial disease. Currently available therapeutic approaches for PD are mainly focused on pharmacological substitution of striatal dopamine and do not prevent the underlying degeneration of dopaminergic neurons. Disease-modifying strategies are thus a major unmet need in the field. With the advance of regenerative medicine, emerging experimental therapies have been proposed, with particular focus on stem cells and gene therapy. Mesenchymal stem cells (MSCs) are a population of adult stem cells that have been particularly harnessed due to their accessibility and neuromodulatory paracrine activity. In this chapter, we will provide an overview of PD at the epidemiological, clinical and pathological level, as well as describe the recent advances on PD disease modeling and experimental disease-modifying therapies, with a particular focus on MSCs and their secretome.

1. Parkinson's disease: understanding what needs to be modified

Parkinson's disease (PD) was originally described by James Parkinson in 1817 as a *shaking palsy* characterized by "*involuntary tremulous motion, with lessened muscular power, in parts not in action and even when supported; with a propensity to bend the trunk forwards, and to pass from a walking to a running pace: the senses and intellects being uninjured*" (Goetz, 2011; Parkinson, 2002). More than two hundred years after shaking palsy, massive scientific breakthroughs have been achieved at the clinical and experimental level, revealing the true complexity of this multifactorial disease. Nonetheless, disease-modifying therapies that prevent the progressive degeneration of dopaminergic neurons are still an unmet need. In this section, we will provide a broad characterization of PD at the epidemiological and clinical level, as well as present the current understanding of the pathophysiological, pathological and molecular mechanisms underlying its etiology and progression.

1.1. *Epidemiology*

Neurological disorders are the second leading cause of global deaths, after heart disease, and the leading cause of disability worldwide (Carroll, 2019). These data were reported on the Global Burden of Diseases, Injuries, and Risk Factors Study (GBD) 2016, which estimated the prevalence, deaths, years of life lost (YLLs), years lived with disability (YLDs), and disability-adjusted life-years (DALYs) by age and sex from 195 countries from 1990 to 2016 for 15 neurological disorders (Carroll, 2019). From these, PD is the fastest growing neurological disorder.

1.1.1. *Prevalence, incidence and demographics*

In 2016, 6.1 million individuals suffered from PD globally, which represents a more than double increase in comparison to 1990 (2.5 million) (Dorsey *et al.*, 2018). Worldwide population ageing has greatly contributed for this increase, however age-standardized prevalence indicates a 22% increase from 1990 to 2016 (Dorsey *et al.*, 2018). Other possible reasons for this increase include the existence of higher quality studies and diagnostic measures, as well as increasing life expectancy which contributes for longer disease duration in PD patients (Dorsey *et al.*, 2018). Still, PD caused 211 296 global deaths, which accounts for a 19.5% increase in age-standardized rates in comparison to 1990 (Dorsey *et al.*, 2018). It is estimated that PD affects 828 703 individuals in western Europe, from which 18 496 were identified in Portugal. Indeed, Portugal holds the third highest increase in age-standardized prevalence (31.9%), death counts (34.3%) and DALYs (32.9%) from 1990 to 2016 within western Europe (Dorsey *et al.*, 2018).

Regarding incidence rates, it is reported that 10 to 20 per 100 000 of total population are diagnosed with PD, annually (Tysnes *et al.*, 2017). This rate dramatically increases in people aged 65 years or older to 160 per 100 000 (Ascherio *et al.*, 2016). PD is uncommon before 50 years of age, representing only less than 5% of the cases in population-based cohorts, being usually linked to genetic variants that cause monogenic forms of PD (Dorsey *et al.*, 2018; Tysnes *et al.*, 2017).

Besides age, PD numbers are also influenced by the countries' socio-demographic index (SDI). In 2016, approximately 34.4% of the people living with PD were from high SDI countries, 50.8% from high middle or middle SDI and 14.8% were from low-middle or low SDI countries (Dorsey *et al.*, 2018). Environmental exposures coupled to industrialization in higher SDI countries are one possible explanation for this variation, although possible underestimation of PD diagnosis in lower SDI countries cannot be excluded (Dorsey *et al.*, 2018). Ethnicity has been also reported to influence PD incidence within the same country (United States of America) which could represent a genetic susceptibility; it was highest among Hispanics, followed by Caucasians, Asians and Africans (Abbas *et al.*, 2018; Van Den Eeden *et al.*, 2003). Nevertheless, both African Americans and Japanese Americans show the higher occurrence of PD, when compared to similar populations in their native country, pinpointing an environmental role in PD development (Abbas *et al.*, 2018; Morens *et al.*, 1996; Schoenberg *et al.*, 1988).

Overall, these studies evidence the increasing global burden of PD over the past generation and identify demographic and environmental incidence patterns that might play a role in disease occurrence, thereby providing measures of risk factor assessment.

1.1.2. *Risk factors*

In addition to age, which is the greatest risk factor for developing PD, gender and genetics are among other internal non-modifiable risk factors, whereas occupational solvent exposure, regular pesticide exposure, nonuse of caffeine and nicotine are identified as external, modifiable risk factors (figure 1.1). Other putative factors such as non-steroidal anti-inflammatory drugs, head injury and calcium-channel blocker intake have also been suggested (Ascherio *et al.*, 2016), yet with limited evidence and/or low predictive value (Berg *et al.*, 2015).

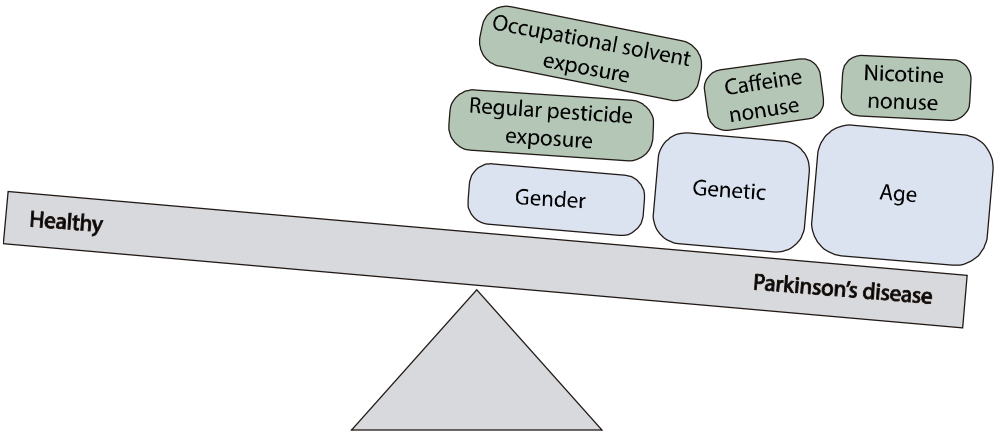

Figure 1.1 – Risk factors associated to Parkinson's disease. Internal non-modifiable risk factors are presented in blue, whereas the most significant external, modifiable risk factors are depicted in green. The different sizes of the boxes represent the estimated contribution of each risk factor for developing PD.

Gender

PD affects 2.9 million women (47.5%) and 3.2 million men (52.5%) worldwide (Dorsey *et al.*, 2018). This gender imbalance has been suggested to be related to a protective effect of female-specific hormones and genetic mechanisms, as well as differences in exposure to environmental risk factors (Dorsey et al., 2018; Haaxma et al., 2007; Poewe et al., 2017). Even though the underlying mechanism is not completely understood, it is described that men have approximately 1.5 fold increased risk of developing PD (Berg *et al.*, 2015).

Occupational exposure to pesticides and solvents

The discovery that intravenous use of 1-methyl-4-phenyl-1,2,3,6-tetrahydropyridine (MPTP), sold as a new "synthetic heroin" in a limited region of northern California during 1982, caused severe parkinsonism in a number of addicted individuals (Langston *et al.*, 1983), prompted the field to explore the influence of pesticide exposure on PD development (Pezzoli *et al.*, 2013). MPTP is converted in the body to a pro-parkinsonian molecule (MPP^+) that has a similar structure to the herbicide paraquat (Ascherio *et al.*, 2016; Richardson *et al.*, 2005). A similar association was then reported between solvent abuse and acute parkinsonism development with an unusual disturbance of striatal dopaminergic function (Uitti *et al.*, 1994). Using *in vitro* and *in vivo* models, specific environmental factors were further demonstrated to be selectively toxic to dopaminergic neurons (Brown *et al.*, 2006; Richardson *et al.*, 2005). Based on these studies and available meta-analysis, regular pesticide exposure and occupational solvent exposure are described to increase the probability of developing PD by 1.5, independently (Berg *et al.*, 2015; Noyce *et al.*, 2012).

Caffeine and nicotine nonuse

Several epidemiologic studies have consistently reported a strong inverse association between PD occurrence and coffee drinking and cigarette smoking (Chen *et al.*, 2010; Hernán *et al.*, 2002; Powers *et al.*, 2008; Ritz *et al.*, 2014; Thacker *et al.*, 2007). It is estimated that the risk is 30% lower among coffee drinkers than among non–coffee drinkers and 60% lower among current cigarette smokers than among never smokers (Hernán *et al.*, 2002). Nevertheless, the nature of this relationship is controversial. Some studies suggest that caffeine and nicotine may have a "protective role" by modulating dopaminergic transmission and competing with neurotoxins binding (Ascherio *et al.*, 2001; Hernán *et al.*, 2002; Thacker *et al.*, 2007). In contrast, other authors propose a "reverse causation", suggesting that nonuse of caffeine and nicotine relates to a lower sensitivity of the brain reward system and thus ease of quitting may act as an early prodromal PD marker (Ritz *et al.*, 2014). Despite this ongoing debate, nonuse of caffeine (less than 3 cups of coffee per week) represents a 1.35 increase of probability of developing PD, whereas never smoking increases PD risk by 1.25 (Berg *et al.*, 2015).

Genetics

For assessing the risk of developing PD based on genetics, either familial history or the identification of genetic variants associated to PD can be used (Berg *et al.*, 2015). The contribution of genetics to PD pathogenesis was initially stirred by the discovery of rare PD forms with Mendelian inheritance (5 -10% of PD cases) and has been supported by genome-wide association studies, providing evidence of polymorphic genes that can directly contribute for the development of sporadic PD or increase its risk and progression (Corti *et al.*, 2011; Iwaki *et al.*, 2019; Nalls *et al.*, 2014). A list of these genes and associated mutations is presented in table 1.1.

Table 1.1 – List of Parkinson's disease associated gene and estimated risk of known mutation variants.

	Gene	Protein	Function(s)	Locus symbol	Mutation(s)	Estimated risk*	Clinical manifestations
Autosomal-dominant/Sporadic	SNCA	α-Synuclein	Synaptic vesicle dynamics Mitochondrial function Intracellular trafficking Potential chaperone	PARK1	Missense mutations (A53T, A30P, E46K G50D)	400	Classic
				PARK4	Duplication	33	Early-onset with prominent dementia
					Triplication	400	
	LRRK2	Leucine-rich repeat kinase 2	Neurite outgrowth Synaptic morphogenesis Membrane trafficking Autophagy Protein synthesis	PARK8	G2019S	25	Classic
					R1441C/G/H, Y1699C, I2020T	10 (conservative)	Classic
Autosomal- recessive	*Parkin*	Parkin	E3 ubiquitin ligase	PARK2	Homozygous or compound heterozygous	400	Lower limb dystonia
					One heterozygous mutation	-	
	PINK1	PTEN-induced putative kinase 1	Mitochondrial serine-threonine protein kinase	PARK6	Homozygous or compound heterozygous	400	Common psychiatric features
					One heterozygous mutation	-	
	DJ-1	DJ-1	Putative antioxidant	PARK7	Homozygous or compound heterozygous	400	Early-onset
Risk	GBA		Lysosomal enzyme	-	Low risk (N370S, S2716)	2	
					High risk	10	
	SNCA			-	rs356219	-	
	MAPT			-	rs393152	-	
	HLA			-	rs3129882	-	

*****Estimated risk is represented as likelihood ratios (LRs), a measure of how much a positive test result increases disease probability as described by (Berg *et al.*, 2015).

The gene encoding α-synuclein (SNCA) was the first reported PD-linked gene, after the discovery of a mutation in the Contursi kindred, a large family of Italian descent with autosomal dominant inheritance of PD (Polymeropoulos *et al.*, 1997). Point mutations (e.g. A53T) leading to missense variations in α-synuclein are less common than whole-locus multiplications causing pathogenic overexpression of the wild-type protein, which represent 2% of all familial forms of parkinsonism (Corti *et al.*, 2011). LRRK2 is

another gene frequently associated with late-onset familial PD (10%) and sporadic PD (3.6%) (Corti *et al.*, 2011). It was later on added to the list of PD-linked genes, following its identification and sequencing in a subset of families of white ancestry with autosomal dominant parkinsonism (Funayama *et al.*, 2002; Zimprich *et al.*, 2004a; Zimprich *et al.*, 2004b). Six mutations are considered "pathogenic", being G2019S the most common. G2019S mutation is found in 1% of patients with sporadic PD and 4% of patients with hereditary PD, although it is associated with incomplete and age-dependent penetrance (Healy *et al.*, 2008). The role of SNCA and LRRK2 mutations in PD pathogenesis is well-documented (approximately 5% mutation frequency in autosomal dominant PD), whereas the association between PD and other dominant genes, including UCHL1, GIGYF2, HTRA2, is still controversial (Corti *et al.*, 2011).

Regarding mutations in the recessive genes *parkin,* PINK1 and DJ-1, a clear association is observed with heritable and early-age onset PD, which may occur due to a loss of function of the encoded protein (Corti *et al.*, 2011). Mutations in the *parkin* gene have a worldwide frequency of 10-20% in PD patients with onset before 50 years old (Lücking *et al.*, 2000; Periquet *et al.*, 2003). Mutations in PINK1 are the second most frequent cause (up to 15% worldwide frequency) of autosomal recessive early onset, followed by mutations in DJ-1, which only account for 1% of early-onset PD (Corti *et al.*, 2011).

In the past decade, accumulating evidence has linked mutations in GBA with a higher risk for developing PD. This association was firstly recognized in the clinic, after the observation of parkinsonism phenotype in patients with Gaucher's disease, caused by alterations in the lysosomal enzyme β-glucocerebrosidase encoded in GBA (Sidransky, 2004). Subsequent findings, obtained from a large multicenter study on GBA mutation frequency, have showed odds ratio greater than 5 for any GBA mutation in PD patients versus controls (Sidransky *et al.*, 2009). Although the underlying mechanism of this association is unclear, GBA coding variants have been linked to an early-age onset, an increased cognitive decline and motor symptom progression (Iwaki *et al.*, 2019; Sidransky *et al.*, 2012).

Genetic factors have been increasingly recognized as part of PD etiology. Accordingly, the application of modern molecular genetic approaches hold great potential for the identification of new variants linked to monogenic PD, as well as susceptibility loci associated with a higher risk for sporadic PD (Elbaz *et al.*, 2006; Iwaki *et al.*, 2019; Soldner *et al.*, 2016). Advances in this field may provide a better understanding of PD pathogenesis and consequently contribute for designing tailored diseased-modifying therapeutic strategies.

1.2. *Clinical features*

Since the first report presented by James Parkinson over 200 years ago, PD clinical characterization has greatly evolved. Nowadays, PD is regarded as an heterogenous and multidimensional disease that spans beyond classic motor features (Obeso *et al.*, 2017). As for other neurodegenerative diseases, cell death occurs progressively, being only clinically evident when approximately 70–80% of striatal dopamine is depleted and 30–50% of the dopaminergic neurons have been lost (Cheng *et al.*, 2010; Postuma *et al.*, 2012). The occurrence of nonmotor symptoms, even before the onset of motor alterations, has also greatly contributed for redefining the disease conceptualization (Berg *et al.*, 2014). According to the Movement Disorder Society (MDS) terminology, PD should be divided into three stages, depicted in figure 1.2: 1) *preclinical*, in which the neurodegenerative processes have started, but there are no evident symptoms or signs; 2) *prodromal*, wherein symptoms or signs are present, but insufficient to perform the clinical diagnosis; 3) *clinical*, when classical motor signs become definite (Berg *et al.*, 2015).

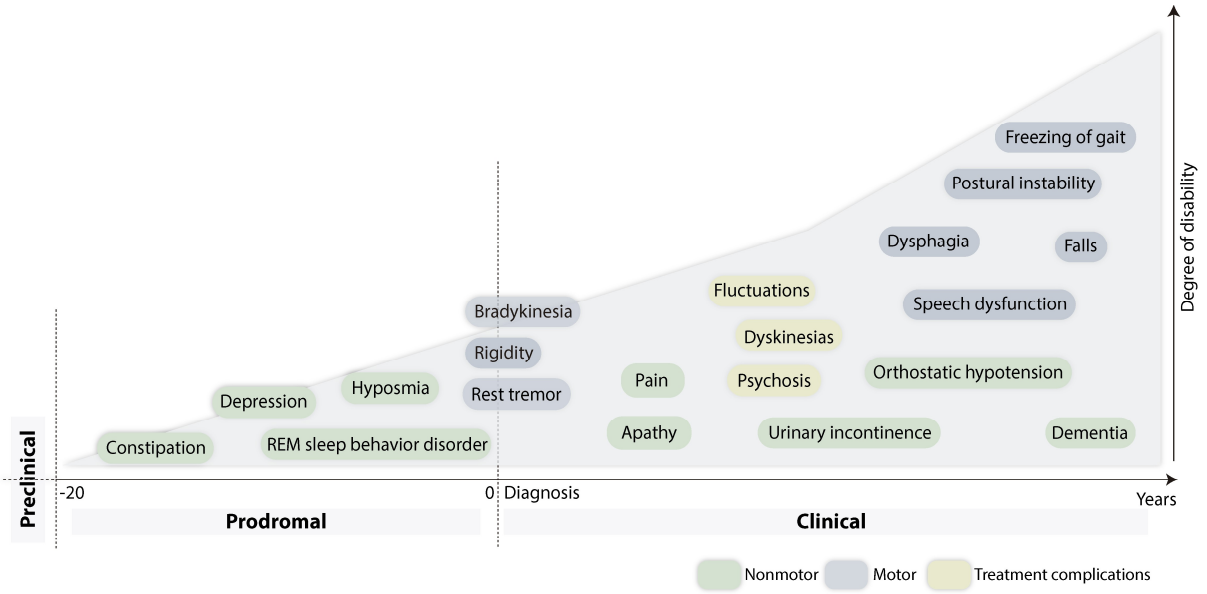

Figure 1.2 – Clinical manifestations associated the different stages of Parkinson's disease progression. Preclinical stage comprises the presence of neurodegeneration before the manifestation of clinical symptoms, which sets the beginning of prodromal stage. This stage is marked by the presence of nonmotor manifestations, such as depression and constipation that may occur up to 20 years before the evidence of PD cardinal motor symptoms – bradykinesia, rigidity and rest tremor – that allow PD diagnosis and establish the beginning of clinical PD. As the disease progresses, other motor and nonmotor symptoms are developed, as well as treatment-associated complications that further increase the degree of disability caused by the disease.

1.2.1. *Prodromal PD*

Whereas the preclinical phase depends on the availability of disease biomarkers to assess neurodegeneration, prodromal PD is regarded as a true stage of the disease (Berg *et al.*, 2015). Prodromal PD criteria defined by MDS refer to a high probability (>80%) of the disease being present. They are based on estimates of background risk combined with diagnostic measures of nonmotor and motor manifestations and imaging markers (Berg *et al.*, 2015).

Nonmotor manifestations

One of the best described early nonmotor feature is **rapid eye movement sleep behavior disorder** (RBD). This parasomnia is characterized by the occurrence of vivid, often frightening dreams associated with prominent motor activity and polysomnographic (PSG) alterations (Boeve, 2010). PSG-confirmed idiopathic RBD has been demonstrated to be a powerful predictor of neurodegenerative synucleinopathy, including PD, dementia with Lewy bodies (DLB) and multiple system atrophy (MSA) (Postuma *et al.*, 2015b). Indeed, different prospective studies have documented more than 75% of conversion rate, within a 7 to 14 years range (Iranzo *et al.*, 2014; Postuma *et al.*, 2015b; Postuma *et al.*, 2015c; Schenck *et al.*, 2013). Excessive daytime somnolence (EDS) is another common sleep disorder affecting up to 60% of PD patients (Chahine *et al.*, 2017; Knie *et al.*, 2011). Despite being listed as a clinical nonmotor marker of prodromal PD (Berg *et al.*, 2015), population studies are lacking to address whether EDS can serve as a predictor of PD, or if it is a consequence of PD-associated sleep disorders, such as RBD.

Olfactory dysfunction has long been associated with PD (Ansari *et al.*, 1975; Mesholam *et al.*, 1998). Yet, it was only recently demonstrated that impaired olfaction, measured by odor identification recognition or threshold, could predate clinical PD by at least 4 years (Haehner *et al.*, 2007; Ponsen *et al.*, 2009; Ross *et al.*, 2008). Remarkably, combination of RBD diagnosis with olfactory dysfunction was shown to provide a diagnostic accuracy for PD conversion of 82,4% within 5 years (Mahlknecht *et al.*, 2015).

Constipation is the most common complaint of autonomic system, with 32% prevalence in PD patients within 2 years before diagnosis (Schrag *et al.*, 2015). Nonetheless, it has been reported to occur as early as 20 years before the onset of motor symptoms, being associated with an increased risk of PD in a dose-dependent manner (Abbott *et al.*, 2001; Lin *et al.*, 2014; Savica *et al.*, 2009). Other less common, but significant autonomic alterations include orthostatic hypotension, urinary and erectile dysfunction (Berg *et al.*, 2015; Schrag *et al.*, 2015).

The most frequent neuropsychiatric manifestation before PD onset is **depression**, affecting up to 10% of the patients within 2 years before diagnosis (Schrag *et al.*, 2015). Although the association is stronger in the years in close proximity to clinical PD, depression diagnosis has been detected more than 15 years prior to the onset of PD motor symptoms (Fang *et al.*, 2010; Gustafsson *et al.*, 2015).

Motor manifestations

In addition to nonmotor signs and symptoms, subtle motor alterations have been described to occur before PD diagnosis (Berg *et al.*, 2015). In a cohort study following patients with idiopathic RBD, a score above 3 on the Unified Parkinson's Disease Rating Scale[1] (UPDRS), was shown to identify prodromal PD (Postuma *et al.*, 2012). First signs occur 4.5 years before PD diagnosis, including voice and face akinesia, followed by rigidity, gait abnormalities, limb bradykinesia and finally tremor (Postuma *et al.*, 2012). Similar motor presentations were observed to predate PD diagnosis in a large primary care database (Schrag *et al.*, 2015).

Imaging markers

Different imaging techniques have been employed to identify subclinical PD. For instance, radiotracer imaging with single photon emission computed tomography (SPECT) or positron emission tomography (PET) allow the identification of dopamine terminal dysfunction, evidenced by a 40-50% reduction in tracer binding (Brooks, 2010; Noyce *et al.*, 2016). Recently, dopamine transporter imaging revealed a reduced striatal binding in 11% of subjects with hyposmia, thereby providing an additional assessment strategy to detect prodromal PD (Jennings *et al.*, 2014). Additionally, transcranial sonography (TCS), which detects ultrasound echoes from brain structures, has been considered a valuable tool to identify hyperechogenicity of the substantia nigra in PD (Berg, 2011). Although it is not specific for PD, it is considered a vulnerability marker that may arise from the ongoing signs of degeneration, such as iron accumulation and microglia activation (Berg, 2011). PD associated midbrain structural and functional abnormalities have also been detected on diffusion weighted magnetic resonance imaging (MRI) and functional MRI, respectively, though their value as prodromal PD markers has not been established (Brooks, 2010; Noyce *et al.*, 2016). Finally, involvement of cardiac sympathetic nerve has also been reported in patients with early nonmotor features of PD in ^{123}I-meta-iodobenzylguanidine (MIBG) myocardial scintigraphy (Sakakibara *et al.*, 2014).

[1] Clinical rating scale widely used for Parkinson's disease; a score of 199 on the UPDRS scale represents the worst (total disability) with a score of zero representing (no disability).

So far, despite several attempts to detect biochemical markers of PD in biological tissues and fluids (e.g. α-synuclein species in cerebrospinal fluid), none added (pre)diagnostic value to PD (Poewe *et al.*, 2017). Nevertheless, the available clinical and imaging markers not only provide important insights on PD pathology, but also offer a therapeutic window for initiating neuroprotective treatment in patients at risk (Noyce *et al.*, 2016).

1.2.2. *Clinical PD*

According to MSD criteria, PD is clinically defined in two steps. First, parkinsonism is diagnosed, being defined by the presence of bradykinesia[2] in combination with either rest tremor[3], rigidity, or both (Postuma *et al.*, 2015a). Next, supportive and exclusion criteria must be applied to address whether parkinsonism is attributable to PD (Postuma *et al.*, 2015a). Supportive criteria include: L-DOPA responsiveness, the presence of classic rest tremor, the presence of L-DOPA-induced dyskinesias, the presence of either olfactory loss or cardiac sympathetic denervation on MIBG scintigraphy (Postuma *et al.*, 2015a). Clinical criteria also exclude red flags, including rapid progression of gait impairment requiring use of wheelchair within 5 years after onset and severe autonomic dysfunction, which suggest atypical parkinsonian syndromes such as progressive supranuclear palsy, multiple system atrophy, and corticobasal degeneration (Kalia *et al.*, 2015; Postuma *et al.*, 2015a).

The onset of cardinal motor features is usually unilateral and the asymmetry persists with disease progression (Poewe *et al.*, 2017). Nonetheless, there is a great heterogeneity regarding motor and cognitive features, age at onset, rate of progression among PD patients, which is thought to represent underlying biological or pathophysiological differences between individuals. As a result, numerous studies have suggested the existence of PD subtypes in an attempt to refine studies of etiology, course and treatment responsiveness in PD (Marras *et al.*, 2013). Although consensus on the classification of PD subtypes has not been achieved, empirical clinical observations point out the occurrence of two subtypes: *tremor-dominant PD*, with very few other motor symptoms; and *non-tremor-dominant PD*, which includes other phenotypes, such as postural instability gait disorder (PIGD) or akinetic-rigid syndrome, with a faster rate of progression and more functional disability (Kalia *et al.*, 2015; Marras *et al.*, 2013).

Increased severity of motor symptoms, which can initially be managed with symptomatic therapies, is one of the hallmarks of disease progression (Coelho *et al.*, 2012). Nonetheless, long-term symptomatic

[2] Slowness of movement and a decrement in amplitude or speed (or progressive hesitations or halts) as movements are continued

[3] 4- to 6-Hz tremor in the fully resting limb, which is suppressed during movement initiation

treatment complications, including motor and nonmotor fluctuations, dyskinesia and psychosis, are major challenges of clinical management of the advanced PD stage (Kalia *et al.*, 2015). Late-stage PD is marked by treatment-resistant motor symptoms, such as postural instability, freezing of gait, falls, dysphagia and speech dysfunction (Hely *et al.*, 2005). In addition, nonmotor features also become increasingly prevalent, being major determinants of quality of life, overall disability and nursing home placement (Coelho *et al.*, 2012; Poewe *et al.*, 2017). In a follow-up study of newly diagnosed PD patients surviving for more than 20 years, 83% presented dementia, followed by increased prevalence of other nonmotor symptoms, such as hallucinosis (74%), excessive daytime sleepiness (70%), urinary incontinence (71%), orthostatic hypotension (48%) and constipation (40%) (Hely *et al.*, 2008). These features of late-stage PD start an exponential curve of disease progression, leading to death within approximately 5 years (Coelho *et al.*, 2012).

1.3. *Pathophysiology*

1.3.1. *Motor*

The main neurobiological substrate of motor alterations featured in parkinsonian disorders is the dopamine striatal depletion, as a consequence of the loss of dopaminergic neurons in the substantia nigra pars compacta (SNc) (Hernandez *et al.*, 2019; Hornykiewicz, 2008). Striatum and SNc are part of a group of subcortical nuclei, commonly referred to as basal ganglia, primarily responsible for motor control along with motor learning, executive functions and behaviors, and emotions (Lanciego *et al.*, 2012).

According to their role in these complex information system, basal ganglia and related nuclei can be organized as: 1) *input nuclei* - striatum, which receive incoming information from different sources, mainly from cortical, thalamic, and nigral origin; 2) *output nuclei* - globus pallidus internal segment (GPi), and substantia nigra pars reticulata (SNr), which send basal ganglia information to the thalamus; and 3) *intrinsic nuclei* - external segment of the globus pallidus (GPe), subthalamic nucleus (STN) and SNc, which are located between the input and output nuclei in the relay of information (Lanciego *et al.*, 2012).

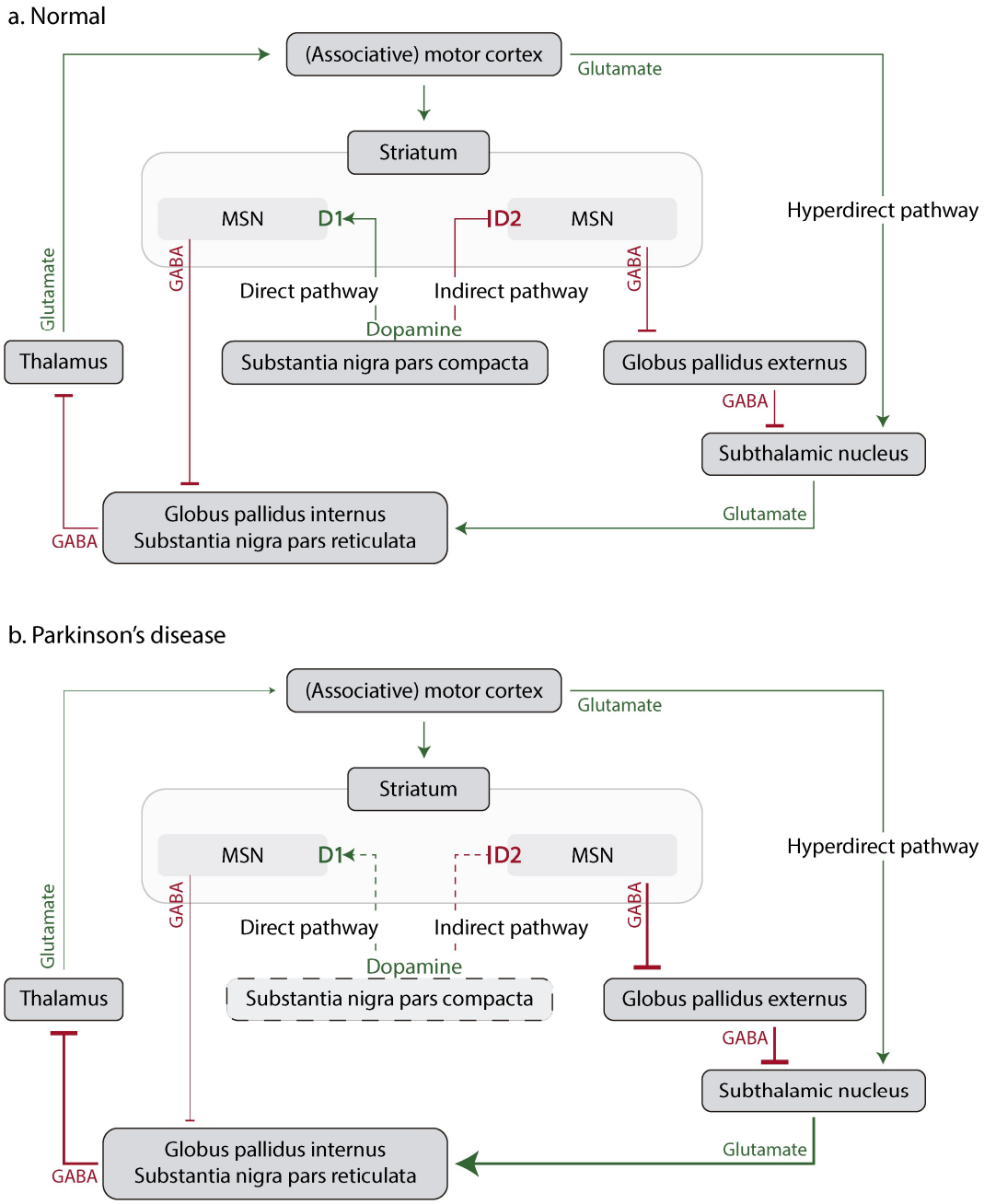

Figure 1.3 – Motor circuitry affected in Parkinson's disease. a) Normal activity of basal ganglia and related nuclei, depicting the type of neurotransmitters leading to their inhibition (red) or activation (green); **b)** depicts the alterations of the activity of this motor circuitry induced by the lack of dopamine release into the striatum, as a consequence of the loss of dopaminergic neurons in the substantia nigra *pars compacta*.

The appropriate functioning of these circuitry requires dopamine release in the striatum, which is mainly originated from nigrostriatal innervation (figure 1.3a). Dopaminergic input has a dichotomous effect on the striatal projecting neurons, also known as medium spiny neurons (MSNs), depending on the subtype of dopamine receptor expressed in the MSNs they bind to. Dopamine receptor subtype 1 (D1) activates adenyl-cyclase signaling, thereby increasing neuronal excitability; whereas binding to dopamine receptor

subtype 2 (D2) expressing neurons exerts an inhibitory effect. Both D1 and D2 expressing striatal MSNs are inhibitory neurons (GABAergic), but project to distinguishable nuclei within basal ganglia. D1 expressing striatal MSNs inhibit GABAergic neurons in GPi and SNr in a monosynaptic connection, giving rise to the direct pathway. On the other hand, the indirect pathway originates from D2 expressing MSNs, which first inhibits GPe, leading to STN disinhibition that, in turn, excites GPi/SNr neurons (Lanciego *et al.*, 2012; Neumann *et al.*, 2018; Poewe *et al.*, 2017). Balance between these opposing functional projection systems are responsible for movement facilitation and inhibition. A third "hyperdirect" pathway formed by glutamatergic projections from the cerebral cortex to the SNT, has been recently identified, being suggested to play a role in preventing premature responses by reinforcing indirect pathway activity (Nambu *et al.*, 2002; Neumann *et al.*, 2018).

A simplified, but still useful, model to explain impaired movement initiation and execution in PD (figure 1.3b), suggests that dopamine depletion, resultant from SNc cell loss, shifts the balance of basal ganglia activity toward the indirect pathway, leading to excessive activity of the STN that overstimulates the GPi/SNr (Albin *et al.*, 1989; Neumann *et al.*, 2018). Recently, abnormal neural synchronization and cortico–subcortical coupling in specific frequency bands have also been proposed as more complex changes in this information processing system (Kühn *et al.*, 2008). In addition, changes in cerebellar activity and its interaction with the basal ganglia have been suggested to explain PD associated tremor (Dirkx *et al.*, 2016). The authors suggest that tremulous activity first arises in the GPi, which switches the cerebello-thalamo-cortical loop on and off, modulating tremor intensity (Dirkx *et al.*, 2016). Overall, the increasing understanding of the PD associated motor networks has contributed for designing new therapeutic strategies, such as deep brain stimulation (DBS), targeting specific symptom profiles.

1.3.2. *Nonmotor*

Conversely to motor alterations, the pathophysiology of nonmotor symptoms remains poorly understood. Most of the studies suggest alterations on other dopaminergic pathways, such as the mesolimbic pathway to explain mood disorders, whereas the involvement of nondopaminergic systems has also been proposed to explain cognitive and autonomic dysfunction.

Loss of dopaminergic neurons in the ventral tegmental area (VTA) is one of the possible explanations for depression in PD patients (Torack *et al.*, 1988). This central structure of the reward system contains dopaminergic neurons of the mesocortical and mesolimbic circuitry innervating the medial prefrontal cortex (mPFC), the nucleus accumbens (NAc), hippocampus and amygdala, thus playing an important role on modulating mood and motivation (Russo *et al.*, 2013). The proposed model suggests that primary

degeneration of dopaminergic neurons from mesolimbic and mesocortical pathways leads to dysfunction of the orbitofrontal cortex, subsequently affecting serotonergic cell bodies in the dorsal raphe nuclei (Aarsland *et al.*, 2012).

Increased neurodegeneration of the locus coeruleus (LC) is also well-documented in PD, even in early stages and thus, has been linked to a myriad of nonmotor symptoms in PD patients (Gratwicke *et al.*, 2015; Szabadi, 2013). LC is the major noradrenergic structure in the brain, projecting to extensive areas of the brain, brainstem and spinal cord (Szabadi, 2013). As a consequence, progressive degeneration of LC in PD might be responsible for: 1) cognitive changes and dementia, due to loss of noradrenergic input to the prefrontal cortex (Gratwicke *et al.*, 2015); 2) sleep disorders, as a result of loss of noradrenaline in pedunculopontine/laterodorsal tegmental nucleus (Dugger *et al.*, 2012; Tubert *et al.*, 2019); and 3) depression, caused by loss of noradrenergic input in the limbic system (Chan-Palay, 1993; Pålhagen *et al.*, 2010; Remy *et al.*, 2005).

Additional networks implicated in PD nonmotor manifestations include cholinergic cells in the nucleus basalis of Meynert, associated with cognitive deficits, and hypocretin cells in the hypothalamus, which may underlie sleep disorders (Gratwicke *et al.*, 2015; Obeso *et al.*, 2010). Accumulation of α-synuclein aggregates in autonomic control areas have also been put forward as possible explanations for gastrointestinal and genitourinary dysfunctions associated to PD, though with little evidence of being a PD specific mechanism (Jellinger, 2014). Given the multifactorial nature of PD nonmotor alterations, identifying the neural networks implicated in their pathophysiology is a challenging task. Nevertheless, future studies on this field may provide important insights of PD etiology and help in designing innovative neuroprotective strategies.

1.4. *Neuropathology*

Neuropathological criteria for PD diagnosis are moderate to severe neuronal loss in the SNc associated with widespread Lewy pathology, which is characterized by the presence of α-synuclein immunoreactive neuronal inclusions (Gelb *et al.*, 1999). Additional neuronal loss assessment might include the presence of fibrillary astrocytosis and extraneuronal neuromelanin (Dickson *et al.*, 2009).

Loss of dopaminergic neurons usually begins in the lateral ventral tier of the SNc, containing the neurons that project to the dorsal putamen of the striatum, being estimated to represent a 68% cell loss at the onset of motor symptoms (Fearnley *et al.*, 1991). Nevertheless, it has been reported that, at early stages

of PD, striatal dopaminergic loss exceeds SN neuron cell death, pointing towards the occurrence of a retrograde degeneration of the nigrostriatal pathway (Cheng *et al.*, 2010; Hernandez *et al.*, 2019).

Even though the mechanisms underlying nigrostriatal degeneration are not completely understood, several hypotheses have been proposed to explain SNc vulnerability to cell damage (Sulzer, 2007). First, nigral dopaminergic neurons have particularly long, unmyelinated axons with large number of synapses, thereby requiring a great amount of energy supply (Bolam *et al.*, 2012; Pissadaki *et al.*, 2013). Secondly, dopamine metabolism, by itself, produces highly reactive species that oxidize lipids and other compounds, leading to increased oxidative stress and mitochondrial dysfunction (Obeso *et al.*, 2010; Zucca *et al.*, 2017). Third, auto-oxidation of dopamine at neutral pH may possibly also occur due to reduced sequestration of dopamine into synaptic vesicles, where the pH is lower (González-Hernández *et al.*, 2004; Zucca *et al.*, 2017). Last, calcium-mediated toxicity has also been suggested, as result of the autonomous pacemaking activity of nigral dopaminergic neurons, which involve cytosolic calcium oscillations and calcium extrusion at the expense of energy (Mosharov *et al.*, 2009).

An additional neuropathological hallmark of PD is the accumulation of α-synuclein filamentous structures as Lewy neurites in axons, or as Lewy bodies in the somatodendritic compartments of certain neurons in the central, peripheral and autonomic nervous system (Obeso *et al.*, 2010; Volpicelli-Daley *et al.*, 2014). Lewy pathology can also be found in 5–20% of non-symptomatic elder individuals, which is interpreted as a byproduct of neuronal aging, or preclinical PD cases (Dickson *et al.*, 2009; Frigerio *et al.*, 2011). Notwithstanding, Lewy pathology is well-established as a neuropathological feature of PD and has been suggested to follow a stepwise progression over the course of PD. According to Braak staging scheme (Braak *et al.*, 2003), α-synuclein pathology progresses over six successive caudal-to-rostral stages and can be related to the onset of nonmotor symptoms that antedate disease onset (figure 1.4). Thereby, α-synuclein first accumulates in the olfactory bulb coinciding with the appearance of olfactory dysfunction. Subsequent accumulation in the SNc establishes the onset of motor symptoms, and lastly, progressive accumulation in the temporal cortex pave the way for cognitive decline and dementia (Braak *et al.*, 2003).

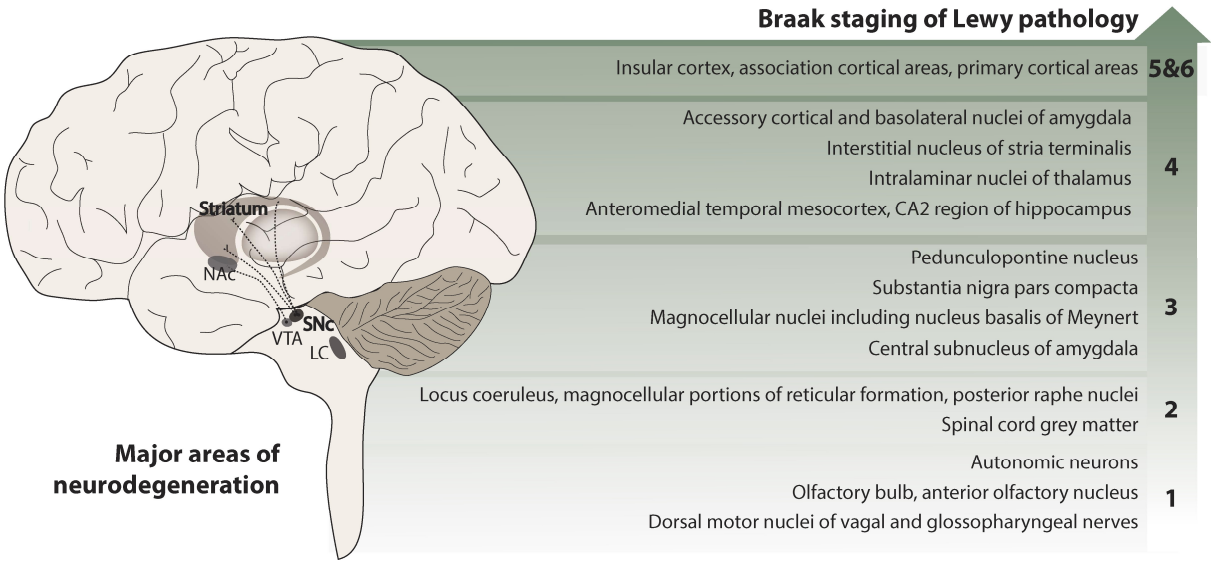

Figure 1.4 – Neuropathological hallmarks in Parkinson's disease. Major degenerated areas are represented on the left, whereas Braak staging of Lewy pathology progression is depicted on the right, showing the areas affected on each stage.

One of the hypotheses currently being considered to explain the progression of Lewy pathology in PD is the prion-like spreading, in which small amounts of fibrillar of α-synuclein act as seeds and are transmitted from one neuron to another, triggering the conversion of normal, soluble α-synuclein into insoluble aggregates (Olanow *et al.*, 2009; Volpicelli-Daley *et al.*, 2018). This idea was initially speculated by Braak and colleagues (Braak *et al.*, 2003). However, clinical evidences for this only emerged with the discovery of α-synuclein in the cerebrospinal fluid and with the detection of Lewy bodies inside fetal grafts transplanted in the striatum of PD patients (Brundin *et al.*, 2008; El-Agnaf *et al.*, 2003; Kordower *et al.*, 2008; Li *et al.*, 2008). Further evidences on this hypothesis were obtained after the injection of α-synuclein fibrils into the duodenum of wild-type and transgenic rat models (overexpressing the wild-type complete human SNCA gene) and subsequent identification of trans-synaptic spreading of the pathology (Holmqvist *et al.*, 2014; Van Den Berge *et al.*, 2019). The injected fibrils were detected within 6 days on dorsal motor nucleus of the vagus of wild-type rats (Holmqvist *et al.*, 2014), as well as in key structures along the sympathetic and parasympathetic pathways (enteric nervous system, autonomic ganglia, intermediolateral nucleus of the spinal cord, heart, dorsal motor nucleus of the vagus and LC) for at least 4 months post-injection in the transgenic animal model (Van Den Berge *et al.*, 2019).

Although compelling evidence has been collected on this hypothesis, a number of limitations hamper its full reconciliation with current understanding of PD pathophysiology (Surmeier *et al.*, 2017). First, Braak staging model is not consistent with about half of PD patients, and some of them do not present Lewy pathology at all (Berg *et al.*, 2014). Secondly, trans-synaptic spread of the pathology implies a correlation

with neuronal synaptic connectome. Nonetheless, some prominent sites of Lewy pathology do not receive projections from affected areas, suggesting that spreading cannot be solely governed by synaptic connectivity (Surmeier *et al.*, 2017). Lastly, another major caveat of synuclein-centered PD etiopathology is the lack of correlation between Lewy pathology and neuronal death (Dickson *et al.*, 2009; Surmeier *et al.*, 2017). Indeed, there is no substantial neurodegeneration in regions presenting Lewy pathology, suggesting the existence of cell-autonomous or regionally autonomous mechanisms underlying neurodegeneration in vulnerable neuronal phenotypes, such as SNc (Surmeier *et al.*, 2017).

1.5. *Cellular and molecular mechanisms*

Knowledge obtained from genetic studies and postmortem brain tissue analysis have shed some light on potential molecular pathways leading to α-synuclein aggregation and/or neurodegeneration, mainly involving a vicious cycle of impaired α-synuclein proteostasis, mitochondrial dysfunction, oxidative stress, impaired calcium homeostasis, iron accumulation and neuroinflammation (Corti *et al.*, 2011; Michel *et al.*, 2016; Poewe *et al.*, 2017; Zucca *et al.*, 2017). A schematic representation of the interplay between these pathways is presented in figure 1.5.

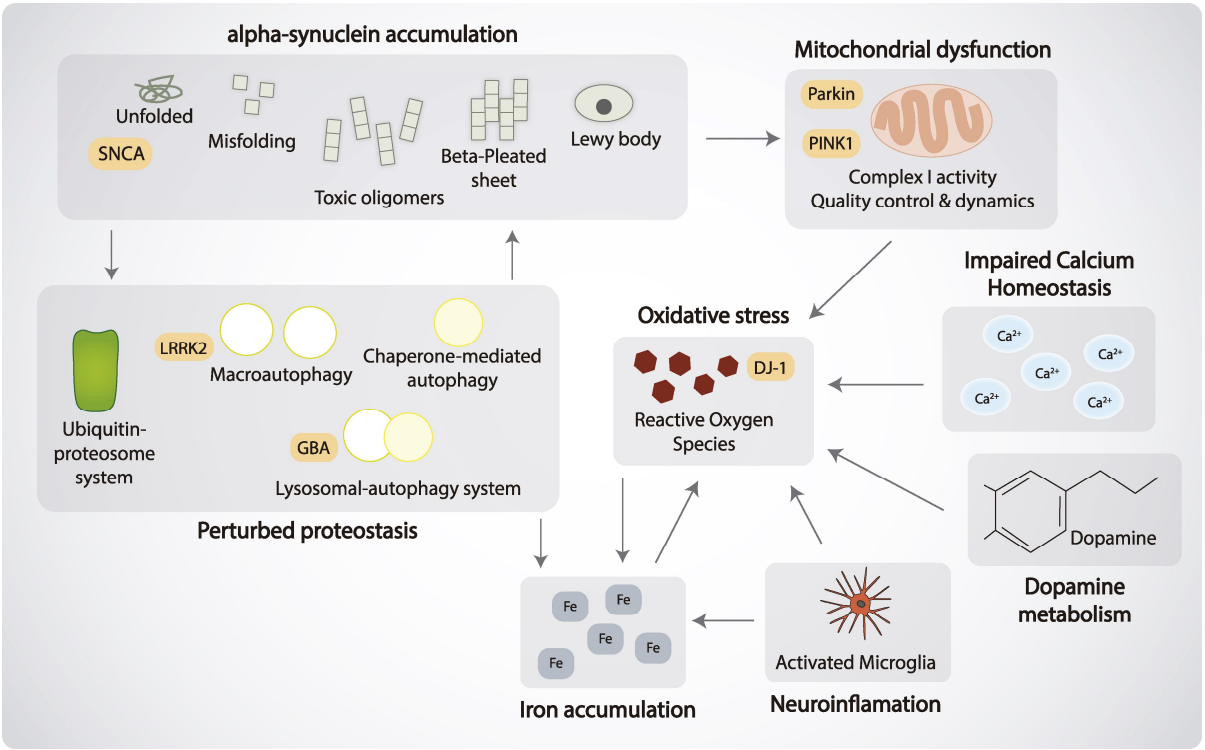

Figure 1.5 – Interplay between molecular pathways associated to neurodegeneration. Parkinson's disease-linked genes are depicted in orange within the pathway associated to their function.

1.5.1. *Impaired α-synuclein proteostasis*

The physiological role of α-synuclein is still unclear. It is localized at the presynaptic terminals in association with the distal pool of synaptic vesicles, thereby suggesting a role in neurotransmitter release, synaptic function and plasticity (Burré *et al.*, 2010; Lashuel *et al.*, 2013). In addition, nuclear and mitochondrial localization has also been reported, though with limited hints on their functions (Pinho *et al.*, 2019; Wales *et al.*, 2013). α-synuclein aggregation is described to be initiated by the combination of unfolded or misfolded monomers into dimers, that stabilize in small oligomeric species through β-sheet-like interactions. Subsequently, these oligomeric species evolve to higher molecular weight insoluble protofibrils, and finally to amyloid-like fibrils that build up pathological structures, such as Lewy bodies (Michel *et al.*, 2016).

As mentioned above, the identification of mutations that lead to α-synuclein overproduction, or that increase the likelihood for its misfolding and oligomerization, are possible triggers for aggregation (Corti *et al.*, 2011; Poewe *et al.*, 2017). Nevertheless, imbalance between protein synthesis and degradation may also arise from alterations in the molecular pathways responsible for clearance of native or misfolded proteins, as a consequence of aging or genetic mutations (Kaushik *et al.*, 2015; Lashuel *et al.*, 2013; Michel *et al.*, 2016). Moreover, accumulated α-synuclein induces a pathological feedback loop, wherein α-synuclein aggregates further impair these degradation pathways (Lindersson *et al.*, 2004; Winslow *et al.*, 2010). The ubiquitin-proteasome system (UPS) and the lysosomal autophagy system (LAS) are the two major intracellular proteolytic systems involved in α-synuclein degradation (Xilouri *et al.*, 2013).

The identification of two PD-linked genes encoding for UPS-related proteins (parkin and UCH-L1) suggested the involvement of UPS-dependent protein processing in PD pathogenesis (Kitada *et al.*, 1998; Maraganore *et al.*, 2004). Nevertheless, it has been suggested that only very specific species of α-synuclein, of small, soluble oligomers, are degraded through the UPS under conditions of endogenous and increased protein burden (Xilouri *et al.*, 2013). In contrast, LAS is suggested to act in pathologic conditions (Xilouri *et al.*, 2013). LAS is responsible for the vesicle-mediated degradation of long-lived proteins, which can occur via macroautophagy or chaperone-mediated autophagy. Macroautophagy, is a tightly regulated process involving the formation of double-membrane-bound structures (autophagosomes) to engulf intracellular constituents, thereby generating the autophagic vacuoles that subsequently fuse with the lysosome for degradation, creating the autophagolysosome (Michel *et al.*, 2016; Xilouri *et al.*, 2013). Chaperone-mediated autophagy is also responsible for lysosomal degradation, though only of a very specific subset of soluble cytosolic proteins (Michel *et al.*, 2016). α-synuclein

belongs to this selective group, as it contains a KFERQ-like motif, which is recognized by the cytosolic chaperone heat shock cognate protein 70 (HSC70) (Cuervo *et al.*, 2004; Xilouri *et al.*, 2013).

Supporting evidence on the involvement of impaired proteostasis on PD pathogenesis comes with the observation of increased expression of autophagosomes, decreased expression of lysosomal marker proteins, as well as, proteins of chaperone-mediated autophagy (LAMP2A and HSC70) in postmortem analysis of PD patients' brains (Alvarez-Erviti *et al.*, 2010; Anglade *et al.*, 1997; Chu *et al.*, 2009).

Moreover, several mutations associated to familial and sporadic PD, were identified in genes encoding for proteins involved in LAS. The G2019S mutation in LRRK2 gene, which upregulates LRRK2 kinase activity, increases a pool of α-synuclein that is more susceptible to form inclusions (Bieri *et al.*, 2019; Lin *et al.*, 2009; Volpicelli-Daley *et al.*, 2016a), as well as increases the number of autophagosomes and decreases the number of acidic lysosomes, thereby decreasing their hydrolytic activity (Gómez-Suaga *et al.*, 2011). Heterozygous mutations in GBA, which encode for a lysosomal enzyme, are also associated with reduced LAS function and subsequent accumulation of α-synuclein (Fernandes *et al.*, 2016; Sardi *et al.*, 2013). Surprisingly, patients without mutations in the GBA gene also present reduced GBA activity in CSF and brain tissue, suggesting the existence of a positive feedback mechanism, whereby reduced GBA lysosomal activity causes accumulation of α-synuclein and vice versa (Mazzulli *et al.*, 2011; Murphy *et al.*, 2014). Mutations in vacuolar protein sorting-associated protein 35 (VPS35) have also been linked to autosomal dominant PD (Vilariño-Güell *et al.*, 2011; Zimprich *et al.*, 2011). VPS35 is part of the retromer complex, being responsible for the regulation of the retrograde transport of proteins from early endosomes to the Golgi apparatus (Williams *et al.*, 2017). Dysfunction of VPS35 has been linked to alterations in the chaperone-mediated autophagy due to impaired endosome-to-Golgi retrieval and consequently, accelerated degradation of LAMP2A (Tang *et al.*, 2015). Finally, mutations in ATP13A2, which is localized in acidic membrane compartments of lysosomes, where it is expected to act as a cation metal transporter, cause rare juvenile-onset neurological condition (Kufor-Rakeb syndrome) characterized by early-onset parkinsonism (Ramirez *et al.*, 2006). ATP13A2 loss of function has been reported to impair lysosomal catabolism and increase accumulation of α-synuclein (Usenovic *et al.*, 2012).

1.5.2. *Mitochondrial dysfunction*

Mitochondria are not only important for producing energy to sustain cell activities, but are also often essential for initiating apoptotic cell death (Tait *et al.*, 2013). First hints on the involvement of mitochondria on PD progression arouse from observations of brain tissue samples from PD patients, wherein deficits on the activity of mitochondrial complex I, part of the electron transport chain, were

identified (Pollard *et al.*, 2016; Schapira *et al.*, 1990). This energy deficiency is potentially an upstream and early neurodegenerative event in PD and has been associated with axonal degeneration (Poewe *et al.*, 2017). Moreover, complex I inhibitors, such as MPP^+ and rotenone, induce irreversible lesions on dopaminergic neurons when systemically administered to animal models (Langston *et al.*, 1984; Sherer *et al.*, 2003). Finally, mitochondrial complex I deficits are also reported to occur as a result of accumulation of α-synuclein protein inside the mitochondria (Devi *et al.*, 2008; Martin *et al.*, 2006).

The identification of two recessive genes associated to familial PD, PINK1 and parkin, further suggested the contribution of mitochondrial quality control and dynamics for PD pathogenesis (Narendra *et al.*, 2012). These two proteins act collectively on the functional and morphological maintenance of mitochondrial network, and are also critical regulators of the removal of bioenergetically compromised mitochondria, through mitophagy (Deas *et al.*, 2011; Gautier *et al.*, 2008; Palacino *et al.*, 2004). PINK1 accumulation at the outer mitochondrial membrane of dysfunctional mitochondria is required and sufficient to recruit and activate parkin, which, in turn, drives ubiquitination and degradation of mitochondrial substrates in autophagosomes (Bertolin *et al.*, 2013; Michel *et al.*, 2016; Narendra *et al.*, 2010). Consequently, mutations in PINK1 or parkin may lead to the accumulation of toxic dysfunctional mitochondria (Michel *et al.*, 2016; Narendra *et al.*, 2010).

1.5.3. *Impaired calcium homeostasis*

Alterations in calcium homeostasis are particularly detrimental for dopaminergic neurons, due to their calcium-dependent pacemaking activity and low intrinsic calcium buffering capacity (Michel *et al.*, 2016). Additionally, impaired calcium homeostasis, may also occur as an indirect consequence of PD related events, including α-synuclein aggregation, mitochondrial and endoplasmic reticulum (ER) dysfunction (Michel *et al.*, 2016).

In an homeostatic state, autonomous pacemaking rely on L-type voltage-dependent calcium channels, thereby increasing the levels of Ca^2 in the cytosol, and secondarily in the mitochondria, either directly or via ER (Chan *et al.*, 2007). In an hypoactive state, decreased levels of basal cytosolic Ca^{2+} and consequently mitochondrial Ca^{2+}, may act as trigger for cell death (Michel *et al.*, 2013). This hypoactive state, may occur early during degeneration and may precede an hyperactive state that triggers oxidative stress and activation of calpains (i.e., calcium-activated proteases) (Dufty *et al.*, 2007). Both hypo- and hyper-active states are exacerbated by mutations in PD-related genes, including DJ-1, parkin, PINK or α-synuclein (Gandhi *et al.*, 2009; Michel *et al.*, 2016). Alternatively, abnormal calcium influx may occur as a consequence of subthalamic nucleus (STN)-mediated excitotoxicity (Blandini *et al.*, 2004).

1.5.4. *Iron accumulation*

Iron plays an essential role in many physiological functions, including neuronal metabolism, neurotransmission and myelination (Sian-Hülsmann *et al.*, 2011). Under normal physiological conditions, excess iron levels can be sequestrated in ferritin and neuromelanin, reducing the availability of redox-active (free) iron (Jiang *et al.*, 2017; Sian-Hülsmann *et al.*, 2011). The presence of increased iron deposition in the SNc of PD patients, spurs the disruption of iron metabolism as a key mechanism of neurodegeneration in PD (Dias *et al.*, 2013; Jiang *et al.*, 2017; Sofic *et al.*, 1988). Then again, it is debatable whether elevated iron levels represent a cause or consequence of neurodegeneration triggered by oxidative stress, inflammation, excitotoxicity, mitochondrial dysfunction and altered proteostasis (Sian-Hülsmann *et al.*, 2011). Iron-mediated cellular destruction is primarily derived from oxidative stress. It is hypothesized that the combination of intracellular iron overload with hydrogen peroxide, produced during normal cell metabolism, generates an extremely toxic hydroxyl radical that induces cellular damage, lipid peroxidation and eventually apoptosis (Jiang *et al.*, 2017; Sian-Hülsmann *et al.*, 2011).

1.5.5. *Neuroinflammation*

Neuronal loss in PD has also been linked to chronic neuroinflammation, primarily by microglia, the resident innate immune cells in the central nervous system (Bachiller *et al.*, 2018). The role of neuroinflammation in neurodegenerative process has been supported by several postmortem analysis, as well as genetic and imaging studies (Moehle *et al.*, 2015). Microglia are responsible for clearance of neuronal death-related debris in response to injury or toxic insult (Hwang, 2013). However, their activation triggers the release of pro-inflammatory cytokines along with free radicals, such as nitric oxide and superoxide, which contribute for oxidative stress and PD progression (Bachiller *et al.*, 2018; Gao *et al.*, 2008; Hwang, 2013). Moreover, it was recently reported that lesion in the LC, might be involved in dopaminergic neurons degeneration via altered microglia function, namely increased expression of pro-inflammatory cytokines, reduced neurotrophic factors release and antioxidant activity in the SNc (Yao *et al.*, 2015). Indeed, BDNF and GDNF, which are trophic factors known to be released by microglia, are found to be decreased in the basal ganglia of PD patients (Siegel *et al.*, 2000).

1.5.6. *Oxidative stress*

Oxidative stress occurs upon imbalance between the production of reactive oxygen species (ROS) and the cellular antioxidant activity (Dias *et al.*, 2013). This imbalance is thought to be the main cause of cell death in both idiopathic and genetic cases of PD (Hwang, 2013). Indeed, increased oxidative stress is

evident in brain tissue of PD patients, as determined by the increased levels of oxidized lipids, proteins and DNA (Bosco *et al.*, 2006; Nakabeppu *et al.*, 2007).

Despite the large body of evidence on the role of oxidative stress in PD pathogenesis, it is not clear whether it is a cause or a consequence of previously described cellular dysfunctions, such as mitochondrial dysfunction, impaired calcium homeostasis, neuroinflammation and iron accumulation (Dias *et al.*, 2013). As previously discussed, dopamine, by itself is also a major source of ROS production, which may explain vulnerability for neurodegeneration (Obeso *et al.*, 2010). In addition, dopamine auto-oxidation in the cytosol leads to the formation of dopamine quinones, which can cyclize to form the highly reactive aminochrome, leading to the generation of superoxide and depletion of cellular NADPH (Hastings, 2009).

The imbalance leading to oxidative stress may also arise from decreased activity of antioxidant proteins, such as DJ-1, which is linked to autosomal recessive, early-onset PD (Bonifati *et al.*, 2003; Kahle *et al.*, 2009). Loss of DJ-1 in dopaminergic neurons has been associated with compromised ability to attenuate oxidative stress evoked by normal autonomous pacemaking, in addition to mitochondria dysfunction and accumulation of autophagy markers (Guzman *et al.*, 2010; Kim *et al.*, 2005; Thomas *et al.*, 2010).

In conclusion, over the past decades, significant advances have been achieved on the identification of cellular and molecular mechanisms associated to PD pathogenesis. Nonetheless, rather than identifying a single cause for neurodegeneration, these observations reveal the high complexity of the disease. Still, most of these studies have been centered on dopaminergic neurons, whereas the mechanisms underlying alterations in non-dopaminergic neurons and glial cells, remain poorly explored.

2. Experimental models of Parkinson's disease

Besides clinical data, the increasing availability of PD experimental models has also contributed for the discovery of potential cellular and molecular mechanisms underlying PD pathogenesis, whereas their use as preclinical models has been hampered by the lack of full recapitulation of PD hallmarks. The existing models attempt to reproduce specific features of PD pathology either *in vitro* or *in vivo*, through the use of toxic agents, such as 6-hydroxydopamine (6-OHDA) and MPTP that selectively destroy dopaminergic neurons or genetic approaches to mimic the most commonly known mutations associated to monogenic PD. Although none of these approaches yields a *bona fide* PD model, the discovery of innovative cellular and genetic tools has provided significant advances in PD disease modeling.

2.1. *In vitro*

Modeling PD in a dish allows a quick development of the pathology, easier pharmacological and genetic modifications, as well as large-scale testing using disease-specific cell types (Falkenburger *et al.*, 2016). The available PD cellular models include cell lines, primary cultures, organotypic cultures, as well as induced pluripotent stem cells (iPSCs) that can be differentiated into disease-specific cell types.

2.1.1. *Cell lines*

Cell lines are naturally (e.g. human neuroblastoma cell line SH-SY5Y) or artificially immortalized cells (e.g. Lund human mesencephalic (LUHMES) cells), lacking some cell cycle checkpoint pathways and normal cellular senescence (Lopes *et al.*, 2017; Lotharius *et al.*, 2002; Maqsood *et al.*, 2013). Despite this high proliferative state, which does not mimic neuronal phenotype, cell lines offer high-throughput and reproducible testing, which is useful to rapidly screen large panels of drugs (Lopes *et al.*, 2017).

2.1.2. *Primary and organotypic cultures*

Primary and organotypic cultures, obtained from rodent brain tissue, have been employed as models to investigate properties and characteristics of dopaminergic neurons (Gaven *et al.*, 2014; Testa *et al.*, 2005). Although primary dopaminergic cultures may contain glial cells, organotypic slice culture models comprise more mature neurons, which remain in cultures for weeks to months, maintaining both inter-neuronal and neuronal–glial interactions (Gähwiler *et al.*, 1997). After established, both cultures types can be challenged with toxic agents, thus providing relevant platforms to assess the neuroprotective effect of given agents (Testa *et al.*, 2005; Toulorge *et al.*, 2011). Nevertheless, the technical difficulty along with the heterogeneity of these cultures, affects reproducibility of experiments, thereby hampering their use in large-scale screening (Lopes *et al.*, 2017).

2.1.3. *Induced pluripotent stem cells*

In 2007, the discovery of human iPSCs has greatly revolutionized the human disease modeling field (figure 1.6). iPSCs are embryonic-like stem cells (ESCs) obtained through the reprogramming of somatic cells, by forced expression of four transcription factors: Oct4, Sox2, c-Myc, and Klf4 (Takahashi *et al.*, 2007). Therefore, human iPSCs offer an unique resource to investigate otherwise inaccessible patient-specific cells, using easily accessible cell types, such as skin fibroblasts and blood cells (Loh *et al.*, 2009; Takahashi *et al.*, 2007). Besides their importance in understanding PD pathogenic mechanisms in disease modelling studies, iPSCs are also relevant for generating large-scale screenings in drug discovery,

and hold great promise to provide a source of cell-based therapeutics for regenerative medicine (Shi *et al.*, 2016).

Since its discovery, the technology employed to deliver the reprograming factors to somatic has greatly evolved from integrating viral vectors, such as retroviral or lentiviral vectors to non-integrating methods, such as Sendai virus, episomal and mRNA reprogramming (Schlaeger *et al.*, 2015). The use of these non-integrating methods allow the generation of iPSCs without the risk of insertional mutagenesis and genetic alterations thus, maintaining the genomic identity of the patient in disease modelling studies (Shi *et al.*, 2016). Moreover, these non-integrating methods allow the generation of high quality human iPSCs, although presenting significant differences regarding aneuploidy rates, reprogramming efficiency, reliability and workload (Schlaeger *et al.*, 2015).

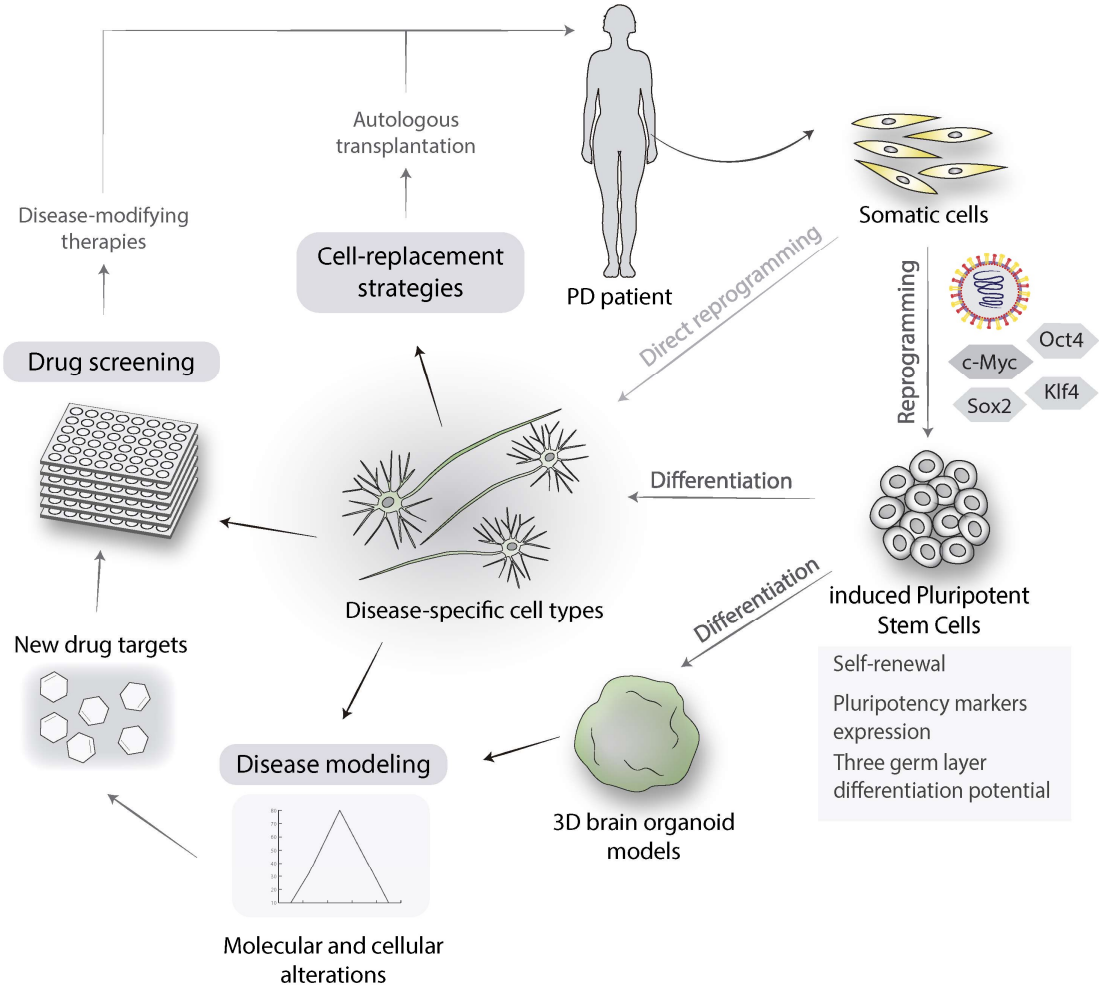

Figure 1.6 – Induced pluripotent stem cells and their applications in disease modeling, drug screening and cell-replacement strategies. Schematic representation of induced pluripotent stem cells generation, characterization and differentiation into disease-specific cell types or 3D brain organoid models.

Essentially, iPSCs are similar to ESCs, as they are able to self-renewal, express human pluripotent factors and surface markers and present developmental potential intro the three germ layers (Shi *et al.*, 2016). After derivation and proper characterization, iPSCs can be differentiated into almost any cell type, by adding timed combinations of mitogens and morphogens to the culture medium that gradually specify temporal and positional identity by mimicking developmental cues (Little *et al.*, 2019; Mertens *et al.*, 2016). This tool enables the generation of large amounts of human disease-relevant cells, with all the genetic background of the donor (Holmqvist *et al.*, 2016; Soldner *et al.*, 2017). Accordingly, dopaminergic neurons obtained from iPSCs of familial and sporadic PD patients display cellular abnormalities previously described (section 1.5), including mitochondrial dysfunction, oxidative stress, lysosomal and autophagy alterations, as well as α-synuclein aggregates in specific genotypes, as summarized in table 1.2 (Cobb *et al.*, 2018; Ghaffari *et al.*, 2018; Li *et al.*, 2018; Sison *et al.*, 2018).

Table 1.2 – Phenotypic cellular alterations displayed by familial and idiopathic iPSC - derived dopaminergic neurons. Adapted from (Shi *et al.*, 2016) and (Cobb *et al.*, 2018).

Genotype	Phenotype
Idiopathic	Increased apoptosis Reduced number of neurites and neurite arborization Impaired autophagy and mitophagy Irregular dopamine metabolism
SNCA Trplication, A53T	α-synuclein accumulation Decreased neuronal activity Reduced neurite outgrowth Impaired synapse formation Increased vulnerability to mitochondrial toxin-induced cell death
LRRK2 G2019S	α-synuclein accumulation Increased oxidative stress Increased vulnerability to environmental factors Reduced neurites and neurite arborization
Parkin Exon deletion	Increased oxidative stress Increased spontaneous dopamine release and decreased dopamine reuptake Increased bursting of spontaneous excitatory postsynaptic currents Reduced neurite length and complexity
PINK1 Q456Stop, V170G	α-synuclein accumulation Abnormal mitochondrial morphology
DJ-1 E64D	α-synuclein accumulation Increased dopamine oxidation and neuromelanin-like pigmented aggregates

Despite the numerous advantages of using patient-derived iPSCs as an experimental model system, they still present technical limitations that should be addressed to create a more robust and reproducible disease-relevant model. First, due to the reprogramming process, iPSCs acquire a "rejuvenation" phenotype, and thus do not fully recapitulate age-related cellular alterations (La Manno *et al.*, 2016; Sison *et al.*, 2018; Zhang *et al.*, 2019). Some reported approaches to induce aging in iPSCs-derived cultures include: 1) progerin expression, which is a premature aging-associated protein (Miller *et al.*, 2013); 2) telomerase inhibition at the iPSC stage, even though the role of telomere length in aging is not fully understood (Vera *et al.*, 2016); and 3) oxidative stress induction to elicit PD neuron-specific phenotypes (Nguyen *et al.*, 2011). Notwithstanding, these strategies only recapitulate specific aspects of aging and thus, do not provide a complete representation of cellular aging in neurons (Mertens *et al.*, 2018). Direct conversion of somatic cells into induced neurons (iNs), without going through the pluripotent stage, has been proposed as an alternative approach to generate human neurons for studying PD in a dish (Mertens *et al.*, 2018). Indeed, it has been shown that features of age are directly transferred from one cell type to another. Yet, PD modeling using iNs is economically challenging, in part, due to the limited expandability of fibroblasts (Mertens *et al.*, 2018).

Another major challenge in iPSC-based disease modeling is the system-immanent variability regarding their differentiation into functional cells (Soldner *et al.*, 2017). Inconsistency between protocols to generate homogeneous cultures of differentiated cells is one of the potential sources of variability (Arenas *et al.*, 2015). Moreover, genetic background differences between patient-derived iPSCs may influence their propensity to differentiate into functional cell types, thereby hampering the establishment of appropriate control lines (Soldner *et al.*, 2017). Recent progress in gene editing technologies, such as the CRISPR/Cas9 system and engineered zinc finger nucleases, has provided a solution for generating controlled iPSCs lines that only differ at known PD-associated mutation variants (Arias-Fuenzalida *et al.*, 2017; Soldner *et al.*, 2011). Nevertheless, this approach is limited to cases in which disease-causing genetic alterations are known, which only represent part of PD cases (Soldner *et al.*, 2017).

Finally, most studies have used two-dimensional (2D)-based iPSCs differentiation protocols, often generating homogeneous cultures that unlikely recapitulate the complexity and cellular diversity of the human brain (Schwamborn, 2018; Zhang *et al.*, 2019). Recently, 3D brain organoid models have been developed, which consist of multiple cell types that self-organize spatially, displaying enhanced cellular maturation and functionality (Kelava *et al.*, 2016; Marotta *et al.*, 2020). Human midbrain-like organoids (hMLOs) are of particular interest for PD modeling studies. The first hMLOs were generated from iPSCs,

containing mature mDA neurons that readily produce neuromelanin granules (Jo *et al.*, 2016; Marton *et al.*, 2016). Subsequently, hMLOs were generated from more fate-restricted neural stem cells, and were shown to contain spatially patterned groups of dopaminergic neurons, displaying synaptic connections, electrophysiological activity and neurite myelination (Monzel *et al.*, 2017). Importantly, this culture system was recently used to create hMLOs PD patients carrying the *LRRK2*-G2019S mutation that exhibit disease-relevant phenotypes, including reduced number and complexity of midbrain dopaminergic neurons and an increased number of FOXA2-positive progenitor cells (Smits *et al.*, 2019).

In summary, the discovery of iPSCs has offered an unprecedented avenue for studying human physiology and disease at the cellular level. The aforementioned limitations may depict the infancy of this powerful technology, yet they provide unique research opportunities to move towards more consistent and relevant PD models.

2.2. *In vivo*

Regardless of patient-derived cells' great potential in disease modeling, they are still unable to fully recapitulate *in vivo* physiology. Therefore, animal models have been widely used to replicate PD at the pathological and behavioral level. The ideal PD animal model should exhibit 1) *construct validity*, showing similar alterations in cellular and molecular mechanisms underlying PD pathogenesis; 2) *face validity*, displaying similar symptomatology at the motor and nonmotor level, as well as similar pathological and biochemical alterations, in an age-dependent and progressive manner; and 3) *predictive validity*, providing the possibility to identify agents that are clinically effective (Duty *et al.*, 2011; Jiang *et al.*, 2018; Titova *et al.*, 2017; Vingill *et al.*, 2018). Even though none of the existing models entirely meet these criteria, there are a myriad of animal models, from nonmammalian organisms to non-human primates, exhibiting individual or multiple disease features that can be selected according to each research purpose.

Nonmammalian model organisms, such as the nematode *Caenorhabditis elegans*, the fruit fly *Drosophila melanogaster*, and the zebrafish *Danio rerio ,* offer numerous advantages, including reduced experimental cost, small size, rapid reproductive cycle, easily generated genetic manipulations and well-defined neuropathology and behavior (Cooper *et al.*, 2018; Konnova *et al.*, 2018; Trigo-Damas *et al.*, 2018). Despite their limited face validity, due to the nature of the 'symptoms' displayed by these species, they provide ideal platforms for high-throughput screenings and may contribute for the development of new disease-modifying strategies (Duty *et al.*, 2011; Konnova *et al.*, 2018).

On the other hand, non-human primates mimic key neuroanatomical, neurophysiological, immunological, and genetic features of humans, thereby providing a valuable model for studying PD pathology and therapy (Grow *et al.*, 2016). Nevertheless, their size, lifespan, associated care and cost, as well as ethical considerations, limit the use of these animals for preclinical evaluation of therapies (Konnova *et al.*, 2018). Indeed, only 10% of the total of publications on PD animal studies are performed in non-human primates, usually based on MPTP or viral vector-mediated PD pathology (Duty *et al.*, 2011; Konnova *et al.*, 2018).

The majority of animal studies of PD are performed in rodents, particularly in rats (48%) and mice (35%), using diverse toxin or genetic -based strategies (Jiang *et al.*, 2018; Konnova *et al.*, 2018). These species are extensively studied due to their suitability to be used in laboratory conditions, relative rapid breeding cycle, mammalian genome and existence of well-established experimental protocols for drug administration, generation of transgenic strains and behavioral assessment (Konnova *et al.*, 2018; Vingill *et al.*, 2018). Therefore, in this section, rodent PD models based on toxin and genetic approaches will be described.

2.2.1. *Toxin models*

Toxin-based approaches include the use of classical neurotoxins, namely 6-OHDA and MPTP, as well as agrochemicals, such as the pesticide rotenone, the herbicide paraquat and the fungicide maneb (table 1.3). Despite mimicking important features of PD, such as slow dopaminergic degeneration and α-synuclein aggregation, agrochemical-based models lack reproducibility and may have systemic effects leading to high mortality rates (Blandini *et al.*, 2012; Blesa *et al.*, 2014; Konnova *et al.*, 2018). On the other hand, classical toxin-based models selectively affect the dopaminergic nigrostriatal pathway, thereby being widely used as pre-clinical PD models (Konnova *et al.*, 2018). Of these, the 6-OHDA rat model presents a more robust behavioral phenotype, whereas MPTP mouse model offers the advantage of being easier to construct (Duty *et al.*, 2011). Recent studies have also attempted to model PD pathogenesis via inflammation, showing a progressive nigrostriatal degeneration and behavioral impairment after LPS intrastriatal injection (Hunter *et al.*, 2009; Hunter *et al.*, 2007).

Table 1.3 – Properties of toxin-based PD models. 6-OHDA - 6-hydroxydopamine; MPTP - 1-methyl-4-phenyl-1,2,3,6-tetrahydropyridine; SNc – Substantia nigra pars compacta; STR – Striatum.

Toxin	Mechanism of action	Model	α-syn aggregation	SNc cell loss	Striatal abnormalities	Behavioral deficits	Limitations
6-OHDA	ROS production Mitochondrial dysfunction	Complete	No	Yes	Yes	Yes	High mortality in bilateral model
		Partial (SNc)	No	Yes	Yes	Yes	
		Partial (STR)	No	Yes	Yes	Not consistent	
MPTP	Mitochondrial dysfunction	Acute	No	Yes	Yes	Yes	Rats are resistant
		Chronic	Not consistent	Yes	Yes	Not consistent	High variability
Rotenone	Mitochondrial dysfunction		Yes	Yes	Yes	Yes	Systemic effects
Paraquat and Maneb	Oxidative stress		Yes	Yes	Yes	Yes	High variability

6-ODHA model

6-OHDA, a hydroxylated analogue of dopamine, was the first toxin demonstrated to induce nigrostriatal dopaminergic degeneration (Ungerstedt, 1968). Because 6-OHDA does not cross the blood-brain barrier (BBB), intra-cranial injection is required to deliver the toxin to the nigrostriatal tract (Blandini *et al.*, 2012; Duty *et al.*, 2011). Unilateral lesions are typically preferred, due to the high-risk mortality resulting from bilateral 6-OHDA injections, as a consequence of severe and long-lasting adipsia and aphagia (Björklund *et al.*, 2019; Pienaar *et al.*, 2012). After injection, 6-OHDA is taken up by dopaminergic neurons via the dopamine transporter (DAT), being thereafter autoxidized, which contributes for ROS formation, antioxidant enzyme levels reduction, iron accumulation and complex I of the mitochondrial respiratory chain inhibition, further increasing oxidative stress (Blandini *et al.*, 2012; Duty *et al.*, 2011; Konnova *et al.*, 2018). Therefore, the level of construct validity of this model is high, as it mimics many cellular and molecular alterations underlying PD pathogenesis (Duty *et al.*, 2011).

Regarding pathological features, the 6-OHDA model fails to replicate Lewy pathology, but provides robust degeneration of the nigrostriatal tract, which is dosage and injection-site dependent (Duty *et al.*, 2011). Injection of high amounts of 6-OHDA in the SNc or in the medial forebrain bundle (MFB), a compacted area containing the ascending nigrostriatal fiber pathway, causes massive and acute anterograde degeneration of the nigrostriatal pathway (Blandini *et al.*, 2012; Heuer *et al.*, 2012). SNc cell loss begins

12h after injection, whereas striatal dopamine depletion takes place 2-3 days post injection (Blesa *et al.*, 2014; Duty *et al.*, 2011). Partial lesion models can be achieved by decreasing the dosage of 6-OHDA delivered into SNc, which induces a 70% cell loss and dopamine depletion within 2 weeks (Visanji *et al.*, 2006). Intrastriatal 6-OHDA administration has also been described as an alternative approach to mimic a progressive retrograde degeneration, leading to 50-70% SNc cell loss over 4-6 weeks (Kirik *et al.*, 1998; Sauer *et al.*, 1994). Despite the severity of complete 6-OHDA model, most likely reflecting an end-stage of the disease, it provides robust behavioral phenotypes that can be used to monitor the efficacy of novel therapeutic strategies (Duty *et al.*, 2011). On the other hand, partial lesion models attempt to mimic an earlier PD stage, yet the behavioral readouts are less consistent and spontaneous recovery, due to sprouting of dopaminergic fibers, can occur around 4 months post-lesion (Stanic *et al.*, 2003).

MPTP model

MPTP is another commonly used toxin to model PD, after being described to induce parkinsonism in humans (Langston *et al.*, 1983). MPTP is a lipophilic protoxin that rapidly crosses the BBB after systemic administration, being subsequently converted into $MPDP^+$ by monoamine oxidase B (MAO-B) in astrocytes (Kin *et al.*, 2019). Subsequently, $MPDP^+$ oxidizes to MPP^+, a toxic metabolite that is transported into dopaminergic neurons by DAT (Dauer *et al.*, 2003; Schober, 2004). Cytoplasmatic MPP^+ triggers the production of ROS, while its accumulation inside the mitochondria leads to complex I inhibition, further contributing for oxidative stress and subsequent cell death (Nicklas *et al.*, 1987). Similarly to 6-OHDA, MPTP model presents a high degree of construct validity, displaying oxidative stress and mitochondrial dysfunction as common mechanisms underlying disease pathogenesis (Duty *et al.*, 2011).

Because rats are resistant to the toxic effects of MPTP, possibly due to absence of a particular isoform of MAO-B or rapid clearance of MPP^+, only specific strains of mice and non-human primates, which are sensitive to MPTP, have been used to develop a PD model (Dunnett *et al.*, 2010; Johannessen *et al.*, 1985). The time course and extent of the nigrostriatal damage is modulated by the schedule and dose of MPTP administration, allowing the generation of different MPTP mouse models that may correlate with the different stages of the human PD (Schmidt *et al.*, 2001; Schober, 2004). An acute regimen, comprising four intra-peritoneal injections of an acute dose (up to 20 mg/kg) at 2h intervals, induces a rapid dopaminergic cell death in the SNc (70%), and massive striatal dopaminergic depletion (90%) within 7 days (Jackson-Lewis *et al.*, 2007). Importantly, dopaminergic degeneration correlates with motor deficits, although functional recovery can occur few days post-acute injection (Sedelis *et al.*, 2001). Sub-acute or chronic administration regimens have also been described, which consist of one injection

per day for several consecutive or non-consecutive days, inducing a delayed nigrostriatal degeneration (Jackson-Lewis *et al.*, 2007; Schober, 2004). Chronic MPTP administration regimens have been reported to result in a progressive accumulation of α-synuclein aggregates and motor deficits; however, these findings are not consistent in literature (Blandini *et al.*, 2012; Duty *et al.*, 2011).

Overall, both 6-OHDA and MPTP approaches induce efficient dopaminergic degeneration of the nigrostriatal tract, via oxidative stress and mitochondrial dysfunction, which is thought to mediate PD pathogenesis in humans. Although they do not reliably replicate the progressive loss of dopaminergic neurons and the presence of Lewy pathology, these models have provided crucial information on PD pathology. Moreover, 6-OHDA model has remained at the forefront of preclinical drug discovery for PD, due to its high level of predictive validity for symptomatic therapeutic strategies (Duty *et al.*, 2011). Conversely, their potential as preclinical models for disease-modifying strategies might be hindered by the severity of dopaminergic degeneration induced by 6-OHDA and MPTP.

2.2.2. *Genetic models*

Genetic animal models have offered invaluable opportunities to understand PD pathogenesis, whereas their use in drug discovery has been compromised by the lack of consistent recapitulation of PD at the neuropathological and behavioral level. These models include overexpression strategies for autosomal dominant genes such as α-synuclein and LRRK2, and knockout or knockdown strategies for autosomal recessive genes, such as parkin, DJ-1, and PINK1. Besides traditional transgenic mouse models, the development of new genetic tools has allowed the establishment of viral vector-based PD models, that mediate a spatiotemporally and quantitatively controlled transgene expression (Van Der Perren *et al.*, 2015).

α-synuclein – based models

One of the major failures of toxin-based animal models is the inability to mimic α-synuclein pathology presented by PD patients. Since the discovery of PD-linked SNCA mutations, a variety of α-synuclein overexpression strategies have been developed, recapitulating the neuropathological and behavioral alterations found in PD patients to variable extents (Konnova *et al.*, 2018; Magen *et al.*, 2010).

Transgenic mouse models were the first approach used to mimic mutated and overexpressed α-synuclein, leading to distinct pathological and behavioral phenotypes. The great variability among these models arises from differences in their generation, primarily depending on the transgene used (wild-type (WT), mutant (A53T, A30P or hE46K) or C-terminally truncated α-synuclein) and on the promoter used to drive

transgene expression (table 1.4) (Koprich *et al.*, 2017; Magen *et al.*, 2010). Despite the strong construct validity of transgenic mouse models, as they are based on SNCA mutations associated to human disease, the degree of face validity is debatable. First, intracellular α-synuclein inclusions are present in most transgenic mice; however, in contrast to human disease, they are not always located in the SNc (Koprich *et al.*, 2017). Moreover, even in models presenting α-synuclein aggregates in SNc, there is no significant dopaminergic neuron loss (Koprich *et al.*, 2017; Magen *et al.*, 2010). On the other hand, some models display striatal abnormalities, such as reduced TH staining, decreased dopamine levels and increased DAT expression, which might suggest an effect of α-synuclein accumulation on early nigrostriatal dysfunction (Oaks *et al.*, 2013; Richfield *et al.*, 2002). Accordingly, most models present motor impairments, though the phenotypes are greatly variable and may also arise from non-PD-related neuronal dysfunction (Magen *et al.*, 2010).

Table 1.4 – α-synuclein transgenic mouse models. PDGFB – Human platelet-derived growth factor subunit B; Thy1 – mouse thymus cell antigen 1; Prnp – mouse prion promoter; Th – tyrosine hydroxylase.

Promoter	Transgene	α-synuclein aggregation	SNc cell loss	Striatal abnormalities	Behavioral deficits
Thy1	hWT	Yes	No	Yes	Yes
	hA53T	Yes	?	Yes	?
	hA30P	Yes	?	No	Yes
PDGFB	hWT	Yes	No	Yes	Yes
Prnp	hA53T	Yes	No	No	Yes
	hA30P	No	No	No	Yes
	hE46K	Yes	?	?	Yes
Th	hWT_{1-120}	Yes	No	Yes	Yes
	$hA53T_{1-130}$	No	Yes	Yes	Yes
	hA53T + A30P	No	Yes	Yes	Yes

To circumvent the lack of correct spatial transgene expression profile, new transgenic models, based on bacterial artificial chromosome (BAC) technology, have been used to drive α-synuclein overexpression, leading to age-dependent loss of nigrostriatal dopamine neurons and motor impairments (Janezic *et al.*, 2013). Conditional expression of α-synuclein, using tetracycline-controlled transcriptional activation, has also been reported, with the advantage of eliminating transgene effects during embryonic development

(Lin *et al.*, 2012). Transgenic mice with inducible expression of human WT or A53T α-synuclein present loss of midbrain dopaminergic neurons and progressive motor decline, thereby providing valuable genetic models to understand α-synuclein-induced neurodegeneration (Lin *et al.*, 2012; Nuber *et al.*, 2008).

Viral-vector based models are an alternative approach to directly induce α-synuclein overexpression in the SNc, with high transgene expression levels in multiple species, without requiring the extensive crossbreeding associated to transgenic mice (Van Der Perren *et al.*, 2015; Volpicelli-Daley *et al.*, 2016b). Moreover, in contrast to α-synuclein transgenic mice, these models display progressive loss of dopaminergic neurons in the SNc, along with synuclein pathology in surviving neurons (Volpicelli-Daley *et al.*, 2016b). Recombinant adeno-associated virus (rAAV) are the gold standard gene delivery system, due to their efficiency and safety (Van Der Perren *et al.*, 2015). Since the initial report on rAAV-mediated α-synuclein expression (Kirik *et al.*, 2002), several modifications of this gene delivery system have been explored to decrease the outcome variability, latency for degeneration and lack of overt behavioral impairments (Koprich *et al.*, 2017). Therefore, a third generation of α-synuclein viral-vector models, with an optimized promoter, rAAV serotype, vector construct and preparation, has been developed, yielding significant (>80%) cell loss in SNc (Van Der Perren *et al.*, 2015). These systems are able to induce profound motor deficits in both mice and rats, either using WT or mutant α-synuclein as transgene (Decressac *et al.*, 2012b; Oliveras-Salvá *et al.*, 2013). Nonetheless, one of the major limitations of this model is the restricted degeneration on the site of focal delivery, *i.e.* the nigrostriatal pathway, which may explain the absence of nonmotor symptoms (Campos *et al.*, 2013; Koprich *et al.*, 2017).

α-synuclein transmission models have been recently put forward as attractive approaches to model PD progression based on Braak staging scheme of Lewy pathology (Braak *et al.*, 2003). Pre-formed α-synuclein fibrils (PFFs) injection into mice SNc and striatum lead to the cell-to-cell transmission of pathologic α-synuclein, Lewy pathology development, along with a progressive loss of dopaminergic neurons in the SNc and reduced striatal dopamine levels (Luk *et al.*, 2012; Masuda-Suzukake *et al.*, 2013). Importantly, these alterations are translated into motor dysfunction with intrastriatal PFF delivery (Luk *et al.*, 2012), but not after injection in the SNc (Masuda-Suzukake *et al.*, 2013). Subsequent studies evidenced similar phenotypes after injection of PFF into rat striatum, either alone (Paumier *et al.*, 2015), or in combination with viral vector-mediated overexpression of SNCA (Thakur *et al.*, 2017). The later approach is particularly relevant, as it induces moderate degeneration in a short time span, thereby producing an attractive experimental model for disease-modifying strategies (Thakur *et al.*, 2017). Still,

the construct validity of PD models based on α-synuclein spread is dependent on the validity of prion-like spreading on PD pathogenesis (Koprich *et al.*, 2017).

LRRK2 - based models

Shortly after the identification of LRRK2 mutations linked to autosomal dominant PD, a number of animal models were generated, mainly expressing the two most frequent mutations, G2019S and R1441C/G.

Transgenic models based on LRRK2 mutations have not been successful in mimicking PD hallmarks. LRRK2 R1441G BAC transgenic mice recapitulate age-dependent and slowness of movement associated with decreased striatal dopamine release; yet, they lack clear dopaminergic neurodegeneration and formation of α-synuclein inclusions (Li *et al.*, 2009). In another study, conditional transgenic mice selectively expressing human R1441C LRRK2 in dopaminergic neurons were shown to exhibit normal motor activity, without SNc degeneration or striatal dopamine deficits in mice up to 2 years of age (Tsika *et al.*, 2014). In contrast, transgenic mice expressing G2019S mutant LRRK2 present age-dependent degeneration of dopaminergic neurons from the nigrostriatal pathway, possibly mediated by MKK4-JNK-c-Jun pathway activation (Chen *et al.*, 2012; Ramonet *et al.*, 2011). Nevertheless, both transgenic G2019S mice and inducible transgenic rats expressing human LRRK2 with G2019S substitution, failed to demonstrate deficits in locomotor activity (Ramonet *et al.*, 2011; Zhou *et al.*, 2011).

Viral-vector models are scarce, mainly due to the large size of the LRRK2 gene and the limited packaging capacity of viral vectors (Van Der Perren *et al.*, 2015). Initial studies from Lee and colleagues (Lee *et al.*, 2010), reported 50% neuronal loss in SNc associated with reduced striatal dopaminergic fibers density at 3 weeks post intrastriatal injection of herpes simplex virus (HSV) amplicon containing G2019S mutant LRRK2 in mice. Subsequently, progressive degeneration of nigral dopaminergic neurons was also verified, after intrastriatal delivery of adenoviral vectors carrying mutant G2019S human LRRK2 in rats (Dusonchet *et al.*, 2011). Age-dependent neurodegeneration, preferentially guided by glial adenoviral-mediated transduction of LRRK2 G2019S, was also recently demonstrated; yet, with no consistent behavioral alterations (Kritzinger *et al.*, 2018).

Parkin, PINK1 and DJ-1-based models

A number of animal models based on knockout or knockdown of the autosomal recessive genes parkin, PINK1 and DJ-1, have been generated over the past decade. Although they fail to display pronounced dopaminergic cell loss or motor deficits, they have allowed the identification of possible mechanisms underlying genetic-linked neurodegeneration.

Parkin knockout models are typically generated by deletion of exon 3, exon 7, or exon 2 in the parkin gene (Blesa *et al.*, 2014). Deletion of exon 3 of the parkin gene, which is the most common mutation in patients with autosomal recessive early-onset parkinsonism, results in mitochondrial dysfunction, oxidative damage, decreased dopamine release and impairment of certain aspects of motor activity and memory, with no evidence for a reduction of nigrostriatal dopamine neurons in the parkin mutant mice (Goldberg *et al.*, 2003; Itier *et al.*, 2003; Kitada *et al.*, 2009; Palacino *et al.*, 2004). Moreover, deletion of parkin exon 7 was shown to induce loss of catecholaminergic neurons in the LC, along with loss of norepinephrine in the olfactory bulb and the spinal cord, whereas the nigrostriatal system was unaffected (Von Coelln *et al.*, 2004).

Conversely to the reports on the role of parkin loss-of-function in PD pathogenesis, recent studies have explored the role of heterozygous parkin mutations, which have been put forward as a risk factor for PD (Klein *et al.*, 2007). For instance, a BAC transgenic mice expressing a truncated mutant parkin were shown to display age-dependent hypokinetic motor deficits associated with significant dopaminergic neuronal degeneration and progressive α-synuclein accumulation (Lu *et al.*, 2009). A gain of toxic function has also been demonstrated after rAAV2/8-mediated overexpression of WT and T240R mutant parkin in the rat SNc. Both transgenes induced progressive and dose-dependent dopaminergic cell death in rats, starting from 8 weeks after injection and were linked to modest motor impairment (Van Rompuy *et al.*, 2014).

Similarly to models of parkin loss-of-function, PINK1 knockout rodent models do not exhibit detectable neuronal loss, although mitochondrial dysfunction, enhanced oxidative stress and striatal dopamine depletion accompanied by age-dependent spontaneous locomotion impairment, have been reported (Gautier *et al.*, 2008; Gispert *et al.*, 2009; Ren *et al.*, 2019; Zhi *et al.*, 2019). Similar outcomes have been reported for DJ-1-deficient mice, which display altered dopaminergic neurotransmission and hypokinesia, yet, normal numbers of dopaminergic neurons in the SNc (Goldberg *et al.*, 2005). Nonetheless, this animal model presents decreased number of dopaminergic neurons in the VTA, along with motivational and cognitive impairments (Pham *et al.*, 2010). In another subset of DJ-1 nullzygous mice, fully backcrossed to a C57BL/6J background, early-onset unilateral cell loss is present in the SNc, progressing to an age-dependent bilateral degeneration of the nigrostriatal pathway and LC associated to mild motor behavior impairment (Rousseaux *et al.*, 2012). Importantly, both PINK1 and DJ-1 knockout models present hypersensitivity to dopaminergic insults, such as MPTP and α-synuclein accumulation,

thereby providing combined models of disease-associated pathways that enhance PD hallmarks (Haque *et al.*, 2012; Kim *et al.*, 2005; Oliveras-Salvá *et al.*, 2014).

Table 1.5 – Summary of outcomes of genetic-based models. WT – wild type; PFF – preformed fibrils; *not consistent, depends on promoter and transgene expressed.

Gene	Approach	Genotype	α-syn aggregation	SNc cell loss	Striatal abnormalities	Behavioral deficits
SNCA	Transgenic	WT, A53T, truncated	Yes*	No*	Yes*	Yes
	Viral vector	WT	Yes	Yes	Yes	Yes
	Spread	*PFF*	Yes	Yes	Yes	Yes
LRRK2	Transgenic	R1441C	No	No	Yes	Yes
		G2019S	No	Yes	No	No
	Viral vector	G2019S	No	Yes	?	No
Parkin	Knockout		No	No	Yes	Yes
	Transgenic	Truncated	Yes	Yes	Yes	Yes
	Viral vector	WT, T240R	?	Yes	Yes	Yes
PINK1	Knockout		No	No	Yes	Yes
DJ-1	Knockout		No	No	Yes	Yes

In summary, despite major efforts in the field, none of these models fully reproduces human condition. Toxin-based approaches, particularly 6-OHDA provide robust and reproducible nigrostriatal degeneration that strongly correlate with behavioral deficits, but do not replicate age-dependent disease progression and α-synuclein pathology (table 1.3). On the other hand, most of α-synuclein-based models recapitulate Lewy pathology, but often fail to consistently present a significant loss of dopaminergic neurons and consequently, the reliability and utility of motor phenotypes as outcome measures are limited (table 1.4 and 1.5). Finally, other genetic-based approaches (LRRK2, parkin, PINK1 and DJ-1 PD-linked mutations) display age-dependent altered cellular functions associated to PD, but are insufficient to induce marked nigrostriatal degeneration (table 1.5).

It is unlikely that a single model can provide a phenocopy of PD, not only due to disease heterogeneity, but also because its etiology its not completely understood. Therefore, there is a reciprocal demand for

using these disease models to study PD pathogenesis and, at the same time, refining them to provide better preclinical models for disease-modifying strategies. For instance, improving the characterization of viral vector and PFF-based α-synuclein models may, not only increase our understanding of the impact α-synuclein pathology on disease progression, but also provide robust preclinical models for therapeutic strategies interfering with its accumulation and spreading (Koprich *et al.*, 2017). Moreover, combination of genetic animal models and toxin may better recapitulate the proposed "multiple hit" hypothesis associated to neurodegeneration in PD (Sulzer, 2007).

2.2.3. *Behavioral readouts*

Another challenging task in the development of *in vivo* PD animal models is the selection of behavioral readouts that provide reliable and quantifiable measures of functional impairment and recovery (Chesselet *et al.*, 2011; Pienaar *et al.*, 2012). PD behavior analysis has been mainly centered on motor performance, as a consequence of the widely used classical PD models leading to dopaminergic depletion in the nigrostriatal pathway. Indeed, besides being easier to observe and measure, motor symptoms display face validity of cardinal symptoms present in PD patients (Dunnett *et al.*, 2010). Nonetheless, nonmotor symptoms have been increasingly recognized as part of PD clinical picture and thus, in recent years, nonmotor behavior has been considered in many animal studies (Magnard *et al.*, 2016).

Motor behavior

Several tests have been established for assessing different features of motor performance (table 1.6). Of note, a number of tests were designed for the evaluation of asymmetric motor behavior displayed by unilateral 6-OHDA or α-synuclein induced nigrostriatal degeneration models. Indeed, these lesions lead to quantifiable deficits in the contralateral limb that can be compared with the ipsilateral limb, thereby providing an internal control of motor performance (Decressac *et al.*, 2012a; Konnova *et al.*, 2018).

Table 1.6 – Motor behavioral tests used in rodent PD models.

Type	Test	Description	Ref
Drug-induced rotation	Apomorphine	Contralateral rotations	(Ungerstedt *et al.*, 1970)
	Amphetamine	Ipsilateral rotations	
Sensorimotor asymmetry	Cylinder test	Independent forelimb use in weight shifting during vertical exploration	(Schallert *et al.*, 2000a)
	Stepping test	Adjusting steps during a passive, lateral translocation of the body	(Olsson *et al.*, 1995)
	Corridor task	Assessment of lateralized food retrieval	(Dowd *et al.*, 2005)
Skilled forelimb use	Staircase test	Independent limb use for reaching and grasping food pellets	(Montoya *et al.*, 1991)
Motor coordination and balance	Rotarod test	General locomotor coordination	(Rozas *et al.*, 1997)
	Beam walking	Ability to keep balance while traversing a narrow beam	(Perry *et al.*, 1995)
	Gait analysis	Gait pattern and stride length using non-automated (footprint) or automated video analysis (DigiGait, CatWalk)	(Brooks *et al.*, 2009)

For instance, spontaneous rotation towards the lesioned side has been described in unilaterally lesioned animals (Francardo *et al.*, 2011; Ungerstedt *et al.*, 1970). Nevertheless, **drug-induced rotational behavior** is most frequently assessed, as it can predict the extent of nigrostriatal degeneration and correlates with motor impairment induced by the lesion (Ungerstedt *et al.*, 1970). Systemic administration of apomorphine leads to a contralateral rotation behavior, *i.e.* in the opposite to the lesion side, when approximately 90% of the dopaminergic neurons have been lost (Björklund *et al.*, 2019). As a dopamine receptor agonist, apomorphine acts post-synaptically, inducing an hyperstimulation of the supersensitive dopamine receptors in the lesioned striatum (Hudson *et al.*, 1993). On the other hand, amphetamine acts pre-synaptically, stimulating dopamine release in the intact striatum and thus, results in a rotational behavior in the ipsilateral direction to the lesion, with as little as 50% cell loss (Björklund *et al.*, 2019; Duty *et al.*, 2011). Therefore, amphetamine-induced rotation may be a useful test to discriminate partially lesioned animals, such as intra-striatal 6-OHDA administration in both rats and mice (Boix *et al.*, 2015; Lee *et al.*, 1996).

Besides drug-induced rotational behavior, **sensorimotor asymmetry** toward the ipsilateral side is also evident in other tests commonly used in unilateral PD models:

1) The cylinder test takes advantage of rats' innate drive to explore, as it evaluates independent forelimb use during vertical exploration and landing after a rearing movement (Schallert *et al.*, 2000b). In rats, complete unilateral lesions induced by 6-OHDA infusion in the MFB lead to approximately 10% of contralateral paw use during supporting wall contacts, whereas partial lesion models, induced by intrastriatal 6-OHDA administration or intranigral AAV-mediated overexpression of α-synuclein, lead to approximately 30% of contralateral paw use (Decressac *et al.*, 2012a). Although initially developed for rats, the cylinder test has also been employed in mice (Boix *et al.*, 2015; Grealish *et al.*, 2010). Nevertheless, it was useful to characterize complete lesions in the MFB (Boix *et al.*, 2015), but not intranigral 6-OHDA lesions (Grealish *et al.*, 2010).

2) The stepping test is another measure of asymmetry, which assesses rats' ability to use their impaired forelimb to adjust its steps to maintain the center of gravity in response to experimenter imposed lateral movements (Olsson *et al.*, 1995). Rats with unilateral lesions display dramatic deficits in this test, essentially making very few or no adjusting steps with the contralateral forelimb and dragging it across the table (Cenci *et al.*, 2005; Decressac *et al.*, 2012a). Adaptation and validation of stepping test in mice has also been established, being able to discriminate partial lesion groups from sham and total lesion groups in an 6-OHDA-induced MFB lesion (Boix *et al.*, 2015), as well as forelimb akinesia in a bilateral MPTP-based mouse model (Blume *et al.*, 2009), but not in intranigral 6-OHDA lesioned mice (Grealish *et al.*, 2010; Heuer *et al.*, 2012).

3) The corridor task was more recently established to assess lateralized neglect, which consists in a failure to respond to a stimuli applied in the contralateral side of animals with unilateral lesions (Dowd *et al.*, 2005). In this task, the stimulus consists of food (sugar pellets) contained in plastic lids placed along left and right sides of a long narrow corridor at regular intervals (Dowd *et al.*, 2005). Both complete and partially lesioned animals present a pronounced ipsilateral retrieval bias that correlates with the level of nigrostriatal degeneration induced by 6-OHDA lesion, but not by AAV-mediated overexpression of α-synuclein (Decressac *et al.*, 2012a; Grealish *et al.*, 2010).

In addition to these spontaneous and reflexive behaviors, fine motor control during **skilled forelimb use** in a goal-directed movement is also profoundly impaired in nigrostriatal lesions. This behavior is commonly assessed using the staircase test, originally introduced by Montoya and colleagues (Montoya *et al.*, 1991). The staircase test, also called "paw-reaching test" evaluates rats' ability to reach, grasp and retrieve food pellets from the steps of a staircase, providing quantifiable measures of motor performance, such as successful reaches (pellets eaten), overall attempts (pellets eaten plus pellets dropped) and

success rate, given by the ratio between both (Dunnett *et al.*, 2010; Winkler *et al.*, 2000). Motor performance in the contralateral paw correlates with the degree of dopamine depletion in rats (Cenci *et al.*, 2005), but not in mice (Heuer *et al.*, 2012). Moreover, the performance of this test is very sensitive to the effects of interventions that induce a precise anatomical restoration of striatal dopaminergic fibers in rats (Cenci *et al.*, 2005).

Finally, **motor coordination and balance** are also commonly evaluated in PD animal models, bearing either unilateral or bilateral lesions, using numerous tests.

1) Rotarod is widely used to assess motor function in both rats and mice (Brooks *et al.*, 2009). The test apparatus consists of a rotating rod, in which the animal is placed and has to maintain its balance. As soon as the animal falls and touches the floor of the apparatus, the latency is automatically recorded (Rozas *et al.*, 1997). An accelerating speed is commonly used to provide quicker and more efficient recordings, although it can lead to a misinterpretations between motor coordination and fatigue (Brooks *et al.*, 2009). Moreover, another caveat of rotarod test is animals' willingness to perform the test, which can be compromised by any stressful situation (Cenci *et al.*, 2005). Notwithstanding, this test is sensitive to unilateral and bilateral nigrostriatal lesions, as evidenced by the decreased latency to fall in comparison with non-lesioned animals (Campos *et al.*, 2013; Rozas *et al.*, 1997).

2) Balance beam is used in mice and rats to assess their ability to maintain balance while moving onto a series of elevated narrow beams to reach a safe platform (Brooks *et al.*, 2009). Therefore, this test provides a measure of motor coordination of the hindlimbs and forelimbs and has been shown to be sensitive to unilateral 6-OHDA lesions in both rats and mice (Allbutt *et al.*, 2007; Heuer *et al.*, 2012).

3) Gait analysis provides a more detailed analysis of motor coordination during normal walking. Footprint analysis, by the use of dyes of different colors to paint fore and hind paws, offer a simple and effective way to characterize animals' gait during normal walking (Brooks *et al.*, 2009). Automated video analysis is also possible, using home-made walking track systems (Hsieh *et al.*, 2011; Lee *et al.*, 2012) or commercially available systems, such as CatWalk™ XT system (Boix *et al.*, 2018). These methodologies have allowed the identification of significant alterations of gait dynamics on hemi-parkinsonian rats, including decreased walking speed and step/stride length, as well as increased base of support (Boix *et al.*, 2018; Hsieh *et al.*, 2011; Klein *et al.*, 2009; Lee *et al.*, 2012). Regarding PD mouse models, no differences were found in unilateral 6-OHDA-induced lesions (Glajch *et al.*, 2012; Heuer *et al.*, 2012), whereas data on MPTP-induced effects are not consensual (Guillot *et al.*, 2008; Hampton *et al.*, 2010).

The existence and validation of these motor behavioral tests in PD animal models not only provide an opportunity to understand the functional impairment induced by toxin- or genetic- mediated nigrostriatal degeneration, but also allow the assessment of functional recovery in preclinical screening of symptomatic or potential disease-modifying therapeutic strategies. Of note, behavioral tests yielding wider dynamic ranges, *i.e.* range of outcome variable between two endpoints, such as staircase and rotarod, are more appropriate to compare different degrees of motor improvement. On the other hand, tests of spontaneous asymmetric behavior, such as the cylinder test, present a strong correlation with the level of nigrostriatal degeneration, but a rather narrow dynamic range (Cenci *et al.*, 2005).

Nonmotor behavior

Whereas motor behavior has been extensively quantified in PD rodent models, the evaluation of nonmotor symptoms has been hitherto generally neglected. In fact, the assessment of nonmotor phenotypes such as neuropsychiatric symptoms is challenging, not only because their anatomical correlates are not completely understood, but also due to the possible bias introduced by motor impairment during the execution of nonmotor behavioral tests (Dunnett *et al.*, 2010). Furthermore, although hemi-parkinsonian models are convenient to characterize and quantify motor deficits, their suitability to provide measurable nonmotor outcomes is arguable (Magnard *et al.*, 2016).

Depression is one of the nonmotor phenotypes most frequently explored in PD rodent models. This complex psychiatric disorder has been demonstrated to be characterized not only by mood deficits, such as anhedonia and learned helplessness, but has also been associated to anxiety and impaired cognition (Bessa *et al.*, 2009). Indeed, these three behavioral dimensions – mood, anxiety and cognition - have been assessed in different PD rodent models, employing the behavioral paradigms established in models of depression and anxiety.

Anhedonia is one of the core symptoms of depression, characterized by a relative lack of pleasure in response to a formerly rewarding stimulus (Hoffman, 2016; Mateus-Pinheiro *et al.*, 2014). This behavioral dimension has been tested in both rat and mouse models of PD using the gold standard method, sucrose consumption test to evaluate the preference for a sweetened solution in relation to water (Hoffman, 2016). Depressed animals are expected to display a decreased preference for the rewarding sweetened solution (Papp *et al.*, 1991). The reported outcomes in PD rodent models are not consistent and do not seem to arise simply from differences in the type of lesion applied (Magnard *et al.*, 2016). Indeed, bilateral intranigral 6-OHDA administration in rats, was shown to lead to a reduction of sucrose consumption at 7 and 21 days after lesion (Santiago *et al.*, 2014), but not after 10 days (Campos *et al.*, 2013). The same

distinct outcome has been reported in bilateral intrastriatal 6-OHDA administration (Branchi *et al.*, 2008; Chen *et al.*, 2014) and unilateral MFB lesions (Carvalho *et al.*, 2013; Delaville *et al.*, 2012). Recently, decreased sucrose preference was reported to occur 8 weeks after bilateral nigral injection of AAV-α-synuclein, opening new avenues for exploring the involvement of genetic and viral approaches in the etiology of neuropsychiatric symptoms in PD (Caudal *et al.*, 2015).

Learned helplessness is another core symptom of depression, commonly expressed in rodents by an increase in time of immobility and a decrease in latency to immobility in the forced-swim test, in which animals are placed in cylinders filled with water (Bessa *et al.*, 2009). Less conflicting results are found in this behavior, as the majority of the bilateral partial and few unilateral lesions were shown to lead to increased immobility time (Branchi *et al.*, 2008; Santiago *et al.*, 2014; Tadaiesky *et al.*, 2008). Importantly, this outcome does not seem to be influenced by the presence of motor impairments, as most of the models presenting strong motor deficits do not display alterations in this test (Magnard *et al.*, 2016).

Anxiety-like behavior can be assessed using 1) the elevated plus maze test, which employs a maze elevated above the floor level, consisting of two opposing open arms and two opposing closed arms with side and end walls, to evaluate the animal's state of anxiety expressed by a reduced number of open arm entries and time spent on the open arms; 2) light/dark box test based on the innate aversion of rodents to brightly illuminated areas and expressed by a decrease in the number of visits and time spent in the large illuminated compartment of the test apparatus; and 3) novelty suppressed feeding test, which measures the consumption of a familiar food in a novel environment, wherein anxiety-like behavior is expressed by an increased latency to feed in the open-field arena (Sousa *et al.*, 2006). Most bilateral toxin-induced lesion models report anxiety-like behavior both in mice (Bonito-Oliva *et al.*, 2014) and rats (Campos *et al.*, 2013; Chen *et al.*, 2014; Drui *et al.*, 2014; Tadaiesky *et al.*, 2008), whereas no consistency was found among unilateral MFB lesions (Magnard *et al.*, 2016). Conversely to bilateral toxin-induced models, bilateral nigral injection of AAV-α-synuclein do not lead to increased anxiety-like behavior in the elevated plus maze test (Caudal *et al.*, 2015).

Cognitive impairments have also been considered in few PD animal models. Hippocampal-dependent learning is usually assessed with the Morris water maze task, in which animals learn to navigate to a platform placed in a pool filed with water (Sousa *et al.*, 2006). Overall, the few studies addressing this behavioral feature, do not evidence significant differences between sham and lesioned animals,

regardless of lesion area and severity (Branchi *et al.*, 2008; Campos *et al.*, 2013; Carvalho *et al.*, 2013; Tadaiesky *et al.*, 2008).

Besides neuropsychiatric impairments, hyposmia and sleep disturbances have also been addressed to a lesser extent in various rodent PD models, reproducing some of the alterations associated to PD (Asakawa *et al.*, 2016; Medeiros *et al.*, 2019).

Despite being overlooked in the past decades, nonmotor symptoms have been increasingly explored in PD animal models. A certain degree of recapitulation of PD nonmotor symptoms has been achieved in several PD rodent models. Nonetheless, there is a great variability among the reported outcomes for the same behavioral test, even within the same type of lesion. This is particularly evident on the sucrose consumption test and can be partially explained by differences in experimental protocols used, revealing the need to use more refined behavioral tests towards the characterization of hedonic behavior in PD rodent models. Another limitation of the assessment of nonmotor behavior is the impossibility to perform a longitudinal characterization of some behavioral deficits, such as anxiety-like behaviors, due to animals' habituation to the test (Sousa *et al.*, 2006). Overcoming these constraints is of utmost importance to better understand the circuits involved in these neuropsychiatric manifestations, as well as to design of therapeutic strategies for the full spectrum of PD symptoms.

3. Therapeutic approaches for Parkinson's disease: a focus on the potential of Mesenchymal Stem Cell secretome

The extensive description of the clinical and experimental picture of PD provided so far, reveals the complexity of this neurodegenerative disease and the inability of existing disease models to fully recapitulate PD complexity. Ultimately, these findings may explain the lack of disease-modifying therapies that slow, halt, or reverse PD progression (Athauda *et al.*, 2015). Currently available therapies are symptom-alleviating, based on pharmacotherapy substitution of striatal dopamine loss or surgical approaches, namely deep brain stimulation (DBS) that modulate or disrupt patterns of neural signaling within a targeted region of the basal ganglia (Okun, 2012; Pires *et al.*, 2017). Nevertheless, there are a number of experimental therapies currently being tested at the preclinical and clinical level, aiming at providing structural and neurochemical brain repair or modifying the disease by targeting the genetic and cellular alterations (e.g. α-synuclein aggregates) underlying PD pathogenesis (Dawson *et al.*, 2019; Poewe *et al.*, 2017). In this section, we will provide an overview of the therapeutic approaches currently being used to manage PD symptoms, as well as describe promising experimental therapies, with a focus on mesenchymal stem cells (MSCs) and their paracrine activity.

3.1. *Symptomatic therapy*

Symptomatic therapy should target not only motor function, but also autonomic, cognitive and psychiatric alterations. Pharmacological and surgical approaches are the mainstay of symptomatic therapy, whereas physiotherapy, speech therapy and dietary measures have been suggested as supportive approaches in PD treatment (Oertel *et al.*, 2016).

3.1.1. *Pharmacological targets*

The dopamine precursor amino acid L-DOPA was the firstly established, and remains the "gold standard", symptomatic treatment for PD, aiming at substituting striatal dopamine loss (Poewe *et al.*, 2017). Treatment with L-DOPA is recommended for all patients with PD (Connolly *et al.*, 2014). Nevertheless, long-term L-DOPA administration is associated with the occurrence of motor and nonmotor complications, such as fluctuations, dyskinesia and psychosis (Pires *et al.*, 2017). Non-physiological pulsatile striatal dopamine receptor stimulation, due to the short half-life of L-DOPA and the variability in its gastrointestinal absorption and blood–brain barrier transport, are thought to mediate these drug-induced complications (Kalia *et al.*, 2015; Poewe *et al.*, 2017). Multiple additional targets have therefore been developed to regulate dopaminergic transmission, both at presynaptic and postsynaptic level.

Inhibition of peripheral metabolism of L-DOPA is one of the approaches used to increase the bioavailability and half-life of L-DOPA. Both inhibitors of aromatic amino acid decarboxyalse (AADC), which catalyzes the conversion of L-DOPA to dopamine, and inhibitors of catechol-O-methyltransferase (COMT), involved the ortho-methylation of L-DOPA, are currently available for clinical use. In addition, increased synaptic availability of dopamine can be achieved through inhibition of monoamine oxidase type B (MAOB), an enzyme involved in dopamine metabolism. Modulation of postsynaptic activity is mediated by the use of dopamine agonists with activity in dopamine receptors in MSNs and a longer half-life than L-DOPA and thus are believed to induce less pulsatile striatal dopamine receptor stimulation (Connolly *et al.*, 2014; Pires *et al.*, 2017; Poewe *et al.*, 2017).

Besides dopaminergic therapy, non-dopaminergic targets have also been explored to address L-DOPA induced complications, as well as motor and nonmotor features that do not respond to dopaminergic replacement therapy. For instance, anti-cholinergic and anti-glutamatergic drugs have been approved for the treatment of PD-associated tremor and L-DOPA-induced dyskinesias, respectively (Pires *et al.*, 2017). Regarding PD depression, although it is likely to differ considerably from non-PD patients, possibly with the involvement of dopaminergic, serotonergic and noradrenergic systems, there is some evidence for

the efficacy of selective serotonin reuptake inhibitors (SSRIs), serotonin and norepinephrine reuptake inhibitor (SSNRIs), tricylic antidepressants and dopamine agonists (Seppi *et al.*, 2019). Table 1.7 summarizes the pharmacologic approaches currently being used for PD treatment.

Table 1.7 – Pharmacological treatment of motor and non-motor symptoms of Parkinson's disease. Adapted from (Connolly *et al.*, 2014; Kalia *et al.*, 2015; Poewe *et al.*, 2017)

	Indication	Mechanism of action	Examples
Motor symptoms	All motor symptoms	Dopamine precursor	Levodopa
		Aromatic amino acid decarboxyalse inhibitors	Carbidopa, Benserazide
		Catechol-O-methyltransferase inhibitors	Entacapone, Opicapone, Tolcapone
		Monoamine oxidase type B (MAOB) inhibitors	Rasagiline, Selegiline, Safinamide
		Dopamine agonists	Pramipexole, Ropinirole, Piribedil Apomorphine, Rotigotine
	Motor fluctuations and parkinsonism	Adenosine A_{2A} receptor antagonists	Istradefylline, Preladenant,Tozadenant
		Mixed activity - inhibition of sodium/calcium channels and MAOB activity	Safinamide, Zonisamide
	Tremor	Anticholinergics	Trihexyphenidyl, Benztropine
	L-DOPA-induced dyskinesia	N-methyl-d-aspartate receptor antagonists	Amantadine
	Gait disorders, falls and freezing of gait	Procholinergic therapy (cholinesterase inhibitors)	Donepezil, Rivastigmine
		Noradrenaline reuptake inhibitor	Methylphenidate
Non-motor symptoms	Dementia	Acetylcholinesterase inhibitor	Rivastigmine
	Depression	Dopamine agonist	Pramipexole
		Selective serotonin reuptake inhibitors	Citalopram, Escitalopram, Fluoxetine, Paroxetine, Sertraline
		Serotonin and norepinephrine reuptake inhibitor	Venlafaxine extended release
		Tricyclic antidepressant	Desipramine, nortriptyline
	REM sleep behavior disorder	Benzodiazepine	Clonazepam
		Hormone	Melatonin
	Constipation	Osmotic laxative	Polyethylene glycol
		Chloride channel activator	Lubiprostone

3.1.2. *Surgical interventions*

DBS is a surgical approach for PD treatment, based on the implantation of electrodes in specific targets of the basal ganglia that generate high-frequency electrical stimulation to modulate or disrupt patterns of neural signaling (Okun, 2012). Subthalamic nucleus and the internal segment of the globus pallidus are well-established as surgical targets for the treatment of motor complications (Poewe et al., 2017). Besides their effect on neuronal signaling, electrical current is also thought to have beneficial effects mediated by astrocyte release of a wave of calcium, blood flow increase and neurogenesis stimulation (Okun, 2012). Nevertheless, it is unclear how these additional effects will influence changes in PD symptoms.

Magnetic resonance-guided focused ultrasound is an emerging technology currently being used for tremor-dominant PD, which consists in non-invasive intracranial thermal ablative procedure with multiple ultrasound beams that allow for non-incisional pallidotomy or subthalotomy (Martínez-Fernández et al., 2018). Moreover, this technology is currently being investigated for drug delivery as it can be used to deliver pulsed ultrasound to microbubble-enriched cerebral vasculature, thereby leading to BBB opening (Lee et al., 2019).

3.2. *Experimental therapies*

Future therapies for PD should move from symptom-alleviating to disease-modifying approaches, also aiming at reducing the prevalence of nonmotor symptoms (Obeso *et al.*, 2010). Although successful preclinical research findings have not been translated into clinical applications, there are a number of experimental strategies currently being explored as disease-modifiers or as alternative approaches for symptom management (Poewe *et al.*, 2017). Gene therapy and cell-based regenerative medicine have been in the forefront of these innovative experimental approaches (Poewe *et al.*, 2017). Nevertheless, novel potential neuroprotective therapies are currently being tested, targeting cellular mechanisms that are known to be implicated in PD pathogenesis, such as calcium homeostasis, oxidative stress, mitochondrial dysfunction, as well as α-synuclein accumulation, aggregation and cell-to-cell transmission, as reviewed elsewhere (Athauda *et al.*, 2015; Dawson *et al.*, 2019).

3.2.1. *Gene therapy*

Gene transfer through the use of AAV vector has become intensively explored for PD treatment (Axelsen et al., 2018). Possible targets for gene therapy can be classified as non-disease modifying, which aim at modulating basal ganglia neurotransmission through the expression of dopaminergic and GABAergic enzymes; or disease modifying, which attempt to stop neurodegeneration by nigral overexpression of

growth factors with neuroprotective potential (e.g. glial cell-derived neurotrophic factor (GDNF) or neurturin) or by correction of gene deficits (Axelsen et al., 2018; Deverman et al., 2018; Pires et al., 2017). Although clinical gene therapy using AAV has been shown to be safe and to result in stable long-term in vivo gene expression, their clinical benefit has only been established for symptomatic strategies, in reducing the need for medication in advanced PD patients (Axelsen et al., 2018; Deverman et al., 2018; Pires et al., 2017).

3.2.2. *Cell-based therapy*

Cell-based therapy has long been proposed as an attractive strategy to replace degenerating dopaminergic neurons and thus, restore normal physiological pattern of striatal dopamine transmission (Barker et al., 2015; Pires et al., 2017). Pioneering clinical studies in this field were based on the transplantation of mesencephalic dopaminergic neurons precursors from allogeneic fetal tissue to the striata of PD patients (Lindvall et al., 1990; Lindvall et al., 1989; Lindvall et al., 1992). These studies provided proof of concept of tissue implantation, yet yielded variable clinical benefits. One of the reasons for this variability was the use of fetal tissue as a cell source, due to their limited availability and standardization (Parmar et al., 2020). The recent advances in stem cell biology field, including the discovery of iPSCs and the development of robust dopaminergic neuron differentiation protocols, have rebooted the promise of cell-replacement therapy in providing more robust and consistent clinical outcomes (Kriks et al., 2011; Shi et al., 2016). Despite the great potential as a therapy for PD, cell-based approaches have been targeted at replacing dopaminergic neurons from the nigrostriatal pathway, whereas extranigral degeneration is also known to contribute for motor and nonmotor symptoms. Moreover, the use of cell-replacement therapy for PD may also benefit from the use of adjunctive strategies to increase cell survival and functional connectivity (Parmar et al., 2020). Finally, another major concern of cell-based therapy is the possibility of spread of α-synuclein pathology into grafted cells, as well as the likely vulnerability of autologous grafts (derived from iPSCs) to develop the pathology (Parmar et al., 2020). A better understanding of PD pathogenesis is therefore required to develop strategies to overcome these limitations in next generation of cell-based therapies.

3.3. *MSCs secretome as a cell-replacement free therapy for PD*

An alternative cell type that has been considered for cell replacement strategies in PD, are mesenchymal stem cells (MSCs) (figure 1.7) (Barker *et al.*, 2015; Pires *et al.*, 2017). MSCs were firstly identified by Friedenstein in mouse bone marrow as clonogenic fibroblast precursor cells (Friedenstein *et al.*, 1976) and later named as *mesenchymal stem cells* by Arnold Caplan (Caplan, 1991). Although their

nomenclature and origin remains highly controversial (Caplan, 2017, 2019; Sipp *et al.*, 2018), their regenerative potential has been widely recognized (Caplan *et al.*, 2011; Fan *et al.*, 2020; Konala *et al.*, 2016)

3.3.1. *MSCs identity & sources*

MSCs are described as adult multipotent progenitors isolated from various adult tissues (Pittenger *et al.*, 1999). Bone marrow is the conventional source of MSCs, nevertheless MSCs have been successfully isolated from fetal, neonatal and adult tissues, including adipose tissue (ASCs), dental pulp, placenta, amniotic fluid, umbilical cord blood, umbilical cord Wharton's jelly (WJ-MSCs) and its perivascular region (HUCPVCs), and even the brain (Salgado *et al.*, 2015; Teixeira *et al.*, 2013).

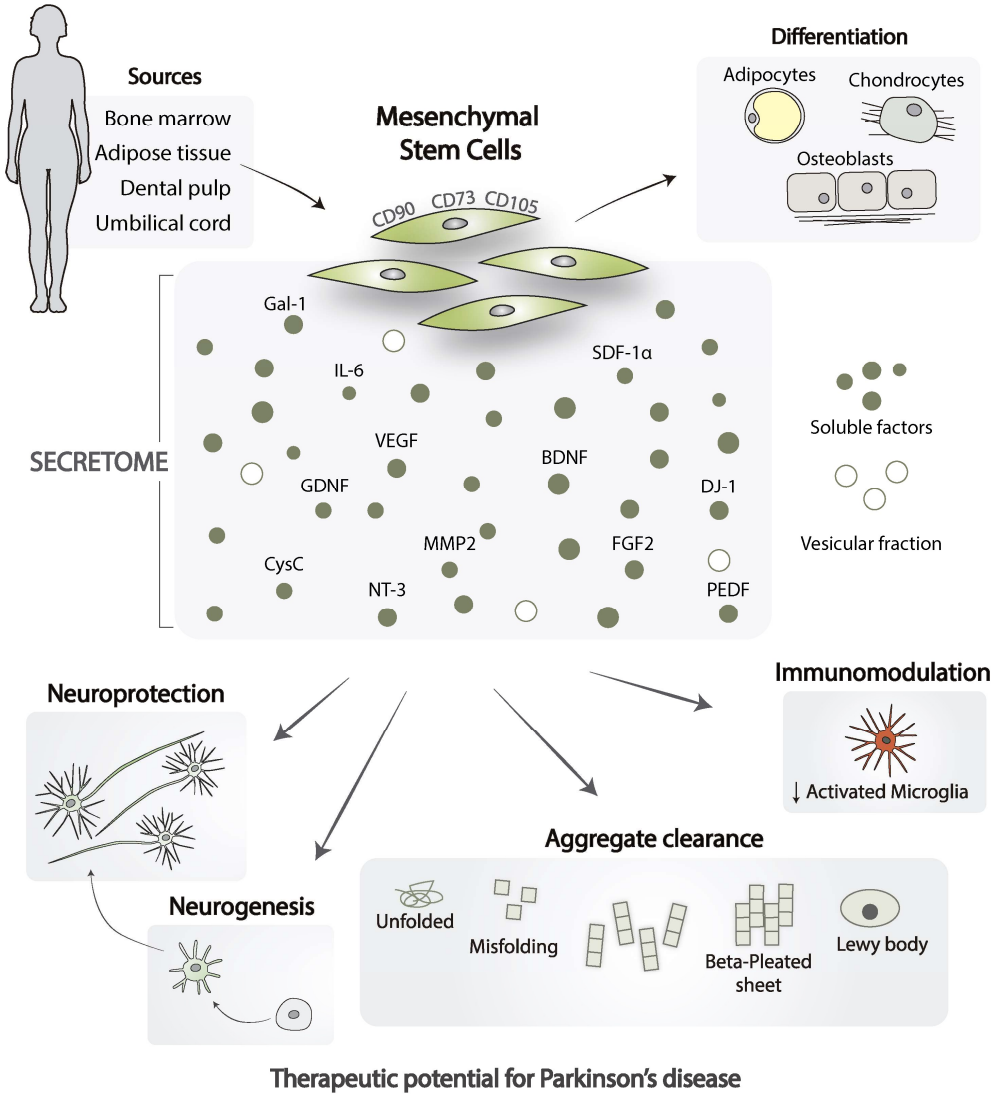

Figure 1.7 – Mesenchymal Stem Cells (MSCs) and their therapeutic potential for Parkinson's disease. Schematic representation of MSCs isolation sources, characterization and possible mechanisms underlying the effects of their secretome on Parkinson's disease.

Whereas their precise *in vivo* origin is unclear, MSCs *in vitro* identity has been established. MSCs present a spindle-shaped morphology upon tissue culture plastic adherence and are further characterized by a unique expression profile of cluster of differentiation (CD) cell surface markers and trilineage differentiation potential, as described by the minimal criteria for designating a cell as an MSC established by the International Society for Cellular Therapy (ISCT) (Dominici *et al.*, 2006). According to these criteria, besides plastic adherence in standard culture conditions, MSCs must express CD105, CD73 and CD90, and lack expression of CD45, CD34, CD14, CD19 and HLA-DR surface molecules, as well as be able to differentiate to osteoblasts, adipocytes and chondroblasts *in vitro* (Dominici et al., 2006).

In spite of the efforts to provide a uniform characterization, culture-expanded MSCs are considered a heterogeneous population of cells, influenced not only by their origin properties, such as species, tissue and donor, but also by culture conditions, including expansion media and passage number (Ankrum *et al.*, 2014; Fan *et al.*, 2020). For instance, the number of BM-MSCs and their differentiation potential is known to be dependent on donor's age; whereas the osteogenic and chondrogenic potential of BM-MSCs is superior to ASCs (Fan *et al.*, 2020).

3.3.2. *MSCs therapeutic potential*

Despite possible dissimilarities among MSCs according to their isolation source, overall, MSCs present a number of properties that have greatly contributed for their use in regenerative medicine, including the minimal invasive procedures associated to their isolation, simple culturing protocols, ability to expand for several passages, as well as low immunogenic and tumorigenic potential that make them suitable for allogeneic transplantation strategies (Ankrum *et al.*, 2014; Salgado *et al.*, 2015). Based on these properties, initial therapeutic applications of MSCs were focused on their differentiation potential in cell replacement strategies aiming to restore compromised adult mesenchymal tissues, although some authors have also reported MSCs differentiation into ectodermal lineages (Bagher *et al.*, 2016; Donega *et al.*, 2014; Takeda *et al.*, 2015).

Nonetheless, it has been increasingly accepted that the major mechanism underlying MSCs' therapeutic potential is their paracrine function, through the secretion of soluble factors and vesicles, collectively referred to as *secretome* (Caplan *et al.*, 2006; Gnecchi *et al.*, 2005; Teixeira *et al.*, 2013). Indeed, a number of soluble factors, including growth factors and cytokines with immunomodulatory, angiogenic, trophic, antiapoptotic and antioxidative effects have been identified in MSCs secretome (figure 1.7) (Pinho *et al.*, 2020). Moreover, MSCs secretome is known to contain a vesicular fraction, composed of exosomes and microvesicles packed with cell-type specific combinations of proteins, lipids, coding, and non-coding

RNAs that are major mediators of cell–cell communication (Lai *et al.*, 2010; Marote *et al.*, 2016). The identification of these secreted factors, and particularly their immunomodulatory effect has allowed the development of treatments for graft versus host disease, as well as autoimmune disorders, such as Chron's disease (Fitzsimmons *et al.*, 2018). Notwithstanding, a wide range of therapeutic applications are being exploited and modulated by 1) combining MSCs with other cell types, 2) using biomaterials as substrates for MSCs culture; as well as 3) increasing the release of paracrine factors by genetic manipulation or pre-conditioning, to generate novel therapeutic approaches (Bagno *et al.*, 2018).

3.3.3. *MSCs therapeutic effects in PD*

The therapeutic potential of MSCs has been widely reported in the context of PD (Chen *et al.*, 2020; Marques *et al.*, 2018; Teixeira *et al.*, 2013). Table 1.8 summarizes the main findings on the use of MSCs in PD animal models. Although most studies, report beneficial outcomes after MSCs local or systemic delivery, their effects are proposed to be mainly mediated by the activity of secreted factors on neurogenesis, neuroprotection, immunomodulation and aggregate clearance (Volkman *et al.*, 2017).

Neurogenesis

Neurogenesis is a neuroadaptative phenomenon that allows the generation of new neuronal cells, involving several steps, such as cell division, commitment of the new cell to a neuronal phenotype, migration and morphophysiological maturation of the neuroblasts, and finally, the establishment of appropriate synaptic contacts to fully integrate a pre-existent network (Salgado *et al.*, 2015). The subependymal zone (SEZ) of the lateral ventricles and the subgranular zone (SGZ) of the hippocampal dentate gyrus are two neurogenic brain regions described in the adult mammalian brain, wherein neural stem cells (NSCs) are maintained, proliferate and differentiate (Salgado *et al.*, 2015).

MSCs and particularly their secretome, have been shown to modulate these neurogenic niches, by increasing proliferation of NSCs, neuronal survival and differentiation in mouse and rat hippocampus (Munoz *et al.*, 2005; Teixeira *et al.*, 2015). Similar observations have been reported after transplantation of BM-MSCs and ASCs in the striatum and SNc of rat PD models in the subventricular zone, possibly explaining the reduced cell loss in the SNc (Cova *et al.*, 2010; Schwerk *et al.*, 2015a; Schwerk *et al.*, 2015b). This neurogenic effect of MSCs in PD has been proposed to be mediated by the *in vivo* MSCs secretion of brain-derived neurotrophic factor (BDNF) (Cova *et al.*, 2010), yet other factors present in MSCs secretome are known to play a role in neurogenesis, such as vascular endothelial growth factor

(VEGF), glial cell line-derived neurotrophic factor (GDNF), fibroblast growth factor 2 (FGF2), and neurotrophin-3 (NT-3) and thus, might also be involved in this response (Volkman *et al.*, 2017).

Neuroprotection

MSCs effect on neuroprotection is another mechanism that has been put forward to explain the vast number of studies reporting reduced cell loss in the nigrostriatal tract and improved motor function, following 6-OHDA-induced neuronal death in PD animal models (Choi *et al.*, 2015; Mccoy *et al.*, 2008; Mendes-Pinheiro *et al.*, 2019; Sadan *et al.*, 2009; Teixeira *et al.*, 2017; Wang *et al.*, 2010; Weiss *et al.*, 2006). Moreover, several *in vitro* studies have allowed the identification of MSCs secretome neuroprotective effect and role of some secreted factors in protection from 6-OHDA cytotoxicity (Cova *et al.*, 2012; Parga *et al.*, 2018; Wang *et al.*, 2010; Yalvaç *et al.*, 2013).

Among these factors, SDF-1α has been shown to mediate apoptotic cell death of PC12 cells with consequent increase of DA release from the cells (Wang *et al.*, 2010). Moreover, prostaglandin E2 receptors have also been identified as main mediators of the observed neuroprotective and neurorescue activities of MSCs secretome (Parga *et al.*, 2018). In our group, proteomic analysis of hBM-MSCs secretome revealed the presence of important neurotrophic factors, such as VEGF, BDNF, interleukin-6 (IL-6) and GDNF, as well as potential neuroregulatory molecules, namely DJ-1, cystatin C (Cys C), glial-derived nexin, galectin-1, and pigment epithelium-derived factor, which may mediate the behavioral recovery in 6-OHDA lesioned rats supported by an increase of DA neurons and neuronal terminals in the SNpc and striatum, respectively (Mendes-Pinheiro *et al.*, 2019; Teixeira *et al.*, 2017). Finally, exosomes isolated from dental pulp stem cells have also been demonstrated to rescue human DA neurons from 6-OHDA induced apoptosis (Jarmalaviciute *et al.*, 2015).

Despite the identification of these neuroregulatory factors in naïve MSCs, some studies have suggested the modulation of MSCs secretion profile by exposure to neurotrophic factors (Sadan *et al.*, 2009) or overexpression of a specific factor in MSCs. For instance, GDNF-transduced rat BM-MSCs were shown to induced protection and sprouting of DA terminals in the striatum of neurotoxin-induced and inflammation-induce rat PD models (Hoban *et al.*, 2015; Moloney *et al.*, 2010). On the other hand, HGF overexpression in human umbilical cord-MSCs, was also able to protect SH-SY5Y cells exposed to MPP^+, probably mediated through the regulation of intracellular Ca^{2+} by modulating the expression of CaBP-D28K, an intracellular calcium-binding protein (Liu *et al.*, 2014).

Table 1.8 – Main findings on the use of mesenchymal stem cells (MSCs) in PD animal models. hWJ-MSCs – human Wharton's Jelly derived MSCs; rBM-MSCs – rat bone marrow derived MSCs; hBM-MSCs – human bone marrow derived MSCs; rASCs – rat adipose tissue derived MSCs; hASCs – human adipose tissue derived MSCs; SNc – substantia nigra pars compacta; MFB – medial forebrain bundle; CM – conditioned medium.

Cell Source	Modification	Product	Route	Model	Histological outcome	Behavioral outcome	Mechanism	Ref.
hWJ-MSCs	No	Cells	Stereotaxic injection (Striatum)	Unilateral (MFB) 6-OHDA rat model	-	Reduced apomorphine-induced rotations	No positive staining for transplanted cells	(Weiss *et al.*, 2006)
rBM-MSCs	No	Cells	Intravenous	Unilateral (striatum) 6-OHDA rat model	Preservation of TH^+ fibers in the striatum Reduced cell loss in the SNc	Reduced forelimb akinesia in cylinder test Reduced amphetamine-induced rotations	No detection of transplanted cells SDF-1α *in vitro* studies	(Wang *et al.*, 2010)
hBM-MSCs	No	Cells	Intravenous	Unilateral (striatum) 6-OHDA rat model	Reduced cell loss in the SNc	Reduced amphetamine-induced rotations	Suppressed glial activation	(Suzuki *et al.*, 2015)
rBM-MSCs	Enriched medium	Cells	Stereotaxic injection (Striatum)	Unilateral (striatum) 6-OHDA rat model	Preservation of TH^+ fibers in the striatum Reduced cell loss in the SNc	Reduced amphetamine-induced rotations	-	(Bouchez *et al.*, 2008)
rBM-MSCs	No	Cells	Intranasal	Unilateral (MFB) 6-OHDA rat model	Preservation of TH^+ fibers in the striatum Reduced cell loss in the SNc	Improvement of forelimb akinesia in stepping test	Modulation of inflammatory response	(Danielyan *et al.*, 2011)
rASCs	No	Cells	Stereotaxic injection (SNc)	Unilateral (striatum) 6-OHDA rat model	Preservation of TH^+ fibers in the striatum Reduced cell loss in the SNc	Reduced amphetamine-induced rotations	Attenuation of microglial activation Neuroprotection	(Mccoy *et al.*, 2008)

mBM-MSCs	Neuron-like differentiation	Cells	Stereotaxic injection (Striatum)	Unilateral (striatum) 6-OHDA mouse model	-	Reduced amphetamine-induced rotations	-	(Offen *et al.*, 2007)
hMSCs	No	Cells	Stereotaxic injection (Striatum)	Unilateral (striatum) 6-OHDA rat model	Preservation of TH+ fibers in the striatum	-	Enhanced neurogenesis mediated by BDNF secretion	(Cova *et al.*, 2010)
hASCs	No	Cells	Stereotaxic injection (SNc)	Unilateral (MFB) 6-OHDA rat model	No protection from cell loss in the SNc	-	Increased subventricular neurogenesis	(Schwerk *et al.*, 2015b)
hASCs	No	Cells	Intravenously	Unilateral (SNc) 6-OHDA mouse model	Reduced cell loss in the SNc	Reduced apomorphine-induced rotations Improved motor coordination and balance on the Rotarod test and pole test	Restored mitochondrial complex I activity	(Choi *et al.*, 2015)
hASCs	No	Cells	Stereotaxic injection (SNc)	Unilateral (MFB) 6-OHDA rat model	Reduced cell loss in the SNc	Improved working memory in the radial-arm-maze test Does not improve motor function	Increased subventricular neurogenesis Increased peripheral EPO & Il-10 levels	(Schwerk *et al.*, 2015a)
hMSCs	No	Cells	Stereotaxic injection (Striatum)	Unilateral (striatum) 6-OHDA rat model	Preservation of TH+ fibers in the striatum Reduced cell loss in the SNc	Reduced apomorphine-induced rotations	-	(Blandini *et al.*, 2010)
hBM-MSCs	Exposure to neurotrophins	Cells	Stereotaxic injection (Striatum)	Unilateral (striatum) 6-OHDA rat model	Reduced dopamine depletion in the striatum	Reduced amphetamine-induced rotations	Neurotrophic effect	(Sadan *et al.*, 2009)

hBM-MSCs	Cultured in bioreactors	CM	Stereotaxic injection (Striatum & SNc)	Unilateral (MFB) 6-OHDA rat model	Preservation of TH+ fibers in the striatum Reduced cell loss in the SNc	Improved motor function in the Rotarod test and Staircase test	Neuroregulatory molecules	(Teixeira *et al.*, 2017)
hBM-MSCs	No	CM	Stereotaxic injection (Striatum & SNc)	Unilateral (MFB) 6-OHDA rat model	Preservation of TH+ fibers in the striatum Reduced cell loss in the SNc	Improved motor function in the Rotarod test and Staircase test	Neuroregulatory molecules	(Mendes-Pinheiro *et al.*, 2019)
hMSCs	No	Cells	Intravenously	MPTP mouse model	Decreased expression of α-synuclein oligomers and induction of pathogenic α-synuclein Attenuated apoptotic cell death signaling	-	Matrix metalloproteinase-2 (MMP-2) plays a role in the degradation of extracellular α-synuclein	(Oh *et al.*, 2017)
	No	CM		α-synuclein inoculation mouse model				
hMSCs	No	Cells/ CM	Intravenously	α-synuclein fibrils inoculation (striatum) mouse model	Attenuated immunoreactivity of the phosphorylated form of α-synuclein in the midbrain and dopaminergic neurons Reduced cell loss in the SNc	Improved motor coordination and balance on the Rotarod test and pole test	Inhibition of α-synuclein transmission by blocking the clathrin-mediated endocytosis of extracellular α-synuclein via modulation of the interaction with N-methyl-D-aspartate receptors Galectin-1 played a role in the transmission control of aggregated α-synuclein	(Oh *et al.*, 2016)

An additional approach for harnessing the neuroprotective potential of MSCs secretome, is their combination with cell replacement strategies to provide trophic support. Pretreatment of embryonic DA neurons with rat BM-MSCs secretome increased their survival after grafting in a 6-OHDA rat model of PD (Shintani *et al.*, 2007), whereas functional improvement has been reported after transplantation of secretome-treated NSCs into PD rats (Yao *et al.*, 2016).

Immunomodulation

MSC immunomodulatory properties have also been suggested to render them for potential use for many therapeutic applications (Ankrum *et al.*, 2014). In the context of PD animal models, modulation of inflammatory response has been proposed to play a major role in therapeutic potential for PD (Danielyan *et al.*, 2011; Kim *et al.*, 2009; Mccoy *et al.*, 2008; Suzuki *et al.*, 2015). Although both pro- and anti-inflammatory cytokines have been identified in MSCs secretome, anti-inflammatory actions, such as suppression of microglia activation have been described to account for the therapeutic effects of MSCs in PD (Kim *et al.*, 2009; Suzuki *et al.*, 2015). Although the immunomodulatory mediators of MSCs paracrine activity on peripheric immune system have been described (such as, IL-6, IL-10, prostaglandin E2 and inducible indoleamine 2,3-dioxygenase (IDO)) (Fan *et al.*, 2020), the specific mechanism underlying suppression of microglia activation on PD animal models has not been elucidated.

Aggregate clearance

Recently, with the development of PD animal models based on α-synuclein aggregation, it was also demonstrated that MSCs secretome is able to degrade extracellular α-synuclein both *in vitro* and *in vivo*, an effect partially mediated by metalloproteinase-2 (MMP-2) (Oh *et al.*, 2017), as well as to block clathrin-mediated endocytosis thereby inhibiting α-synuclein transmission (Oh *et al.*, 2016). With the advance of this type of models and with a better understanding of the involvement of α-synuclein on PD pathology, future studies may further reveal other mediators of MSCs secretome participating in this mechanism.

4. Conclusions & Future perspectives

PD is a complex and multifactorial neurodegenerative disorder affecting millions of people worldwide, significantly decreasing their quality of life, as a consequence of the increasing disability caused by disease progression. PD complexity is expressed in a myriad of clinical symptoms displayed by PD patients, at the motor and non-motor level, in distinct neuropathological findings in multiple areas of the central nervous system (CNS), and in the diversity of cellular and molecular mechanisms that have been proposed for explaining disease-associated neurodegeneration.

Despite the recognition of this complexity, most of the past and ongoing therapeutic approaches with potential disease-modifying features have been focused in the modulation of a specific pathway in a specific cell type, which may not be able to modify disease progression. For instance, overexpression of growth factors through gene therapy may provide local neurotrophic support, but may be insufficient to modulate protein aggregation. On the other hand, the role of α-synuclein aggregates in PD pathogenesis is not completely understood and thus, therapeutic approaches exclusively targeting α-synuclein may also fail to halt neuronal degeneration.

Essentially, whilst the identification of a single mechanism underlying PD etiology is not achieved, it is reasonable to anticipate that a multitargeted approach may provide a better outcome as a disease-modifying strategy. MSCs' secretome has been shown to contain a variety of growth factors, cytokines and other signaling factors involved in neuroprotection, immunomodulation, as well as aggregate clearance, which are known to in part contribute for PD pathogenesis. Moreover, loss of neurotrophic support has been reported in the basal ganglia of PD patients, wherein reduced expression levels of neurotrophic factors, such as GDNF and BDNF, are found (Siegel *et al.*, 2000). Therefore, the administration of MSCs secretome containing these molecules may address this depletion, as well as provide local neurotrophic support, when combined with cell-replacement strategies (Brundin *et al.*, 2008).

Nevertheless, despite these promising results in preclinical studies, moving MSCs secretome-based approaches to clinical applications requires future improvements, namely regarding the source of MSCs from which the secretome is collected. For instance, the isolation procedure of BM-MSCs, one of the most commonly utilized source of MSCs, consists in a bone marrow biopsy that is painful and holds a risk of infection for the donor (Fan *et al.*, 2020). Moreover, MSCs isolated from adult tissues have limited proliferative capacity in culture and their quality and number decreases with donors' age (Fitzsimmons *et al.*, 2018). As a consequence, these limitations do not allow the expansion of MSCs in sufficient number to provide large batches of secretome for PD clinical applications.

iPSCs have been recently suggested as an alternative source for acquiring a large number of MSCs and circumvent the drawbacks associated to the isolation of tissue-derived MSCs. iPSCs can be obtained by reprogramming easily accessible somatic cell sources, such as fibroblasts and peripheral blood mononuclear cells. Due to their self-renewal capacity, this embryonic-like stem cells can be extensively expanded prior to their differentiation into MSCs, thus providing a readily available and inexhaustible source for MSCs differentiation. Moreover, even after differentiation, iPSC-derived MSCs (iMSCs) display

a higher proliferative capacity and lower cell senescence in comparison to tissue-derived MSCs, thereby allowing the acquisition of a large number of cells, without ageing-associated drawbacks.

Although several studies have addressed the therapeutic potential of iMSCs (Hu *et al.*, 2015; Lian *et al.*, 2010; Zhang *et al.*, 2015), the effects of their secretome in the context of PD have not been addressed. Therefore, in view of future clinical applications, it is of utmost importance to explore the paracrine potential of iMSCs in PD to establish an alternative source to the gold standard use of BM-MSCs. Besides providing additional evidence on the role of MSCs as medicinal signaling cells, these studies may open new avenues for a better standardization and characterization of MSCs secretome, ultimately leading to a better understanding of the mechanisms underlying the effects of this potential disease-modifying strategy.

References

Aarsland D, Påhlhagen S, Ballard CG, Ehrt U, & Svenningsson P. (2012). Depression in Parkinson disease—epidemiology, mechanisms and management. *Nature Reviews Neurology, 8*(1), 35-47. doi:10.1038/nrneurol.2011.189

Abbas MM, Xu Z, & Tan LCS. (2018). Epidemiology of Parkinson's Disease—East Versus West. *Movement Disorders Clinical Practice, 5*(1), 14-28. doi:10.1002/mdc3.12568

Abbott RD, Petrovitch H, White LR, Masaki KH, Tanner CM, Curb JD, Grandinetti A, Blanchette PL, Popper JS, & Ross GW. (2001). Frequency of bowel movements and the future risk of Parkinson's disease. *Neurology, 57*(3), 456-462. doi:10.1212/wnl.57.3.456

Albin RL, Young AB, & Penney JB. (1989). The functional anatomy of basal ganglia disorders. *Trends in neurosciences, 12*(10), 366-375. doi:10.1016/0166-2236(89)90074-x

Allbutt HN, & Henderson JM. (2007). Use of the narrow beam test in the rat, 6-hydroxydopamine model of Parkinson's disease. *Journal of Neuroscience Methods, 159*(2), 195-202. doi:10.1016/j.jneumeth.2006.07.006

Alvarez-Erviti L, Rodriguez-Oroz MC, Cooper JM, Caballero C, Ferrer I, Obeso JA, & Schapira AHV. (2010). Chaperone-mediated autophagy markers in Parkinson disease brains. *Archives of neurology, 67*(12), 1464-1472. doi:10.1001/archneurol.2010.198

Anglade P, Vyas S, Javoy-Agid F, Herrero MT, Michel PP, Marquez J, Mouatt-Prigent A, Ruberg M, Hirsch EC, & Agid Y. (1997). Apoptosis and autophagy in nigral neurons of patients with Parkinson's disease. *Histology and histopathology, 12*(1), 25-31.

Ankrum JA, Ong JF, & Karp JM. (2014). Mesenchymal stem cells: immune evasive, not immune privileged. *Nat Biotechnol, 32*(3), 252-260. doi:10.1038/nbt.2816

Ansari KA, & Johnson A. (1975). Olfactory function in patients with Parkinson's disease. *Journal of chronic diseases, 28*(9), 493-497. doi:10.1016/0021-9681(75)90058-2

Arenas E, Denham M, & Villaescusa JC. (2015). How to make a midbrain dopaminergic neuron. *Development, 142*(11), 1918-1936. doi:10.1242/dev.097394

Arias-Fuenzalida J, Jarazo J, Qing X, Walter J, Gomez-Giro G, Nickels SL, Zaehres H, Schöler HR, & Schwamborn JC. (2017). FACS-Assisted CRISPR-Cas9 Genome Editing Facilitates Parkinson's Disease Modeling. *Stem Cell Reports, 9*(5), 1423-1431. doi:10.1016/j.stemcr.2017.08.026

Asakawa T, Fang H, Sugiyama K, Nozaki T, Hong Z, Yang Y, Hua F, Ding G, Chao D, Fenoy AJ, Villarreal SJ, Onoe H, Suzuki K, Mori N, Namba H, & Xia Y. (2016). Animal behavioral assessments in current research of Parkinson's disease. *Neuroscience and biobehavioral reviews, 65*, 63-94. doi:10.1016/j.neubiorev.2016.03.016

Ascherio A, & Schwarzschild MA. (2016). The epidemiology of Parkinson's disease: risk factors and prevention. *The Lancet. Neurology, 15*(12), 1257-1272. doi:10.1016/s1474-4422(16)30230-7

Ascherio A, Zhang SM, Hernán MA, Kawachi I, Colditz GA, Speizer FE, & Willett WC. (2001). Prospective study of caffeine consumption and risk of Parkinson's disease in men and women. *Annals of neurology, 50*(1), 56-63. doi:10.1002/ana.1052

Athauda D, & Foltynie T. (2015). The ongoing pursuit of neuroprotective therapies in Parkinson disease. *Nature Reviews Neurology, 11*(1), 25-40. doi:10.1038/nrneurol.2014.226

Axelsen TM, & Woldbye DPD. (2018). Gene Therapy for Parkinson's Disease, An Update. *J Parkinsons Dis, 8*(2), 195-215. doi:10.3233/jpd-181331

Bachiller S, Jiménez-Ferrer I, Paulus A, Yang Y, Swanberg M, Deierborg T, & Boza-Serrano A. (2018). Microglia in Neurological Diseases: A Road Map to Brain-Disease Dependent-Inflammatory Response. *Front Cell Neurosci, 12*(488). doi:10.3389/fncel.2018.00488

Bagher Z, Azami M, Ebrahimi-Barough S, Mirzadeh H, Solouk A, Soleimani M, Ai J, Nourani MR, & Joghataei MT. (2016). Differentiation of Wharton's Jelly-Derived Mesenchymal Stem Cells into Motor Neuron-Like Cells on Three-Dimensional Collagen-Grafted Nanofibers. *Molecular Neurobiology, 53*(4), 2397-2408. doi:10.1007/s12035-015-9199-x

Bagno L, Hatzistergos KE, Balkan W, & Hare JM. (2018). Mesenchymal Stem Cell-Based Therapy for Cardiovascular Disease: Progress and Challenges. *Molecular therapy : the journal of the American Society of Gene Therapy, 26*(7), 1610-1623. doi:10.1016/j.ymthe.2018.05.009

Barker RA, Drouin-Ouellet J, & Parmar M. (2015). Cell-based therapies for Parkinson disease—past insights and future potential. *Nature reviews. Neurology, 11*(9), 492-503. doi:10.1038/nrneurol.2015.123

Berg D. (2011). Hyperechogenicity of the substantia nigra: pitfalls in assessment and specificity for Parkinson's disease. *Journal of neural transmission (Vienna, Austria : 1996), 118*(3), 453-461. doi:10.1007/s00702-010-0469-5

Berg D, Postuma RB, Adler CH, Bloem BR, Chan P, Dubois B, Gasser T, Goetz CG, Halliday G, Joseph L, Lang AE, Liepelt-Scarfone I, Litvan I, Marek K, Obeso J, Oertel W, Olanow CW, Poewe W, Stern M, & Deuschl G. (2015). MDS research criteria for prodromal Parkinson's disease. *Movement Disorders, 30*(12), 1600-1611. doi:10.1002/mds.26431

Berg D, Postuma RB, Bloem B, Chan P, Dubois B, Gasser T, Goetz CG, Halliday GM, Hardy J, Lang AE, Litvan I, Marek K, Obeso J, Oertel W, Olanow CW, Poewe W, Stern M, & Deuschl G. (2014). Time to redefine PD? Introductory statement of the MDS Task Force on the definition of Parkinson's disease. *Movement disorders : official journal of the Movement Disorder Society, 29*(4), 454-462. doi:10.1002/mds.25844

Bertolin G, Ferrando-Miguel R, Jacoupy M, Traver S, Grenier K, Greene AW, Dauphin A, Waharte F, Bayot A, Salamero J, Lombès A, Bulteau A-L, Fon EA, Brice A, & Corti O. (2013). The TOMM machinery is a molecular switch in PINK1 and PARK2/PARKIN-dependent mitochondrial clearance. *Autophagy, 9*(11), 1801-1817. doi:10.4161/auto.25884

Bessa J, Mesquita A, Oliveira M, Pêgo J, Cerqueira J, Palha J, Almeida O, & Sousa N. (2009). A trans-dimensional approach to the behavioral aspects of depression. *Front Behav Neurosci, 3*(1). doi:10.3389/neuro.08.001.2009

Bieri G, Brahic M, Bousset L, Couthouis J, Kramer NJ, Ma R, Nakayama L, Monbureau M, Defensor E, Schüle B, Shamloo M, Melki R, & Gitler AD. (2019). LRRK2 modifies α-syn pathology and spread in mouse models and human neurons. *Acta neuropathologica, 137*(6), 961-980. doi:10.1007/s00401-019-01995-0

Björklund A, & Dunnett SB. (2019). The Amphetamine Induced Rotation Test: A Re-Assessment of Its Use as a Tool to Monitor Motor Impairment and Functional Recovery in Rodent Models of Parkinson's Disease. *J Parkinsons Dis, 9*(1), 17-29. doi:10.3233/jpd-181525

Blandini F, & Armentero M-T. (2012). Animal models of Parkinson's disease. *The FEBS journal, 279*(7), 1156-1166. doi:10.1111/j.1742-4658.2012.08491.x

Blandini F, Braunewell KH, Manahan-Vaughan D, Orzi F, & Sarti P. (2004). Neurodegeneration and energy metabolism: from chemistry to clinics. *Cell Death & Differentiation, 11*(4), 479-484. doi:10.1038/sj.cdd.4401323

Blandini F, Cova L, Armentero M-T, Zennaro E, Levandis G, Bossolasco P, Calzarossa C, Mellone M, Giuseppe B, Deliliers GL, Polli E, Nappi G, & Silani V. (2010). Transplantation of undifferentiated human mesenchymal stem cells protects against 6-hydroxydopamine neurotoxicity in the rat. *Cell transplantation, 19*(2), 203-217. doi:10.3727/096368909x479839

Blesa J, & Przedborski S. (2014). Parkinson's disease: animal models and dopaminergic cell vulnerability. *Frontiers in Neuroanatomy, 8*(155). doi:10.3389/fnana.2014.00155

Blume SR, Cass DK, & Tseng KY. (2009). Stepping test in mice: a reliable approach in determining forelimb akinesia in MPTP-induced Parkinsonism. *Experimental Neurology, 219*(1), 208-211. doi:10.1016/j.expneurol.2009.05.017

Boeve BF. (2010). REM sleep behavior disorder: Updated review of the core features, the REM sleep behavior disorder-neurodegenerative disease association, evolving concepts, controversies, and future directions. *Annals of the New York Academy of Sciences, 1184*, 15-54. doi:10.1111/j.1749-6632.2009.05115.x

Boix J, Padel T, & Paul G. (2015). A partial lesion model of Parkinson's disease in mice – Characterization of a 6-OHDA-induced medial forebrain bundle lesion. *Behavioural Brain Research, 284*, 196-206. doi:https://doi.org/10.1016/j.bbr.2015.01.053

Boix J, von Hieber D, & Connor B. (2018). Gait Analysis for Early Detection of Motor Symptoms in the 6-OHDA Rat Model of Parkinson's Disease. *Front Behav Neurosci, 12*(39). doi:10.3389/fnbeh.2018.00039

Bolam JP, & Pissadaki EK. (2012). Living on the edge with too many mouths to feed: why dopamine neurons die. *Movement disorders : official journal of the Movement Disorder Society, 27*(12), 1478-1483. doi:10.1002/mds.25135

Bonifati V, Rizzu P, van Baren MJ, Schaap O, Breedveld GJ, Krieger E, Dekker MCJ, Squitieri F, Ibanez P, Joosse M, van Dongen JW, Vanacore N, van Swieten JC, Brice A, Meco G, van Duijn CM, Oostra BA, & Heutink P. (2003). Mutations in the DJ-1 gene associated with autosomal recessive early-onset parkinsonism. *Science (New York, N.Y.), 299*(5604), 256-259. doi:10.1126/science.1077209

Bonito-Oliva A, Masini D, & Fisone G. (2014). A mouse model of non-motor symptoms in Parkinson's disease: focus on pharmacological interventions targeting affective dysfunctions. *Front Behav Neurosci, 8*, 290-290. doi:10.3389/fnbeh.2014.00290

Bosco DA, Fowler DM, Zhang Q, Nieva J, Powers ET, Wentworth P, Jr., Lerner RA, & Kelly JW. (2006). Elevated levels of oxidized cholesterol metabolites in Lewy body disease brains accelerate alpha-synuclein fibrilization. *Nature chemical biology, 2*(5), 249-253. doi:10.1038/nchembio782

Bouchez G, Sensebé L, Vourc'h P, Garreau L, Bodard S, Rico A, Guilloteau D, Charbord P, Besnard J-C, & Chalon S. (2008). Partial recovery of dopaminergic pathway after graft of adult mesenchymal stem cells in a rat model of Parkinson's disease. *Neurochemistry international, 52*(7), 1332-1342. doi:10.1016/j.neuint.2008.02.003

Braak H, Del Tredici K, Rüb U, de Vos RAI, Jansen Steur ENH, & Braak E. (2003). Staging of brain pathology related to sporadic Parkinson's disease. *Neurobiol Aging, 24*(2), 197-211. doi:10.1016/s0197-4580(02)00065-9

Branchi I, D'Andrea I, Armida M, Cassano T, Pèzzola A, Potenza RL, Morgese MG, Popoli P, & Alleva E. (2008). Nonmotor symptoms in Parkinson's disease: investigating early-phase onset of behavioral dysfunction in the 6-hydroxydopamine-lesioned rat model. *J Neurosci Res, 86*(9), 2050-2061. doi:10.1002/jnr.21642

Brooks DJ. (2010). Imaging approaches to Parkinson disease. *Journal of nuclear medicine : official publication, Society of Nuclear Medicine, 51*(4), 596-609. doi:10.2967/jnumed.108.059998

Brooks SP, & Dunnett SB. (2009). Tests to assess motor phenotype in mice: a user's guide. *Nature reviews. Neuroscience, 10*(7), 519-529. doi:10.1038/nrn2652

Brown TP, Rumsby PC, Capleton AC, Rushton L, & Levy LS. (2006). Pesticides and Parkinson's disease--is there a link? *Environmental health perspectives, 114*(2), 156-164. doi:10.1289/ehp.8095

Brundin P, Li J-Y, Holton JL, Lindvall O, & Revesz T. (2008). Research in motion: the enigma of Parkinson's disease pathology spread. *Nature reviews. Neuroscience, 9*(10), 741-745. doi:10.1038/nrn2477

Burré J, Sharma M, Tsetsenis T, Buchman V, Etherton MR, & Südhof TC. (2010). Alpha-synuclein promotes SNARE-complex assembly in vivo and in vitro. *Science (New York, N.Y.), 329*(5999), 1663-1667. doi:10.1126/science.1195227

Campos FL, Carvalho MM, Cristovao AC, Je G, Baltazar G, Salgado AJ, Kim YS, & Sousa N. (2013). Rodent models of Parkinson's disease: beyond the motor symptomatology. *Front Behav Neurosci, 7*, 175. doi:10.3389/fnbeh.2013.00175

Caplan AI. (1991). Mesenchymal stem cells. *Journal of orthopaedic research : official publication of the Orthopaedic Research Society, 9*(5), 641-650. doi:10.1002/jor.1100090504

Caplan AI. (2017). Mesenchymal Stem Cells: Time to Change the Name! *Stem Cells Translational Medicine, 6*(6), 1445-1451. doi:10.1002/sctm.17-0051

Caplan AI. (2019). There Is No "Stem Cell Mess". *Tissue engineering. Part B, Reviews, 25*(4), 291-293. doi:10.1089/ten.TEB.2019.0049

Caplan Arnold I, & Correa D. (2011). The MSC: An Injury Drugstore. *Cell Stem Cell, 9*(1), 11-15. doi:10.1016/j.stem.2011.06.008

Caplan AI, & Dennis JE. (2006). Mesenchymal stem cells as trophic mediators. *Journal of Cellular Biochemistry, 98*(5), 1076-1084. doi:10.1002/jcb.20886

Carroll WM. (2019). The global burden of neurological disorders. *The Lancet Neurology, 18*(5), 418-419. doi:10.1016/s1474-4422(19)30029-8

Carvalho MM, Campos FL, Coimbra B, Pêgo JM, Rodrigues C, Lima R, Rodrigues AJ, Sousa N, & Salgado AJ. (2013). Behavioral characterization of the 6-hydroxidopamine model of Parkinson's disease and pharmacological rescuing of non-motor deficits. *Molecular Neurodegeneration, 8*, 14-14. doi:10.1186/1750-1326-8-14

Caudal D, Alvarsson A, Björklund A, & Svenningsson P. (2015). Depressive-like phenotype induced by AAV-mediated overexpression of human α-synuclein in midbrain dopaminergic neurons. *Experimental Neurology, 273*, 243-252. doi:10.1016/j.expneurol.2015.09.002

Cenci MA, & Lundblad M. (2005). CHAPTER B7 - Utility of 6-Hydroxydopamine Lesioned Rats in the Preclinical Screening of Novel Treatments for Parkinson Disease. In M. LeDoux (Ed.), *Animal Models of Movement Disorders* (pp. 193-208). Burlington: Academic Press.

Chahine LM, Amara AW, & Videnovic A. (2017). A systematic review of the literature on disorders of sleep and wakefulness in Parkinson's disease from 2005 to 2015. *Sleep medicine reviews, 35*, 33-50. doi:10.1016/j.smrv.2016.08.001

Chan-Palay V. (1993). Depression and dementia in Parkinson's disease. Catecholamine changes in the locus ceruleus, a basis for therapy. *Advances in neurology, 60*, 438-446.

Chan CS, Guzman JN, Ilijic E, Mercer JN, Rick C, Tkatch T, Meredith GE, & Surmeier DJ. (2007). 'Rejuvenation' protects neurons in mouse models of Parkinson's disease. *Nature, 447*(7148), 1081-1086. doi:10.1038/nature05865

Chen CY, Weng YH, Chien KY, Lin KJ, Yeh TH, Cheng YP, Lu CS, & Wang HL. (2012). (G2019S) LRRK2 activates MKK4-JNK pathway and causes degeneration of SN dopaminergic neurons in a transgenic mouse model of PD. *Cell death and differentiation, 19*(10), 1623-1633. doi:10.1038/cdd.2012.42

Chen H, Huang X, Guo X, Mailman RB, Park Y, Kamel F, Umbach DM, Xu Q, Hollenbeck A, Schatzkin A, & Blair A. (2010). Smoking duration, intensity, and risk of Parkinson disease. *Neurology, 74*(11), 878-884. doi:10.1212/WNL.0b013e3181d55f38

Chen L, Deltheil T, Turle-Lorenzo N, Liberge M, Rosier C, Watabe I, Sreng L, Amalric M, & Mourre C. (2014). SK channel blockade reverses cognitive and motor deficits induced by nigrostriatal dopamine lesions in rats. *The international journal of neuropsychopharmacology, 17*(8), 1295-1306. doi:10.1017/s1461145714000236

Chen Y, Shen J, Ke K, & Gu X. (2020). Clinical potential and current progress of mesenchymal stem cells for Parkinson's disease: a systematic review. *Neurological sciences : official journal of the Italian Neurological Society and of the Italian Society of Clinical Neurophysiology*, 10.1007/s10072-10020-04240-10079. doi:10.1007/s10072-020-04240-9

Cheng H-C, Ulane CM, & Burke RE. (2010). Clinical progression in Parkinson disease and the neurobiology of axons. *Annals of neurology, 67*(6), 715-725. doi:10.1002/ana.21995

Chesselet M-F, & Richter F. (2011). Modelling of Parkinson's disease in mice. *The Lancet. Neurology, 10*(12), 1108-1118. doi:10.1016/s1474-4422(11)70227-7

Choi HS, Kim HJ, Oh J-H, Park H-G, Ra JC, Chang K-A, & Suh Y-H. (2015). Therapeutic potentials of human adipose-derived stem cells on the mouse model of Parkinson's disease. *Neurobiol Aging, 36*(10), 2885-2892. doi:10.1016/j.neurobiolaging.2015.06.022

Chu Y, Dodiya H, Aebischer P, Olanow CW, & Kordower JH. (2009). Alterations in lysosomal and proteasomal markers in Parkinson's disease: relationship to alpha-synuclein inclusions. *Neurobiology of Disease, 35*(3), 385-398. doi:10.1016/j.nbd.2009.05.023

Cobb MM, Ravisankar A, Skibinski G, & Finkbeiner S. (2018). iPS cells in the study of PD molecular pathogenesis. *Cell and tissue research, 373*(1), 61-77. doi:10.1007/s00441-017-2749-y

Coelho M, & Ferreira JJ. (2012). Late-stage Parkinson disease. *Nature Reviews Neurology, 8*(8), 435-442. doi:10.1038/nrneurol.2012.126

Connolly BS, & Lang AE. (2014). Pharmacological treatment of Parkinson disease: a review. *JAMA, 311*(16), 1670-1683. doi:10.1001/jama.2014.3654

Cooper JF, & Van Raamsdonk JM. (2018). Modeling Parkinson's Disease in C. elegans. *J Parkinsons Dis, 8*(1), 17-32. doi:10.3233/jpd-171258

Corti O, Lesage S, & Brice A. (2011). What genetics tells us about the causes and mechanisms of Parkinson's disease. *Physiological reviews, 91*(4), 1161-1218. doi:10.1152/physrev.00022.2010

Cova L, Armentero MT, Zennaro E, Calzarossa C, Bossolasco P, Busca G, Lambertenghi Deliliers G, Polli E, Nappi G, Silani V, & Blandini F. (2010). Multiple neurogenic and neurorescue effects of human mesenchymal stem cell after transplantation in an experimental model of Parkinson's disease. *Brain Res., 1311:12-27.*(doi), 10.1016/j.brainres.2009.1011.1041. Epub 2009 Nov 1026.

Cova L, Bossolasco P, Armentero M-T, Diana V, Zennaro E, Mellone M, Calzarossa C, Cerri S, Deliliers GL, Polli E, Blandini F, & Silani V. (2012). Neuroprotective effects of human mesenchymal stem cells on neural cultures exposed to 6-hydroxydopamine: implications for reparative therapy in Parkinson's disease. *Apoptosis : an international journal on programmed cell death, 17*(3), 289-304. doi:10.1007/s10495-011-0679-9

Cuervo AM, Stefanis L, Fredenburg R, Lansbury PT, & Sulzer D. (2004). Impaired degradation of mutant alpha-synuclein by chaperone-mediated autophagy. *Science (New York, N.Y.), 305*(5688), 1292-1295. doi:10.1126/science.1101738

Danielyan L, Schäfer R, von Ameln-Mayerhofer A, Bernhard F, Verleysdonk S, Buadze M, Lourhmati A, Klopfer T, Schaumann F, Schmid B, Koehle C, Proksch B, Weissert R, Reichardt HM, van den Brandt J, Buniatian GH, Schwab M, Gleiter CH, & Frey WH, 2nd. (2011). Therapeutic efficacy of intranasally delivered mesenchymal stem cells in a rat model of Parkinson disease. *Rejuvenation research, 14*(1), 3-16. doi:10.1089/rej.2010.1130

Dauer W, & Przedborski S. (2003). Parkinson's disease: mechanisms and models. *Neuron., 39*(6), 889-909.

Dawson VL, & Dawson TM. (2019). Promising disease-modifying therapies for Parkinson's disease. *Science translational medicine, 11*(520), eaba1659. doi:10.1126/scitranslmed.aba1659

Deas E, Wood NW, & Plun-Favreau H. (2011). Mitophagy and Parkinson's disease: the PINK1-parkin link. *Biochim Biophys Acta, 1813*(4), 623-633. doi:10.1016/j.bbamcr.2010.08.007

Decressac M, Mattsson B, & Björklund A. (2012a). Comparison of the behavioural and histological characteristics of the 6-OHDA and α-synuclein rat models of Parkinson's disease. *Experimental Neurology, 235*(1), 306-315. doi:10.1016/j.expneurol.2012.02.012

Decressac M, Mattsson B, Lundblad M, Weikop P, & Bjorklund A. (2012b). Progressive neurodegenerative and behavioural changes induced by AAV-mediated overexpression of alpha-synuclein in midbrain dopamine neurons. *Neurobiology of Disease, 45*(3), 939-953.

Delaville C, Chetrit J, Abdallah K, Morin S, Cardoit L, De Deurwaerdère P, & Benazzouz A. (2012). Emerging dysfunctions consequent to combined monoaminergic depletions in Parkinsonism. *Neurobiology of Disease, 45*(2), 763-773. doi:10.1016/j.nbd.2011.10.023

Deverman BE, Ravina BM, Bankiewicz KS, Paul SM, & Sah DWY. (2018). Gene therapy for neurological disorders: progress and prospects. *Nature Reviews Drug Discovery, 17*(9), 641-659. doi:10.1038/nrd.2018.110

Devi L, Raghavendran V, Prabhu BM, Avadhani NG, & Anandatheerthavarada HK. (2008). Mitochondrial import and accumulation of alpha-synuclein impair complex I in human dopaminergic neuronal cultures and Parkinson disease brain. *The Journal of biological chemistry, 283*(14), 9089-9100. doi:10.1074/jbc.M710012200

Dias V, Junn E, & Mouradian MM. (2013). The role of oxidative stress in Parkinson's disease. *J Parkinsons Dis, 3*(4), 461-491. doi:10.3233/jpd-130230

Dickson DW, Braak H, Duda JE, Duyckaerts C, Gasser T, Halliday GM, Hardy J, Leverenz JB, Del Tredici K, Wszolek ZK, & Litvan I. (2009). Neuropathological assessment of Parkinson's disease: refining the diagnostic criteria. *The Lancet. Neurology, 8*(12), 1150-1157. doi:10.1016/s1474-4422(09)70238-8

Dirkx MF, den Ouden H, Aarts E, Timmer M, Bloem BR, Toni I, & Helmich RC. (2016). The Cerebral Network of Parkinson's Tremor: An Effective Connectivity fMRI Study. *J Neurosci, 36*(19), 5362-5372. doi:10.1523/jneurosci.3634-15.2016

Dominici M, Le Blanc K, Mueller I, Slaper-Cortenbach I, Marini F, Krause D, Deans R, Keating A, Prockop D, & Horwitz E. (2006). Minimal criteria for defining multipotent mesenchymal stromal cells. The International Society for Cellular Therapy position statement. *Cytotherapy., 8*(4), 315-317. doi: 310.1080/14653240600855905.

Donega V, Nijboer CH, Braccioli L, Slaper-Cortenbach I, Kavelaars A, van Bel F, & Heijnen CJ. (2014). Intranasal administration of human MSC for ischemic brain injury in the mouse: in vitro and in vivo neuroregenerative functions. *PLoS One, 9*(11), e112339. doi:10.1371/journal.pone.0112339

Dorsey ER, Elbaz A, Nichols E, Abd-Allah F, Abdelalim A, Adsuar JC, Ansha MG, Brayne C, Choi J-YJ, Collado-Mateo D, Dahodwala N, Do HP, Edessa D, Endres M, Fereshtehnejad S-M, Foreman KJ, Gankpe FG, Gupta R, Hankey GJ, Hay SI, Hegazy MI, Hibstu DT, Kasaeian A, Khader Y, Khalil I, Khang Y-H, Kim YJ, Kokubo Y, Logroscino G, Massano J, Mohamed Ibrahim N, Mohammed MA, Mohammadi A, Moradi-Lakeh M, Naghavi M, Nguyen BT, Nirayo YL, Ogbo FA, Owolabi MO, Pereira DM, Postma MJ, Qorbani M, Rahman MA, Roba KT, Safari H, Safiri S, Satpathy M, Sawhney M, Shafieesabet A, Shiferaw MS, Smith M, Szoeke CEI, Tabarés-Seisdedos R, Truong NT, Ukwaja KN, Venketasubramanian N, Villafaina S, weldegwergs Kg, Westerman R, Wijeratne T, Winkler AS, Xuan BT, Yonemoto N, Feigin VL, Vos T, & Murray CJL. (2018). Global, regional, and national burden of Parkinson's disease, 1990–2016: a systematic analysis for the Global Burden of Disease Study 2016. *The Lancet Neurology, 17*(11), 939-953. doi:10.1016/s1474-4422(18)30295-3

Dowd E, Monville C, Torres EM, & Dunnett SB. (2005). The Corridor Task: a simple test of lateralised response selection sensitive to unilateral dopamine deafferentation and graft-derived dopamine replacement in the striatum. *Brain research bulletin, 68*(1-2), 24-30. doi:10.1016/j.brainresbull.2005.08.009

Drui G, Carnicella S, Carcenac C, Favier M, Bertrand A, Boulet S, & Savasta M. (2014). Loss of dopaminergic nigrostriatal neurons accounts for the motivational and affective deficits in Parkinson's disease. *Molecular psychiatry, 19*(3), 358-367. doi:10.1038/mp.2013.3

Dufty BM, Warner LR, Hou ST, Jiang SX, Gomez-Isla T, Leenhouts KM, Oxford JT, Feany MB, Masliah E, & Rohn TT. (2007). Calpain-Cleavage of α-Synuclein: Connecting Proteolytic Processing to Disease-Linked Aggregation. *The American Journal of Pathology, 170*(5), 1725-1738. doi:https://doi.org/10.2353/ajpath.2007.061232

Dugger BN, Murray ME, Boeve BF, Parisi JE, Benarroch EE, Ferman TJ, & Dickson DW. (2012). Neuropathological analysis of brainstem cholinergic and catecholaminergic nuclei in relation to rapid eye movement (REM) sleep behaviour disorder. *Neuropathol Appl Neurobiol, 38*(2), 142-152. doi:10.1111/j.1365-2990.2011.01203.x

Dunnett SB, & Lelos M. (2010). Chapter 3 - Behavioral analysis of motor and non-motor symptoms in rodent models of Parkinson's disease. In A. Björklund & M. A. Cenci (Eds.), *Progress in Brain Research* (Vol. 184, pp. 35-51): Elsevier.

Dusonchet J, Kochubey O, Stafa K, Young SM, Jr., Zufferey R, Moore DJ, Schneider BL, & Aebischer P. (2011). A rat model of progressive nigral neurodegeneration induced by the Parkinson's disease-associated G2019S mutation in LRRK2. *J Neurosci, 31*(3), 907-912. doi:10.1523/jneurosci.5092-10.2011

Duty S, & Jenner P. (2011). Animal models of Parkinson's disease: a source of novel treatments and clues to the cause of the disease. *British journal of pharmacology, 164*(4), 1357-1391. doi:10.1111/j.1476-5381.2011.01426.x

El-Agnaf OMA, Salem SA, Paleologou KE, Cooper LJ, Fullwood NJ, Gibson MJ, Curran MD, Court JA, Mann DMA, Ikeda S-i, Cookson MR, Hardy J, & Allsop D. (2003). Alpha-synuclein implicated in Parkinson's disease is present in extracellular biological fluids, including human plasma. *FASEB journal : official publication of the Federation of American Societies for Experimental Biology, 17*(13), 1945-1947. doi:10.1096/fj.03-0098fje

Elbaz A, Nelson LM, Payami H, Ioannidis JPA, Fiske BK, Annesi G, Carmine Belin A, Factor SA, Ferrarese C, Hadjigeorgiou GM, Higgins DS, Kawakami H, Krüger R, Marder KS, Mayeux RP, Mellick GD, Nutt JG, Ritz B, Samii A, Tanner CM, Van Broeckhoven C, Van Den Eeden SK, Wirdefeldt K, Zabetian CP, Dehem M, Montimurro JS, Southwick A, Myers RM, & Trikalinos TA. (2006). Lack of replication of thirteen single-nucleotide polymorphisms implicated in Parkinson's disease: a large-scale international study. *The Lancet. Neurology, 5*(11), 917-923. doi:10.1016/s1474-4422(06)70579-8

Falkenburger BH, Saridaki T, & Dinter E. (2016). Cellular models for Parkinson's disease. *Journal of Neurochemistry, 139*(S1), 121-130. doi:10.1111/jnc.13618

Fan X-L, Zhang Y, Li X, & Fu Q-L. (2020). Mechanisms underlying the protective effects of mesenchymal stem cell-based therapy. *Cell Mol Life Sci*, 10.1007/s00018-00020-03454-00016. doi:10.1007/s00018-020-03454-6

Fang F, Xu Q, Park Y, Huang X, Hollenbeck A, Blair A, Schatzkin A, Kamel F, & Chen H. (2010). Depression and the subsequent risk of Parkinson's disease in the NIH-AARP Diet and Health Study. *Movement disorders : official journal of the Movement Disorder Society, 25*(9), 1157-1162. doi:10.1002/mds.23092

Fearnley JM, & Lees AJ. (1991). Ageing and Parkinson's disease: substantia nigra regional selectivity. *Brain : a journal of neurology, 114 (Pt 5)*, 2283-2301. doi:10.1093/brain/114.5.2283

Fernandes HJR, Hartfield EM, Christian HC, Emmanoulidou E, Zheng Y, Booth H, Bogetofte H, Lang C, Ryan BJ, Sardi SP, Badger J, Vowles J, Evetts S, Tofaris GK, Vekrellis K, Talbot K, Hu MT, James W, Cowley SA, & Wade-Martins R. (2016). ER Stress and Autophagic Perturbations Lead to Elevated Extracellular α-Synuclein in GBA-N370S Parkinson's iPSC-Derived Dopamine Neurons. *Stem Cell Reports, 6*(3), 342-356. doi:10.1016/j.stemcr.2016.01.013

Fitzsimmons REB, Mazurek MS, Soos A, & Simmons CA. (2018). Mesenchymal Stromal/Stem Cells in Regenerative Medicine and Tissue Engineering. *Stem Cells Int, 2018*, 8031718-8031718. doi:10.1155/2018/8031718

Francardo V, Recchia A, Popovic N, Andersson D, Nissbrandt H, & Cenci MA. (2011). Impact of the lesion procedure on the profiles of motor impairment and molecular responsiveness to L-DOPA in the 6-hydroxydopamine mouse model of Parkinson's disease. *Neurobiology of Disease, 42*(3), 327-340. doi:10.1016/j.nbd.2011.01.024

Friedenstein AJ, Gorskaja JF, & Kulagina NN. (1976). Fibroblast precursors in normal and irradiated mouse hematopoietic organs. *Exp Hematol., 4*(5), 267-274.

Frigerio R, Fujishiro H, Ahn T-B, Josephs KA, Maraganore DM, DelleDonne A, Parisi JE, Klos KJ, Boeve BF, Dickson DW, & Ahlskog JE. (2011). Incidental Lewy body disease: do some cases represent a preclinical stage of dementia with Lewy bodies? *Neurobiol Aging, 32*(5), 857-863. doi:10.1016/j.neurobiolaging.2009.05.019

Funayama M, Hasegawa K, Kowa H, Saito M, Tsuji S, & Obata F. (2002). A new locus for Parkinson's disease (PARK8) maps to chromosome 12p11.2-q13.1. *Annals of neurology, 51*(3), 296-301. doi:10.1002/ana.10113

Gähwiler BH, Capogna M, Debanne D, McKinney RA, & Thompson SM. (1997). Organotypic slice cultures: a technique has come of age. *Trends in neurosciences, 20*(10), 471-477. doi:10.1016/s0166-2236(97)01122-3

Gandhi S, Wood-Kaczmar A, Yao Z, Plun-Favreau H, Deas E, Klupsch K, Downward J, Latchman DS, Tabrizi SJ, Wood NW, Duchen MR, & Abramov AY. (2009). PINK1-Associated Parkinson's Disease Is Caused by Neuronal Vulnerability to Calcium-Induced Cell Death. *Molecular Cell, 33*(5), 627-638. doi:https://doi.org/10.1016/j.molcel.2009.02.013

Gao H-M, Kotzbauer PT, Uryu K, Leight S, Trojanowski JQ, & Lee VMY. (2008). Neuroinflammation and oxidation/nitration of alpha-synuclein linked to dopaminergic neurodegeneration. *J Neurosci, 28*(30), 7687-7698. doi:10.1523/jneurosci.0143-07.2008

Gautier CA, Kitada T, & Shen J. (2008). Loss of PINK1 causes mitochondrial functional defects and increased sensitivity to oxidative stress. *Proceedings of the National Academy of Sciences of the United States of America, 105*(32), 11364-11369. doi:10.1073/pnas.0802076105

Gaven F, Marin P, & Claeysen S. (2014). Primary culture of mouse dopaminergic neurons. *Journal of visualized experiments : JoVE*(91), e51751-e51751. doi:10.3791/51751

Gelb DJ, Oliver E, & Gilman S. (1999). Diagnostic criteria for Parkinson disease. *Archives of neurology, 56*(1), 33-39. doi:10.1001/archneur.56.1.33

Ghaffari LT, Starr A, Nelson AT, & Sattler R. (2018). Representing Diversity in the Dish: Using Patient-Derived in Vitro Models to Recreate the Heterogeneity of Neurological Disease. *Frontiers in Neuroscience, 12*(56). doi:10.3389/fnins.2018.00056

Gispert S, Ricciardi F, Kurz A, Azizov M, Hoepken H-H, Becker D, Voos W, Leuner K, Müller WE, Kudin AP, Kunz WS, Zimmermann A, Roeper J, Wenzel D, Jendrach M, García-Arencíbia M, Fernández-Ruiz J, Huber L, Rohrer H, Barrera M, Reichert AS, Rüb U, Chen A, Nussbaum RL, & Auburger G. (2009). Parkinson phenotype in aged PINK1-deficient mice is accompanied by progressive mitochondrial dysfunction in absence of neurodegeneration. *PLoS One, 4*(6), e5777-e5777. doi:10.1371/journal.pone.0005777

Glajch KE, Fleming SM, Surmeier DJ, & Osten P. (2012). Sensorimotor assessment of the unilateral 6-hydroxydopamine mouse model of Parkinson's disease. *Behavioural brain research, 230*(2), 309-316. doi:10.1016/j.bbr.2011.12.007

Gnecchi M, He H, Liang OD, Melo LG, Morello F, Mu H, Noiseux N, Zhang L, Pratt RE, Ingwall JS, & Dzau VJ. (2005). Paracrine action accounts for marked protection of ischemic heart by Akt-modified mesenchymal stem cells. *Nature medicine, 11*(4), 367-368. doi:10.1038/nm0405-367

Goetz CG. (2011). The history of Parkinson's disease: early clinical descriptions and neurological therapies. *Cold Spring Harbor perspectives in medicine, 1*(1), a008862-a008862. doi:10.1101/cshperspect.a008862

Goldberg MS, Fleming SM, Palacino JJ, Cepeda C, Lam HA, Bhatnagar A, Meloni EG, Wu N, Ackerson LC, Klapstein GJ, Gajendiran M, Roth BL, Chesselet M-F, Maidment NT, Levine MS, & Shen J. (2003). Parkin-deficient mice exhibit nigrostriatal deficits but not loss of dopaminergic neurons. *The Journal of biological chemistry, 278*(44), 43628-43635. doi:10.1074/jbc.M308947200

Goldberg MS, Pisani A, Haburcak M, Vortherms TA, Kitada T, Costa C, Tong Y, Martella G, Tscherter A, Martins A, Bernardi G, Roth BL, Pothos EN, Calabresi P, & Shen J. (2005). Nigrostriatal Dopaminergic Deficits and Hypokinesia Caused by Inactivation of the Familial Parkinsonism-Linked Gene DJ-1. *Neuron, 45*(4), 489-496. doi:10.1016/j.neuron.2005.01.041

Gómez-Suaga P, Luzón-Toro B, Churamani D, Zhang L, Bloor-Young D, Patel S, Woodman PG, Churchill GC, & Hilfiker S. (2011). Leucine-rich repeat kinase 2 regulates autophagy through a calcium-dependent pathway involving NAADP. *Hum Mol Genet, 21*(3), 511-525. doi:10.1093/hmg/ddr481

González-Hernández T, Barroso-Chinea P, De La Cruz Muros I, Del Mar Pérez-Delgado M, & Rodríguez M. (2004). Expression of dopamine and vesicular monoamine transporters and differential vulnerability of mesostriatal dopaminergic neurons. *The Journal of comparative neurology, 479*(2), 198-215. doi:10.1002/cne.20323

Gratwicke J, Jahanshahi M, & Foltynie T. (2015). Parkinson's disease dementia: a neural networks perspective. *Brain : a journal of neurology, 138*(Pt 6), 1454-1476. doi:10.1093/brain/awv104

Grealish S, Mattsson B, Draxler P, & Björklund A. (2010). Characterisation of behavioural and neurodegenerative changes induced by intranigral 6-hydroxydopamine lesions in a mouse model of Parkinson's disease. *The European journal of neuroscience, 31*(12), 2266-2278. doi:10.1111/j.1460-9568.2010.07265.x

Grow DA, McCarrey JR, & Navara CS. (2016). Advantages of nonhuman primates as preclinical models for evaluating stem cell-based therapies for Parkinson's disease. *Stem Cell Res, 17*(2), 352-366. doi:10.1016/j.scr.2016.08.013

Guillot TS, Asress SA, Richardson JR, Glass JD, & Miller GW. (2008). Treadmill gait analysis does not detect motor deficits in animal models of Parkinson's disease or amyotrophic lateral sclerosis. *Journal of motor behavior, 40*(6), 568-577. doi:10.3200/jmbr.40.6.568-577

Gustafsson H, Nordström A, & Nordström P. (2015). Depression and subsequent risk of Parkinson disease: A nationwide cohort study. *Neurology, 84*(24), 2422-2429. doi:10.1212/wnl.0000000000001684

Guzman JN, Sanchez-Padilla J, Wokosin D, Kondapalli J, Ilijic E, Schumacker PT, & Surmeier DJ. (2010). Oxidant stress evoked by pacemaking in dopaminergic neurons is attenuated by DJ-1. *Nature, 468*(7324), 696-700. doi:10.1038/nature09536

Haaxma CA, Bloem BR, Borm GF, Oyen WJG, Leenders KL, Eshuis S, Booij J, Dluzen DE, & Horstink MWIM. (2007). Gender differences in Parkinson's disease. *Journal of neurology, neurosurgery, and psychiatry, 78*(8), 819-824. doi:10.1136/jnnp.2006.103788

Haehner A, Hummel T, Hummel C, Sommer U, Junghanns S, & Reichmann H. (2007). Olfactory loss may be a first sign of idiopathic Parkinson's disease. *Movement disorders : official journal of the Movement Disorder Society, 22*(6), 839-842. doi:10.1002/mds.21413

Hampton TG, & Amende I. (2010). Treadmill gait analysis characterizes gait alterations in Parkinson's disease and amyotrophic lateral sclerosis mouse models. *Journal of motor behavior, 42*(1), 1-4. doi:10.1080/00222890903272025

Haque ME, Mount MP, Safarpour F, Abdel-Messih E, Callaghan S, Mazerolle C, Kitada T, Slack RS, Wallace V, Shen J, Anisman H, & Park DS. (2012). Inactivation of Pink1 gene in vivo sensitizes dopamine-producing neurons to 1-methyl-4-phenyl-1,2,3,6-tetrahydropyridine (MPTP) and can be rescued by autosomal recessive Parkinson disease genes, Parkin or DJ-1. *The Journal of biological chemistry, 287*(27), 23162-23170. doi:10.1074/jbc.M112.346437

Hastings TG. (2009). The role of dopamine oxidation in mitochondrial dysfunction: implications for Parkinson's disease. *Journal of bioenergetics and biomembranes, 41*(6), 469-472. doi:10.1007/s10863-009-9257-z

Healy DG, Falchi M, O'Sullivan SS, Bonifati V, Durr A, Bressman S, Brice A, Aasly J, Zabetian CP, Goldwurm S, Ferreira JJ, Tolosa E, Kay DM, Klein C, Williams DR, Marras C, Lang AE, Wszolek ZK, Berciano J, Schapira AHV, Lynch T, Bhatia KP, Gasser T, Lees AJ, & Wood NW. (2008). Phenotype, genotype, and worldwide genetic penetrance of LRRK2-associated Parkinson's disease: a case-control study. *The Lancet Neurology, 7*(7), 583-590. doi:https://doi.org/10.1016/S1474-4422(08)70117-0

Hely MA, Morris JGL, Reid WGJ, & Trafficante R. (2005). Sydney Multicenter Study of Parkinson's disease: non-L-dopa-responsive problems dominate at 15 years. *Movement disorders : official journal of the Movement Disorder Society, 20*(2), 190-199. doi:10.1002/mds.20324

Hely MA, Reid WGJ, Adena MA, Halliday GM, & Morris JGL. (2008). The Sydney multicenter study of Parkinson's disease: the inevitability of dementia at 20 years. *Movement disorders : official journal of the Movement Disorder Society, 23*(6), 837-844. doi:10.1002/mds.21956

Hernán MA, Takkouche B, Caamaño-Isorna F, & Gestal-Otero JJ. (2002). A meta-analysis of coffee drinking, cigarette smoking, and the risk of Parkinson's disease. *Annals of neurology, 52*(3), 276-284. doi:10.1002/ana.10277

Hernandez LF, Obeso I, Costa RM, Redgrave P, & Obeso JA. (2019). Dopaminergic Vulnerability in Parkinson Disease: The Cost of Humans’ Habitual Performance. *Trends in Neurosciences, 42*(6), 375-383. doi:10.1016/j.tins.2019.03.007

Heuer A, Smith GA, Lelos MJ, Lane EL, & Dunnett SB. (2012). Unilateral nigrostriatal 6-hydroxydopamine lesions in mice I: motor impairments identify extent of dopamine depletion at three different lesion sites. *Behavioural brain research, 228*(1), 30-43. doi:10.1016/j.bbr.2011.11.027

Hoban DB, Howard L, & Dowd E. (2015). GDNF-secreting mesenchymal stem cells provide localized neuroprotection in an inflammation-driven rat model of Parkinson's disease. *Neuroscience, 303*, 402-411. doi:10.1016/j.neuroscience.2015.07.014

Hoffman KL. (2016). New dimensions in the use of rodent behavioral tests for novel drug discovery and development. *Expert opinion on drug discovery, 11*(4), 343-353. doi:10.1517/17460441.2016.1153624

Holmqvist S, Chutna O, Bousset L, Aldrin-Kirk P, Li W, Björklund T, Wang Z-Y, Roybon L, Melki R, & Li J-Y. (2014). Direct evidence of Parkinson pathology spread from the gastrointestinal tract to the brain in rats. *Acta neuropathologica, 128*(6), 805-820. doi:10.1007/s00401-014-1343-6

Holmqvist S, Lehtonen Š, Chumarina M, Puttonen KA, Azevedo C, Lebedeva O, Ruponen M, Oksanen M, Djelloul M, Collin A, Goldwurm S, Meyer M, Lagarkova M, Kiselev S, Koistinaho J, & Roybon L. (2016). Creation of a library of induced pluripotent stem cells from Parkinsonian patients. *npj Parkinson's Disease, 2*(1), 16009. doi:10.1038/npjparkd.2016.9

Hornykiewicz O. (2008). Basic research on dopamine in Parkinson's disease and the discovery of the nigrostriatal dopamine pathway: the view of an eyewitness. *Neuro-degenerative diseases, 5*(3-4), 114-117. doi:10.1159/000113678

Hsieh T-H, Chen J-JJ, Chen L-H, Chiang P-T, & Lee H-Y. (2011). Time-course gait analysis of hemiparkinsonian rats following 6-hydroxydopamine lesion. *Behavioural brain research, 222*(1), 1-9. doi:10.1016/j.bbr.2011.03.031

Hu GW, Li Q, Niu X, Hu B, Liu J, Zhou SM, Guo SC, Lang HL, Zhang CQ, Wang Y, & Deng ZF. (2015). Exosomes secreted by human-induced pluripotent stem cell-derived mesenchymal stem cells attenuate limb ischemia by promoting angiogenesis in mice. *Stem Cell Res Ther., 6*(10). doi:10.1186/scrt546

Hudson JL, van Horne CG, Strömberg I, Brock S, Clayton J, Masserano J, Hoffer BJ, & Gerhardt GA. (1993). Correlation of apomorphine- and amphetamine-induced turning with nigrostriatal dopamine content in unilateral 6-hydroxydopamine lesioned rats. *Brain Res, 626*(1-2), 167-174. doi:10.1016/0006-8993(93)90576-9

Hunter RL, Cheng B, Choi D-Y, Liu M, Liu S, Cass WA, & Bing G. (2009). Intrastriatal lipopolysaccharide injection induces parkinsonism in C57/B6 mice. *J Neurosci Res, 87*(8), 1913-1921. doi:10.1002/jnr.22012

Hunter RL, Dragicevic N, Seifert K, Choi DY, Liu M, Kim H-C, Cass WA, Sullivan PG, & Bing G. (2007). Inflammation induces mitochondrial dysfunction and dopaminergic neurodegeneration in the nigrostriatal system. *Journal of neurochemistry, 100*(5), 1375-1386. doi:10.1111/j.1471-4159.2006.04327.x

Hwang O. (2013). Role of oxidative stress in Parkinson's disease. *Experimental neurobiology, 22*(1), 11-17. doi:10.5607/en.2013.22.1.11

Iranzo A, Fernández-Arcos A, Tolosa E, Serradell M, Molinuevo JL, Valldeoriola F, Gelpi E, Vilaseca I, Sánchez-Valle R, Lladó A, Gaig C, & Santamaría J. (2014). Neurodegenerative disorder risk in idiopathic REM sleep behavior disorder: study in 174 patients. *PLoS One, 9*(2), e89741-e89741. doi:10.1371/journal.pone.0089741

Itier J-M, Ibáñez P, Mena MA, Abbas N, Cohen-Salmon C, Bohme GA, Laville M, Pratt J, Corti O, Pradier L, Ret G, Joubert C, Periquet M, Araujo F, Negroni J, Casarejos MJ, Canals S, Solano R, Serrano A, Gallego E, Sánchez M, Denèfle P, Benavides J, Tremp G, Rooney TA, Brice A, & García de Yébenes J. (2003). Parkin gene inactivation alters behaviour and dopamine neurotransmission in the mouse. *Hum Mol Genet, 12*(18), 2277-2291. doi:10.1093/hmg/ddg239

Iwaki H, Blauwendraat C, Leonard HL, Liu G, Maple-Grødem J, Corvol J-C, Pihlstrøm L, van Nimwegen M, Hutten SJ, Nguyen K-DH, Rick J, Eberly S, Faghri F, Auinger P, Scott KM, Wijeyekoon R, Van Deerlin VM, Hernandez DG, Day-Williams AG, Brice A, Alves G, Noyce AJ, Tysnes O-B, Evans JR, Breen DP, Estrada K, Wegel CE, Danjou F, Simon DK, Ravina B, Toft M, Heutink P, Bloem BR, Weintraub D, Barker RA, Williams-Gray CH, van de Warrenburg BP, Van Hilten JJ, Scherzer CR, Singleton AB, & Nalls MA. (2019). Genetic risk of Parkinson disease and progression. *Neurology Genetics, 5*(4), e348. doi:10.1212/nxg.0000000000000348

Jackson-Lewis V, & Przedborski S. (2007). Protocol for the MPTP mouse model of Parkinson's disease. *Nat Protoc, 2*(1), 141-151. doi:10.1038/nprot.2006.342

Janezic S, Threlfell S, Dodson PD, Dowie MJ, Taylor TN, Potgieter D, Parkkinen L, Senior SL, Anwar S, Ryan B, Deltheil T, Kosillo P, Cioroch M, Wagner K, Ansorge O, Bannerman DM, Bolam JP, Magill PJ, Cragg SJ, & Wade-Martins R. (2013). Deficits in dopaminergic transmission precede neuron loss and dysfunction in a new Parkinson model. *Proceedings of the National Academy of Sciences of the United States of America, 110*(42), E4016-E4025. doi:10.1073/pnas.1309143110

Jarmalaviciute A, Tunaitis V, Pivoraite U, Venalis A, & Pivoriunas A. (2015). Exosomes from dental pulp stem cells rescue human dopaminergic neurons from 6-hydroxy-dopamine-induced apoptosis. *Cytotherapy, 17*(7), 932-939. doi:10.1016/j.jcyt.2014.07.013

Jellinger KA. (2014). The pathomechanisms underlying Parkinson's disease. *Expert review of neurotherapeutics, 14*(2), 199-215. doi:10.1586/14737175.2014.877842

Jennings D, Siderowf A, Stern M, Seibyl J, Eberly S, Oakes D, Marek K, & Investigators P. (2014). Imaging prodromal Parkinson disease: the Parkinson Associated Risk Syndrome Study. *Neurology, 83*(19), 1739-1746. doi:10.1212/wnl.0000000000000960

Jiang H, Wang J, Rogers J, & Xie J. (2017). Brain Iron Metabolism Dysfunction in Parkinson's Disease. *Molecular Neurobiology, 54*(4), 3078-3101. doi:10.1007/s12035-016-9879-1

Jiang P, & Dickson DW. (2018). Parkinson's disease: experimental models and reality. *Acta neuropathologica, 135*(1), 13-32. doi:10.1007/s00401-017-1788-5

Jo J, Xiao Y, Sun AX, Cukuroglu E, Tran H-D, Göke J, Tan ZY, Saw TY, Tan C-P, Lokman H, Lee Y, Kim D, Ko HS, Kim S-O, Park JH, Cho N-J, Hyde TM, Kleinman JE, Shin JH, Weinberger DR, Tan EK, Je HS, & Ng H-H. (2016). Midbrain-like Organoids from Human Pluripotent Stem Cells Contain Functional Dopaminergic and Neuromelanin-Producing Neurons. *Cell Stem Cell, 19*(2), 248-257. doi:10.1016/j.stem.2016.07.005

Johannessen JN, Chiueh CC, Burns RS, & Markey SP. (1985). Differences in the metabolism of MPTP in the rodent and primate parallel differences in sensitivity to its neurotoxic effects. *Life sciences, 36*(3), 219-224. doi:10.1016/0024-3205(85)90062-1

Kahle PJ, Waak J, & Gasser T. (2009). DJ-1 and prevention of oxidative stress in Parkinson's disease and other age-related disorders. *Free radical biology & medicine, 47*(10), 1354-1361. doi:10.1016/j.freeradbiomed.2009.08.003

Kalia LV, & Lang AE. (2015). Parkinson's disease. *Lancet (London, England), 386*(9996), 896-912. doi:10.1016/s0140-6736(14)61393-3

Kaushik S, & Cuervo AM. (2015). Proteostasis and aging. *Nature Medicine, 21*(12), 1406-1415. doi:10.1038/nm.4001

Kelava I, & Lancaster MA. (2016). Dishing out mini-brains: Current progress and future prospects in brain organoid research. *Developmental Biology, 420*(2), 199-209. doi:https://doi.org/10.1016/j.ydbio.2016.06.037

Kim RH, Smith PD, Aleyasin H, Hayley S, Mount MP, Pownall S, Wakeham A, You-Ten AJ, Kalia SK, Horne P, Westaway D, Lozano AM, Anisman H, Park DS, & Mak TW. (2005). Hypersensitivity of DJ-1-deficient mice to 1-methyl-4-phenyl-1,2,3,6-tetrahydropyrindine (MPTP) and oxidative stress. *Proceedings of the National Academy of Sciences of the United States of America, 102*(14), 5215-5220. doi:10.1073/pnas.0501282102

Kim Y-J, Park H-J, Lee G, Bang OY, Ahn YH, Joe E, Kim HO, & Lee PH. (2009). Neuroprotective effects of human mesenchymal stem cells on dopaminergic neurons through anti-inflammatory action. *Glia, 57*(1), 13-23. doi:10.1002/glia.20731

Kin K, Yasuhara T, Kameda M, & Date I. (2019). Animal Models for Parkinson's Disease Research: Trends in the 2000s. *International journal of molecular sciences, 20*(21), 5402. doi:10.3390/ijms20215402

Kirik D, Rosenblad C, & Björklund A. (1998). Characterization of behavioral and neurodegenerative changes following partial lesions of the nigrostriatal dopamine system induced by intrastriatal 6-hydroxydopamine in the rat. *Experimental Neurology, 152*(2), 259-277. doi:10.1006/exnr.1998.6848

Kirik D, Rosenblad C, Burger C, Lundberg C, Johansen TE, Muzyczka N, Mandel RJ, & Bjorklund A. (2002). Parkinson-like neurodegeneration induced by targeted overexpression of alpha-synuclein in the nigrostriatal system. *J Neurosci., 22*(7), 2780-2791.

Kitada T, Asakawa S, Hattori N, Matsumine H, Yamamura Y, Minoshima S, Yokochi M, Mizuno Y, & Shimizu N. (1998). Mutations in the parkin gene cause autosomal recessive juvenile parkinsonism. *Nature, 392*(6676), 605-608. doi:10.1038/33416

Kitada T, Pisani A, Karouani M, Haburcak M, Martella G, Tscherter A, Platania P, Wu B, Pothos EN, & Shen J. (2009). Impaired dopamine release and synaptic plasticity in the striatum of Parkin−/− mice. *Journal of Neurochemistry, 110*(2), 613-621. doi:10.1111/j.1471-4159.2009.06152.x

Klein A, Wessolleck J, Papazoglou A, Metz GA, & Nikkhah G. (2009). Walking pattern analysis after unilateral 6-OHDA lesion and transplantation of foetal dopaminergic progenitor cells in rats. *Behavioural brain research, 199*(2), 317-325. doi:10.1016/j.bbr.2008.12.007

Klein C, Lohmann-Hedrich K, Rogaeva E, Schlossmacher MG, & Lang AE. (2007). Deciphering the role of heterozygous mutations in genes associated with parkinsonism. *The Lancet. Neurology, 6*(7), 652-662. doi:10.1016/s1474-4422(07)70174-6

Knie B, Mitra MT, Logishetty K, & Chaudhuri KR. (2011). Excessive daytime sleepiness in patients with Parkinson's disease. *CNS drugs, 25*(3), 203-212. doi:10.2165/11539720-000000000-00000

Konala VB, Mamidi MK, Bhonde R, Das AK, Pochampally R, & Pal R. (2016). The current landscape of the mesenchymal stromal cell secretome: A new paradigm for cell-free regeneration. *Cytotherapy., 18*(1), 13-24. doi:10.1016/j.jcyt.2015.10.008

Konnova E, & Swanberg M. (2018). Animal Models of Parkinson's Disease. In T. Stoker & J. Greenland (Eds.), *Parkinson's Disease: Pathogenesis and Clinical Aspects [Internet]*. Brisbane (AU): Codon Publications.

Koprich JB, Kalia LV, & Brotchie JM. (2017). Animal models of α-synucleinopathy for Parkinson disease drug development. *Nature reviews. Neuroscience, 18*(9), 515-529. doi:10.1038/nrn.2017.75

Kordower JH, Chu Y, Hauser RA, Freeman TB, & Olanow CW. (2008). Lewy body–like pathology in long-term embryonic nigral transplants in Parkinson's disease. *Nature Medicine, 14*(5), 504-506. doi:10.1038/nm1747

Kriks S, Shim J-W, Piao J, Ganat YM, Wakeman DR, Xie Z, Carrillo-Reid L, Auyeung G, Antonacci C, Buch A, Yang L, Beal MF, Surmeier DJ, Kordower JH, Tabar V, & Studer L. (2011). Dopamine neurons derived from human ES cells efficiently engraft in animal models of Parkinson/'s disease. *Nature, 480*(7378), 547-551. doi:http://www.nature.com/nature/journal/v480/n7378/abs/nature10648.html#supplementary-information

Kritzinger A, Ferger B, Gillardon F, Stierstorfer B, Birk G, Kochanek S, & Ciossek T. (2018). Age-related pathology after adenoviral overexpression of the leucine-rich repeat kinase 2 in the mouse striatum. *Neurobiol Aging, 66*, 97-111. doi:https://doi.org/10.1016/j.neurobiolaging.2018.02.008

Kühn AA, Kempf F, Brücke C, Gaynor Doyle L, Martinez-Torres I, Pogosyan A, Trottenberg T, Kupsch A, Schneider G-H, Hariz MI, Vandenberghe W, Nuttin B, & Brown P. (2008). High-frequency stimulation of the subthalamic nucleus suppresses oscillatory beta activity in patients with Parkinson's disease in parallel with improvement in motor performance. *J Neurosci, 28*(24), 6165-6173. doi:10.1523/jneurosci.0282-08.2008

La Manno G, Gyllborg D, Codeluppi S, Nishimura K, Salto C, Zeisel A, Borm LE, Stott SRW, Toledo EM, Villaescusa JC, Lönnerberg P, Ryge J, Barker RA, Arenas E, & Linnarsson S. (2016). Molecular Diversity of Midbrain Development in Mouse, Human, and Stem Cells. *Cell, 167*(2), 566-580.e519. doi:10.1016/j.cell.2016.09.027

Lai RC, Arslan F, Lee MM, Sze NS, Choo A, Chen TS, Salto-Tellez M, Timmers L, Lee CN, El Oakley RM, Pasterkamp G, de Kleijn DP, & Lim SK. (2010). Exosome secreted by MSC reduces myocardial ischemia/reperfusion injury. *Stem Cell Res, 4*(3), 214-222. doi:10.1016/j.scr.2009.12.003

Lanciego JL, Luquin N, & Obeso JA. (2012). Functional neuroanatomy of the basal ganglia. *Cold Spring Harbor perspectives in medicine, 2*(12), a009621-a009621. doi:10.1101/cshperspect.a009621

Langston JW, Ballard P, Tetrud JW, & Irwin I. (1983). Chronic Parkinsonism in humans due to a product of meperidine-analog synthesis. *Science (New York, N.Y.), 219*(4587), 979-980. doi:10.1126/science.6823561

Langston JW, Langston EB, & Irwin I. (1984). MPTP-induced parkinsonism in human and non-human primates–clinical and experimental aspects. *Acta neurologica Scandinavica. Supplementum, 100*, 49-54.

Lashuel HA, Overk CR, Oueslati A, & Masliah E. (2013). The many faces of α-synuclein: from structure and toxicity to therapeutic target. *Nature Reviews Neuroscience, 14*(1), 38-48. doi:10.1038/nrn3406

Lee BD, Shin J-H, VanKampen J, Petrucelli L, West AB, Ko HS, Lee Y-I, Maguire-Zeiss KA, Bowers WJ, Federoff HJ, Dawson VL, & Dawson TM. (2010). Inhibitors of leucine-rich repeat kinase-2 protect against models of Parkinson's disease. *Nature medicine, 16*(9), 998-1000. doi:10.1038/nm.2199

Lee CS, Sauer H, & Bjorklund A. (1996). Dopaminergic neuronal degeneration and motor impairments following axon terminal lesion by instrastriatal 6-hydroxydopamine in the rat. *Neuroscience, 72*(3), 641-653. doi:10.1016/0306-4522(95)00571-4

Lee EJ, Fomenko A, & Lozano AM. (2019). Magnetic Resonance-Guided Focused Ultrasound : Current Status and Future Perspectives in Thermal Ablation and Blood-Brain Barrier Opening. *Journal of Korean Neurosurgical Society, 62*(1), 10-26. doi:10.3340/jkns.2018.0180

Lee H-Y, Hsieh T-H, Liang J-I, Yeh M-L, & Chen J-JJ. (2012). Quantitative video-based gait pattern analysis for hemiparkinsonian rats. *Medical & biological engineering & computing, 50*(9), 937-946. doi:10.1007/s11517-012-0933-5

Li H, Jiang H, Zhang B, & Feng J. (2018). Modeling Parkinson's Disease Using Patient-specific Induced Pluripotent Stem Cells. *J Parkinsons Dis, 8*(4), 479-493. doi:10.3233/jpd-181353

Li J-Y, Englund E, Holton JL, Soulet D, Hagell P, Lees AJ, Lashley T, Quinn NP, Rehncrona S, Björklund A, Widner H, Revesz T, Lindvall O, & Brundin P. (2008). Lewy bodies in grafted neurons in subjects with Parkinson's disease suggest host-to-graft disease propagation. *Nature Medicine, 14*(5), 501-503. doi:10.1038/nm1746

Li Y, Liu W, Oo TF, Wang L, Tang Y, Jackson-Lewis V, Zhou C, Geghman K, Bogdanov M, Przedborski S, Beal MF, Burke RE, & Li C. (2009). Mutant LRRK2(R1441G) BAC transgenic mice recapitulate cardinal features of Parkinson's disease. *Nature neuroscience, 12*(7), 826-828. doi:10.1038/nn.2349

Lian Q, Zhang Y, Zhang J, Zhang HK, Wu X, Lam FF, Kang S, Xia JC, Lai WH, Au KW, Chow YY, Siu CW, Lee CN, & Tse HF. (2010). Functional mesenchymal stem cells derived from human induced pluripotent stem cells attenuate limb ischemia in mice. *Circulation, 121*(9), 1113-1123.

Lin C-H, Lin J-W, Liu Y-C, Chang C-H, & Wu R-M. (2014). Risk of Parkinson's disease following severe constipation: a nationwide population-based cohort study. *Parkinsonism & related disorders, 20*(12), 1371-1375. doi:10.1016/j.parkreldis.2014.09.026

Lin X, Parisiadou L, Gu X-L, Wang L, Shim H, Sun L, Xie C, Long C-X, Yang W-J, Ding J, Chen ZZ, Gallant PE, Tao-Cheng J-H, Rudow G, Troncoso JC, Liu Z, Li Z, & Cai H. (2009). Leucine-Rich Repeat Kinase 2 Regulates the Progression of Neuropathology Induced by Parkinson's-Disease-Related Mutant α-synuclein. *Neuron, 64*(6), 807-827. doi:https://doi.org/10.1016/j.neuron.2009.11.006

Lin X, Parisiadou L, Sgobio C, Liu G, Yu J, Sun L, Shim H, Gu X-L, Luo J, Long C-X, Ding J, Mateo Y, Sullivan PH, Wu L-G, Goldstein DS, Lovinger D, & Cai H. (2012). Conditional expression of Parkinson's disease-related mutant α-synuclein in the midbrain dopaminergic neurons causes progressive neurodegeneration and degradation of transcription factor nuclear receptor related 1. *J Neurosci, 32*(27), 9248-9264. doi:10.1523/jneurosci.1731-12.2012

Lindersson E, Beedholm R, Højrup P, Moos T, Gai W, Hendil KB, & Jensen PH. (2004). Proteasomal inhibition by alpha-synuclein filaments and oligomers. *The Journal of biological chemistry, 279*(13), 12924-12934. doi:10.1074/jbc.M306390200

Lindvall O, Brundin P, Widner H, Rehncrona S, Gustavii B, Frackowiak R, Leenders KL, Sawle G, Rothwell JC, & Marsden CD. (1990). Grafts of fetal dopamine neurons survive and improve motor function in Parkinson's disease. *Science (New York, N.Y.), 247*(4942), 574-577. doi:10.1126/science.2105529

Lindvall O, Rehncrona S, Brundin P, Gustavii B, Astedt B, Widner H, Lindholm T, Björklund A, Leenders KL, Rothwell JC, Frackowiak R, Marsden D, Johnels B, Steg G, Freedman R, Hoffer BJ, Seiger A, Bygdeman M, Strömberg I, & Olson L. (1989). Human fetal dopamine neurons grafted into the striatum in two patients with severe Parkinson's disease. A detailed account of methodology and

a 6-month follow-up. *Archives of neurology, 46*(6), 615-631. doi:10.1001/archneur.1989.00520420033021

Lindvall O, Widner H, Rehncrona S, Brundin P, Odin P, Gustavii B, Frackowiak R, Leenders KL, Sawle G, & Rothwell JC. (1992). Transplantation of fetal dopamine neurons in Parkinson's disease: one-year clinical and neurophysiological observations in two patients with putaminal implants. *Annals of neurology, 31*(2), 155-165. doi:10.1002/ana.410310206

Little D, Ketteler R, Gissen P, & Devine MJ. (2019). Using stem cell-derived neurons in drug screening for neurological diseases. *Neurobiol Aging, 78*, 130-141. doi:10.1016/j.neurobiolaging.2019.02.008

Liu X-S, Li J-F, Wang S-S, Wang Y-T, Zhang Y-Z, Yin H-L, Geng S, Gong H-C, Han B, & Wang Y-L. (2014). Human umbilical cord mesenchymal stem cells infected with adenovirus expressing HGF promote regeneration of damaged neuron cells in a Parkinson's disease model. *Biomed Res Int, 2014*, 909657-909657. doi:10.1155/2014/909657

Loh Y-H, Agarwal S, Park I-H, Urbach A, Huo H, Heffner GC, Kim K, Miller JD, Ng K, & Daley GQ. (2009). Generation of induced pluripotent stem cells from human blood. *Blood, 113*(22), 5476.

Lopes FM, Bristot IJ, da Motta LL, Parsons RB, & Klamt F. (2017). Mimicking Parkinson's Disease in a Dish: Merits and Pitfalls of the Most Commonly used Dopaminergic In Vitro Models. *Neuromolecular medicine, 19*(2-3), 241-255. doi:10.1007/s12017-017-8454-x

Lotharius J, Barg S, Wiekop P, Lundberg C, Raymon HK, & Brundin P. (2002). Effect of mutant alpha-synuclein on dopamine homeostasis in a new human mesencephalic cell line. *The Journal of biological chemistry, 277*(41), 38884-38894. doi:10.1074/jbc.M205518200

Lu X-H, Fleming SM, Meurers B, Ackerson LC, Mortazavi F, Lo V, Hernandez D, Sulzer D, Jackson GR, Maidment NT, Chesselet M-F, & Yang XW. (2009). Bacterial artificial chromosome transgenic mice expressing a truncated mutant parkin exhibit age-dependent hypokinetic motor deficits, dopaminergic neuron degeneration, and accumulation of proteinase K-resistant alpha-synuclein. *J Neurosci, 29*(7), 1962-1976. doi:10.1523/jneurosci.5351-08.2009

Lücking CB, Dürr A, Bonifati V, Vaughan J, De Michele G, Gasser T, Harhangi BS, Meco G, Denèfle P, Wood NW, Agid Y, Brice A, French Parkinson's Disease Genetics Study G, & European Consortium on Genetic Susceptibility in Parkinson's D. (2000). Association between early-onset Parkinson's disease and mutations in the parkin gene. *The New England journal of medicine, 342*(21), 1560-1567. doi:10.1056/nejm200005253422103

Luk KC, Kehm V, Carroll J, Zhang B, O'Brien P, Trojanowski JQ, & Lee VMY. (2012). Pathological α-synuclein transmission initiates Parkinson-like neurodegeneration in nontransgenic mice. *Science (New York, N.Y.), 338*(6109), 949-953. doi:10.1126/science.1227157

Magen I, & Chesselet M-F. (2010). Genetic mouse models of Parkinson's disease The state of the art. *Progress in brain research, 184*, 53-87. doi:10.1016/s0079-6123(10)84004-x

Magnard R, Vachez Y, Carcenac C, Krack P, David O, Savasta M, Boulet S, & Carnicella S. (2016). What can rodent models tell us about apathy and associated neuropsychiatric symptoms in Parkinson's disease? *Translational psychiatry, 6*(3), e753-e753. doi:10.1038/tp.2016.17

Mahlknecht P, Iranzo A, Högl B, Frauscher B, Müller C, Santamaría J, Tolosa E, Serradell M, Mitterling T, Gschliesser V, Goebel G, Brugger F, Scherfler C, Poewe W, Seppi K, & Sleep Innsbruck Barcelona G. (2015). Olfactory dysfunction predicts early transition to a Lewy body disease in idiopathic RBD. *Neurology, 84*(7), 654-658. doi:10.1212/wnl.0000000000001265

Maqsood MI, Matin MM, Bahrami AR, & Ghasroldasht MM. (2013). Immortality of cell lines: challenges and advantages of establishment. *Cell biology international, 37*(10), 1038-1045. doi:10.1002/cbin.10137

Maraganore DM, Lesnick TG, Elbaz A, Chartier-Harlin M-C, Gasser T, Krüger R, Hattori N, Mellick GD, Quattrone A, Satoh J-I, Toda T, Wang J, Ioannidis JPA, de Andrade M, Rocca WA, & Consortium UGG. (2004). UCHL1 is a Parkinson's disease susceptibility gene. *Annals of neurology, 55*(4), 512-521. doi:10.1002/ana.20017

Marote A, Teixeira FG, Mendes-Pinheiro B, & Salgado AJ. (2016). MSCs-Derived Exosomes: Cell-Secreted Nanovesicles with Regenerative Potential. *Frontiers in Pharmacology, 7*(231). doi:10.3389/fphar.2016.00231

Marotta N, Kim S, & Krainc D. (2020). Organoid and pluripotent stem cells in Parkinson's disease modeling: an expert view on their value to drug discovery. *Expert opinion on drug discovery*, 1-15. doi:10.1080/17460441.2020.1703671

Marques CR, Marote A, Mendes-Pinheiro B, Teixeira FG, & Salgado AJ. (2018). Cell secretome based approaches in Parkinson's disease regenerative medicine. *Expert Opinion on Biological Therapy, 18*(12), 1235-1245. doi:10.1080/14712598.2018.1546840

Marras C, & Lang A. (2013). Parkinson's disease subtypes: lost in translation? *Journal of Neurology, Neurosurgery & Psychiatry, 84*(4), 409. doi:10.1136/jnnp-2012-303455

Martin LJ, Pan Y, Price AC, Sterling W, Copeland NG, Jenkins NA, Price DL, & Lee MK. (2006). Parkinson's disease alpha-synuclein transgenic mice develop neuronal mitochondrial degeneration and cell death. *J Neurosci, 26*(1), 41-50. doi:10.1523/jneurosci.4308-05.2006

Martínez-Fernández R, Rodríguez-Rojas R, del Álamo M, Hernández-Fernández F, Pineda-Pardo JA, Dileone M, Alonso-Frech F, Foffani G, Obeso I, Gasca-Salas C, de Luis-Pastor E, Vela L, & Obeso JA. (2018). Focused ultrasound subthalamotomy in patients with asymmetric Parkinson's disease: a pilot study. *The Lancet Neurology, 17*(1), 54-63. doi:10.1016/s1474-4422(17)30403-9

Marton Rebecca M, & Paşca Sergiu P. (2016). Neural Differentiation in the Third Dimension: Generating a Human Midbrain. *Cell Stem Cell, 19*(2), 145-146. doi:10.1016/j.stem.2016.07.017

Masuda-Suzukake M, Nonaka T, Hosokawa M, Oikawa T, Arai T, Akiyama H, Mann DMA, & Hasegawa M. (2013). Prion-like spreading of pathological α-synuclein in brain. *Brain : a journal of neurology, 136*(Pt 4), 1128-1138. doi:10.1093/brain/awt037

Mateus-Pinheiro A, Patrício P, Alves ND, Machado-Santos AR, Morais M, Bessa JM, Sousa N, & Pinto L. (2014). The Sweet Drive Test: refining phenotypic characterization of anhedonic behavior in rodents. *Front Behav Neurosci, 8*, 74-74. doi:10.3389/fnbeh.2014.00074

Mazzulli JR, Xu Y-H, Sun Y, Knight AL, McLean PJ, Caldwell GA, Sidransky E, Grabowski GA, & Krainc D. (2011). Gaucher disease glucocerebrosidase and α-synuclein form a bidirectional pathogenic loop in synucleinopathies. *Cell, 146*(1), 37-52. doi:10.1016/j.cell.2011.06.001

McCoy MK, Martinez TN, Ruhn KA, Wrage PC, Keefer EW, Botterman BR, Tansey KE, & Tansey MG. (2008). Autologous transplants of Adipose-Derived Adult Stromal (ADAS) cells afford dopaminergic neuroprotection in a model of Parkinson's disease. *Experimental Neurology, 210*(1), 14-29. doi:10.1016/j.expneurol.2007.10.011

Medeiros DdC, Lopes Aguiar C, Moraes MFD, & Fisone G. (2019). Sleep Disorders in Rodent Models of Parkinson's Disease. *Frontiers in Pharmacology, 10*(1414). doi:10.3389/fphar.2019.01414

Mendes-Pinheiro B, Anjo SI, Manadas B, Da Silva JD, Marote A, Behie LA, Teixeira FG, & Salgado AJ. (2019). Bone Marrow Mesenchymal Stem Cells' Secretome Exerts Neuroprotective Effects in a Parkinson's Disease Rat Model. *Frontiers in bioengineering and biotechnology, 7*, 294-294. doi:10.3389/fbioe.2019.00294

Mertens J, Marchetto MC, Bardy C, & Gage FH. (2016). Evaluating cell reprogramming, differentiation and conversion technologies in neuroscience. *Nature Reviews Neuroscience, 17*(7), 424-437. doi:10.1038/nrn.2016.46

Mertens J, Reid D, Lau S, Kim Y, & Gage FH. (2018). Aging in a Dish: iPSC-Derived and Directly Induced Neurons for Studying Brain Aging and Age-Related Neurodegenerative Diseases. *Annual review of genetics, 52*, 271-293. doi:10.1146/annurev-genet-120417-031534

Mesholam RI, Moberg PJ, Mahr RN, & Doty RL. (1998). Olfaction in neurodegenerative disease: a meta-analysis of olfactory functioning in Alzheimer's and Parkinson's diseases. *Archives of neurology, 55*(1), 84-90. doi:10.1001/archneur.55.1.84

Michel Patrick P, Hirsch Etienne C, & Hunot S. (2016). Understanding Dopaminergic Cell Death Pathways in Parkinson Disease. *Neuron, 90*(4), 675-691. doi:10.1016/j.neuron.2016.03.038

Michel PP, Toulorge D, Guerreiro S, & Hirsch EC. (2013). Specific needs of dopamine neurons for stimulation in order to survive: implication for Parkinson disease. *The FASEB Journal, 27*(9), 3414-3423. doi:10.1096/fj.12-220418

Miller Justine D, Ganat Yosif M, Kishinevsky S, Bowman Robert L, Liu B, Tu Edmund Y, Mandal PK, Vera E, Shim J-w, Kriks S, Taldone T, Fusaki N, Tomishima Mark J, Krainc D, Milner Teresa A, Rossi Derrick J, & Studer L. (2013). Human iPSC-Based Modeling of Late-Onset Disease via Progerin-Induced Aging. *Cell Stem Cell, 13*(6), 691-705. doi:10.1016/j.stem.2013.11.006

Moehle MS, & West AB. (2015). M1 and M2 immune activation in Parkinson's Disease: Foe and ally? *Neuroscience, 302*, 59-73. doi:10.1016/j.neuroscience.2014.11.018

Moloney TC, Rooney GE, Barry FP, Howard L, & Dowd E. (2010). Potential of rat bone marrow-derived mesenchymal stem cells as vehicles for delivery of neurotrophins to the Parkinsonian rat brain. *Brain Res, 1359*, 33-43. doi:10.1016/j.brainres.2010.08.040

Montoya CP, Campbell-Hope LJ, Pemberton KD, & Dunnett SB. (1991). The "staircase test": a measure of independent forelimb reaching and grasping abilities in rats. *J Neurosci Methods., 36*(2-3), 219-228.

Monzel AS, Smits LM, Hemmer K, Hachi S, Moreno EL, van Wuellen T, Jarazo J, Walter J, Brüggemann I, Boussaad I, Berger E, Fleming RMT, Bolognin S, & Schwamborn JC. (2017). Derivation of Human Midbrain-Specific Organoids from Neuroepithelial Stem Cells. *Stem Cell Reports, 8*(5), 1144-1154. doi:10.1016/j.stemcr.2017.03.010

Morens DM, Davis JW, Grandinetti A, Ross GW, Popper JS, & White LR. (1996). Epidemiologic observations on Parkinson's disease: incidence and mortality in a prospective study of middle-aged men. *Neurology, 46*(4), 1044-1050. doi:10.1212/wnl.46.4.1044

Mosharov EV, Larsen KE, Kanter E, Phillips KA, Wilson K, Schmitz Y, Krantz DE, Kobayashi K, Edwards RH, & Sulzer D. (2009). Interplay between cytosolic dopamine, calcium, and alpha-synuclein causes selective death of substantia nigra neurons. *Neuron, 62*(2), 218-229. doi:10.1016/j.neuron.2009.01.033

Munoz JR, Stoutenger BR, Robinson AP, Spees JL, & Prockop DJ. (2005). Human stem/progenitor cells from bone marrow promote neurogenesis of endogenous neural stem cells in the hippocampus of mice. *Proceedings of the National Academy of Sciences of the United States of America, 102*(50), 18171-18176. doi:10.1073/pnas.0508945102

Murphy KE, Gysbers AM, Abbott SK, Tayebi N, Kim WS, Sidransky E, Cooper A, Garner B, & Halliday GM. (2014). Reduced glucocerebrosidase is associated with increased α-synuclein in sporadic Parkinson's disease. *Brain, 137*(3), 834-848. doi:10.1093/brain/awt367

Nakabeppu Y, Tsuchimoto D, Yamaguchi H, & Sakumi K. (2007). Oxidative damage in nucleic acids and Parkinson's disease. *J Neurosci Res, 85*(5), 919-934. doi:10.1002/jnr.21191

Nalls MA, Pankratz N, Lill CM, Do CB, Hernandez DG, Saad M, DeStefano AL, Kara E, Bras J, Sharma M, Schulte C, Keller MF, Arepalli S, Letson C, Edsall C, Stefansson H, Liu X, Pliner H, Lee JH, Cheng R, International Parkinson's Disease Genomics C, Parkinson's Study Group Parkinson's Research: The Organized GI, andMe, GenePd, NeuroGenetics Research C, Hussman Institute of Human G, Ashkenazi Jewish Dataset I, Cohorts for H, Aging Research in Genetic E, North American Brain Expression C, United Kingdom Brain Expression C, Greek Parkinson's Disease C, Alzheimer Genetic Analysis G, Ikram MA, Ioannidis JPA, Hadjigeorgiou GM, Bis JC, Martinez M, Perlmutter JS, Goate A, Marder K, Fiske B, Sutherland M, Xiromerisiou G, Myers RH, Clark LN, Stefansson K, Hardy JA, Heutink P, Chen H, Wood NW, Houlden H, Payami H, Brice A, Scott WK, Gasser T, Bertram L, Eriksson N, Foroud T, & Singleton AB. (2014). Large-scale meta-analysis of genome-wide association data identifies six new risk loci for Parkinson's disease. *Nature genetics, 46*(9), 989-993. doi:10.1038/ng.3043

Nambu A, Tokuno H, & Takada M. (2002). Functional significance of the cortico-subthalamo-pallidal 'hyperdirect' pathway. *Neuroscience research, 43*(2), 111-117. doi:10.1016/s0168-0102(02)00027-5

Narendra D, Walker JE, & Youle R. (2012). Mitochondrial quality control mediated by PINK1 and Parkin: links to parkinsonism. *Cold Spring Harbor perspectives in biology, 4*(11), a011338. doi:10.1101/cshperspect.a011338

Narendra DP, Jin SM, Tanaka A, Suen D-F, Gautier CA, Shen J, Cookson MR, & Youle RJ. (2010). PINK1 Is Selectively Stabilized on Impaired Mitochondria to Activate Parkin. *PLOS Biology, 8*(1), e1000298. doi:10.1371/journal.pbio.1000298

Neumann W-J, Schroll H, de Almeida Marcelino AL, Horn A, Ewert S, Irmen F, Krause P, Schneider G-H, Hamker F, & Kühn AA. (2018). Functional segregation of basal ganglia pathways in Parkinson's disease. *Brain : a journal of neurology, 141*(9), 2655-2669. doi:10.1093/brain/awy206

Nguyen Ha N, Byers B, Cord B, Shcheglovitov A, Byrne J, Gujar P, Kee K, Schüle B, Dolmetsch Ricardo E, Langston W, Palmer Theo D, & Pera Renee R. (2011). LRRK2 Mutant iPSC-Derived DA Neurons Demonstrate Increased Susceptibility to Oxidative Stress. *Cell Stem Cell, 8*(3), 267-280. doi:10.1016/j.stem.2011.01.013

Nicklas WJ, Youngster SK, Kindt MV, & Heikkila RE. (1987). MPTP, MPP+ and mitochondrial function. *Life sciences, 40*(8), 721-729. doi:10.1016/0024-3205(87)90299-2

Noyce AJ, Bestwick JP, Silveira-Moriyama L, Hawkes CH, Giovannoni G, Lees AJ, & Schrag A. (2012). Meta-analysis of early nonmotor features and risk factors for Parkinson disease. *Annals of neurology, 72*(6), 893-901. doi:10.1002/ana.23687

Noyce AJ, Lees AJ, & Schrag A-E. (2016). The prediagnostic phase of Parkinson's disease. *Journal of Neurology, Neurosurgery & Psychiatry, 87*(8), 871. doi:10.1136/jnnp-2015-311890

Nuber S, Petrasch-Parwez E, Winner B, Winkler J, von Hörsten S, Schmidt T, Boy J, Kuhn M, Nguyen HP, Teismann P, Schulz JB, Neumann M, Pichler BJ, Reischl G, Holzmann C, Schmitt I, Bornemann A, Kuhn W, Zimmermann F, Servadio A, & Riess O. (2008). Neurodegeneration and motor dysfunction in a conditional model of Parkinson's disease. *J Neurosci, 28*(10), 2471-2484. doi:10.1523/jneurosci.3040-07.2008

Oaks AW, Frankfurt M, Finkelstein DI, & Sidhu A. (2013). Age-dependent effects of A53T alpha-synuclein on behavior and dopaminergic function. *PLoS One, 8*(4), e60378-e60378. doi:10.1371/journal.pone.0060378

Obeso JA, Rodriguez-Oroz MC, Goetz CG, Marin C, Kordower JH, Rodriguez M, Hirsch EC, Farrer M, Schapira AHV, & Halliday G. (2010). Missing pieces in the Parkinson's disease puzzle. *Nat Med, 16*(6), 653-661.

Obeso JA, Stamelou M, Goetz CG, Poewe W, Lang AE, Weintraub D, Burn D, Halliday GM, Bezard E, Przedborski S, Lehericy S, Brooks DJ, Rothwell JC, Hallett M, DeLong MR, Marras C, Tanner CM, Ross GW, Langston JW, Klein C, Bonifati V, Jankovic J, Lozano AM, Deuschl G, Bergman H, Tolosa E, Rodriguez-Violante M, Fahn S, Postuma RB, Berg D, Marek K, Standaert DG, Surmeier DJ, Olanow CW, Kordower JH, Calabresi P, Schapira AHV, & Stoessl AJ. (2017). Past, present, and future of Parkinson's disease: A special essay on the 200th Anniversary of the Shaking Palsy. *Movement disorders : official journal of the Movement Disorder Society, 32*(9), 1264-1310. doi:10.1002/mds.27115

Oertel W, & Schulz JB. (2016). Current and experimental treatments of Parkinson disease: A guide for neuroscientists. *Journal of neurochemistry, 139 Suppl 1*, 325-337. doi:10.1111/jnc.13750

Offen D, Barhum Y, Levy YS, Burshtein A, Panet H, Cherlow T, & Melamed E. (2007). Intrastriatal transplantation of mouse bone marrow-derived stem cells improves motor behavior in a mouse model of Parkinson's disease. *Journal of neural transmission. Supplementum*(72), 133-143. doi:10.1007/978-3-211-73574-9_16

Oh SH, Kim HN, Park HJ, Shin JY, Bae EJ, Sunwoo MK, Lee SJ, & Lee PH. (2016). Mesenchymal Stem Cells Inhibit Transmission of alpha-Synuclein by Modulating Clathrin-Mediated Endocytosis in a Parkinsonian Model. *Cell Rep., 14*(4), 835-849. doi: 810.1016/j.celrep.2015.1012.1075. Epub 2016 Jan 1014.

Oh SH, Kim HN, Park HJ, Shin JY, Kim DY, & Lee PH. (2017). The Cleavage Effect of Mesenchymal Stem Cell and Its Derived Matrix Metalloproteinase-2 on Extracellular α-Synuclein Aggregates in Parkinsonian Models. *Stem Cells Translational Medicine, 6*(3), 949-961. doi:10.5966/sctm.2016-0111

Okun MS. (2012). Deep-brain stimulation for Parkinson's disease. *The New England journal of medicine, 367*(16), 1529-1538. doi:10.1056/NEJMct1208070

Olanow CW, & Prusiner SB. (2009). Is Parkinson's disease a prion disorder? *Proceedings of the National Academy of Sciences, 106*(31), 12571. doi:10.1073/pnas.0906759106

Oliveras-Salvá M, Macchi F, Coessens V, Deleersnijder A, Gérard M, Van der Perren A, Van den Haute C, & Baekelandt V. (2014). Alpha-synuclein-induced neurodegeneration is exacerbated in PINK1 knockout mice. *Neurobiol Aging, 35*(11), 2625-2636. doi:10.1016/j.neurobiolaging.2014.04.032

Oliveras-Salvá M, Van der Perren A, Casadei N, Stroobants S, Nuber S, D'Hooge R, Van den Haute C, & Baekelandt V. (2013). rAAV2/7 vector-mediated overexpression of alpha-synuclein in mouse substantia nigra induces protein aggregation and progressive dose-dependent neurodegeneration. *Molecular Neurodegeneration, 8*, 44-44. doi:10.1186/1750-1326-8-44

Olsson M, Nikkhah G, Bentlage C, & Björklund A. (1995). Forelimb akinesia in the rat Parkinson model: differential effects of dopamine agonists and nigral transplants as assessed by a new stepping test. *J Neurosci, 15*(5 Pt 2), 3863-3875. doi:10.1523/jneurosci.15-05-03863.1995

Palacino JJ, Sagi D, Goldberg MS, Krauss S, Motz C, Wacker M, Klose J, & Shen J. (2004). Mitochondrial dysfunction and oxidative damage in parkin-deficient mice. *The Journal of biological chemistry, 279*(18), 18614-18622. doi:10.1074/jbc.M401135200

Pålhagen S, Qi H, Mårtensson B, Wålinder J, Granérus A-K, & Svenningsson P. (2010). Monoamines, BDNF, IL-6 and corticosterone in CSF in patients with Parkinson's disease and major depression. *J Neurol, 257*(4), 524-532. doi:10.1007/s00415-009-5353-6

Papp M, Willner P, & Muscat R. (1991). An animal model of anhedonia: attenuation of sucrose consumption and place preference conditioning by chronic unpredictable mild stress. *Psychopharmacology, 104*(2), 255-259. doi:10.1007/bf02244188

Parga JA, García-Garrote M, Martínez S, Raya Á, Labandeira-García JL, & Rodríguez-Pallares J. (2018). Prostaglandin EP2 Receptors Mediate Mesenchymal Stromal Cell-Neuroprotective Effects on

Dopaminergic Neurons. *Molecular Neurobiology, 55*(6), 4763-4776. doi:10.1007/s12035-017-0681-5

Parkinson J. (2002). An essay on the shaking palsy. 1817. *J Neuropsychiatry Clin Neurosci., 14*(2), 223-236; discussion 222. doi: 210.1176/jnp.1114.1172.1223.

Parmar M, Grealish S, & Henchcliffe C. (2020). The future of stem cell therapies for Parkinson disease. *Nature Reviews Neuroscience, 21*(2), 103-115. doi:10.1038/s41583-019-0257-7

Paumier KL, Luk KC, Manfredsson FP, Kanaan NM, Lipton JW, Collier TJ, Steece-Collier K, Kemp CJ, Celano S, Schulz E, Sandoval IM, Fleming S, Dirr E, Polinski NK, Trojanowski JQ, Lee VM, & Sortwell CE. (2015). Intrastriatal injection of pre-formed mouse α-synuclein fibrils into rats triggers α-synuclein pathology and bilateral nigrostriatal degeneration. *Neurobiology of Disease, 82*, 185-199. doi:10.1016/j.nbd.2015.06.003

Periquet M, Latouche M, Lohmann E, Rawal N, De Michele G, Ricard S, Teive H, Fraix V, Vidailhet M, Nicholl D, Barone P, Wood NW, Raskin S, Deleuze J-F, Agid Y, Dürr A, Brice A, French Parkinson's Disease Genetics Study G, & European Consortium on Genetic Susceptibility in Parkinson's D. (2003). Parkin mutations are frequent in patients with isolated early-onset parkinsonism. *Brain : a journal of neurology, 126*(Pt 6), 1271-1278. doi:10.1093/brain/awg136

Perry T, Torres E, Czech C, Beyreuther K, Richards S, & Dunnett S. (1995). Cognitive and motor function in transgenic mice carrying excess copies of the 695 and 751 amino acid isoforms of the amyloid precursor protein gene.

Pezzoli G, & Cereda E. (2013). Exposure to pesticides or solvents and risk of Parkinson disease. *Neurology, 80*(22), 2035-2041. doi:10.1212/WNL.0b013e318294b3c8

Pham TT, Giesert F, Röthig A, Floss T, Kallnik M, Weindl K, Hölter SM, Ahting U, Prokisch H, Becker L, Klopstock T, Hrabé de Angelis M, Beyer K, Görner K, Kahle PJ, Vogt Weisenhorn DM, & Wurst W. (2010). DJ-1-deficient mice show less TH-positive neurons in the ventral tegmental area and exhibit non-motoric behavioural impairments. *Genes, Brain and Behavior, 9*(3), 305-317. doi:10.1111/j.1601-183X.2009.00559.x

Pienaar IS, Lu B, & Schallert T. (2012). Closing the gap between clinic and cage: sensori-motor and cognitive behavioural testing regimens in neurotoxin-induced animal models of Parkinson's disease. *Neuroscience and biobehavioral reviews, 36*(10), 2305-2324. doi:10.1016/j.neubiorev.2012.07.009

Pinho AG, Cibrão JR, Silva NA, Monteiro S, & Salgado AJ. (2020). Cell Secretome: Basic Insights and Therapeutic Opportunities for CNS Disorders. *Pharmaceuticals (Basel). 13*(2), E31. doi: 10.3390/ph13020031.

Pinho R, Paiva I, Jercic KG, Fonseca-Ornelas L, Gerhardt E, Fahlbusch C, Garcia-Esparcia P, Kerimoglu C, Pavlou MAS, Villar-Piqué A, Szego É, Lopes da Fonseca T, Odoardi F, Soeroes S, Rego AC, Fischle W, Schwamborn JC, Meyer T, Kügler S, Ferrer I, Attems J, Fischer A, Becker S, Zweckstetter M, Borovecki F, & Outeiro TF. (2019). Nuclear localization and phosphorylation modulate pathological effects of alpha-synuclein. *Hum Mol Genet, 28*(1), 31-50. doi:10.1093/hmg/ddy326

Pires AO, Teixeira FG, Mendes-Pinheiro B, Serra SC, Sousa N, & Salgado AJ. (2017). Old and new challenges in Parkinson's disease therapeutics. *Prog Neurobiol, 156*, 69-89. doi:https://doi.org/10.1016/j.pneurobio.2017.04.006

Pissadaki EK, & Bolam JP. (2013). The energy cost of action potential propagation in dopamine neurons: clues to susceptibility in Parkinson's disease. *Frontiers in computational neuroscience, 7*, 13-13. doi:10.3389/fncom.2013.00013

Pittenger MF, Mackay AM, Beck SC, Jaiswal RK, Douglas R, Mosca JD, Moorman MA, Simonetti DW, Craig S, & Marshak DR. (1999). Multilineage potential of adult human mesenchymal stem cells. *Science, 284*(5411), 143-147.

Poewe W, Seppi K, Tanner CM, Halliday GM, Brundin P, Volkmann J, Schrag A-E, & Lang AE. (2017). Parkinson disease. *Nature Reviews Disease Primers, 3*(1), 17013. doi:10.1038/nrdp.2017.13

Pollard AK, Craig EL, & Chakrabarti L. (2016). Mitochondrial Complex 1 Activity Measured by Spectrophotometry Is Reduced across All Brain Regions in Ageing and More Specifically in Neurodegeneration. *PLoS One, 11*(6), e0157405-e0157405. doi:10.1371/journal.pone.0157405

Polymeropoulos MH, Lavedan C, Leroy E, Ide SE, Dehejia A, Dutra A, Pike B, Root H, Rubenstein J, Boyer R, Stenroos ES, Chandrasekharappa S, Athanassiadou A, Papapetropoulos T, Johnson WG, Lazzarini AM, Duvoisin RC, Di Iorio G, Golbe LI, & Nussbaum RL. (1997). Mutation in the alpha-synuclein gene identified in families with Parkinson's disease. *Science (New York, N.Y.), 276*(5321), 2045-2047. doi:10.1126/science.276.5321.2045

Ponsen MM, Stoffers D, Twisk JWR, Wolters EC, & Berendse HW. (2009). Hyposmia and executive dysfunction as predictors of future Parkinson's disease: a prospective study. *Movement disorders : official journal of the Movement Disorder Society, 24*(7), 1060-1065. doi:10.1002/mds.22534

Postuma RB, Berg D, Stern M, Poewe W, Olanow CW, Oertel W, Obeso J, Marek K, Litvan I, Lang AE, Halliday G, Goetz CG, Gasser T, Dubois B, Chan P, Bloem BR, Adler CH, & Deuschl G. (2015a). MDS clinical diagnostic criteria for Parkinson's disease. *Movement Disorders, 30*(12), 1591-1601. doi:10.1002/mds.26424

Postuma RB, Gagnon J-F, Bertrand J-A, Génier Marchand D, & Montplaisir JY. (2015b). Parkinson risk in idiopathic REM sleep behavior disorder: preparing for neuroprotective trials. *Neurology, 84*(11), 1104-1113. doi:10.1212/wnl.0000000000001364

Postuma RB, Iranzo A, Hogl B, Arnulf I, Ferini-Strambi L, Manni R, Miyamoto T, Oertel W, Dauvilliers Y, Ju Y-E, Puligheddu M, Sonka K, Pelletier A, Santamaria J, Frauscher B, Leu-Semenescu S, Zucconi M, Terzaghi M, Miyamoto M, Unger MM, Carlander B, Fantini M-L, & Montplaisir JY. (2015c). Risk factors for neurodegeneration in idiopathic rapid eye movement sleep behavior disorder: a multicenter study. *Annals of neurology, 77*(5), 830-839. doi:10.1002/ana.24385

Postuma RB, Lang AE, Gagnon JF, Pelletier A, & Montplaisir JY. (2012). How does parkinsonism start? Prodromal parkinsonism motor changes in idiopathic REM sleep behaviour disorder. *Brain : a journal of neurology, 135*(Pt 6), 1860-1870. doi:10.1093/brain/aws093

Powers KM, Kay DM, Factor SA, Zabetian CP, Higgins DS, Samii A, Nutt JG, Griffith A, Leis B, Roberts JW, Martinez ED, Montimurro JS, Checkoway H, & Payami H. (2008). Combined effects of smoking, coffee, and NSAIDs on Parkinson's disease risk. *Movement disorders : official journal of the Movement Disorder Society, 23*(1), 88-95. doi:10.1002/mds.21782

Ramirez A, Heimbach A, Gründemann J, Stiller B, Hampshire D, Cid LP, Goebel I, Mubaidin AF, Wriekat A-L, Roeper J, Al-Din A, Hillmer AM, Karsak M, Liss B, Woods CG, Behrens MI, & Kubisch C. (2006). Hereditary parkinsonism with dementia is caused by mutations in ATP13A2, encoding a lysosomal type 5 P-type ATPase. *Nature Genetics, 38*(10), 1184-1191. doi:10.1038/ng1884

Ramonet D, Daher JPL, Lin BM, Stafa K, Kim J, Banerjee R, Westerlund M, Pletnikova O, Glauser L, Yang L, Liu Y, Swing DA, Beal MF, Troncoso JC, McCaffery JM, Jenkins NA, Copeland NG, Galter D, Thomas B, Lee MK, Dawson TM, Dawson VL, & Moore DJ. (2011). Dopaminergic neuronal loss, reduced neurite complexity and autophagic abnormalities in transgenic mice expressing G2019S mutant LRRK2. *PLoS One, 6*(4), e18568-e18568. doi:10.1371/journal.pone.0018568

Remy P, Doder M, Lees A, Turjanski N, & Brooks D. (2005). Depression in Parkinson's disease: loss of dopamine and noradrenaline innervation in the limbic system. *Brain : a journal of neurology, 128*(Pt 6), 1314-1322. doi:10.1093/brain/awh445

Ren X, Hinchie A, Swomley A, Powell DK, & Butterfield DA. (2019). Profiles of brain oxidative damage, ventricular alterations, and neurochemical metabolites in the striatum of PINK1 knockout rats as functions of age and gender: Relevance to Parkinson disease. *Free radical biology & medicine, 143*, 146-152. doi:10.1016/j.freeradbiomed.2019.08.008

Richardson JR, Quan Y, Sherer TB, Greenamyre JT, & Miller GW. (2005). Paraquat Neurotoxicity is Distinct from that of MPTP and Rotenone. *Toxicological Sciences, 88*(1), 193-201. doi:10.1093/toxsci/kfi304

Richfield EK, Thiruchelvam MJ, Cory-Slechta DA, Wuertzer C, Gainetdinov RR, Caron MG, Di Monte DA, & Federoff HJ. (2002). Behavioral and neurochemical effects of wild-type and mutated human alpha-synuclein in transgenic mice. *Experimental Neurology, 175*(1), 35-48. doi:10.1006/exnr.2002.7882

Ritz B, Lee P-C, Lassen CF, & Arah OA. (2014). Parkinson disease and smoking revisited: ease of quitting is an early sign of the disease. *Neurology, 83*(16), 1396-1402. doi:10.1212/wnl.0000000000000879

Ross GW, Petrovitch H, Abbott RD, Tanner CM, Popper J, Masaki K, Launer L, & White LR. (2008). Association of olfactory dysfunction with risk for future Parkinson's disease. *Annals of neurology, 63*(2), 167-173. doi:10.1002/ana.21291

Rousseaux MWC, Marcogliese PC, Qu D, Hewitt SJ, Seang S, Kim RH, Slack RS, Schlossmacher MG, Lagace DC, Mak TW, & Park DS. (2012). Progressive dopaminergic cell loss with unilateral-to-bilateral progression in a genetic model of Parkinson disease. *Proceedings of the National Academy of Sciences of the United States of America, 109*(39), 15918-15923. doi:10.1073/pnas.1205102109

Rozas G, Guerra MJ, & Labandeira-García JL. (1997). An automated rotarod method for quantitative drug-free evaluation of overall motor deficits in rat models of parkinsonism. *Brain research. Brain research protocols, 2*(1), 75-84. doi:10.1016/s1385-299x(97)00034-2

Russo SJ, & Nestler EJ. (2013). The brain reward circuitry in mood disorders. *Nature reviews. Neuroscience, 14*(9), 609-625. doi:10.1038/nrn3381

Sadan O, Bahat-Stromza M, Barhum Y, Levy YS, Pisnevsky A, Peretz H, Ilan AB, Bulvik S, Shemesh N, Krepel D, Cohen Y, Melamed E, & Offen D. (2009). Protective effects of neurotrophic factor-secreting cells in a 6-OHDA rat model of Parkinson disease. *Stem Cells Dev, 18*(8), 1179-1190. doi:10.1089/scd.2008.0411

Sakakibara R, Tateno F, Kishi M, Tsuyusaki Y, Terada H, & Inaoka T. (2014). MIBG myocardial scintigraphy in pre-motor Parkinson's disease: a review. *Parkinsonism & related disorders, 20*(3), 267-273. doi:10.1016/j.parkreldis.2013.11.001

Salgado AJ, Sousa JC, Costa BM, Pires AO, Mateus-Pinheiro A, Teixeira FG, Pinto L, & Sousa N. (2015). Mesenchymal stem cells secretome as a modulator of the neurogenic niche: basic insights and therapeutic opportunities. *Front Cell Neurosci, 9*(249). doi:10.3389/fncel.2015.00249

Santiago RM, Barbiero J, Gradowski RW, Bochen S, Lima MMS, Da Cunha C, Andreatini R, & Vital MABF. (2014). Induction of depressive-like behavior by intranigral 6-OHDA is directly correlated with deficits in striatal dopamine and hippocampal serotonin. *Behavioural brain research, 259*, 70-77. doi:10.1016/j.bbr.2013.10.035

Sardi SP, Clarke J, Viel C, Chan M, Tamsett TJ, Treleaven CM, Bu J, Sweet L, Passini MA, Dodge JC, Yu WH, Sidman RL, Cheng SH, & Shihabuddin LS. (2013). Augmenting CNS glucocerebrosidase activity as a therapeutic strategy for parkinsonism and other Gaucher-related synucleinopathies. *Proceedings of the National Academy of Sciences of the United States of America, 110*(9), 3537-3542. doi:10.1073/pnas.1220464110

Sauer H, & Oertel WH. (1994). Progressive degeneration of nigrostriatal dopamine neurons following intrastriatal terminal lesions with 6-hydroxydopamine: a combined retrograde tracing and immunocytochemical study in the rat. *Neuroscience, 59*(2), 401-415. doi:10.1016/0306-4522(94)90605-x

Savica R, Carlin JM, Grossardt BR, Bower JH, Ahlskog JE, Maraganore DM, Bharucha AE, & Rocca WA. (2009). Medical records documentation of constipation preceding Parkinson disease: A case-control study. *Neurology, 73*(21), 1752-1758. doi:10.1212/WNL.0b013e3181c34af5

Schallert T, Fleming SM, Leasure JL, Tillerson JL, & Bland ST. (2000a). CNS plasticity and assessment of forelimb sensorimotor outcome in unilateral rat models of stroke, cortical ablation, parkinsonism and spinal cord injury. *Neuropharmacology, 39*(5), 777-787. doi:https://doi.org/10.1016/S0028-3908(00)00005-8

Schallert T, & Tillerson JL. (2000b). Intervention Strategies for Degeneration of Dopamine Neurons in Parkinsonism. In D. F. Emerich, R. L. Dean, & P. R. Sanberg (Eds.), *Central Nervous System Diseases: Innovative Animal Models from Lab to Clinic* (pp. 131-151). Totowa, NJ: Humana Press.

Schapira AHV, Cooper JM, Dexter D, Clark JB, Jenner P, & Marsden CD. (1990). Mitochondrial Complex I Deficiency in Parkinson's Disease. *Journal of Neurochemistry, 54*(3), 823-827. doi:10.1111/j.1471-4159.1990.tb02325.x

Schenck CH, Boeve BF, & Mahowald MW. (2013). Delayed emergence of a parkinsonian disorder or dementia in 81% of older men initially diagnosed with idiopathic rapid eye movement sleep behavior disorder: a 16-year update on a previously reported series. *Sleep medicine, 14*(8), 744-748. doi:10.1016/j.sleep.2012.10.009

Schlaeger TM, Daheron L, Brickler TR, Entwisle S, Chan K, Cianci A, DeVine A, Ettenger A, Fitzgerald K, Godfrey M, Gupta D, McPherson J, Malwadkar P, Gupta M, Bell B, Doi A, Jung N, Li X, Lynes MS, Brookes E, Cherry ABC, Demirbas D, Tsankov AM, Zon LI, Rubin LL, Feinberg AP, Meissner A, Cowan CA, & Daley GQ. (2015). A comparison of non-integrating reprogramming methods. *Nat Biotechnol, 33*(1), 58-63. doi:10.1038/nbt.3070

Schmidt N, & Ferger B. (2001). Neurochemical findings in the MPTP model of Parkinson's disease. *Journal of neural transmission (Vienna, Austria : 1996), 108*(11), 1263-1282. doi:10.1007/s007020100004

Schober A. (2004). Classic toxin-induced animal models of Parkinson's disease: 6-OHDA and MPTP. *Cell and tissue research, 318*(1), 215-224. doi:10.1007/s00441-004-0938-y

Schoenberg BS, Osuntokun BO, Adeuja AO, Bademosi O, Nottidge V, Anderson DW, & Haerer AF. (1988). Comparison of the prevalence of Parkinson's disease in black populations in the rural United States and in rural Nigeria: door-to-door community studies. *Neurology, 38*(4), 645-646. doi:10.1212/wnl.38.4.645

Schrag A, Horsfall L, Walters K, Noyce A, & Petersen I. (2015). Prediagnostic presentations of Parkinson's disease in primary care: a case-control study. *The Lancet. Neurology, 14*(1), 57-64. doi:10.1016/s1474-4422(14)70287-x

Schwamborn JC. (2018). Is Parkinson's Disease a Neurodevelopmental Disorder and Will Brain Organoids Help Us to Understand It? *Stem Cells Dev, 27*(14), 968-975. doi:10.1089/scd.2017.0289

Schwerk A, Altschüler J, Roch M, Gossen M, Winter C, Berg J, Kurtz A, Akyüz L, & Steiner B. (2015a). Adipose-derived human mesenchymal stem cells induce long-term neurogenic and anti-inflammatory effects and improve cognitive but not motor performance in a rat model of Parkinson's disease. *Regenerative medicine, 10*(4), 431-446. doi:10.2217/rme.15.17

Schwerk A, Altschüler J, Roch M, Gossen M, Winter C, Berg J, Kurtz A, & Steiner B. (2015b). Human adipose-derived mesenchymal stromal cells increase endogenous neurogenesis in the rat subventricular zone acutely after 6-hydroxydopamine lesioning. *Cytotherapy, 17*(2), 199-214. doi:10.1016/j.jcyt.2014.09.005

Sedelis M, Schwarting RK, & Huston JP. (2001). Behavioral phenotyping of the MPTP mouse model of Parkinson's disease. *Behavioural brain research, 125*(1-2), 109-125. doi:10.1016/s0166-4328(01)00309-6

Seppi K, Ray Chaudhuri K, Coelho M, Fox SH, Katzenschlager R, Perez Lloret S, Weintraub D, Sampaio C, & the collaborators of the Parkinson's Disease Update on Non-Motor Symptoms Study Group

on behalf of the Movement Disorders Society Evidence-Based Medicine C. (2019). Update on treatments for nonmotor symptoms of Parkinson's disease-an evidence-based medicine review. *Movement disorders : official journal of the Movement Disorder Society, 34*(2), 180-198. doi:10.1002/mds.27602

Sherer TB, Betarbet R, Testa CM, Seo BB, Richardson JR, Kim JH, Miller GW, Yagi T, Matsuno-Yagi A, & Greenamyre JT. (2003). Mechanism of Toxicity in Rotenone Models of Parkinson's Disease. *The Journal of Neuroscience, 23*(34), 10756. doi:10.1523/jneurosci.23-34-10756.2003

Shi Y, Inoue H, Wu JC, & Yamanaka S. (2016). Induced pluripotent stem cell technology: a decade of progress. *Nature Reviews Drug Discovery, 16*, 115. doi:10.1038/nrd.2016.245

Shintani A, Nakao N, Kakishita K, & Itakura T. (2007). Protection of dopamine neurons by bone marrow stromal cells. *Brain Res, 1186*, 48-55. doi:10.1016/j.brainres.2007.09.086

Sian-Hülsmann J, Mandel S, Youdim MBH, & Riederer P. (2011). The relevance of iron in the pathogenesis of Parkinson's disease. *Journal of Neurochemistry, 118*(6), 939-957. doi:10.1111/j.1471-4159.2010.07132.x

Sidransky E. (2004). Gaucher disease: complexity in a "simple" disorder. *Molecular genetics and metabolism, 83*(1-2), 6-15. doi:10.1016/j.ymgme.2004.08.015

Sidransky E, & Lopez G. (2012). The link between the GBA gene and parkinsonism. *The Lancet. Neurology, 11*(11), 986-998. doi:10.1016/s1474-4422(12)70190-4

Sidransky E, Nalls MA, Aasly JO, Aharon-Peretz J, Annesi G, Barbosa ER, Bar-Shira A, Berg D, Bras J, Brice A, Chen CM, Clark LN, Condroyer C, De Marco EV, Dürr A, Eblan MJ, Fahn S, Farrer MJ, Fung HC, Gan-Or Z, Gasser T, Gershoni-Baruch R, Giladi N, Griffith A, Gurevich T, Januario C, Kropp P, Lang AE, Lee-Chen GJ, Lesage S, Marder K, Mata IF, Mirelman A, Mitsui J, Mizuta I, Nicoletti G, Oliveira C, Ottman R, Orr-Urtreger A, Pereira LV, Quattrone A, Rogaeva E, Rolfs A, Rosenbaum H, Rozenberg R, Samii A, Samaddar T, Schulte C, Sharma M, Singleton A, Spitz M, Tan EK, Tayebi N, Toda T, Troiano AR, Tsuji S, Wittstock M, Wolfsberg TG, Wu YR, Zabetian CP, Zhao Y, & Ziegler SG. (2009). Multicenter analysis of glucocerebrosidase mutations in Parkinson's disease. *The New England journal of medicine, 361*(17), 1651-1661. doi:10.1056/NEJMoa0901281

Siegel GJ, & Chauhan NB. (2000). Neurotrophic factors in Alzheimer's and Parkinson's disease brain. *Brain research. Brain research reviews, 33*(2-3), 199-227. doi:10.1016/s0165-0173(00)00030-8

Sipp D, Robey PG, & Turner L. (2018). Clear up this stem-cell mess. *Nature, 561*(7724), 455-457. doi:10.1038/d41586-018-06756-9

Sison SL, Vermilyea SC, Emborg ME, & Ebert AD. (2018). Using Patient-Derived Induced Pluripotent Stem Cells to Identify Parkinson's Disease-Relevant Phenotypes. *Curr Neurol Neurosci Rep, 18*(12), 84-84. doi:10.1007/s11910-018-0893-8

Smits LM, Reinhardt L, Reinhardt P, Glatza M, Monzel AS, Stanslowsky N, Rosato-Siri MD, Zanon A, Antony PM, Bellmann J, Nicklas SM, Hemmer K, Qing X, Berger E, Kalmbach N, Ehrlich M,

Bolognin S, Hicks AA, Wegner F, Sterneckert JL, & Schwamborn JC. (2019). Modeling Parkinson's disease in midbrain-like organoids. *NPJ Parkinson's disease, 5*, 5-5. doi:10.1038/s41531-019-0078-4

Sofic E, Riederer P, Heinsen H, Beckmann H, Reynolds GP, Hebenstreit G, & Youdim MB. (1988). Increased iron (III) and total iron content in post mortem substantia nigra of parkinsonian brain. *Journal of Neural Transmission, 74*(3), 199-205. doi:10.1007/bf01244786

Soldner F, & Jaenisch R. (2017). In Vitro Modeling of Complex Neurological Diseases. In R. Jaenisch, F. Zhang, & F. Gage (Eds.), *Genome Editing in Neurosciences* (pp. 1-19). Cham: Springer International Publishing.

Soldner F, Laganiere J, Cheng AW, Hockemeyer D, Gao Q, Alagappan R, Khurana V, Golbe LI, Myers RH, Lindquist S, Zhang L, Guschin D, Fong LK, Vu BJ, Meng X, Urnov FD, Rebar EJ, Gregory PD, Zhang HS, & Jaenisch R. (2011). Generation of isogenic pluripotent stem cells differing exclusively at two early onset Parkinson point mutations. *Cell., 146*(2), 318-331. doi: 310.1016/j.cell.2011.1006.1019. Epub 2011 Jul 1014.

Soldner F, Stelzer Y, Shivalila CS, Abraham BJ, Latourelle JC, Barrasa MI, Goldmann J, Myers RH, Young RA, & Jaenisch R. (2016). Parkinson-associated risk variant in distal enhancer of α-synuclein modulates target gene expression. *Nature, 533*(7601), 95-99. doi:10.1038/nature17939

Sousa N, Almeida OFX, & Wotjak CT. (2006). A hitchhiker's guide to behavioral analysis in laboratory rodents. *Genes, brain, and behavior, 5 Suppl 2*, 5-24. doi:10.1111/j.1601-183X.2006.00228.x

Stanic D, Finkelstein DI, Bourke DW, Drago J, & Horne MK. (2003). Timecourse of striatal re-innervation following lesions of dopaminergic SNpc neurons of the rat. *The European journal of neuroscience, 18*(5), 1175-1188. doi:10.1046/j.1460-9568.2003.02800.x

Sulzer D. (2007). Multiple hit hypotheses for dopamine neuron loss in Parkinson's disease. *Trends in neurosciences, 30*(5), 244-250. doi:10.1016/j.tins.2007.03.009

Surmeier DJ, Obeso JA, & Halliday GM. (2017). Parkinson's Disease Is Not Simply a Prion Disorder. *The Journal of Neuroscience, 37*(41), 9799. doi:10.1523/jneurosci.1787-16.2017

Suzuki S, Kawamata J, Iwahara N, Matsumura A, Hisahara S, Matsushita T, Sasaki M, Honmou O, & Shimohama S. (2015). Intravenous mesenchymal stem cell administration exhibits therapeutic effects against 6-hydroxydopamine-induced dopaminergic neurodegeneration and glial activation in rats. *Neuroscience letters, 584*, 276-281. doi:10.1016/j.neulet.2014.10.039

Szabadi E. (2013). Functional neuroanatomy of the central noradrenergic system. *Journal of psychopharmacology (Oxford, England), 27*(8), 659-693. doi:10.1177/0269881113490326

Tadaiesky MT, Dombrowski PA, Figueiredo CP, Cargnin-Ferreira E, Da Cunha C, & Takahashi RN. (2008). Emotional, cognitive and neurochemical alterations in a premotor stage model of Parkinson's disease. *Neuroscience, 156*(4), 830-840. doi:10.1016/j.neuroscience.2008.08.035

Tait SWG, & Green DR. (2013). Mitochondrial regulation of cell death. *Cold Spring Harbor perspectives in biology, 5*(9), a008706. doi:10.1101/cshperspect.a008706

Takahashi K, Tanabe K, Ohnuki M, Narita M, Ichisaka T, Tomoda K, & Yamanaka S. (2007). Induction of pluripotent stem cells from adult human fibroblasts by defined factors. *Cell., 131*(5), 861-872.

Takeda YS, & Xu Q. (2015). Neuronal Differentiation of Human Mesenchymal Stem Cells Using Exosomes Derived from Differentiating Neuronal Cells. *PLoS One., 10*(8), e0135111. doi:10.1371/journal.pone.0135111

Tang F-L, Erion JR, Tian Y, Liu W, Yin D-M, Ye J, Tang B, Mei L, & Xiong W-C. (2015). VPS35 in Dopamine Neurons Is Required for Endosome-to-Golgi Retrieval of Lamp2a, a Receptor of Chaperone-Mediated Autophagy That Is Critical for α-Synuclein Degradation and Prevention of Pathogenesis of Parkinson's Disease. *J Neurosci, 35*(29), 10613-10628. doi:10.1523/jneurosci.0042-15.2015

Teixeira FG, Carvalho MM, Neves-Carvalho A, Panchalingam KM, Behie LA, Pinto L, Sousa N, & Salgado AJ. (2015). Secretome of mesenchymal progenitors from the umbilical cord acts as modulator of neural/glial proliferation and differentiation. *Stem Cell Rev, 11*(2), 288-297. doi:10.1007/s12015-014-9576-2

Teixeira FG, Carvalho MM, Panchalingam KM, Rodrigues AJ, Mendes-Pinheiro B, Anjo S, Manadas B, Behie LA, Sousa N, & Salgado AJ. (2017). Impact of the Secretome of Human Mesenchymal Stem Cells on Brain Structure and Animal Behavior in a Rat Model of Parkinson's Disease. *Stem Cells Transl Med., 6*(2), 634-646. doi: 610.5966/sctm.2016-0071. Epub 2016 Sep 5922.

Teixeira FG, Carvalho MM, Sousa N, & Salgado AJ. (2013). Mesenchymal stem cells secretome: a new paradigm for central nervous system regeneration? *Cellular and Molecular Life Sciences, 70*(20), 3871-3882.

Testa CM, Sherer TB, & Greenamyre JT. (2005). Rotenone induces oxidative stress and dopaminergic neuron damage in organotypic substantia nigra cultures. *Brain research. Molecular brain research, 134*(1), 109-118. doi:10.1016/j.molbrainres.2004.11.007

Thacker EL, O'Reilly EJ, Weisskopf MG, Chen H, Schwarzschild MA, McCullough ML, Calle EE, Thun MJ, & Ascherio A. (2007). Temporal relationship between cigarette smoking and risk of Parkinson disease. *Neurology, 68*(10), 764-768. doi:10.1212/01.wnl.0000256374.50227.4b

Thakur P, Breger LS, Lundblad M, Wan OW, Mattsson B, Luk KC, Lee VMY, Trojanowski JQ, & Björklund A. (2017). Modeling Parkinson's disease pathology by combination of fibril seeds and α-synuclein overexpression in the rat brain. *Proceedings of the National Academy of Sciences of the United States of America, 114*(39), E8284-E8293. doi:10.1073/pnas.1710442114

Thomas KJ, McCoy MK, Blackinton J, Beilina A, van der Brug M, Sandebring A, Miller D, Maric D, Cedazo-Minguez A, & Cookson MR. (2010). DJ-1 acts in parallel to the PINK1/parkin pathway to control mitochondrial function and autophagy. *Hum Mol Genet, 20*(1), 40-50. doi:10.1093/hmg/ddq430

Titova N, Schapira AHV, Chaudhuri KR, Qamar MA, Katunina E, & Jenner P. (2017). Nonmotor Symptoms in Experimental Models of Parkinson's Disease. *International review of neurobiology, 133*, 63-89. doi:10.1016/bs.irn.2017.05.018

Torack RM, & Morris JC. (1988). The Association of Ventral Tegmental Area Histopathology With Adult Dementia. *Archives of Neurology, 45*(5), 497-501. doi:10.1001/archneur.1988.00520290025008

Toulorge D, Guerreiro S, Hild A, Maskos U, Hirsch EC, & Michel PP. (2011). Neuroprotection of midbrain dopamine neurons by nicotine is gated by cytoplasmic Ca2+. *FASEB journal : official publication of the Federation of American Societies for Experimental Biology, 25*(8), 2563-2573. doi:10.1096/fj.11-182824

Trigo-Damas I, Del Rey NL-G, & Blesa J. (2018). Novel models for Parkinson's disease and their impact on future drug discovery. *Expert opinion on drug discovery, 13*(3), 229-239. doi:10.1080/17460441.2018.1428556

Tsika E, Kannan M, Foo CS-Y, Dikeman D, Glauser L, Gellhaar S, Galter D, Knott GW, Dawson TM, Dawson VL, & Moore DJ. (2014). Conditional expression of Parkinson's disease-related R1441C LRRK2 in midbrain dopaminergic neurons of mice causes nuclear abnormalities without neurodegeneration. *Neurobiology of Disease, 71*, 345-358. doi:10.1016/j.nbd.2014.08.027

Tubert C, Galtieri D, & Surmeier DJ. (2019). The pedunclopontine nucleus and Parkinson's disease. *Neurobiology of Disease, 128*, 3-8. doi:10.1016/j.nbd.2018.08.017

Tysnes OB, & Storstein A. (2017). Epidemiology of Parkinson's disease. *J Neural Transm (Vienna). 124*(8), 901-905. doi: 910.1007/s00702-00017-01686-y. Epub 02017 Feb 00701.

Uitti RJ, Snow BJ, Shinotoh H, Vingerhoets FJ, Hayward M, Hashimoto S, Richmond J, Markey SP, Markey CJ, & Calne DB. (1994). Parkinsonism induced by solvent abuse. *Annals of neurology, 35*(5), 616-619. doi:10.1002/ana.410350516

Ungerstedt U. (1968). 6-Hydroxy-dopamine induced degeneration of central monoamine neurons. *European journal of pharmacology, 5*(1), 107-110. doi:10.1016/0014-2999(68)90164-7

Ungerstedt U, & Arbuthnott GW. (1970). Quantitative recording of rotational behavior in rats after 6-hydroxy-dopamine lesions of the nigrostriatal dopamine system. *Brain Res, 24*(3), 485-493. doi:https://doi.org/10.1016/0006-8993(70)90187-3

Usenovic M, & Krainc D. (2012). Lysosomal dysfunction in neurodegeneration. *Autophagy, 8*(6), 987-988. doi:10.4161/auto.20256

Van Den Berge N, Ferreira N, Gram H, Mikkelsen TW, Alstrup AKO, Casadei N, Tsung-Pin P, Riess O, Nyengaard JR, Tamgüney G, Jensen PH, & Borghammer P. (2019). Evidence for bidirectional and trans-synaptic parasympathetic and sympathetic propagation of alpha-synuclein in rats. *Acta Neuropathologica, 138*(4), 535-550. doi:10.1007/s00401-019-02040-w

Van Den Eeden SK, Tanner CM, Bernstein AL, Fross RD, Leimpeter A, Bloch DA, & Nelson LM. (2003). Incidence of Parkinson's disease: variation by age, gender, and race/ethnicity. *American journal of epidemiology, 157*(11), 1015-1022. doi:10.1093/aje/kwg068

Van der Perren A, Van den Haute C, & Baekelandt V. (2015). Viral vector-based models of Parkinson's disease. *Curr Top Behav Neurosci., 22:271-301.*(doi), 10.1007/7854_2014_1310.

Van Rompuy A-S, Lobbestael E, Van der Perren A, Van den Haute C, & Baekelandt V. (2014). Long-term overexpression of human wild-type and T240R mutant Parkin in rat substantia nigra induces progressive dopaminergic neurodegeneration. *Journal of neuropathology and experimental neurology, 73*(2), 159-174. doi:10.1097/nen.0000000000000039

Vera E, Bosco N, & Studer L. (2016). Generating Late-Onset Human iPSC-Based Disease Models by Inducing Neuronal Age-Related Phenotypes through Telomerase Manipulation. *Cell reports, 17*(4), 1184-1192. doi:10.1016/j.celrep.2016.09.062

Vilariño-Güell C, Wider C, Ross OA, Dachsel JC, Kachergus JM, Lincoln SJ, Soto-Ortolaza AI, Cobb SA, Wilhoite GJ, Bacon JA, Behrouz B, Melrose HL, Hentati E, Puschmann A, Evans DM, Conibear E, Wasserman WW, Aasly JO, Burkhard PR, Djaldetti R, Ghika J, Hentati F, Krygowska-Wajs A, Lynch T, Melamed E, Rajput A, Rajput AH, Solida A, Wu R-M, Uitti RJ, Wszolek ZK, Vingerhoets F, & Farrer MJ. (2011). VPS35 mutations in Parkinson disease. *American journal of human genetics, 89*(1), 162-167. doi:10.1016/j.ajhg.2011.06.001

Vingill S, Connor-Robson N, & Wade-Martins R. (2018). Are rodent models of Parkinson's disease behaving as they should? *Behavioural Brain Research, 352*, 133-141. doi:https://doi.org/10.1016/j.bbr.2017.10.021

Visanji NP, O'Neill MJ, & Duty S. (2006). Nicotine, but neither the alpha4beta2 ligand RJR2403 nor an alpha7 nAChR subtype selective agonist, protects against a partial 6-hydroxydopamine lesion of the rat median forebrain bundle. *Neuropharmacology, 51*(3), 506-516. doi:10.1016/j.neuropharm.2006.04.015

Volkman R, & Offen D. (2017). Concise Review: Mesenchymal Stem Cells in Neurodegenerative Diseases. *Stem Cells, 35*(8), 1867-1880. doi:10.1002/stem.2651

Volpicelli-Daley L, & Brundin P. (2018). Prion-like propagation of pathology in Parkinson disease. *Handbook of clinical neurology, 153*, 321-335. doi:10.1016/b978-0-444-63945-5.00017-9

Volpicelli-Daley LA, Abdelmotilib H, Liu Z, Stoyka L, Daher JPL, Milnerwood AJ, Unni VK, Hirst WD, Yue Z, Zhao HT, Fraser K, Kennedy RE, & West AB. (2016a). G2019S-LRRK2 Expression Augments α-Synuclein Sequestration into Inclusions in Neurons. *J Neurosci, 36*(28), 7415-7427. doi:10.1523/jneurosci.3642-15.2016

Volpicelli-Daley LA, Gamble KL, Schultheiss CE, Riddle DM, West AB, & Lee VMY. (2014). Formation of α-synuclein Lewy neurite-like aggregates in axons impedes the transport of distinct endosomes. *Molecular biology of the cell, 25*(25), 4010-4023. doi:10.1091/mbc.E14-02-0741

Volpicelli-Daley LA, Kirik D, Stoyka LE, Standaert DG, & Harms AS. (2016b). How can rAAV-α-synuclein and the fibril α-synuclein models advance our understanding of Parkinson's disease? *Journal of neurochemistry, 139 Suppl 1*(Suppl 1), 131-155. doi:10.1111/jnc.13627

Von Coelln R, Thomas B, Savitt JM, Lim KL, Sasaki M, Hess EJ, Dawson VL, & Dawson TM. (2004). Loss of locus coeruleus neurons and reduced startle in parkin null mice. *Proceedings of the National Academy of Sciences of the United States of America, 101*(29), 10744-10749. doi:10.1073/pnas.0401297101

Wales P, Pinho R, Lázaro DF, & Outeiro TF. (2013). Limelight on alpha-synuclein: pathological and mechanistic implications in neurodegeneration. *J Parkinsons Dis, 3*(4), 415-459. doi:10.3233/jpd-130216

Wang F, Yasuhara T, Shingo T, Kameda M, Tajiri N, Yuan WJ, Kondo A, Kadota T, Baba T, Tayra JT, Kikuchi Y, Miyoshi Y, & Date I. (2010). Intravenous administration of mesenchymal stem cells exerts therapeutic effects on parkinsonian model of rats: focusing on neuroprotective effects of stromal cell-derived factor-1alpha. *BMC neuroscience, 11*, 52-52. doi:10.1186/1471-2202-11-52

Weiss ML, Medicetty S, Bledsoe AR, Rachakatla RS, Choi M, Merchav S, Luo Y, Rao MS, Velagaleti G, & Troyer D. (2006). Human umbilical cord matrix stem cells: preliminary characterization and effect of transplantation in a rodent model of Parkinson's disease. *Stem cells (Dayton, Ohio), 24*(3), 781-792. doi:10.1634/stemcells.2005-0330

Williams ET, Chen X, & Moore DJ. (2017). VPS35, the Retromer Complex and Parkinson's Disease. *J Parkinsons Dis, 7*(2), 219-233. doi:10.3233/jpd-161020

Winkler C, Kirik D, Björklund A, & Dunnett SB. (2000). Transplantation in the rat model of Parkinson's disease: ectopic versus homotopic graft placement. *Progress in brain research, 127*, 233-265. doi:10.1016/s0079-6123(00)27012-x

Winslow AR, Chen C-W, Corrochano S, Acevedo-Arozena A, Gordon DE, Peden AA, Lichtenberg M, Menzies FM, Ravikumar B, Imarisio S, Brown S, O'Kane CJ, & Rubinsztein DC. (2010). α-Synuclein impairs macroautophagy: implications for Parkinson's disease. *The Journal of Cell Biology, 190*(6), 1023-1037. doi:10.1083/jcb.201003122

Xilouri M, Brekk OR, & Stefanis L. (2013). α-Synuclein and protein degradation systems: a reciprocal relationship. *Molecular Neurobiology, 47*(2), 537-551. doi:10.1007/s12035-012-8341-2

Yalvaç ME, Yarat A, Mercan D, Rizvanov AA, Palotás A, & Şahin F. (2013). Characterization of the secretome of human tooth germ stem cells (hTGSCs) reveals neuro-protection by fine-tuning micro-environment. *Brain Behav Immun, 32*, 122-130. doi:10.1016/j.bbi.2013.03.007

Yao N, Wu Y, Zhou Y, Ju L, Liu Y, Ju R, Duan D, & Xu Q. (2015). Lesion of the locus coeruleus aggravates dopaminergic neuron degeneration by modulating microglial function in mouse models of Parkinson′s disease. *Brain Res, 1625*, 255-274. doi:10.1016/j.brainres.2015.08.032

Yao Y, Huang C, Gu P, & Wen T. (2016). Combined MSC-Secreted Factors and Neural Stem Cell Transplantation Promote Functional Recovery of PD Rats. *Cell transplantation, 25*(6), 1101-1113. doi:10.3727/096368915x689938

Zhang X, Hu D, Shang Y, & Qi X. (2019). Using induced pluripotent stem cell neuronal models to study neurodegenerative diseases. *Biochimica et biophysica acta. Molecular basis of disease*, 165431-165431. doi:10.1016/j.bbadis.2019.03.004

Zhang Y, Liang X, Liao S, Wang W, Wang J, Li X, Ding Y, Liang Y, Gao F, Yang M, Fu Q, Xu A, Chai YH, He J, Tse HF, & Lian Q. (2015). Potent Paracrine Effects of human induced Pluripotent Stem Cell-derived Mesenchymal Stem Cells Attenuate Doxorubicin-induced Cardiomyopathy. *Scientific Reports, 5*, 112-135.

Zhi L, Qin Q, Muqeem T, Seifert EL, Liu W, Zheng S, Li C, & Zhang H. (2019). Loss of PINK1 causes age-dependent decrease of dopamine release and mitochondrial dysfunction. *Neurobiol Aging, 75*, 1-10. doi:10.1016/j.neurobiolaging.2018.10.025

Zhou H, Huang C, Tong J, Hong WC, Liu Y-J, & Xia X-G. (2011). Temporal expression of mutant LRRK2 in adult rats impairs dopamine reuptake. *International journal of biological sciences, 7*(6), 753-761. doi:10.7150/ijbs.7.753

Zimprich A, Benet-Pagès A, Struhal W, Graf E, Eck SH, Offman MN, Haubenberger D, Spielberger S, Schulte EC, Lichtner P, Rossle SC, Klopp N, Wolf E, Seppi K, Pirker W, Presslauer S, Mollenhauer B, Katzenschlager R, Foki T, Hotzy C, Reinthaler E, Harutyunyan A, Kralovics R, Peters A, Zimprich F, Brücke T, Poewe W, Auff E, Trenkwalder C, Rost B, Ransmayr G, Winkelmann J, Meitinger T, & Strom TM. (2011). A mutation in VPS35, encoding a subunit of the retromer complex, causes late-onset Parkinson disease. *American journal of human genetics, 89*(1), 168-175. doi:10.1016/j.ajhg.2011.06.008

Zimprich A, Biskup S, Leitner P, Lichtner P, Farrer M, Lincoln S, Kachergus J, Hulihan M, Uitti RJ, Calne DB, Stoessl AJ, Pfeiffer RF, Patenge N, Carbajal IC, Vieregge P, Asmus F, Müller-Myhsok B, Dickson DW, Meitinger T, Strom TM, Wszolek ZK, & Gasser T. (2004a). Mutations in LRRK2 cause autosomal-dominant parkinsonism with pleomorphic pathology. *Neuron, 44*(4), 601-607. doi:10.1016/j.neuron.2004.11.005

Zimprich A, Müller-Myhsok B, Farrer M, Leitner P, Sharma M, Hulihan M, Lockhart P, Strongosky A, Kachergus J, Calne DB, Stoessl J, Uitti RJ, Pfeiffer RF, Trenkwalder C, Homann N, Ott E, Wenzel K, Asmus F, Hardy J, Wszolek Z, & Gasser T. (2004b). The PARK8 locus in autosomal dominant parkinsonism: confirmation of linkage and further delineation of the disease-containing interval. *American journal of human genetics, 74*(1), 11-19. doi:10.1086/380647

Zucca FA, Segura-Aguilar J, Ferrari E, Muñoz P, Paris I, Sulzer D, Sarna T, Casella L, & Zecca L. (2017). Interactions of iron, dopamine and neuromelanin pathways in brain aging and Parkinson's disease. *Prog Neurobiol, 155*, 96-119. doi:10.1016/j.pneurobio.2015.09.012

CHAPTER 2

GENERATION OF PATIENT-DERIVED INDUCED PLURIPOTENT STEM CELLS

***This chapter is based on the following publications:**

Marote A, Pomeshchik Y, Collin A, Goldwurm S, Lamas NJ, Pinto L, Salgado AJ, & Roybon L. (2018). Generation of an induced pluripotent stem cell line (CSC-41) from a Parkinson's disease patient carrying a p.G2019S mutation in the LRRK2 gene. *Stem Cell Res*, 28, 44-47. doi:10.1016/j.scr.2018.01.022

Marote A, Pomeshchik Y, Goldwurm S, Collin A, Lamas NJ, Pinto L, Salgado AJ, & Roybon L. (2018). Generation of an integration-free induced pluripotent stem cell line (CSC-43J) from a patient with sporadic Parkinson's disease. *Stem Cell Res*, 27, 82-85. doi:10.1016/j.scr.2018.01.007

Marote A, Pomeshchik Y, Goldwurm S, Collin A, Lamas NJ, Pinto L, Salgado AJ, & Roybon L. (2018). Generation of an induced pluripotent stem cell line (CSC-44) from a Parkinson's disease patient carrying a compound heterozygous mutation (c.823C > T and EX6 del) in the PARK2 gene. *Stem Cell Res*, 27, 90-94. doi:10.1016/j.scr.2018.01.006

Russ K, Marote A, Savchenko E, Collin A, Goldwurm S, Pomeshchik Y, & Roybon L. (2018). Generation of a human induced pluripotent stem cell line (CSC-40) from a Parkinson's disease patient with a PINK1 p.Q456X mutation. *Stem Cell Res*, 27, 61-64. doi:10.1016/j.scr.2018.01.001

Savchenko E, Marote A, Russ K, Collin A, Goldwurm S, Roybon L, & Pomeshchik Y. (2018). Generation of a human induced pluripotent stem cell line (CSC-42) from a patient with sporadic form of Parkinson's disease. *Stem Cell Res*, 27, 78-81. doi:10.1016/j.scr.2018.01.

Gustavsson N, Marote A, Pomeshchik Y, Russ K, Azevedo C, Chumarina M, Goldwurm S, Collin A, Pinto L, Salgado AJ, Klementieva O, Roybon L, & Savchenko E. (2019). Generation of an induced pluripotent stem cell line (CSC-46) from a patient with Parkinson's disease carrying a novel p.R301C mutation in the GBA gene. *Stem Cell Res*, 34. doi:10.1016/j.scr.2018.101373

Chapter 2 | Generation of patient-derived induced pluripotent stem cells

Abstract

The possibility of inducing pluripotency in cells isolated from adult tissue has revolutionized the stem biology field, paving the way for an era of patient- and disease—specific modeling studies. Additionally, these induced pluripotent stem cells (iPSCs) can be differentiated into any cell type, thereby providing an important resource for cell replacement strategies. In this chapter, we report the generation of 11 iPSC lines from healthy subjects (n=3), Parkinson's disease (PD) patients with idiopathic (n=4) or genetically-associated (n=4) forms of the disease. For that, patient-derived skin fibroblasts and peripheral blood mononuclear cells (PBMCs) were reprogrammed using the Sendai virus vectors containing the four transcription factors known to induce pluripotency - Oct4, Sox2, c-Myc and Klf4. After colony picking and expansion of selected clones, cells were tested for pluripotency, genomic stability and presence of Sendai virus. All generated iPSC lines exhibit expression of common pluripotency markers, differentiate into the three germ layers, have a normal karyotype and do not present Sendai virus expression. These lines can be further used in disease modeling studies addressing the molecular mechanisms underlying PD progression. Particularly, iPSCs from patients carrying known or new variants of mutations in PD-related genes, such as PINK1, *parkin*, LRRK2 and GBA are an important contribution for assessing their induced phenotypic alterations in disease-specific cell types (*i.e.* dopaminergic neurons), neuronal precursor cells or 3D brain organoids. Ultimately, these studies may provide a better understanding of the etiology of neurodegeneration and thus identify new targets for the development of disease-modifying therapies.

1. Introduction

Successful reprogramming of human somatic cells into a embryonic pluripotent state was a revolutionary discovery in stem cell research field. Through the forced expression of a defined set of transcription factors, it was possible to generate induced pluripotent stem cells (iPSCs), which display embryonic stem cells (ESCs) properties (Takahashi *et al.*, 2007; Takahashi *et al.*, 2006). Besides circumventing the ethical concerns associated with ESCs use in research, iPSCs can be generated from easily accessible somatic sources, such as skin fibroblasts (Takahashi *et al.*, 2007), blood cells (Loh *et al.*, 2009; Staerk *et al.*, 2010) and urine-derived cells (Gaignerie *et al.*, 2018). The possibility to differentiate patient-specific iPSCs into any cell type offers unprecedent opportunities to develop personalized medicine strategies for disease modelling, drug discovery and regenerative medicine purposes (Shi *et al.*, 2016).

Identifying the pathological mechanisms underlying neurodegenerative diseases, such as Parkinson's disease (PD) is of key importance to design novel therapeutic strategies (Shi *et al.*, 2016). Although most of PD cases present unknown etiology, 5-10% of the cases present mutations in specific genes that are linked to the familial forms of the disease. Mutations in α-synuclein (α-syn) and leucine rich repeat kinase 2 (LRRK2) have been associated with autosomal-dominant PD, whereas mutations in parkin, DJ-1, and phosphatase and tensin homolog (PTEN)-induced novel kinase 1 (PINK1) have been identified in autosomal-recessive PD (Holmqvist *et al.*, 2016).

Disease modelling studies based on patient-derived iPSCs carrying known PD mutations have revealed phenotypical alterations in differentiated dopaminergic neurons and neural precursor cells, including impaired oxidative stress response, decreased neurite outgrowth, reduced dopamine uptake and release, mitochondrial dysfunction, alpha-synuclein accumulation and nuclear-architecture defects (Chung *et al.*, 2013; Chung *et al.*, 2016; Cooper *et al.*, 2012; Imaizumi *et al.*, 2012; Jiang *et al.*, 2012; Liu *et al.*, 2012; Nguyen *et al.*, 2011; Ren *et al.*, 2015; Seibler *et al.*, 2011; Shaltouki *et al.*, 2015). In addition, midbrain-specific organoids from sporadic PD-patient carrying a G2019S-LRRK2 mutation were reported to recapitulate disease-relevant phenotypes, such as decreased number and complexity of dopaminergic neurons, as well as increased FOXA2-positive progenitor cells (Kim *et al.*, 2019; Smits *et al.*, 2019).

The process for obtaining *in vitro* disease models based on iPSCs begins with the reprogramming of somatic tissue into pluripotency. Since the discovery of iPSCs in 2006, different technologies have been developed to efficiently deliver the reprogramming factors without inducing mutagenesis (Malik *et al.*, 2013; Takahashi *et al.*, 2006). Indeed, the integrating viral vector systems that were initially used (e.g. retrovirus and lentivirus) have been replaced by non-integrating methods, such as episomal DNAs, Sendai

virus and synthetically modified mRNAs, due to their high efficiency, safety and simple use (Shi *et al.*, 2016). After reprograming, generated cells must undergo a panel of tests to validate the conversion to embryonic-like state at the phenotypic, *i.e.* pluripotency markers expression, and functional level, *i.e.* three-germ layer differentiation. Moreover, it is also required to check for the presence of the gene delivery method, genomic stability and iPSCs identity (Holmqvist *et al.*, 2016). In this chapter, we report the generation of 11 iPSCs lines from healthy subjects, idiopathic and genetic PD patients by non-integrating Sendai virus technology, which can be used as a source of pre-clinical models of neurodegeneration and/or be used in therapeutic strategies for PD.

2. Materials and methods

2.1. *Human samples culture*

2.1.1. *Fibroblasts*

Dermal fibroblasts were obtained from the Parkinson Institute Biobank (part of the Telethon Genetic Biobank Network http://biobanknetwork. telethon.it/): approved by Ethics Committee "Milano Area C" (http://comitatoeticoareac.ospedaleniguarda. it/) on the 26/06/2015, Numero Registro dei pareri: 370-062015. The fibroblasts, collected by punch skin biopsy, were maintained in fibroblast growth medium, composed of DMEM media with 10% fetal bovine serum and 1% Penicillin-Streptomycin and passaged with 0.05% trypsin.

2.1.2. *Peripheral Blood Mononuclear Cells (PBMCs)*

PBMCs were obtained from patients recruited at Hospital de Braga and Hospital da Senhora da Oliveira after informed consent acquisition and ethical approval (CNPD:11739/2016; Hospital de Braga:CESHB-137/2016). Mononuclear cells were isolated from peripheral blood using a density gradient centrifugation protocol (Serre-Miranda *et al.*, 2015). Briefly, human peripheral blood was combined with Histopaque ®-1077 (Sigma-Aldrich) and centrifuged for 30 min at room temperature, according to manufacturer's instructions. Cells were then collected, washed twice with sterile PBS, counted using trypan blue exclusion dye and cryopreserved until further use.

2.2. *iPSC generation*

Human fibroblasts and PBMCs were reprogrammed using the CytoTune™-iPS 2.0 Sendai Reprogramming Kit (Thermo Fisher Scientific), according to the manufacturer's instructions.

2.2.1. *Fibroblasts reprogramming*

For fibroblast reprogramming, two days prior to transduction, 75 000 cells were seeded on a 12-well tissue culture plate and maintained in fibroblast growth medium. On the transduction day, cells were incubated with the three vector preparations (MOI = 5, 5, 3), according to the lot-specific virus titer. On the following day and on every other day, the medium was replaced with fresh fibroblast growth medium. At day 7, the cells were re-seeded onto irradiated mouse embryonic fibroblasts (MEF) feeder cells (CF-1 MEF IRR, Gibco, USA Gibco) with fibroblast growth medium. On the day after and until colony picking, cells were cultured in WiCell medium composed of advanced DMEM/F12, 20% Knock-Out Serum Replacement, 2 mM L-glutamine, 1% non-essential amino acids and 0.1mM β-mercaptoethanol, supplemented with 20 ng/ml FGF2 (Gibco).

2.2.2. *PBMCs reprogramming*

For PBMCs reprogramming, 500 000 cells were seeded on a 24-well tissue culture plate and maintained in culture for four days with half medium changes in complete PBMC medium composed of StemPro®-34 SFM, StemPro®-34 Nutrient Mix (Gibco), 2mM L-Glutamine (Gibco), StemSpan™ Erythroid Expansion Supplement (STEMCELL Technologies). On transduction day, 250 000 cells were combined with the three vector preparations (MOI=5 5 3) in a low-attachment 24-well tissue culture plate in 0.3mL of complete PBMC medium. On the day after, the medium was totally replaced with fresh complete PBMC medium. Three days after, transduced PBMCs were transferred onto tissue culture dishes containing MEFs and kept in PBMC medium lacking the Erythroid Expansion Supplement. Seven days after transduction, half of the medium was replaced with WiCell medium supplemented with 20 ng/ml FGF2. Thenceforward and until colony picking, daily medium changes were performed in transduced PBMCs with WiCell medium supplemented with 20 ng/ml FGF2.

2.2.3. *Colony picking and expansion*

Approximately 21 – 28 days after transduction, 12 colonies showing embryonic-like morphology were manually picked and expanded as individual clones (A – L). From these, three clones were selected based on their morphology for further expansion and characterization. iPSCs cultured in feeder-dependent system, were kept in WiCell medium, supplemented with 20 ng/mL FGF2 and passaged with dispase (1mg/mL, Gibco). On later passages, iPSCs were cultured in a feeder-free system, in mTeSR™ medium onto vitronectin-coated 6-well tissue culture plates and passaged with ReLeSR (all products from STEMCELL Technologies).

2.3. *iPSCs characterization*

2.3.1. *Phenotypic*

To confirm the phenotype of generated iPSCs, the expression of pluripotency markers was assessed by immunocytochemistry. For that, iPSCs cultures were fixed with 4% paraformaldehyde for 15 min at room temperature (RT), permeabilized and blocked for 1h at RT with PBS containing 10% donkey or fetal calf serum and 0.1% TritonX-10 (blocking buffer) and incubated for two hours at RT or overnight at 4°C with the primary antibodies (table 2.1) diluted in blocking buffer. The secondary antibodies (table 2.1) were thereafter added for two hours at RT in the dark, followed by nuclei counterstain with DAPI (1:1000) and image acquisition on inverted epifluorescence microscope LRI - Olympus IX-73 or Olympus Widefield Upright Microscope BX61 microscope.

Table 2.1 – List of antibodies used for iPSCs phenotypic characterization

	Antibody	Reference	Host	Dilution
Primary antibodies	anti-Oct4	Millipore, Cat# MAB4401	Mouse	1:200
	anti-OCT3/4	R&D systems, Cat# AF1759	Goat	1:20
	PE-conjugated anti-human Nanog	BD Biosciences, Cat# 560483	Mouse	1:200
	anti-NANOG	Sigma-Aldrich, Cat#AB9220,	Rabbit	1:100
Secondary antibodies	anti-mouse Alexa Fluor® 488	Molecular Probes Cat# A21202	Donkey	1:400
	anti-mouse Alexa Fluor® 555	Invitrogen, Cat# A31570	Donkey	1:400
	anti-mouse Alexa Fluor® 488	Invitrogen, Cat# A32723	Goat	1:1000
	anti-rabbit Alexa Fluor® 594	Invitrogen, Cat# A32740	Goat	1:1000
	anti-rabbit Alexa Fluor® 594	Invitrogen, Cat# A32754	Donkey	1:1000
	anti-goat Alexa Fluor® 488	Invitrogen, Cat# A32814	Donkey	1:1000

2.3.2. *Functional characterization*

To assess the pluripotency at the functional level, *in vitro* spontaneous differentiation by embryoid body (EBs) formation was performed. For that, human iPSC were grown for two weeks as embryoid bodies (EBs) in low-attachment 24-well plates (Corning) in WiCell medium supplemented with 20 ng/ml FGF2. The EBs were then seeded on a 0.1% gelatin-coated 96-well plate (Greiner Bio-One) in DMEM media containing 10% fetal bovine serum and 1% Penicillin-Streptomycin for subsequent spontaneous differentiation, with media changes every 2-3 days. After 2 weeks, the cells were fixed and stained for three germ-layer markers as described in section 2.3, using the antibodies described in table 2.2.

Table 2.2 – List of antibodies used for iPSCs functional characterization

Germ-layer	Antibody	Reference	Host	Dilution
Endoderm	anti-α-fetoprotein	Santa Cruz, Cat# SC8399 Sigma-Aldrich Cat# A2547	Mouse	1:200
Mesoderm	anti-α-Smooth Muscle Actin	Sigma-Aldrich, Cat# A2547	Mouse	1:200
Ectoderm	anti-β-III Tubulin	Sigma-Aldrich Cat# T8660 Promega, Cat# G7121	Mouse	1:1000

2.3.3. *Karyotype analysis*

The G-banding analysis was performed at 400–550 band resolution in a clinical diagnostic setting after 8 to 14 passages.

2.3.4. *Mutation sequencing*

Genomic DNA from fibroblasts and iPSCs was extracted using conventional lysis buffer composed of 100 mM Tris (pH 8.0), 200 mM NaCl, 5 mM EDTA and 0.2% SDS in distilled autoclaved water supplemented with 1.5 mg/ml Proteinase K. The mutations were confirmed by direct DNA sequencing (Eurofins Genomics). Primers used for amplification and directed sequencing of each gene around the mutation sites are listed in Table 2.3.

Table 2.3 – List of primers used for DNA sequencing.

Gene	Forward/Reverse primer (5′-3′)	Mutation
LRRK2	TTTTGATGCTTGACATAGTGGAC/CACATCTGAGGTCAGTGGTTATC	p.G2019S
PINK1	TGGATCAGGTGATGTGCAGGA/AGGATCTGTCACTGTGGCTCT	p.Q456X
PARK2	AGGATTACAGAAATTGGTCT/TCTGTTCTTCATTAGCATTAGA	c.823C>T and EX6 del
GBA	TGGTCCACTTTCTTGGCCG/AGGGGAATGGTGCTCTAGGA	p.R301C

3. Results

A total of 11 iPSC lines were generated during this study, which were coded as follows: NeuroRegeneration Clulster – *NRC* or iPSC Laboratory for CNS Disease Modeling – *CSC* = lab identification – *number*=patient and *letter*=clone characterization. A total of five lines (NRC 1G, 2H, 3B, 4J and 5H) were generated from patient-derived PBMCs and comprise the first iPSC lines generated at the ICVS. Moreover, six new iPSC lines were also generated from patients' fibroblasts and contribute for the comprehensive library of iPSC lines of sporadic and genetic PD already established at the CSC lab (Holmqvist *et al.*, 2016). All samples were successfully reprogrammed by Sendai virus transduction of 'Yamanaka' factors – Oct, Sox2, Klf4, and c-Myc. iPSC characterization was subsequently performed from passage 8 onwards in either feeder-

dependent (NRC-1G, NRC-2H, CSC-40F, CSC-41C, CSC-42L, CSC-43J, CSC-44I, CSC-46L) or feeder free-culture systems (NRC-3B, NRC-4J, NRC-5H).

Table 2.4 summarizes subjects' information regarding age, sex and identified mutation (if applicable), as well as the genomic stability (chromosomal analysis) of each generated line. Part of these iPSCs were published as lab resources, in which full characterization can be found (Annexes I – VI, (Gustavsson *et al.*, 2019; Marote *et al.*, 2018a; Marote *et al.*, 2018b, 2018c; Russ *et al.*, 2018; Savchenko *et al.*, 2018)). Figures 2.1, 2.2 and 2.3 depict part of the phenotypic and functional characterization performed in healthy, sporadic and genetic PD lines, respectively. All lines express the pluripotency markers Oct4 and Nanog as evidenced by immunocytochemistry analysis. Additionally, all lines were able to grow as embryoid bodies and spontaneously differentiate into cell types of the three germ-layers into a variable extent. Furthermore, the lack of the delivery method is also demonstrated by the absence of Sendai virus antibody expression.

Table 2.4 – Summary of iPSC lines generated in the study. M – male; F – female; N/a - not applicable; PBMCs - peripheral blood monunclear cells.

	Code	Age	Sex	Genotype	Somatic cell source	Karyotype	Published lab resource
Healthy	NRC – 2H	68	F	N/a	PBMCs	46, XX	No
	NRC – 4J	-	F	N/a	PBMCs	46, XX	No
	NRC – 5H	-	F	N/a	PBMCs	(-)	No
Idiopathic PD	CSC – 42L	38*	F	N/a	Fibroblasts	46, XX	*Annex I* (Savchenko *et al.*, 2018)
	CSC – 43J	31*	M	N/a	Fibroblasts	46, XY	*Annex II* (Marote *et al.*, 2018c)
	NRC – 1G	62	F	N/a	PBMCs	46, XX	No
	NRC – 3B	-	F	N/a	PBMCs	(-)	No
Genetic PD	CSC – 40F	36*	M	PINK1 (p.Q456X)	Fibroblasts	46, XY	*Annex III* (Russ *et al.*, 2018)
	CSC – 41C	75	F	LRRK2 (p.G2019S)	Fibroblasts	46, XX	*Annex IV* (Marote *et al.*, 2018a)
	CSC – 44I	33*	F	PARK2 (c.823CNT and EX6 del)	Fibroblasts	46, XX	*Annex V* (Marote *et al.*, 2018b)
	CSC – 46L	60	M	GBA (p.R301C)	Fibroblasts	46, XY	*Annex VI* (Gustavsson *et al.*, 2019)

*age at onset; (-) not analyzed yet

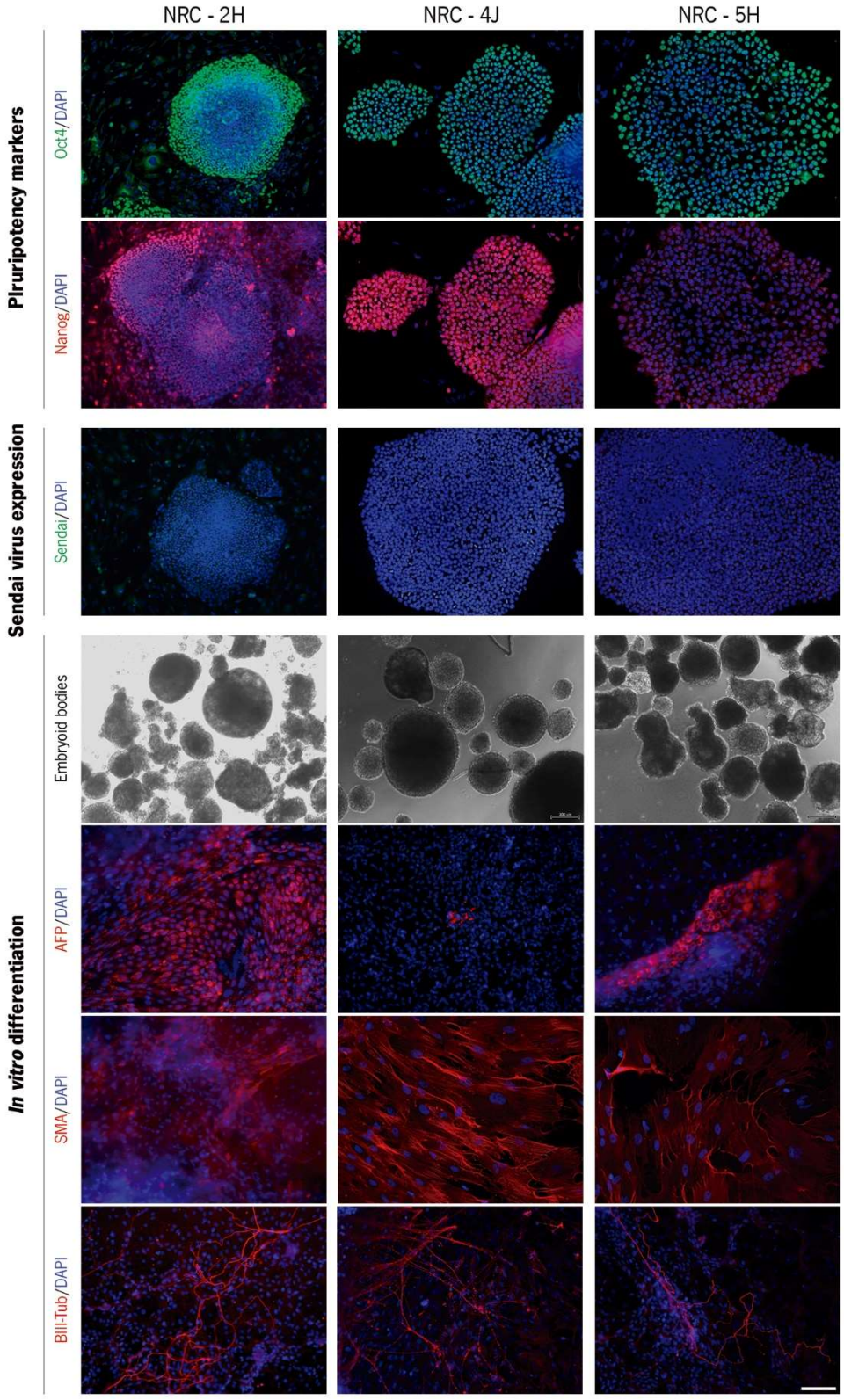

Figure 2.1 – Phenotypical and functional characterization of iPSC lines from healthy individuals (NRC-2H, NRC-4J and NRC-5H). Scale bar represents 100 μm. AFP – alpha fetoprotein; SMA – smooth muscle actin; BIII-tub – B-III tubulin.

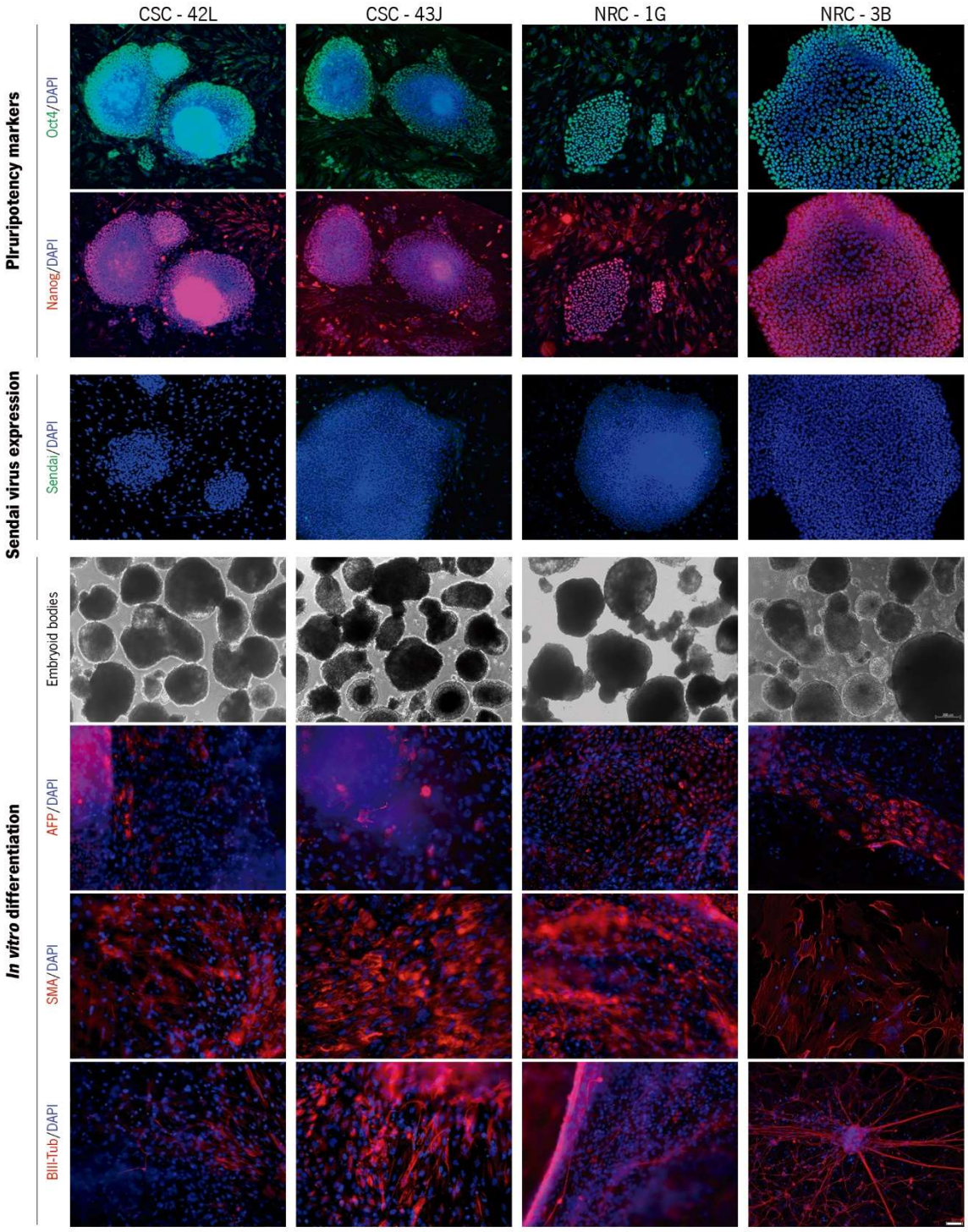

Figure 2.2 – Phenotypical and functional characterization of iPSC lines from idiopathic PD patients (CSC-42L, CSC-43J, NRC-1G, NRC-3B). Scale bar represents 100 μm. AFP – alpha fetoprotein; SMA – smooth muscle actin; BIII-tub – B-III tubulin.

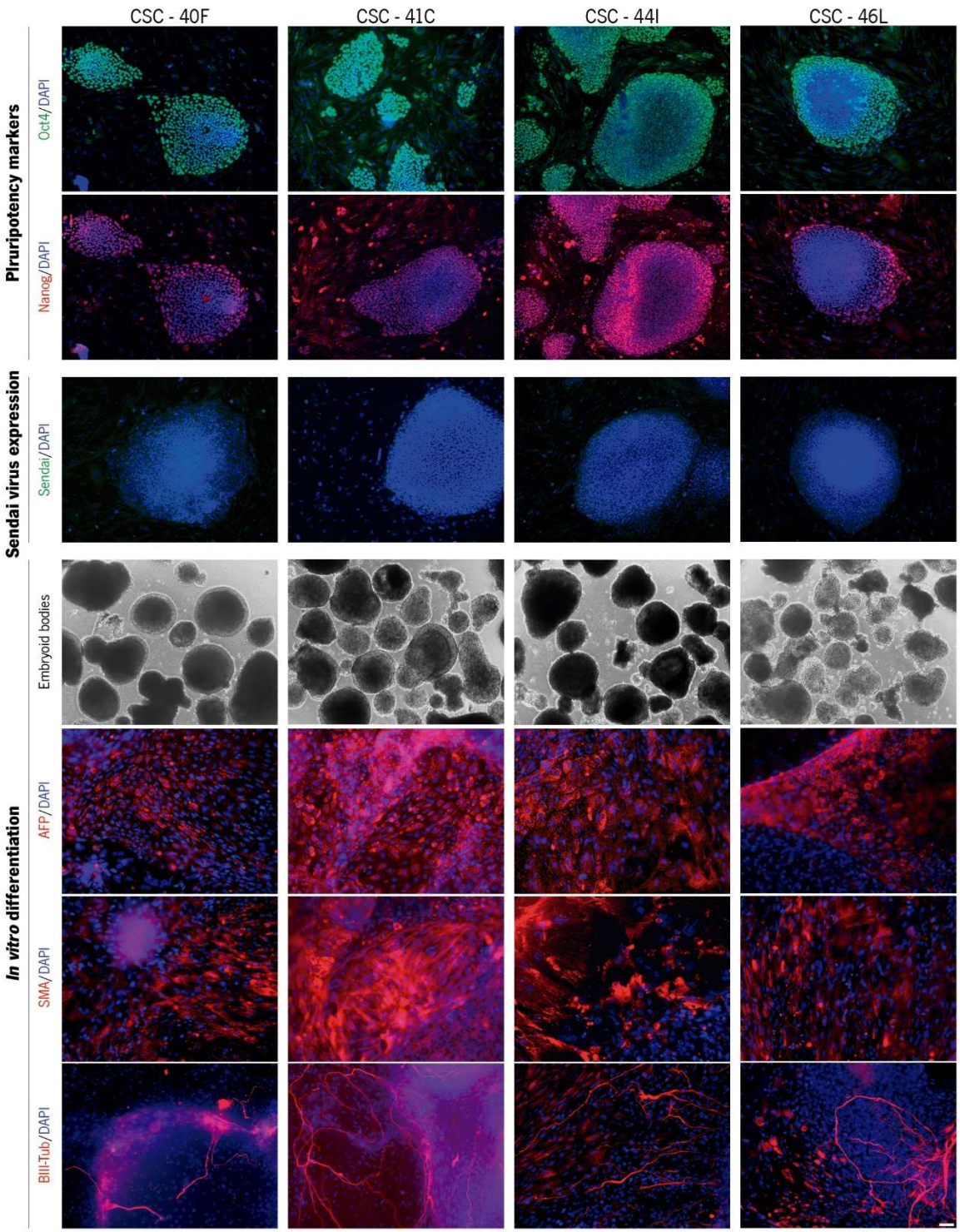

Figure 2.3 – Phenotypical and functional characterization of iPSC lines from genetic PD patients (CSC-40F, CSC-41C, CSC-44I, CSC-46L). Scale bar represents 100 μm. AFP – alpha fetoprotein; SMA – smooth muscle actin; BIII-tub – B-III tubulin.

4. Discussion

Since the revolutionary discovery of iPSC technology, different somatic cell types have been reprogrammed. In this study, we report the successful generation of iPSCs from patient-derived fibroblasts and PBMCs. Although direct comparison between sources was not the aim of the present study, we verified a higher chromosomic stability of PBMC-derived iPSCs as no karyotype abnormalities were found in all the analysed clones (data not shown). Indeed, skin cells are more likely to have acquired DNA damage due to UV-induced mutations and need to be expanded for several passages in culture before reprograming, thereby increasing the probability to acquire genetic alterations (Maherali *et al.*, 2008). In contrast, PBMCs are an easily accessible source of patient tissue and do not need extensive cell culture maintenance prior to reprogramming. (Staerk *et al.*, 2010). Regardless of the cell source used, no visible differences were found between reprogramming efficiency of healthy and PD lines, despite recent reports of cellular alterations in PD patient-derived fibroblasts (Teves *et al.*, 2018) as well as changes in PBMCs' survival and response to stimuli (Nissen *et al.*, 2019).

From the eight PD-derived iPSCs lines, four lines were originated from patients carrying mutations in PD associated genes: CSC-40F, CSC-41C, CSC-44I and CSC-46L. CSC-40F line presented a PINK1 p.Q456X mutation that leads to a decrease in mRNA and a loss of protein function (Siuda *et al.*, 2014). PINK1 encodes a serine/threonine protein kinase that localizes to mitochondria and is thought to protect cells from stress-induced mitochondrial dysfunction (Russ *et al.*, 2018). Human DA neurons derived from iPSCs carrying PINK1 p.Q456X mutation have shown diminished recruitment of parkin to mitochondria and increase in PGC-1α expression, a protein involved in mitochondrial biogenesis (Seibler *et al.*, 2011). Interestingly, progerin-induced aging of dopaminergic neurons derived from PINK1 p.Q456X mutated iPSCs led to loss of dendrite length, increased apoptosis and decreased number of TH^+ neurons in grafts of 6-OHDA lesioned mice (Miller *et al.*, 2013).

A LRRK2 G2019S mutation is present in line CSC-41C, which is linked to autosomal-dominant familial PD cases and has also been identified in sporadic PD cases with no family history of the disease. LRRK2 encodes for dardarin, a protein with GTPase and kinase activity (Marote *et al.*, 2018a). The G2019S mutation is the most frequent among PD patients. This glycine-to-serine substitution at amino acid 2019 causes increased kinase activity and has been reported to have implications in oxidative stress response, nuclear structure and dopaminergic neurons maturation (Liu *et al.*, 2012; Reinhardt *et al.*, 2013; Smits *et al.*, 2019).

CSC-44 iPSC line was generated from a PD patient with a compound heterozygous mutation in PARK2, which accounts for the second most common known cause of PD and result in autosomal-recessive familial PD (Marote *et al.*, 2018b). PARK2 encodes for parkin, a E3 ubiquitin ligase that plays a role in targeting proteins for degradation and maintaining mitochondrial function (Nuytemans *et al.*, 2010). Among the identified PARK2 mutations, both deletions and insertions of one or more exons and missense mutations have been described. CSC-44I line carries a compound heterozygous PARK2 mutation: point mutation c.823CNT in exon 7 and deletion of exon 6. The c.823CNT mutation in PARK2 gene predicts an arginine to tryptophan substitution at amino acid residue 275 (p.R275W), which is located within the RING1 domain of PARK2. This mutation disrupts the charge distribution and leads to local rearrangements in the RING1-IBR interface, which hampers ubiquitin ligase activity and confers a toxic gain of function to PARKIN, leading to its aggregation (Fiesel et al., 2015; Oczkowska et al., 2013). Even though this point mutation has been well characterized and associated with other mutations in compound heterozygotes, its association with the deletion of exon 6 has not been described. Given the importance of compound heterozygous mutations on PARK2 gene, CSC-44 iPSC line can be used to better understand the impact of both alterations on cellular function (Marote *et al.*, 2018b).

Lastly, CSC-46L line, contains a new mutation variant (R301C) on the GBA gene, a gene that is associated with the development of PD. GBA encodes for the enzyme glucocerebrosidase that is deficient in Gaucher's disease, a recessive lysosomal storage disorder. Mutations in the GBA gene are linked to an increased risk of developing PD and present early-onset of the motor symptoms and increased cognitive impairment (Mata *et al.*, 2016; Sidransky *et al.*, 2012). Several mutations have been identified in the GBA gene, being N370S and L444P most frequently described in genetic screening studies (Asselta *et al.*, 2014). CSC-46L line carries a new mutation variant (R301C: arginine to cystein substitution at amino acid 301) on the GBA gene and therefore can be used to explore its contribution of GBA-associated parkinsonism in disease modelling studies (Gustavsson *et al.*, 2019).

In addition to modelling of known PD-linked mutations, iPSCs also provide a new way to study sporadic forms of the disease. CSC-42L, CSC-43-J, NRC-1G, NRC-3B lines were generated from patients with no identified genetic cause of the disease. These lines can be used in genome-wide association studies to identify genetic variants associated with PD (Soldner *et al.*, 2016). Moreover, it has been shown that dopaminergic neurons derived from sporadic PD patients express a pathogenic phenotype, including morphological alterations and accumulation of autophagic vacuoles (Sánchez-Danés *et al.*, 2012).

The lines generated in this study are an important contribution for the growing need of iPSCs biobanks to serve as resources for studying disease development and analyse genetic variations. However, to maximize the statistical power of iPSC-based modelling, a large number of iPSC lines need to be generated and expanded. Standard methods for generating, characterizing and expanding iPSCs are laborious, time- and money-consuming. Therefore, there has been a growing interest to develop high-throughput platforms as well as cheaper media for iPSC expansion. For instance, a robotic platform enabling automated, high-throughput conversion of fibroblasts into iPSCs cells with minimal manual intervention was generated by Paull and colleagues (Paull *et al.*, 2015). On the other hand, high-throughput methods including flow cytometry using fluorescent cell barcoding, qPCR (based on 12 primer pairs) for expression analysis, and SNP arrays for digital karyotyping were proposed for a more cost and time effective characterization (D'antonio *et al.*, 2017). Additionally, a completely xeno-free, chemically defined, synthetic culture system was developed to support long-term iPSC propagation with decreased production cost for clinical applications (Yasuda *et al.*, 2018).

In summary, we have generated 11 integration-free iPSC lines from two different somatic sources that present embryonic-like features and hence can be used in future studies of PD *in vitro* modelling, as well as in regenerative medicine applications.

Acknowledgments

We are greatly thankful to AnnaKarin Oldén and Marianne Juhlin, for their technical assistance and to the 'Cell Line and DNA Biobank from Patients affected by Genetic Diseases' (Istituto G. Gaslini, Genova, Italy) and the 'Parkinson Institute Biobank' (Milan, Italy, http://www.parkinsonbiobank.com), members of the Telethon Network of Genetic Biobanks (project no. GTB12001) funded by Telethon Italy, for providing fibroblasts samples. This work was supported by the Strategic Research Environment MultiPark—multidisciplinary research on Parkinson's disease at Lund University, the Swedish Parkinson foundation (Parkinsonfonden), and Finnish Cultural Foundation (Suomen Kulttuurirahasto). We also acknowledge the Portuguese Foundation for Science and Technology for the doctoral fellowship - PDE/BDE/113598/2015 to AM and IF Development Grant to AJS. This work has been developed under the scope of the project NORTE-01-0145-FEDER-000023, supported by the Northern Portugal Regional Operational Programme (NORTE 2020), under the Portugal 2020 Partnership Agreement, through the European Regional Development Fund (FEDER). This project has been funded by FEDER funds, through the Competitiveness Factors Operational Programme (COMPETE), and by National funds, through FCT, under the scope of the project POCI-01-0145-FEDER-007038.

References

Asselta R, Rimoldi V, Siri C, Cilia R, Guella I, Tesei S, Soldà G, Pezzoli G, Duga S, & Goldwurm S. (2014). Glucocerebrosidase mutations in primary parkinsonism. *Parkinsonism & related disorders, 20*(11), 1215-1220. doi:10.1016/j.parkreldis.2014.09.003

Chung CY, Khurana V, Auluck PK, Tardiff DF, Mazzulli JR, Soldner F, Baru V, Lou Y, Freyzon Y, Cho S, Mungenast AE, Muffat J, Mitalipova M, Pluth MD, Jui NT, Schüle B, Lippard SJ, Tsai L-H, Krainc D, Buchwald SL, Jaenisch R, & Lindquist S. (2013). Identification and Rescue of α-Synuclein Toxicity in Parkinson Patient–Derived Neurons. *Science, 342*(6161), 983-987. doi:10.1126/science.1245296

Chung Sun Y, Kishinevsky S, Mazzulli Joseph R, Graziotto J, Mrejeru A, Mosharov Eugene V, Puspita L, Valiulahi P, Sulzer D, Milner Teresa A, Taldone T, Krainc D, Studer L, & Shim J-w. (2016). Parkin and PINK1 Patient iPSC-Derived Midbrain Dopamine Neurons Exhibit Mitochondrial Dysfunction and α-Synuclein Accumulation. *Stem Cell Reports, 7*(4), 664-677. doi:10.1016/j.stemcr.2016.08.012

Cooper O, Seo H, Andrabi S, Guardia-Laguarta C, Graziotto J, Sundberg M, McLean JR, Carrillo-Reid L, Xie Z, Osborn T, Hargus G, Deleidi M, Lawson T, Bogetofte H, Perez-Torres E, Clark L, Moskowitz C, Mazzulli J, Chen L, Volpicelli-Daley L, Romero N, Jiang H, Uitti RJ, Huang Z, Opala G, Scarffe LA, Dawson VL, Klein C, Feng J, Ross OA, Trojanowski JQ, Lee VM-Y, Marder K, Surmeier DJ, Wszolek ZK, Przedborski S, Krainc D, Dawson TM, & Isacson O. (2012). Pharmacological Rescue of Mitochondrial Deficits in iPSC-Derived Neural Cells from Patients with Familial Parkinson's Disease. *Science translational medicine, 4*(141), 141ra190-141ra190. doi:10.1126/scitranslmed.3003985

D'Antonio M, Woodruff G, Nathanson JL, D'Antonio-Chronowska A, Arias A, Matsui H, Williams R, Herrera C, Reyna SM, Yeo GW, Goldstein LSB, Panopoulos AD, & Frazer KA. (2017). High-Throughput and Cost-Effective Characterization of Induced Pluripotent Stem Cells. *Stem Cell Reports, 8*(4), 1101-1111. doi:10.1016/j.stemcr.2017.03.011

Gaignerie A, Lefort N, Rousselle M, Forest-Choquet V, Flippe L, Francois–Campion V, Girardeau A, Caillaud A, Chariau C, Francheteau Q, Derevier A, Chaubron F, Knöbel S, Gaborit N, Si-Tayeb K, & David L. (2018). Urine-derived cells provide a readily accessible cell type for feeder-free mRNA reprogramming. *Scientific Reports, 8*(1), 14363. doi:10.1038/s41598-018-32645-2

Gustavsson N, Marote A, Pomeshchik Y, Russ K, Azevedo C, Chumarina M, Goldwurm S, Collin A, Pinto L, Salgado AJ, Klementieva O, Roybon L, & Savchenko E. (2019). Generation of an induced pluripotent stem cell line (CSC-46) from a patient with Parkinson's disease carrying a novel p.R301C mutation in the GBA gene. *Stem Cell Res, 34*. doi:10.1016/j.scr.2018.101373

Holmqvist S, Lehtonen Š, Chumarina M, Puttonen KA, Azevedo C, Lebedeva O, Ruponen M, Oksanen M, Djelloul M, Collin A, Goldwurm S, Meyer M, Lagarkova M, Kiselev S, Koistinaho J, & Roybon L. (2016). Creation of a library of induced pluripotent stem cells from Parkinsonian patients. *npj Parkinson's Disease, 2*(1), 16009. doi:10.1038/npjparkd.2016.9

Imaizumi Y, Okada Y, Akamatsu W, Koike M, Kuzumaki N, Hayakawa H, Nihira T, Kobayashi T, Ohyama M, Sato S, Takanashi M, Funayama M, Hirayama A, Soga T, Hishiki T, Suematsu M, Yagi T, Ito

D, Kosakai A, Hayashi K, Shouji M, Nakanishi A, Suzuki N, Mizuno Y, Mizushima N, Amagai M, Uchiyama Y, Mochizuki H, Hattori N, & Okano H. (2012). Mitochondrial dysfunction associated with increased oxidative stress and α-synuclein accumulation in PARK2 iPSC-derived neurons and postmortem brain tissue. *Molecular Brain, 5*(1), 35. doi:10.1186/1756-6606-5-35

Jiang H, Ren Y, Yuen EY, Zhong P, Ghaedi M, Hu Z, Azabdaftari G, Nakaso K, Yan Z, & Feng J. (2012). Parkin controls dopamine utilization in human midbrain dopaminergic neurons derived from induced pluripotent stem cells. *Nature Communications, 3*(1), 668. doi:10.1038/ncomms1669

Kim H, Park HJ, Choi H, Chang Y, Park H, Shin J, Kim J, Lengner CJ, Lee YK, & Kim J. (2019). Modeling G2019S-LRRK2 Sporadic Parkinson's Disease in 3D Midbrain Organoids. *Stem Cell Reports, 12*(3), 518-531. doi:10.1016/j.stemcr.2019.01.020

Liu G-H, Qu J, Suzuki K, Nivet E, Li M, Montserrat N, Yi F, Xu X, Ruiz S, Zhang W, Wagner U, Kim A, Ren B, Li Y, Goebl A, Kim J, Soligalla RD, Dubova I, Thompson J, Iii JY, Esteban CR, Sancho-Martinez I, & Belmonte JCI. (2012). Progressive degeneration of human neural stem cells caused by pathogenic LRRK2. *Nature, 491*, 603. doi:10.1038/nature11557

https://www.nature.com/articles/nature11557#supplementary-information

Loh Y-H, Agarwal S, Park I-H, Urbach A, Huo H, Heffner GC, Kim K, Miller JD, Ng K, & Daley GQ. (2009). Generation of induced pluripotent stem cells from human blood. *Blood, 113*(22), 5476.

Maherali N, & Hochedlinger K. (2008). Guidelines and techniques for the generation of induced pluripotent stem cells. *Cell Stem Cell, 3*(6), 595-605. doi:10.1016/j.stem.2008.11.008

Malik N, & Rao MS. (2013). A review of the methods for human iPSC derivation. *Methods in molecular biology (Clifton, N.J.), 997*, 23-33. doi:10.1007/978-1-62703-348-0_3

Marote A, Pomeshchik Y, Collin A, Goldwurm S, Lamas NJ, Pinto L, Salgado AJ, & Roybon L. (2018a). Generation of an induced pluripotent stem cell line (CSC-41) from a Parkinson's disease patient carrying a p.G2019S mutation in the LRRK2 gene. *Stem Cell Res, 28*, 44-47. doi:10.1016/j.scr.2018.01.022

Marote A, Pomeshchik Y, Goldwurm S, Collin A, Lamas NJ, Pinto L, Salgado AJ, & Roybon L. (2018b). Generation of an induced pluripotent stem cell line (CSC-44) from a Parkinson's disease patient carrying a compound heterozygous mutation (c.823C > T and EX6 del) in the PARK2 gene. *Stem Cell Res, 27*, 90-94. doi:10.1016/j.scr.2018.01.006

Marote A, Pomeshchik Y, Goldwurm S, Collin A, Lamas NJ, Pinto L, Salgado AJ, & Roybon L. (2018c). Generation of an integration-free induced pluripotent stem cell line (CSC-43J) from a patient with sporadic Parkinson's disease. *Stem Cell Res, 27*, 82-85. doi:10.1016/j.scr.2018.01.007

Mata IF, Leverenz JB, Weintraub D, Trojanowski JQ, Chen-Plotkin A, Van Deerlin VM, Ritz B, Rausch R, Factor SA, Wood-Siverio C, Quinn JF, Chung KA, Peterson-Hiller AL, Goldman JG, Stebbins GT, Bernard B, Espay AJ, Revilla FJ, Devoto J, Rosenthal LS, Dawson TM, Albert MS, Tsuang D, Huston H, Yearout D, Hu S-C, Cholerton BA, Montine TJ, Edwards KL, & Zabetian CP. (2016). GBA Variants are associated with a distinct pattern of cognitive deficits in Parkinson's disease. *Movement disorders : official journal of the Movement Disorder Society, 31*(1), 95-102. doi:10.1002/mds.26359

Miller Justine D, Ganat Yosif M, Kishinevsky S, Bowman Robert L, Liu B, Tu Edmund Y, Mandal PK, Vera E, Shim J-w, Kriks S, Taldone T, Fusaki N, Tomishima Mark J, Krainc D, Milner Teresa A, Rossi Derrick J, & Studer L. (2013). Human iPSC-Based Modeling of Late-Onset Disease via Progerin-Induced Aging. *Cell Stem Cell, 13*(6), 691-705. doi:10.1016/j.stem.2013.11.006

Nguyen Ha N, Byers B, Cord B, Shcheglovitov A, Byrne J, Gujar P, Kee K, Schüle B, Dolmetsch Ricardo E, Langston W, Palmer Theo D, & Pera Renee R. (2011). LRRK2 Mutant iPSC-Derived DA Neurons Demonstrate Increased Susceptibility to Oxidative Stress. *Cell Stem Cell, 8*(3), 267-280. doi:10.1016/j.stem.2011.01.013

Nissen SK, Shrivastava K, Schulte C, Otzen DE, Goldeck D, Berg D, Møller HJ, Maetzler W, & Romero-Ramos M. (2019). Alterations in Blood Monocyte Functions in Parkinson's Disease. *Movement Disorders, 0*(0). doi:10.1002/mds.27815

Nuytemans K, Theuns J, Cruts M, & Van Broeckhoven C. (2010). Genetic Etiology of Parkinson Disease Associated with Mutations in the SNCA, PARK2, PINK1, PARK7, and LRRK2 Genes: A Mutation Update. *Human Mutation, 31*(7), 763-780. doi:10.1002/humu.21277

Paull D, Sevilla A, Zhou H, Hahn AK, Kim H, Napolitano C, Tsankov A, Shang L, Krumholz K, Jagadeesan P, Woodard CM, Sun B, Vilboux T, Zimmer M, Forero E, Moroziewicz DN, Martinez H, Malicdan MCV, Weiss KA, Vensand LB, Dusenberry CR, Polus H, Sy KTL, Kahler DJ, Gahl WA, Solomon SL, Chang S, Meissner A, Eggan K, & Noggle SA. (2015). Automated, high-throughput derivation, characterization and differentiation of induced pluripotent stem cells. *Nature Methods, 12*, 885. doi:10.1038/nmeth.3507

https://www.nature.com/articles/nmeth.3507#supplementary-information

Reinhardt P, Schmid B, Burbulla LF, Schondorf DC, Wagner L, Glatza M, Hoing S, Hargus G, Heck SA, Dhingra A, Wu G, Muller S, Brockmann K, Kluba T, Maisel M, Kruger R, Berg D, Tsytsyura Y, Thiel CS, Psathaki OE, Klingauf J, Kuhlmann T, Klewin M, Muller H, Gasser T, Scholer HR, & Sterneckert J. (2013). Genetic correction of a LRRK2 mutation in human iPSCs links parkinsonian neurodegeneration to ERK-dependent changes in gene expression. *Cell Stem Cell., 12*(3), 354-367. doi: 310.1016/j.stem.2013.1001.1008.

Ren Y, Jiang H, Hu Z, Fan K, Wang J, Janoschka S, Wang X, Ge S, & Feng J. (2015). Parkin Mutations Reduce the Complexity of Neuronal Processes in iPSC-Derived Human Neurons. *Stem Cells, 33*(1), 68-78. doi:10.1002/stem.1854

Russ K, Marote A, Savchenko E, Collin A, Goldwurm S, Pomeshchik Y, & Roybon L. (2018). Generation of a human induced pluripotent stem cell line (CSC-40) from a Parkinson's disease patient with a PINK1 p.Q456X mutation. *Stem Cell Res, 27*, 61-64. doi:10.1016/j.scr.2018.01.001

Sánchez-Danés A, Richaud-Patin Y, Carballo-Carbajal I, Jiménez-Delgado S, Caig C, Mora S, Di Guglielmo C, Ezquerra M, Patel B, Giralt A, Canals JM, Memo M, Alberch J, López-Barneo J, Vila M, Cuervo AM, Tolosa E, Consiglio A, & Raya A. (2012). Disease-specific phenotypes in dopamine neurons from human iPS-based models of genetic and sporadic Parkinson's disease. *EMBO Molecular Medicine, 4*(5), 380-395. doi:10.1002/emmm.201200215

Savchenko E, Marote A, Russ K, Collin A, Goldwurm S, Roybon L, & Pomeshchik Y. (2018). Generation of a human induced pluripotent stem cell line (CSC-42) from a patient with sporadic form of Parkinson's disease. *Stem Cell Res, 27*, 78-81. doi:10.1016/j.scr.2018.01.002

Seibler P, Graziotto J, Jeong H, Simunovic F, Klein C, & Krainc D. (2011). Mitochondrial Parkin Recruitment Is Impaired in Neurons Derived from Mutant PINK1 Induced Pluripotent Stem Cells. *The Journal of Neuroscience, 31*(16), 5970-5976. doi:10.1523/jneurosci.4441-10.2011

Serre-Miranda C, Roque S, Santos NC, Portugal-Nunes C, Costa P, Palha JA, Sousa N, & Correia-Neves M. (2015). Effector memory CD4(+) T cells are associated with cognitive performance in a senior population. *Neurol Neuroimmunol Neuroinflamm, 2*(1), e54. doi:10.1212/nxi.0000000000000054

Shaltouki A, Sivapatham R, Pei Y, Gerencser AA, Momčilović O, Rao MS, & Zeng X. (2015). Mitochondrial alterations by PARKIN in dopaminergic neurons using PARK2 patient-specific and PARK2 knockout isogenic iPSC lines. *Stem Cell Reports, 4*(5), 847-859. doi:10.1016/j.stemcr.2015.02.019

Shi Y, Inoue H, Wu JC, & Yamanaka S. (2016). Induced pluripotent stem cell technology: a decade of progress. *Nature Reviews Drug Discovery, 16*, 115. doi:10.1038/nrd.2016.245

Sidransky E, & Lopez G. (2012). The link between the GBA gene and parkinsonism. *The Lancet. Neurology, 11*(11), 986-998. doi:10.1016/s1474-4422(12)70190-4

Siuda J, Jasinska-Myga B, Boczarska-Jedynak M, Opala G, Fiesel FC, Moussaud-Lamodière EL, Scarffe LA, Dawson VL, Ross OA, Springer W, Dawson TM, & Wszolek ZK. (2014). Early-onset Parkinson's disease due to PINK1 p.Q456X mutation–clinical and functional study. *Parkinsonism & related disorders, 20*(11), 1274-1278. doi:10.1016/j.parkreldis.2014.08.019

Smits LM, Reinhardt L, Reinhardt P, Glatza M, Monzel AS, Stanslowsky N, Rosato-Siri MD, Zanon A, Antony PM, Bellmann J, Nicklas SM, Hemmer K, Qing X, Berger E, Kalmbach N, Ehrlich M, Bolognin S, Hicks AA, Wegner F, Sterneckert JL, & Schwamborn JC. (2019). Modeling Parkinson's disease in midbrain-like organoids. *NPJ Parkinson's disease, 5*, 5-5. doi:10.1038/s41531-019-0078-4

Soldner F, Stelzer Y, Shivalila CS, Abraham BJ, Latourelle JC, Barrasa MI, Goldmann J, Myers RH, Young RA, & Jaenisch R. (2016). Parkinson-associated risk variant in distal enhancer of α-synuclein modulates target gene expression. *Nature, 533*, 95. doi:10.1038/nature17939

https://www.nature.com/articles/nature17939#supplementary-information

Staerk J, Dawlaty MM, Gao Q, Maetzel D, Hanna J, Sommer CA, Mostoslavsky G, & Jaenisch R. (2010). Reprogramming of Human Peripheral Blood Cells to Induced Pluripotent Stem Cells. *Cell Stem Cell, 7*(1), 20-24. doi:http://dx.doi.org/10.1016/j.stem.2010.06.002

Takahashi K, Tanabe K, Ohnuki M, Narita M, Ichisaka T, Tomoda K, & Yamanaka S. (2007). Induction of pluripotent stem cells from adult human fibroblasts by defined factors. *Cell., 131*(5), 861-872.

Takahashi K, & Yamanaka S. (2006). Induction of pluripotent stem cells from mouse embryonic and adult fibroblast cultures by defined factors. *Cell, 126*(4), 663-676. doi:10.1016/j.cell.2006.07.024

Teves JMY, Bhargava V, Kirwan KR, Corenblum MJ, Justiniano R, Wondrak GT, Anandhan A, Flores AJ, Schipper DA, Khalpey Z, Sligh JE, Curiel-Lewandrowski C, Sherman SJ, & Madhavan L. (2018). Parkinson's Disease Skin Fibroblasts Display Signature Alterations in Growth, Redox Homeostasis, Mitochondrial Function, and Autophagy. *Frontiers in neuroscience, 11*, 737-737. doi:10.3389/fnins.2017.00737

Yasuda S-y, Ikeda T, Shahsavarani H, Yoshida N, Nayer B, Hino M, Vartak-Sharma N, Suemori H, & Hasegawa K. (2018). Chemically defined and growth-factor-free culture system for the expansion and derivation of human pluripotent stem cells. *Nature Biomedical Engineering, 2*(3), 173-182. doi:10.1038/s41551-018-0200-7

CHAPTER 3

GENERATION OF AN *IN VITRO* MODEL OF PARKINSON'S DISEASE

***This chapter is based on the following publication:**

Marote A, Mendes-Pinheiro B, Gomes ED, Lamas NJ, Pinto L, Roybon L, Salgado AJ. Generation of an *in vitro* model of Parkinson's disease to explore the neuroprotective effects of mesenchymal stem cells secretome.

(manuscript in preparation)

Chapter 3 | Generation of an *in vitro* model of Parkinson's disease

Abstract

Parkinson's disease (PD) is characterized by the loss of dopaminergic neurons from the substantia nigra *pars compacta* leading to the denervation of the nigrostriatal tract, and a significant reduction of dopamine at the striatal level. In this study, we attempted to model these biochemical dysfunctions, by exposing pluripotent stem cell derived dopaminergic neurons to 6-hydroxydopamine (6-OHDA). For that, we have established an embryoid body-based dopaminergic differentiation protocol and provided a collagen matrix to promote neurite outgrowth and render a platform to induce 6-OHDA mediated toxicity. Subsequently, we have assessed cell viability, dopaminergic neurons' morphology and reactive oxygen species production as readouts of 6-OHDA induced toxicity. Using this model, we were able to induce significant morphological alterations in the neurite arborization of 6-OHDA exposed dopaminergic neurons along with decreased cell viability and increased production of reactive oxygen species. Therefore, this model can be used as a simple and affordable tool to investigate the use of new therapeutic tools for PD.

1. Introduction

Parkinson's disease (PD) is the second most common neurodegenerative disease, being characterized by severe loss of dopaminergic neurons at the substantia nigra *pars compacta* (SNc) and consequent denervation of the nigrostriatal tract and reduction of dopamine release at the striatal level (Dauer *et al.*, 2003). Although the exact mechanism underlying dopaminergic cell death is not completely understood, oxidative stress and mitochondrial dysfunction have been suggested to play a major role in PD pathogenesis (Bosco *et al.*, 2006; Michel *et al.*, 2016; Nakabeppu *et al.*, 2007; Pollard *et al.*, 2016; Schapira *et al.*, 1990). The incomplete understanding of the mechanisms underlying PD pathogenesis, in part, due to the inaccessibility of diseased tissue, justifies the current lack of effective treatments to halt PD-associated neurodegeneration (Little *et al.*, 2019).

In vitro experimental PD models, mimicking known PD pathological mechanisms, are extensively used in preclinical studies, as these provide quick and straightforward platforms for large-scale drug screenings (Falkenburger *et al.*, 2016; Lopes *et al.*, 2017). Among the available sources to develop PD relevant cellular models, pluripotent stem cells (PSCs) are ideal, as they comprise an unlimited supply of cells, for which robust differentiation and genetic engineering protocols are available (Studer, 2012). PSCs include embryonic stem cells (ESCs), derived from the inner cell mass of the developing blastocyst and induced pluripotent stem cells (iPSCs), obtained by reprogramming of somatic cells (Little *et al.*, 2019; Takahashi *et al.*, 2007; Takahashi *et al.*, 2006). Despite the potential of human iPSCs for disease modeling studies of PD cases with known mutations, mouse ESCs (mESCs) may provide a time and cost-effective source of dopaminergic neurons for preliminary preclinical studies addressing the neuroprotective potential of new therapies (Studer, 2012).

mESCs were firstly isolated in the early 1980s (Evans *et al.*, 1981); nonetheless, efficient generation of midbrain dopaminergic neurons from this source was only reported in 2000 (Lee *et al.*, 2000). The authors based mESCs dopaminergic differentiation on the generation of embryoid bodies (EBs) and subsequent use of two patterning factors, sonic hedgehog (SHH) and fibroblast growth factor 8 (FGF8) (Lee *et al.*, 2000), which had been previously shown to induce midbrain neuronal fate (Ye *et al.*, 1998). Other mESCs dopaminergic differentiation protocols also include the use of a coculture system with stromal-feeder layer, with or without patterning factors (Barberi *et al.*, 2003; Studer, 2012), as well as forced expression of LMX1A, a transcription factor determining midbrain dopaminergic neurons during embryogenesis (Friling *et al.*, 2009).

Besides extracellular chemical and biological cues, physical and mechanical properties from the extracellular matrix (ECM), including its stiffness, are known to play a major role in stem cell fate determination (Iwashita *et al.*, 2019; Murphy *et al.*, 2017). ECM proteins present in the brain, such as collagen, laminin and fibronectin provide mechanical, as well as molecular cues that influence cell behavior (Murphy *et al.*, 2017). Therefore, a variety of hydrogels have been developed as scaffolds to mimic the mechanical properties of the central nervous system (CNS). Collagen is a highly abundant and natural ECM protein that has a pore size appropriate to the scale of cells, thereby allowing appropriate cell adhesion without any modifications (Caliari *et al.*, 2016; Kratochvil *et al.*, 2019). Despite their popularity as a natural hydrogel material, the use of non-modified collagen to guide dopaminergic neurons differentiation is scarce (Iacovitti *et al.*, 2007; Kothapalli *et al.*, 2013; Lin *et al.*, 2006).

In the present study, we aimed to develop an *in vitro* model of PD, based on the mechanical properties of collagen to provide a 3D culture system of mESCs-derived dopaminergic neurons, and subsequent exposure to 6-hydroxydopamine (6-OHDA), to selectively destroy dopaminergic neurons via oxidative stress and complex I inhibition (Blum *et al.*, 2001). Therefore, this system may provide a simple and affordable platform to assess the effect of potential neuroprotective therapies for PD.

2. Materials and methods

2.1. *Mouse embryonic fibroblasts culture*

A feeder layer composed of mouse embryonic fibroblasts (MEFs) was prepared by seeding irradiated MEFs (CF-1 MEF IRR, Gibco, USA) on T25 flask coated with gelatin (0.1 % gelatin; Millipore, USA) with DMEM GlutaMAX (Gibco, USA) medium supplemented with 10 % fetal bovine serum (FBS; Biochrom, Germany) and 1 % Penicillin-Streptomycin (Gibco, USA).

2.2. *Mouse embryonic stem cells (mESC) culture*

A mESC reporter line (mESC TH::GFP), previously generated from heterozygous transgenic mice expressing green fluorescent protein (GFP) under the control of the rat tyrosine hydroxylase (TH) promotor (Chumarina *et al.*, 2017), was expanded on a MEF-feeder layer in DMEM GlutaMAX, 10 % FBS, 1x Nucleosides (Millipore, USA), 2mM L-glutamine (Life Technologies, USA), 1x Penicillin-Streptomycin and 0.1mM β-mercaptoethanol (Sigma, USA) supplemented with leukemia inhibitory factor (LIF, 1:10 000; Millipore, USA).

2.3. *Dopaminergic differentiation*

2.3.1. *Protocol optimization*

To understand which factors' combination induced a higher level of dopaminergic neurons, we took advantage of the GFP expression on TH^+ cells to measure the yield of differentiated cells in each embryoid body (EB) formation based protocol. For that, mESC cultures exhibiting an appropriate size and morphology were enzymatically dissociated with 0.05% trypsin solution (Life Technologies, USA) and centrifuged at 0.2 x g for 5 min. Afterwards, 10,000 to 20,000 cells/cm^2 were seeded in low-attachment culture surfaces in ADFNK medium consisting of Advanced DMEM-F12 medium (Gibco) and Neurobasal medium (Gibco) mixed at 1:1 ratio, 10% Knockout Serum Replacement (Life Technologies), 2mM L-glutamine, 1x Pen-Strep and 0.1 mM β-mercaptoethanol. On the following day, the medium was replaced by centrifuging small aggregates at 0.2 xg for 4 min. At day 2 of differentiation and on every other day, single factors or a combination of different factors were added to the culture medium and compared to a negative control in which no factors were added. The protocols tested included the following factors: Smoothened agonist (SAG, 0.5 μM, Tocris Bioscience, UK), Fibroblast growth factor 8 (FGF8, 100 ng/mL, Gibco, USA) and CHIR99021 (0.8 μM, Stemgent, USA). From day 8 until day 14, brain-derived neurotrophic factor (BDNF, 10 ng/ml; Peprotech, UK), glial cell line-derived neurotrophic factor (GDNF; 10 ng/mL; Peprotech) and ascorbic acid (AA, 200 μM; Sigma) were also added to the media to induce neuronal differentiation.

2.3.2. *Flow cytometry analysis*

To prepare single cell suspension, EBs from each protocol were collected into a 15mL tube and washed twice with PBS 0.4% glucose. After that, EBs were incubated with trypsin 0.5% for 10 min at 37°C to promote enzymatic dissociation, and rapidly mechanically dissociated with a micropipette until an homogenous single cell suspension was obtained. DNase containing FBS was then added and cell suspension was centrifuged at 0.3 x g for 3 min. The resulting cell pellet was resuspended in fresh ADFNK medium and subjected to flow cytometry analysis in FACSAria (Becton Dickinson, USA) coupled to DIVA software (Becton Dickinson, USA) to quantify GFP^+ cells resultant from each differentiation protocol.

2.3.3. *Seeding on collagen hydrogel*

After identifying the factors yielding the highest amount of GFP^+ cells, dopaminergic differentiated EBs were seeded on collagen hydrogel droplets, which served as a matrix for their adhesion and neurite outgrowth. The matrix was prepared by mixing rat tail collagen type I (3.61 mg/ml; BD Biosciences, USA) with 10x concentrated DMEM medium (Gibco, USA) and a 7.5(m/v)% solution of NaHCO3. After mixing,

collagen droplets (30 µL) were placed at the center of a well of a 48-well tissue culture plate and incubated for 2 hours at 37°C, 5% CO2 to induce polymerization. Afterwards, EBs with similar size were selected and placed on top of polymerized collagen droplets. EBs were kept under these 3D culture system for 6 additional days with daily medium changes with ADFNK medium containing differentiation factors (0.5 µM SAG, 10ng/mL BDNF, 10ng/mL GDNF, 200 µM AA).

2.4. *6-OHDA exposure*

After establishing the differentiated EBs on collagen with visible neurite outgrowth, dopaminergic cell death was induced by adding 6-OHDA hydrochloride (Sigma, USA) to a subset of wells. For that, a stock solution of 100 mM was prepared in 0.2% ascorbic acid solution and kept in dark to prevent oxidation. Afterwards, differentiation medium was removed and Neurobasal A medium (Gibco, USA) containing 500 µM of 6-OHDA (diluted from stock) was added to a subset of wells, while others were kept in Neurobasal A medium containing vehicle (0.2 % ascorbic acid). After 4h of incubation, medium was replaced with either differentiation medium (supplemented ADFNK) or non supplemented Neurobasal A medium and kept in culture for 48h until further analysis.

2.5. *MTS assay*

To measure cell viability after 6-OHDA exposure, the MTS [(5-(3-carboxymethoxyphenyl)-2-(4,5-dimethyl-thiazoly)-3-(4-sulfophenyl) tetrazolium, inner salt) assay was used, which measures the conversion of a tetrazolium salt into a colored formazan by mitochondrial activity of living cells. At the end of the 48h period post 6-OHDA exposure, the medium was replaced with fresh Neurobasal A medium containing MTS in a 5:1 ratio and incubated for 5h at 37 °C and 5 % CO_2. Afterwards, three technical replicates of each sample were placed in wells of a 96-well plate and optical density was measured by spectrometry in a microplate reader (Tecan, Switzerland)

2.6. *Immunocytochemistry*

Cell morphology and neurite arborization was measured by immunocytochemistry. For that, EBs on collagen gels were fixed in 4 % paraformaldehyde (PFA; Sigma) for 45 min and permeabilized with PBS 0.3 % Triton X-100 (Sigma) for 10 min. After blocking the non-specific binding by incubation in PBS 10 % newborn calf serum (NBCS; Biochrom), the cells were incubated with a rabbit polyclonal TH antibody (1:500; Millipore), a marker of dopaminergic neurons, diluted in blocking, for 48 h at 4 °C. After washing, cells were incubated with a goat anti-rabbit IgG secondary antibody conjugated to Alexa Fluor 594 (1:1000; Life Technologies) diluted in PBS with 0.5 % NBCS, overnight at 4°C. Afterwards, the samples

were incubated with the nuclear counterstain 4-6-diamidino-2-phenylindole-dhydrochloride (DAPI, 1:1000; Life Technologies) for 45 min at room temperature. Images were obtained through confocal microscopy (FV1000, Olympus, Japan) using the software FV10-ASW 2.0c (Olympus). Since neurites occupy a large area, the mosaic function was used, assembling single images to form one large super image of the specimen.

2.7. *Reactive oxygen species detection*

To analyze the production of reactive oxygen species (ROS) in 6-OHDA exposed cells, MitoSOX™ Red reagent a fluorogenic dye specifically targeted to mitochondria in live cells was used, following manufacturer's instructions. For that, cells were washed with Neurobasal medium and incubated with 5μM of MitoSOX for 20 min a 37°C. After that, three washes with PBS were performed and wells were incubated with DAPI (1:500) for 10 min, RT. Following three additional washes with PBS, image acquisition was performed through confocal microscopy (FV1000, Olympus, Japan) using the software FV10-ASW 2.0c (Olympus).

2.8. *Statistical analysis*

A confidence interval of 95 % was assumed for all statistical tests. The assumption of normality was tested for all continuous variables through evaluation of the frequency distribution histogram, the values of skewness and kurtosis and through the Shapiro-Wilk test. For the evaluation of mean differences between samples with one independent variable, One-way ANOVA was used, followed by multiple comparisons analysis through Tukey's post hoc test. Results are presented as mean ± SEM. All statistical analysis were performed using Prism GraphPad 8.0.1(GraphPad Software; La Jolla, USA) and results were considered significant for $p \leq 0.05$.

3. Results and discussion

3.1. *Mouse embryonic stem cells dopaminergic differentiation - protocol optimization*

In order to create a model of dopaminergic degeneration, we have firstly generated dopaminergic neurons from a reporter line of mouse embryonic stem cells that expresses GFP under the promoter of TH (mESCs TH::GFP) (Chumarina *et al.*, 2017). TH is a commonly used marker of ventral midbrain neurons, as it is a rate-limiting enzyme involved in dopamine biosynthesis (Studer, 2012). Therefore, the use of this reporter line allows the determination of the success of dopaminergic differentiation in a time course manner and perform a direct quantification of GFP^+ cells without requiring further staining procedures.

We have tested different combinations of morphogens to guide the differentiation of mESC into a dopaminergic fate, *via* embryoid body formation, with slight variations from the protocol described by (Lee *et al.*, 2000). Undifferentiated mESC growing on a MEF-feeder layer (figure 3.1a) were enzymatically dissociated and seeded on ultra-low attachment surfaces in ADFNK medium to promote the generation of embryoid bodies (EBs) during 2 days. Subsequently, the following molecules were added individually or in combination: SAG [0.5 µM], FGF8 [100 ng/mL] and CHIR [0.8 µM] (figure 3.1b). After 8 days of differentiation, neuronal maturation was induced by adding BDNF, GDNF and ascorbic acid to the culture medium. By day 14 of differentiation, EBs with approximately 250 µm of diameter were obtained (Figure 3.1c). Importantly, in some of the protocols tested, these EBs were packed with GFP^+ cells (figure 3.1d). To quantify the expression of GFP on the generated EBs, an enzymatic and mechanical dissociation of these cellular structures was performed to obtain a single cell suspension for flow cytometry analysis.

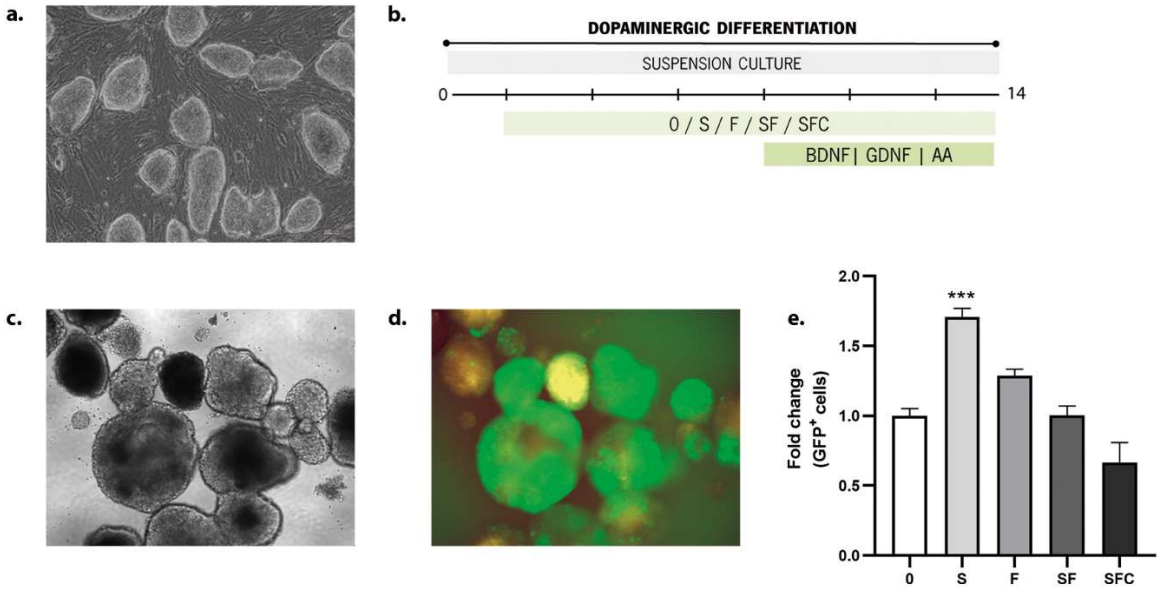

Figure 3.1 – Optimization of mouse embryonic stem cells (mESC) dopaminergic differentiation. a) undifferentiated mESC depicting well-defined colonies on top of a MEF feeder layer; **b)** timeline of dopaminergic differentiation showing the different factors tested in the embryoid-based protocol; **c)** and **d)** embryoid bodies (EBs) at the end of the differentiation protocol in bright field microscopy and under fluorescence microscopy, showing GFP^+ cells inside the EB, respectively; **e)** quantification of GFP^+ cells at the end of the differentiation protocol after EBs dissociation. Data is presented as fold change over the negative control – *O.* (n=4; mean ± SEM ***p≤0.001) *S* – SAG [0.5 µM] , *F* – FGF8 [100 ng/mL], *SF* – SAG [0.5 µM] and FGF8 [100 ng/mL], *SFC* – SAG [0.5 µM], FGF8 [100 ng/mL] and CHIR [0.8 µM].

Quantification of GFP^+ cells from the total cell suspension showed a higher differentiation efficiency of the protocol in which only SAG was added to induce the dopaminergic cell fate (figure 3.1e). Despite the known role of FGF8 in inducing midbrain specification (Ye *et al.*, 1998), in our protocol, the addition of

this patterning factor did not induce a significant increase over the negative control. Using only SAG, we were able to obtain an average of 15% of GFP^+ cells from the total cell population. Conversely, Lee and colleagues had reported 6.9% of TH^+ cells from the 71.9%. neuronal population present in culture (Lee *et al.*, 2000). Higher percentages have been reported for coculture systems with stromal-feeder layer (up to 50% TH^+ cells), described by (Barberi *et al.*, 2003), as well as through forced expression of LMX1A (75%–95% of TH^+ cells from the neuronal population) (Friling *et al.*, 2009). Nevertheless, both feeder layer seeding and viral infection are technically demanding and, therefore, are not suitable for generating an *in vitro* model for drug screening.

On the other hand, the use of an EB-based protocol is simple and has been demonstrated to yield higher proliferation and differentiating capacity for neural induction in human iPSCs (Pauly *et al.*, 2018). Indeed, iPSCs-derived neural cultures using an EB-based protocol have been shown to recapitulate embryonic events, as they display an intrinsic induction of hedgehog signaling (Crompton *et al.*, 2013). This is probably one of the explanations for the existence of GFP^+ cells (8%) in the negative control differentiation protocol, in which no morphogen was added to the EBs in culture. Moreover, mESCs have a default differentiation propensity toward mid/hindbrain fate, as opposed to hESCs that are more prone to differentiate toward the forebrain identity (Studer, 2012).

In summary, at this point, we have optimized the dopaminergic differentiation protocol of mESCs, taking advantage of the GFP expression as a measure of efficiency. Moreover, it was also possible to show that adding only SAG in an EB-based protocol is sufficient to obtain approximately 15% of TH^+ (GFP^+) cells. By eliminating the need to use FGF8 in the differentiation protocol, it is possible to reduce the overall costs of this differentiation protocol and thus, potentiate the generation of a large-scale *in vitro* disease model. Another advantage of using mESCs TH::GFP reporter line, is the possibility to obtain a pure culture of TH^+ cells, by performing fluorescence-activated cell sorting of GFP^+ cells. Nonetheless, in the next steps we kept the generated dopaminergic neurons inside the EB and modulated differentiation, using a more favorable extracellular environment for neuronal differentiation

3.2. *Culture of mouse embryonic stem cells derived embryoid bodies on collagen hydrogel*

In the next step of our protocol we sought to culture each generated EB on top of a collagen hydrogel droplet. For that, at the end of the dopaminergic neuronal differentiation we transferred one EB to a droplet of collagen, previously prepared on a 48-well plate and kept them in culture for an additional period of 6 days with daily medium changes to keep the nutritional support (figure 3.2a). This type of

culture on multi-well plates allows for testing different experimental conditions at the same time, using low amounts of reagents.

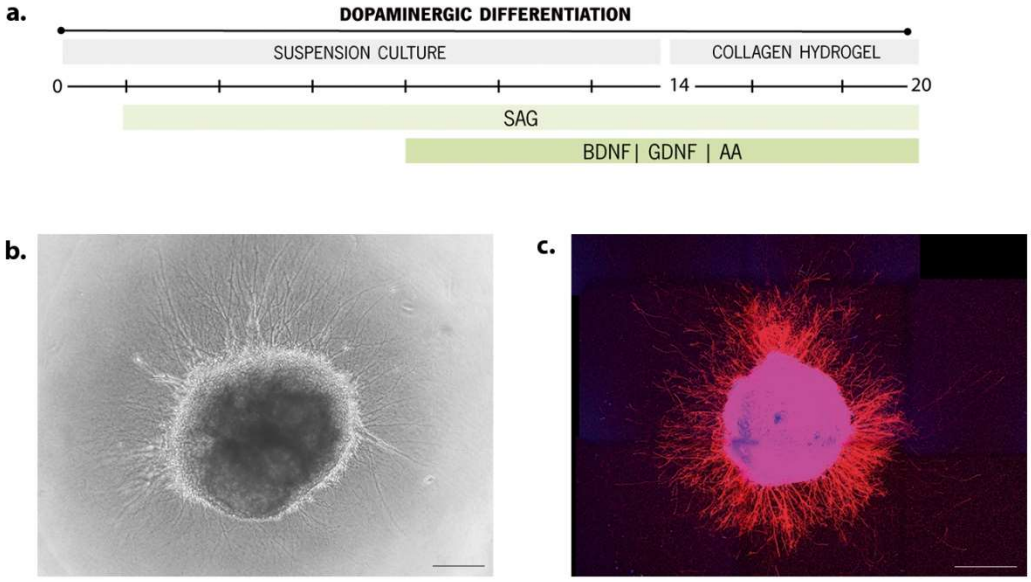

Figure 3.2 – Seeding of mESC-derived embryoid bodies on collagen hydrogel. a) timeline of the differentiation protocol carried out in ultra-low attachment surfaces for the first 14 days and in a collagen hydrogel in the last 6 days; **b)** bright field imaging (4x objective) of an EB extending its neurites on top of collagen; **c)** expression of a dopaminergic markers, tyrosine hydroxylase (TH), on neurites extending on top of the collagen. Scale bars: 200 µm.

After seeding the EBs on collagen it was clearly visible the extension of long neurites on top of the collagen, which arise from all around the body structure (figure 3.2b). To confirm if these neurites were specific of dopaminergic neurons, we performed further immunocytochemistry analysis to check TH expression. As observed in figure 3.2c, TH^+ neurites are present in most of the surrounding areas of the EB, as well as in the central area. Therefore, we confirmed the use of collagen as an ECM protein that potentiates neurite outgrowth (Sundararaghavan *et al.*, 2009), and further validated the ability of its reduced stiffness in promoting dopaminergic differentiation (Keung *et al.*, 2012; Kothapalli *et al.*, 2013). Besides providing a 3D culture system of dopaminergic neurons, seeding the EBs on collagen avoids their dissociation that is often associated with decreased viability of generated neurons.

3.3. *Effects of 6-OHDA exposure on established model*

Finally, we induced neuronal death by incubation with 6-OHDA in the previously obtained dopaminergic neuronal 3D model. 6-OHDA is an hydroxylated analogue of dopamine that has been widely used to model neurodegeneration underlying PD (Oñate *et al.*, 2019). Due to their similar chemical structure, 6-OHDA can be transported into dopaminergic cells, being very rapidly oxidized which produces free radicals and

hydrogen peroxide that induce neuronal damage (Fulceri *et al.*, 2006). Because dopaminergic neurites are enclosed in the collagen, which might confer some degree of protection, we have used a high dosage ([500 µM]) and a long incubation period (4h) to induce a significant decrease of dopaminergic neurons (figure 3.3a). After 6-OHDA exposure, cells were incubated with two distinct media: *NB+* - a complete differentiation medium composed of ADFNK medium supplemented with SAG, BDNF, GDNF and AA, and *NB* - a basal medium without any supplementation.

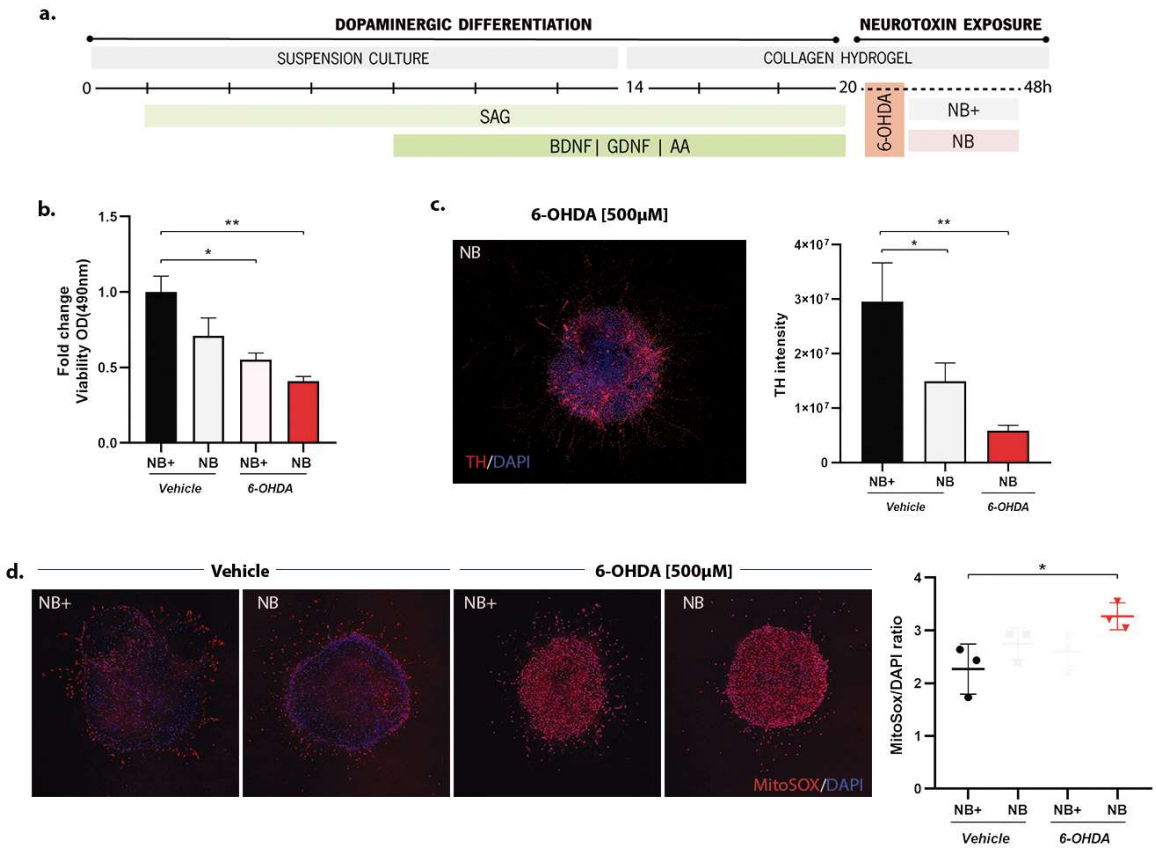

Figure 3.3 – 6-OHDA-induced effects on the established 3D model of dopaminergic neurons. a) timeline of the differentiation protocol carried out in ultra-low attachment surfaces for the first 14 days, collagen hydrogel for the next 6 days followed by exposure to 6-OHDA and analysis 48h after induction; **b)** effects of 6-OHDA exposure on cell viability measured by the MTS assay (n=9-11); **c)** effects of 6-OHDA exposure on TH$^+$ neurons and its quantification (n=3-5); **d)** effects of 6-OHDA exposure on the production of reactive oxygen species (ROS) detected by a MitoSOX probe and quantified (right panel) by the dividing the intensity of MitoSOX by the intensity of DAPI staining (n=3; mean ± SEM; *($p<0.05$)). *NB+* - supplemented medium, *NB* – non-supplemented medium.

To address the effect of 6-OHDA on the overall cell viability, we have employed a MTS assay that is an indirect measure of mitochondrial activity of living cells. Incubation with 6-OHDA induced a significant decrease of cell viability, with or without the presence of supplements after toxin exposure (figure 3.3b).

Further analysis of the morphology of TH neurites after 6-OHDA exposure, revealed a marked decrease of the intensity of TH expression in the EB (Figure 3.3c). As an additional measure of 6-OHDA induced cellular alterations, we have used a live-imaging probe that detects the production of ROS with mitochondria specificity (MitoSOX). Indeed, as depicted in figure 3.3d, 6-OHDA exposure induces a significant increase of the ratio of MitoSOX/DAPI when EBs are maintained with no supplements during the 48h following 6-OHDA incubation.

These cellular alterations confirm the neurotoxicity of 6-OHDA to dopaminergic neurons present in the 3D culture system, thereby providing a reliable model for mimicking PD *in vitro*. To better understand the mechanisms leading to 6-OHDA-induced cell death, it would be relevant to address the expression of dopamine transporter in our 3D culture system to confirm that the toxic effects are mediated by the selective 6-OHDA uptake by dopaminergic neurons and not by its extracellular autoxidation. A better understanding of the intracellular mechanism leading to dopaminergic cell death, may deliver other cellular markers to address possible neuroprotective effects of new therapies tested using this model.

In spite of future improvements of the model at the mechanistic level, we were able to generate an *in vitro* model of PD that mimics the phenotypic features of the underlying neurodegeneration, including decreased cell viability, increased production of ROS and loss of dopaminergic neurites. Because it is based on mESCs, dopaminergic differentiation can be achieved faster, with reduced associated costs of maintenance and amount of factors used for differentiation. Moreover, the use of collagen as a substrate for neurite outgrowth enhances the relevance of the model, thereby yielding a time and cost-effective *in vitro* preclinical PD model.

Acknowledgments

Acknowledgement: Financial support from MultiPark, Crafoord Foundation Sweden, and Portuguese Foundation for Science and Technology (FCT): IF Development Grant (IF/00111/2013) to AJ Salgado and Pre-Doctoral Fellowships to A. Marote (PDE/BDE/113598/2015), B. Mendes-Pinheiro (SFRH/BD/120124/2016) and E. Gomes (SFRH/BD/103075/2014). This work has been developed under the scope of the project NORTE-01-0145-FEDER-000023, supported by the Northern Portugal Regional Operational Programme (NORTE 2020), under the Portugal 2020 Partnership Agreement, through the European Regional Development Fund (FEDER). This project has been funded by FEDER funds, through the Competitiveness Factors Operational Programme (COMPETE), and by National funds, through FCT, under the scope of the project POCI-01-0145-FEDER-007038.

References

Barberi T, Klivenyi P, Calingasan NY, Lee H, Kawamata H, Loonam K, Perrier AL, Bruses J, Rubio ME, Topf N, Tabar V, Harrison NL, Beal MF, Moore MAS, & Studer L. (2003). Neural subtype specification of fertilization and nuclear transfer embryonic stem cells and application in parkinsonian mice. *Nat Biotechnol, 21*(10), 1200-1207. doi:10.1038/nbt870

Blum D, Torch S, Lambeng N, Nissou M, Benabid AL, Sadoul R, & Verna JM. (2001). Molecular pathways involved in the neurotoxicity of 6-OHDA, dopamine and MPTP: contribution to the apoptotic theory in Parkinson's disease. *Prog Neurobiol., 65*(2), 135-172.

Bosco DA, Fowler DM, Zhang Q, Nieva J, Powers ET, Wentworth P, Jr., Lerner RA, & Kelly JW. (2006). Elevated levels of oxidized cholesterol metabolites in Lewy body disease brains accelerate alpha-synuclein fibrilization. *Nature chemical biology, 2*(5), 249-253. doi:10.1038/nchembio782

Caliari SR, & Burdick JA. (2016). A practical guide to hydrogels for cell culture. *Nature Methods, 13*(5), 405-414. doi:10.1038/nmeth.3839

Chumarina M, Azevedo C, Bigarreau J, Vignon C, Kim K-S, Li J-Y, & Roybon L. (2017). Derivation of mouse embryonic stem cell lines from tyrosine hydroxylase reporter mice crossed with a human SNCA transgenic mouse model of Parkinson's disease. *Stem Cell Res, 19*, 17-20. doi:https://doi.org/10.1016/j.scr.2016.12.026

Crompton LA, Byrne ML, Taylor H, Kerrigan TL, Bru-Mercier G, Badger JL, Barbuti PA, Jo J, Tyler SJ, Allen SJ, Kunath T, Cho K, & Caldwell MA. (2013). Stepwise, non-adherent differentiation of human pluripotent stem cells to generate basal forebrain cholinergic neurons via hedgehog signaling. *Stem Cell Res, 11*(3), 1206-1221. doi:https://doi.org/10.1016/j.scr.2013.08.002

Dauer W, & Przedborski S. (2003). Parkinson's disease: mechanisms and models. *Neuron., 39*(6), 889-909.

Evans MJ, & Kaufman MH. (1981). Establishment in culture of pluripotential cells from mouse embryos. *Nature, 292*(5819), 154-156. doi:10.1038/292154a0

Falkenburger BH, Saridaki T, & Dinter E. (2016). Cellular models for Parkinson's disease. *Journal of Neurochemistry, 139*(S1), 121-130. doi:10.1111/jnc.13618

Friling S, Andersson E, Thompson LH, Jönsson ME, Hebsgaard JB, Nanou E, Alekseenko Z, Marklund U, Kjellander S, Volakakis N, Hovatta O, El Manira A, Björklund A, Perlmann T, & Ericson J. (2009). Efficient production of mesencephalic dopamine neurons by Lmx1a expression in embryonic stem cells. *Proceedings of the National Academy of Sciences of the United States of America, 106*(18), 7613-7618. doi:10.1073/pnas.0902396106

Fulceri F, Biagioni F, Lenzi P, Falleni A, Gesi M, Ruggieri S, & Fornai F. (2006). Nigrostriatal damage with 6-OHDA: validation of routinely applied procedures. *Annals of the New York Academy of Sciences, 1074*, 344-348. doi:10.1196/annals.1369.032

Iacovitti L, Donaldson AE, Marshall CE, Suon S, & Yang M. (2007). A protocol for the differentiation of human embryonic stem cells into dopaminergic neurons using only chemically defined human

additives: Studies in vitro and in vivo. *Brain Res, 1127*(1), 19-25. doi:10.1016/j.brainres.2006.10.022

Iwashita M, Ohta H, Fujisawa T, Cho M, Ikeya M, Kidoaki S, & Kosodo Y. (2019). Brain-stiffness-mimicking tilapia collagen gel promotes the induction of dorsal cortical neurons from human pluripotent stem cells. *Scientific Reports, 9*(1), 3068. doi:10.1038/s41598-018-38395-5

Keung AJ, Asuri P, Kumar S, & Schaffer DV. (2012). Soft microenvironments promote the early neurogenic differentiation but not self-renewal of human pluripotent stem cells. *Integrative biology : quantitative biosciences from nano to macro, 4*(9), 1049-1058. doi:10.1039/c2ib20083j

Kothapalli CR, & Kamm RD. (2013). 3D matrix microenvironment for targeted differentiation of embryonic stem cells into neural and glial lineages. *Biomaterials, 34*(25), 5995-6007. doi:10.1016/j.biomaterials.2013.04.042

Kratochvil MJ, Seymour AJ, Li TL, Paşca SP, Kuo CJ, & Heilshorn SC. (2019). Engineered materials for organoid systems. *Nature Reviews Materials, 4*(9), 606-622. doi:10.1038/s41578-019-0129-9

Lee S-H, Lumelsky N, Studer L, Auerbach JM, & McKay RD. (2000). Efficient generation of midbrain and hindbrain neurons from mouse embryonic stem cells. *Nat Biotechnol, 18*(6), 675-679. doi:10.1038/76536

Lin L, & Isacson O. (2006). Axonal growth regulation of fetal and embryonic stem cell-derived dopaminergic neurons by Netrin-1 and Slits. *Stem cells (Dayton, Ohio), 24*(11), 2504-2513. doi:10.1634/stemcells.2006-0119

Little D, Ketteler R, Gissen P, & Devine MJ. (2019). Using stem cell-derived neurons in drug screening for neurological diseases. *Neurobiol Aging, 78*, 130-141. doi:10.1016/j.neurobiolaging.2019.02.008

Lopes FM, Bristot IJ, da Motta LL, Parsons RB, & Klamt F. (2017). Mimicking Parkinson's Disease in a Dish: Merits and Pitfalls of the Most Commonly used Dopaminergic In Vitro Models. *Neuromolecular medicine, 19*(2-3), 241-255. doi:10.1007/s12017-017-8454-x

Michel Patrick P, Hirsch Etienne C, & Hunot S. (2016). Understanding Dopaminergic Cell Death Pathways in Parkinson Disease. *Neuron, 90*(4), 675-691. doi:10.1016/j.neuron.2016.03.038

Murphy AR, Laslett A, O'Brien CM, & Cameron NR. (2017). Scaffolds for 3D in vitro culture of neural lineage cells. *Acta biomaterialia, 54*, 1-20. doi:10.1016/j.actbio.2017.02.046

Nakabeppu Y, Tsuchimoto D, Yamaguchi H, & Sakumi K. (2007). Oxidative damage in nucleic acids and Parkinson's disease. *J Neurosci Res, 85*(5), 919-934. doi:10.1002/jnr.21191

Oñate M, Catenaccio A, Salvadores N, Saquel C, Martinez A, Moreno-Gonzalez I, Gamez N, Soto P, Soto C, Hetz C, & Court FA. (2019). The necroptosis machinery mediates axonal degeneration in a model of Parkinson disease. *Cell Death & Differentiation*. doi:10.1038/s41418-019-0408-4

Pauly MG, Krajka V, Stengel F, Seibler P, Klein C, & Capetian P. (2018). Adherent vs. Free-Floating Neural Induction by Dual SMAD Inhibition for Neurosphere Cultures Derived from Human Induced

Pluripotent Stem Cells. *Frontiers in Cell and Developmental Biology, 6*(3). doi:10.3389/fcell.2018.00003

Pollard AK, Craig EL, & Chakrabarti L. (2016). Mitochondrial Complex 1 Activity Measured by Spectrophotometry Is Reduced across All Brain Regions in Ageing and More Specifically in Neurodegeneration. *PLoS One, 11*(6), e0157405-e0157405. doi:10.1371/journal.pone.0157405

Schapira AHV, Cooper JM, Dexter D, Clark JB, Jenner P, & Marsden CD. (1990). Mitochondrial Complex I Deficiency in Parkinson's Disease. *Journal of Neurochemistry, 54*(3), 823-827. doi:10.1111/j.1471-4159.1990.tb02325.x

Studer L. (2012). Derivation of dopaminergic neurons from pluripotent stem cells. *Progress in brain research, 200*, 243-263. doi:10.1016/b978-0-444-59575-1.00011-9

Sundararaghavan HG, Monteiro GA, Firestein BL, & Shreiber DI. (2009). Neurite growth in 3D collagen gels with gradients of mechanical properties. *Biotechnology and bioengineering, 102*(2), 632-643. doi:10.1002/bit.22074

Takahashi K, Tanabe K, Ohnuki M, Narita M, Ichisaka T, Tomoda K, & Yamanaka S. (2007). Induction of pluripotent stem cells from adult human fibroblasts by defined factors. *Cell., 131*(5), 861-872.

Takahashi K, & Yamanaka S. (2006). Induction of pluripotent stem cells from mouse embryonic and adult fibroblast cultures by defined factors. *Cell, 126*(4), 663-676. doi:10.1016/j.cell.2006.07.024

Ye W, Shimamura K, Rubenstein JLR, Hynes MA, & Rosenthal A. (1998). FGF and Shh Signals Control Dopaminergic and Serotonergic Cell Fate in the Anterior Neural Plate. *Cell, 93*(5), 755-766. doi:10.1016/s0092-8674(00)81437-3

CHAPTER 4

INDUCED PLURIPOTENT STEM CELL-DERIVED MESENCHYMAL STEM CELLS: AN UNLIMITED SOURCE OF NEUROPROTECTIVE FACTORS WITH THERAPEUTIC POTENTIAL FOR PARKINSON'S DISEASE

***This chapter is based on the following publication:**

Marote A, Barata-Antunes S, Mendes-Pinheiro B, Domingues AV, Gomes ED, Patrício P, Soares-Cunha C, Serre-Miranda C, Fernandes-Platzgummer A, Teixeira FG, Lobato da Silva S, Roybon L, Pinto L, Salgado AJ. Induced pluripotent stem cell-derived mesenchymal stem cells: an unlimited source of neuroprotective factors with therapeutic potential for Parkinson's disease

(manuscript and patent in preparation)

Chapter 4 | Induced pluripotent stem cell-derived mesenchymal stem cells: an unlimited source of neuroprotective factors with therapeutic potential for Parkinson's disease

Abstract

Parkinson's disease (PD) is characterized by a progressive loss of dopaminergic neurons (DAn) at the substantia nigra pars compacta, giving rise to motor and non-motor symptoms that severely impair patients' quality of life. Current pharmacologic approaches for PD only target the symptoms, and do not prevent neuronal damage. Mesenchymal stem cells (MSCs) have been proposed as a promising therapeutic strategy to prevent DAn degeneration, particularly due to their paracrine action. Nevertheless, the primary sources from which MSCs are commonly obtained are not suitable for translating this potential therapy into a clinical context, not only due to the invasive protocols inherent to their isolation, but also due to their limited proliferative capacity over continuous passaging. Induced pluripotent stem cells (iPSCs), obtained via somatic cell reprogramming, can be expanded indefinitely and are capable of differentiating into any cell type. Thus, our aim is to address the use of iPSCs as a source of MSCs (iMSCs) and assess the therapeutic potential of their secretome. For that, we have firstly generated iMSCs using a serum-free protocol. Subsequently, we performed a direct comparison between iMSCs and bone-marrow derived MSCs (BM-MSCs) secretome at composition level as well as in understanding their regenerative potential both *in vitro* and *in* vivo using an animal PD model. Our results show that both sources secrete neuroregulatory factors in similar amounts and thus, promote the same level of neurodifferentiation of neural progenitor cells. Moreover, both iMSCs and BM-MSCs secretome significantly improved the motor performance of 6-OHDA lesioned animals, which may be attributed to preservation of dopaminergic neurons in the nigrostriatal pathway. Therefore, our study paves the way for exploring MSCs as a source for future PD therapeutic applications based on secretome administration.

1. Introduction

Parkinson's disease (PD) is the second most common neurodegenerative disorder, affecting 6.1 million people worldwide, and 1% of the population above 60 years-old (Dorsey *et al.*, 2018; Tysnes *et al.*, 2017). Besides the core motor symptoms - bradykinesia, rest tremor and rigidity - on which clinical diagnosis is based, PD has been increasingly associated to the occurrence of nonmotor manifestations, such as olfactory loss, constipation and depression (Aarsland *et al.*, 2012; Berg *et al.*, 2015; Pont-Sunyer *et al.*, 2015; Postuma *et al.*, 2015). Severe neuronal loss in the Substantia nigra *pars compacta* (SNc), as well as widespread α-synuclein immunoreactive neuronal inclusions, are the main PD pathological hallmarks (Dauer *et al.*, 2003). Although PD etiology remains largely unknown, impaired α-synuclein proteostasis, mitochondrial dysfunction and increased oxidative stress have been put forward as key cellular disturbances underlying neurodegeneration (Michel *et al.*, 2016; Poewe *et al.*, 2017). Current therapeutic approaches are focused on the substitution of dopamine in the nigrostriatal system, which is initially effective in modulating motor symptoms, but is often associated to the occurrence of complications after long-term use (Pires *et al.*, 2017). Therefore, one of the major challenges in this field is the development of therapeutic strategies that are able to modify disease progression, *i.e.* that slow, halt, or reverse PD-associated neurodegeneration (Athauda *et al.*, 2015).

Mesenchymal stem cells (MSCs) were initially explored as a source of adult stem cells for cell replacement strategies in PD (Barker *et al.*, 2015). These adult multipotent stem cells can be isolated from different adult tissues, such as bone marrow and adipose tissue, and are characterized by the expression of specific cell surface markers, namely CD105, CD90 and CD73 and the ability to differentiate into osteoblasts, adipocytes and chondroblasts (Dominici et al., 2006). Nonetheless, the therapeutic effects associated to their transplantation in PD preclinical models have been associated to their paracrine activity, rather than to their transdifferentiation into dopaminergic neurons (Mendes-Pinheiro *et al.*, 2019; Teixeira *et al.*, 2013). Indeed, a number of soluble factors, such as cytokines and growth factors, as well as vesicles with immunomodulatory, neurogenic and neuroprotective actions have been identified in MSCs secretome (Caplan *et al.*, 2006; Mendes-Pinheiro *et al.*, 2019; Salgado *et al.*, 2015; Teixeira *et al.*, 2013; Volkman *et al.*, 2017). Therefore, MSCs conditioned medium (CM), which contains their secreted factors (*i.e.* secretome), holds an interesting potential for the development of cell-free therapeutic approaches for PD, without requiring the technical constraints and risks associated to cell transplantation (Marques *et al.*, 2018; Mendes-Pinheiro *et al.*, 2019; Teixeira *et al.*, 2017).

Nevertheless, current sources from which MSCs are obtained limit the expansion of MSCs in large numbers to allow the collection of significant volumes of secretome for clinical applications. Additionally, isolation of MSCs from tissue sources, such as bone marrow, involves an invasive and painful procedure to the donor (Fan *et al.*, 2020). Moreover, their number, quality and proliferative capacity decreases with donor's age, thereby displaying a limited expansion in culture (Fitzsimmons *et al.*, 2018). On the other hand, induced pluripotent stem cells (iPSCs) have been recently put forward as a promising alternative source for obtaining large populations of MSC-like cells (iMSCs) (Hynes *et al.*, 2014; Sabapathy *et al.*, 2016).

iPSCs are embryonic-like stem cells obtained through reprogramming of easily accessible somatic cell sources, such as fibroblasts and peripheral blood mononuclear cells (Takahashi *et al.*, 2007). After being established, these cells present self-renewal capacity and can be differentiated into any desired cell type (Shi *et al.*, 2016). Therefore, iPSCs provide an improved source of MSCs, not only due to the virtually unlimited iPSCs self-renewal capacity, but also due to the rejuvenated phenotype of iPSCs acquired after the reprogramming process. Indeed, this provides a higher proliferative capacity and lower cell senescence to iMSCs in comparison to tissue-derived MSCs (Spitzhorn *et al.*, 2019). Only a limited number of studies has assessed the therapeutic potential of iMSCs, reporting similar outcomes in comparison to tissue-derived MSCs (Lian *et al.*, 2010; Zhang *et al.*, 2015). Nevertheless, their therapeutic action in PD remains elusive.

Therefore, the aim of the present study was to address the potential of iMSCs secretome as a cell-free therapeutic approach for PD. For that we have firstly generated iMSCs from three different iPSCs lines using a serum-free protocol. Subsequently, we have performed a direct comparison on the secretome effects between iMSCs and the gold standard MSCs isolation source, BM-MSCs, using both *in vitro* and *in vivo* PD experimental models of dopaminergic degeneration. Due to the increasing recognition of the importance of nonmotor alterations in PD, we have also addressed the impact of 6-OHDA lesion, as well as treatment administration in depressive-like behavior, including anhedonia and anxious-like behavior. Finally, we present a targeted proteomic analysis of the conditioned medium from both MSCs sources, identifying neuroregulatory molecules in similar amounts in the conditioned medium from both MSCs sources.

2. Materials and methods

2.1. *Generation of induced pluripotent stem cell derived mesenchymal stem cells using a serum-dependent protocol*

MSC-like cells were generated according to the protocol described by Hynes and colleagues (Hynes *et al.*, 2014). A healthy iPSC line (NRC-2H), previously established in the lab, was expanded in MEF-coated flasks in WiCell medium, composed of advanced DMEM/F12, 20% Knock-Out Serum Replacement, 2 mM L-glutamine, 1% non-essential amino acids and 0.1mM β-mercaptoethanol, supplemented with 20 ng/ml FGF2 (Gibco). To initiate MSC differentiation, iPSCs were detached from MEFs using dispase (1mg/mL, Gibco) and seeded on a 0.1% gelatin-coated T25cm^2 flask after breaking colonies into smaller aggregates. Cells were kept in culture for 14 days, with medium changes every 2 days, in Minimum Essential Medium Eagle - alpha modified (alpha-MEM) containing 10% fetal bovine serum (FBS), 2mM L-glutamine, 1% HEPES, 1% non-essential amino acids, 1% sodium pyruvate, 1% penicillin/streptomycin and 100 µM ascorbic acid. After induction period, the resulting heterogeneous culture, was passaged as a single cell suspension using 0.05% trypsin in a 1:3 split ratio. Until passage 2, cells were seeded onto 0.1% gelatin-coated flasks. Afterwards, cells were passaged in the same ratio without gelatin coating.

2.2. *Generation of induced pluripotent stem cell derived mesenchymal stem cells*

To obtain MSCs without serum supplementation and without other products of animal origin, previously generated iPSCs lines (NRC-2H, NRC-4J, NRC-5H – described in chapter 2) were expanded in a feeder-free system in mTeSR™ medium onto vitronectin-coated 6-well tissue culture plates (all products from STEMCELL Technologies, Canada). Afterwards, STEMdiff™ Mesenchymal Progenitor Kit (STEMCELL technologies) was used to differentiate iPSCs into MSC-like cells, according to manufacturer's instructions. Briefly, iPSCs were dissociated into a single cell suspension after incubation with Gentle Cell Dissociation Reagent (STEMCELL Technologies, Canada) for 8 – 10 min. After centrifugation, 500 000 cells were seeded on vitronectin-coated 6-well tissue culture plates in mTeSR™ medium containing 10 µM of ROCK Inhibitor Y-27632 (Selleck Chemicals, USA). After 2 days and for the next 6 days, cells were kept in STEMdiff™-ACF Mesenchymal Induction Medium, with daily medium changes. At day 6, cells were passaged with Gentle Cell Dissociation Reagent (STEMCELL Technologies, Canada) into a new 6-well tissue culture plate in MesenCult™-ACF Plus Medium. From passage 2 onwards, cells were passaged at 2 000 cells/cm^2 using Animal Component-Free Cell Dissociation Kit (STEMCELL Technologies, Canada).

2.3. *Human bone-marrow derived MSCs culture*

Human bone-marrow derived MSCs (BM-MSCs; Lonza, Switzerland) from three different donors were thawed and seeded into T75cm^2 tissue culture flasks and expanded in MesenCult™-ACF Plus Medium (STEMCELL Technologies, Canada). The medium was renewed every 3 days and upon confluence, cells were dissociated using Animal Component-Free Cell Dissociation Kit (STEMCELL Technologies), according to manufacturer's instructions.

2.4. *Flow cytometry*

To perform phenotypical characterization of generated iMSCs and compare with BM-MSCs, single cell suspensions from each donor of BM-MSCs and iMSCs were prepared using Animal Component-Free Cell Dissociation Kit (STEMCELL Technologies). After cell counting using the trypan blue exclusion assay, 1 000 000 cells were transferred to a round-bottom 96-well plate and centrifuged at 1200 rpm, 2min, 4°C. The resulting pellet was diluted in FACS buffer (0.5% bovine serum albumin, 0.01% azide in PBS buffer). Antibody mixes were added to the corresponding well and incubated for 20 min at 4°C with the following antibodies: FITC anti-human CD105, PE anti-human CD90 (Thy1), PE/Cy7 anti-human CD73 (Ecto-5'-nucleotidase), APC/Cyanine7 anti-human CD34, Brilliant Violet 605™ anti-human CD45, PerCP-Cy5.5 Anti-Human TRA-1-60-R, Brilliant Violet 510™ anti-human HLA-DR (all from BioLegend, USA). Cells were then washed and resuspended in 200 μL of FACS buffer. All samples were acquired (minimum of 50000 events/sample) on an eight-color BD LSRII flow cytometer using the FACS DIVA software (BD Biosciences). Data was analyzed using the FlowJo software (Tree Star, Ashland, OR, USA) version 10.0.8.

2.5. *In vitro differentiation of MSCs*

To evaluate the multipotency of MSCs, a human MSC Functional Identification Kit (Catalog #SC006, R&D systems, USA) was used according to manufacturer's instructions. Briefly, after reaching confluence, MSCs from each source and donor were enzymatically dissociated as described in sections 2.1 and 2.2 and the number of viable cells was estimated. For adipogenic and osteogenic differentiation, 210 000 cells/cm^2 and 4 200 cells/cm^2 accordingly, were seeded onto a coverslip placed in a well of a 24-well tissue culture plate in alpha-MEM medium containing 10% FBS. Cells were kept in culture for 21 days with medium changes every 3 – 4 days and supplemented with the corresponding differentiation supplement. Chondrogenic differentiation was carried out by transferring 250 000 cells from the cell suspension into a 15 mL conical tube. After centrifugation at 0.2 x g for 5 min, the resulting pellet was

kept in culture for 21 days in D-MEM/F-12 medium supplemented with the chondrogenic supplement with medium changes every 2 – 3 days. At the end of the differentiation period, cells from each lineage differentiation were fixed in 4% paraformaldehyde (PFA; Merck, Portugal) for 30 min, RT. Chondrogenic pellets were then embedded in Tissue-Tek® O.C.T.™ compound (Sakura Finetek, Japan), gradually frozen in liquid nitrogen and kept at -20°C until sectioning. Serial 10 μm sections of frozen pellets were cut in the cryostat and collected to SuperFrost® Plus slides (ThermoFisher Scientific, USA). All tissues were then processed for immunocytochemistry by permeabilization and blocking for 45min in PBS 0.3% Triton X-100, 1% BSA and 10% newborn calf serum (NBCS; Biochrom, Germany). After that, primary antibodies were prepared in blocking buffer: goat anti-FABP4 [10 μg/mL] for the detection of adipocytes, mouse anti-osteocalcin [10 μg/mL] for the detection of osteoblasts and goat anti-Aggrecan [10 μg/mL] for the detection of chondrocytes. After primary antibody incubation period (3h at RT, ON at 4°C), cells were washed three times with PBS and secondary antibodies Alexa Fluor 488 goat anti-mouse and Alexa Fluor 488 rabbit anti-goat (1:500, Life Technologies) were added for 1h. Afterwards, nuclei counterstaining was performed with 4-6-diamidino-2-phenylindole-dhydrochloride (DAPI, 1:1000; Life Technologies) for 10 min at RT. Finally, coverslips were mounted on glass slides using immu-mount (Thermo Scientific, UK) and image acquisition was performed in a fluorescence microscope (BX61, Olympus, Germany).

2.6. *Secretome collection and concentration*

After confirming the identity of the generated MSCs, their conditioned medium was collected in passage 8 – 9 (P8/ P9) according to protocols already established in our laboratory. Briefly, 5 000 cells/cm^2 were seeded for *in vitro* and *in vivo* experiments and expanded for 72h in MesenCult™-ACF Plus Medium. On the conditioning day, cells were washed with PBS without Ca^{2+}/Mg^{2+} (Invitrogen) and incubated with Neurobasal A medium (TermoFisher Scientific, USA) supplemented with 1% kanamycin (Life Technologies, USA). After 24 h, the media containing the factors secreted by each MSC source were collected and centrifuged at 1200 rpm for 10 min at 4°C to remove any cell debris. For *in vivo* experiments, secretome was 100x concentrated by centrifugation using a 5 kDa cut-off concentrator (Vivaspin, GE Healthcare, UK), and frozen at -80 °C until used.

2.7. *Protein profile array*

To compare the secretory profile of BM-MSCs and generated iMSCs, a membrane-based antibody array (Human Neuro Discovery Array C1, AAH-NEU-1-2, RayBiotech. USA) was used following manufacturer's instructions. For that, after 30 min of blocking, the membrane array was incubated overnight (ON), at

4°C with the non-concentrated conditioned medium containing all the factors secreted by MSCs. On the next day, binding of secreted factors to the antibodies present in the membrane was detected by incubation with Biotinylated Detection Antibody Cocktail, followed by incubation with Streptavidin-Conjugated HRP. Chemiluminescence detection was performed using Sapphire Biomolecular Imager and spot intensity was measured using AzureSpot software (Azure Biosystems, USA).

2.8. *Neuronal differentiation assay with human neural progenitor cells*

For neuronal differentiation studies, pre-isolated and cryopreserved human neural progenitor cells (hNPCs) were thawed at 37°C and grown as neurospheres in serum-free PPRF-h2 medium, as previously described (Teixeira *et al.*, 2016). Cells were isolated in respect with the protocols and strict ethical guidelines previously established and approved by the Conjoint Health Research Ethics Board (CHREB, University of Calgary, Canada; ID: E-18786). After 3 days of expansion, the cells were mechanically dissociated into a single cell suspension and cultured in fresh PPRF-h2 medium. After 14-20 days of growth as neurospheres, hNPCs were passaged and seeded on pre-coated coverslips contained in 24-well plates with poly-D-lysine (100 μg/mL; Sigma) and laminin (10 μg/mL; Sigma) at a density of 60 000 cells per well. The cells were exposed for 5 days to each experimental condition and compared to a negative control group containing Neurobasal A medium with 1% kanamycin. A positive control composed of Neurobasal-A medium; 2% B27 (Gibco, USA), 0.05% basic fibroblast growth factor (bFGF; R&D Systems, USA), 1% kanamycin and 0.5% GlutaMAX (Gibco)] was used to ensure successful assay execution. At the end of the assay cells were fixed in 4% PFA for 30 min at RT, permeabilized in PBS 0.1% Triton X-100 for 5 min and blocked with PBS 10% NBCS for 1h, RT. Afterwards, cells were incubated with anti-microtubule associated protein-2 (MAP-2, mouse monoclonal IgG, 1:500; M4403, Sigma), diluted in PBS with 10% NBCS for 1 h at RT for mature neurons detection. After washing, cells were incubated with the secondary antibody Alexa Fluor 594 goat anti-mouse (1:1000; Life Technologies) for 1 h at RT. Nuclei were stained with DAPI (1:1000; Life Technologies) for 10 min at RT. Afterwards, coverslips were mounted on glass slides using immu-mount (Thermo Scientific, UK). Finally, for quantification analysis, samples were observed under blind conditions using a fluorescence microscope (BX61, Olympus, Germany) and ten representative imaging fields from three coverslips were chosen and analyzed.

2.9. *Neuroprotection assay*

To assess the neuroprotective effect of the secretome from both sources, an *in vitro* PD model (described in chapter 3) was used. Briefly, the model is based on the differentiation of mouse embryonic stem cells

(mESC) into dopaminergic neurons using a 3D culture system. mESCs were maintained in a mouse embryonic fibroblast-feeder layer in DMEM GlutaMAX, 10 % FBS, 1x Nucleosides (Millipore, USA), 2mM L-glutamine (Life Technologies, USA), 1x Penicillin-Streptomycin and 0.1mM β-mercaptoethanol (Sigma, USA) supplemented with leukemia inhibitory factor (LIF, 1:10 000; Millipore, USA).

For dopaminergic differentiation, mESCs were dissociated and cultured for 14 days as embryoid bodies (EBs) in differentiation medium consisting of Advanced DMEM-F12 medium (Gibco) and Neurobasal medium (Gibco) mixed at 1:1 ratio, 10% Knockout Serum Replacement (Life Technologies), 2mM L-glutamine, 1x Pen-Strep and 0.1 mM β-mercaptoethanol, supplemented with smoothened agonist (SAG, 0.5 μM, Tocris Bioscience, UK), brain-derived neurotrophic factor (BDNF, 10 ng/ml; Peprotech, UK), glial cell line-derived neurotrophic factor (GDNF; 10 ng/mL; Peprotech) and ascorbic acid (AA, 200 μM; Sigma). Subsequently, differentiated EBs were placed on top of a collagen hydrogel droplet placed at the center of a well of a 48-well tissue culture plate, wherein differentiation continues for six additional days.

After the establishment of a dopaminergic culture system, 6-hydroxydopamine (6-OHDA) was added to a subset of wells (500 μM of 6-OHDA diluted in 0.2% ascorbic acid), whereas another subset of wells was maintained in vehicle (0.2% ascorbic acid). After 4h exposure, 6-OHDA was removed and the wells were incubated with 1) differentiation medium (NB^+); 2) basal medium (NB), consisting of neurobasal A medium without further supplementation; 3) BM-MSCs conditioned medium; and 4) iMSCs conditioned medium.

Following 48h of incubation, cell viability and reactive oxygen species (ROS) production were assessed using MTS [(5-(3-carboxymethoxyphenyl)-2-(4,5-dimethyl-thiazoly)-3-(4-sulfophenyl) tetrazolium, inner salt) assay and MitoSOX™ Red reagent, respectively as described in chapter 2.

2.10. *Animals & experimental design*

Ten-weeks old Wistar-Han male rats (Charles River, Spain), weighing 305-414 g at the beginning of the experiment, were used, according to the Portuguese national authority for animal research, Direção Geral de Alimentação e Veterinária (ID: DGAV28421) and Ethical Subcommittee in Life and Health Sciences (SECVS; ID: SECVS 142/2016, University of Minho). Animals were housed in pairs, in a temperature and humidity-controlled room, maintained on 12 h light/dark cycles, with access to food and water *ad libitum*. The experimental timeline, including surgical interventions and behavioral assessment is described in figure 4.1.

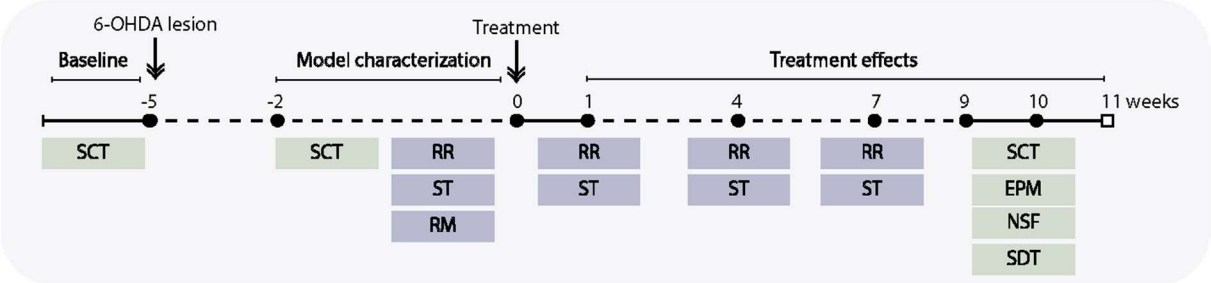

Figure 4.1 – Experimental timeline. Following animals' handling and baseline behavioral assessment of sucrose consumption test (SCT), 6-OHDA lesion surgeries were performed. Three weeks after surgery and during two weeks, a set of behavioral tests, SCT, rotarod (RR), staircase test (ST) and apomorphine-induced rotations (RM) were performed to assess the extent of motor and non-motor deficits elicited by 6-OHDA administration. Subsequently, treatment surgeries were performed and their effects at the motor behavior level were analyzed at 1, 4 and 7 weeks post-surgery using rotarod and staircase test. At 9 weeks after treatment surgery, non-motor behavior analysis was performed using the SweetDrive test (SDT) and SCT for anhedonia assessment and elevated plus maze (EPM) and novelty suppressed feeding (NSF) test to assess anxious-like behavior. After 2 weeks (16 weeks since lesion surgeries), animals were sacrificed and brain tissue was processed according to subsequent analysis.

2.11. *Surgeries*

All surgical procedures were conducted under aseptic conditions. Rats were anesthetized by intraperitoneal injection of ketamine (75 mg/kg) plus medetomidine (0.5 mg/kg) and placed on a stereotaxic apparatus (Stoelting, USA). The skull was exposed and a burr hole was drilled. All surgeries were performed with a Hamilton syringe (30-gauge; Hamilton, Switzerland) at a flow rate of 0.5 µl /min. The lesioned group (n=62) was injected with a total of 8 µg of 6-OHDA (2 µl of 6-OHDA dissolved in saline containing 0.2 mg/ml ascorbic acid; Sigma, USA) in the right medial forebrain bundle (MFB) at the following coordinates related to Bregma: AP =4 .4 mm, ML = -1.0 mm, DV = -7.8 mm). The sham group (n=16) received an equal volume of vehicle solution, at the same stereotaxic coordinates. The syringe was left in place for 2 minutes after injection and then removed slowly to optimize toxin diffusion and to avoid any backflow. The surgical procedures for treatment administration were performed as described above, and the animals were unilaterally injected in the SNpc (4 µl, coordinates related to Bregma: AP = -5.3 mm, ML = 1.8 mm, DV = -7.4 mm) and into four different sites of the striatum (2 µl/site, coordinates related to Bregma: AP = -1.3 mm, ML = 4.7 mm, DV = -4.5 mm and -4.0 mm; AP = -0.4 mm, ML = 4.3 mm, DV = -4.5 mm and 4.0 mm; AP = 0.4 mm, ML = 3.1 mm, DV = -4.5 mm and -4.0 mm; AP = 1.3 mm, ML = 2.7 mm; DV = -4.5 mm and -4.0 mm). The groups were divided as follows: *Sham* – sterile saline (n=14); *6-OHDA [vehicle]* - Neurobasal A medium (n=19); *6-OHDA [BM-MSCs CM]* – BM-MSCs

secretome (n=21); *6-OHDA [iMSCs CM]* – iMSCs secretome (n=21). After surgery all animals were treated with an analgesic – buprenorphine at 0.05 mg kg^{-1} (Bupaq, Richter Pharma, Wels, Austria).

2.12. *Behavioral analysis*

2.12.1. *Rotarod*

Rotarod was used to assess motor coordination and balance in a rotarod apparatus (3376-4R, TSE systems, USA). The protocol consisted of 3 days of training, under an accelerating protocol (4 rpm-40 rpm) during 5 min. At the fourth day using the same protocol, the animal latency to fall was recorded. The animals were allowed to rest at least 20 min between each trial.

2.12.2. *Staircase*

Staircase was used to assess fine motor control. The test apparatus consists of a clear chamber with a hinged lid (Campden Instruments, Lafayette, USA), connected to a narrower compartment with a central raised platform running along its length. A removable double staircase (with seven steps) is inserted into the end of the box, sliding into the troughs on either side of the central platform. To perform the test, five pellets were placed into each well of the double staircase apparatus. One day prior to the test session the rats were allowed to get familiarized with the chambers and pellets during 10 mins. In the test day, animals were kept inside the box for 15 minutes, so that they could reach, retrieve, and eat food pellets. After each test period, animals were removed from the staircase boxes and the remaining pellets were counted. To increase the animal's motivation to eat, we kept them in dietary restriction (10-15 g of standard laboratory food to maintain body weight at 90% of the free feeding level).

2.12.3. *Apomorphine-induced rotations*

Apomorphine-induced rotations were used as a measure of unilateral dopaminergic denervation, allowing the selection of the animals with a successful 6-OHDA lesion. Briefly, animals were injected with apomorphine (0.5 mg/kg in saline containing 0.2% ascorbic acid) and immediately placed into a circular cage and tied to an automated rotameter (MED-RSS, Med Associates, USA). The number of complete turns performed by the animals was recorded for 30 min. The rotational response was calculated by subtracting the total number of ipsilateral rotations to the total number of contralateral turns, and results were expressed as the number of net contralateral rotations.

2.12.4. *Sucrose consumption test*

The gold standard sucrose consumption test (SCT) was used to assess anhedonia. For that, pre-weighed drinking bottles containing water or 2% (m/v) sucrose solution were presented for 1 h to the animals individually placed on home cages. Before each test, rats were food and water-deprived for 12 h. SCT was performed during the nocturnal activity period of animals (starting at 8.30 p.m). Sucrose preference was calculated according to the formula: sucrose preference = (sucrose intake)/(sucrose intake + water intake) × 100, as previously described (Bessa *et al.*, 2009). Baseline sucrose preference values were established during a 1-week habituation period and compared to the values obtained after lesion and after treatment surgeries.

2.12.5. *Sweet-drive test*

A newly-developed test, the Sweet Drive Test (SDT), was also used to measure anhedonic behavior (Mateus-Pinheiro *et al.*, 2014). The SDT apparatus is composed of a black acrylic enclosed arena divided by transparent and perforated walls that define 4 separated chambers. The animal is initially placed in a pre-chamber that is connected by an automatic trap-door to a middle chamber (MC). Once the animal enters the MC, the trap-door closes, and the animal is allowed to move freely between the right chamber, containing 20 pre-weighted Cheerios® (68% Carbohydrates, 3800 $Kcal.Kg^{-1}$) pellets and the left chamber, containing 20 pre-weighted regular food pellets (Mucedola 4RF21-GLP; 53.3% Carbohydrates, 3700 $Kcal.Kg^{-1}$). The trial lasts for 10 min and at the end, pellets consumption is determined and preference for sweet pellets (Cheerios® pellets) is calculated as follows: preference for sweet pellets (%) = Consumption of Sweet Pellets (g)/Total Food Consumption (g) × 100. The test was performed after 8:30 pm (30 min after the beginning of the animals' nocturnal activity period) under red light, after 10h of food deprivation.

In addition to food consumption, animals ultrasonic vocalizations (USVs) during test period were also recorded using ultrasound microphones (CM16/CMPA, Avisoft Bioacoustics) sensitive to frequencies of 10–200 KHz placed 20 cm above the floor and connected via an Avisoft UltrasoundGate 416H (Avisoft Biocoustics) to a personal computer. Vocalizations were recorded using the Avisoft-Recorder (version 5.1.04) with the following settings: sampling rate: 250,000; format: 16 bit. All 50 KHz vocalizations, were identified and assessed by automatic data processing.

2.12.6. *Elevated plus maze*

The EPM test was carried out under bright white light in an apparatus consisting of a black polypropylene plus-shaped platform elevated 72.4 cm above the floor with two open arms (50.8 cm 10.2 cm) and two

closed arms (50.8 cm 10.2 cm 40.6 cm; MedAssociates Inc., USA). Animals were placed individually in the center of the platform and the number of entries into each arm and the time spent therein were recorded during 5 min and analyzed using EthoVision XT (Noldus Information Technology, USA).

2.12.7. *Novelty-suppressed feeding test*

The test apparatus consisted of an open-field arena (MedAssociates Inc, USA) containing a single food pellet at the center. After a 18h food-deprivation period, animals were placed in the arena and the time the animal took to reach the pellet was measured and expressed as the latency to feed. After that, the animals were individually returned to their home cage, where they were allowed to eat a pre-weighed food pellet for 10 min to provide a measure of their appetite drive.

2.13. *Histological analysis*

To further evaluate the degree of dopaminergic preservation, immunohistochemical staining for TH was performed. For that, animals (n=6-8/group) were anaesthetised with pentobarbital (Eutasi, 60 mg/kg, i.p.; Ceva Saúde Animal, Portugal) and transcardially perfused with 0.9% saline followed by 4%PFA in PBS. Brains were collected and transferred to a tube containing 4% PFA in PBS. After 48h of incubation at RT, brains were kept in 30% sucrose in PBS containing 0.01% of sodium azide at 4°C until being rains processed and sectioned coronally on a vibratome (VT1000S, Leica, Germany). Four series of coronal sections of striatum and SNc at a thickness of 50 µm were selected for free-floating immunohistochemistry. For that, sections were initially treated with 3% hydrogen peroxidase for 20 min to block endogenous peroxidase activity, permeabilized in 0.1% PBS-T for 10 min and then blocked in PBS 10% NBCS for 1h. Subsequently, sections were incubated with anti-TH (rabbit polyclonal IgG, 1:1000; Merck Millipore) overnight at 4°C. On the next day, brain sections were incubated during 30 min at RT firstly with a biotinylated secondary antibody (goat anti-polyvalent, TP-125-BN, ThermoFisher Scientific) and then with the streptavidine-peroxidase solution (TP-125-HR, ThermoFisher Scientific). Detection of streptavidin-biotin immunoenzymatic complex was performed using 25 mg of 3,3'-diaminobenzidine tetrahydrocloride (DAB; D5905, Sigma) in 50 ml of Tris-HCl 0.05 M (pH=7.6) with 12.5 µl of H_2O_2. Sections were then mounted on superfrost slides and air dried for 24h. Thionin counter-coloration was then performed, before mounting the sections using entellan (Merck Millipore).

TH^+ fibers in the striatum were imaged using brightfield illumination (SZX16, Olympus) and the optical density was measured using the ImageJ software (National Institute of Health, v1.48, USA), to draw the striatal area in each slice and compare it to the non-lesioned side. TH-positive cells in the SNc were

visualized and counted using a bright-field microscope (BX51; Olympus, Center Valley, PA) equipped with a digital camera (PixeLINK PL-A622, CANIMPEX Enterprises, Halifax, NS, Canada). Using the Visiomorph software (V2.12.3.0; Visiopharm, Hørsholm, Denmark) the boundaries of the SNc area were drawn and total TH^+ cells in the SNc area were counted in both hemispheres.

2.14. *Neurochemical analysis*

Macrodissection was performed in set of animals (n=10/group) after deeply anesthetizing with lethal dose of pentobarbital, decapitation and brain snap-freezing in liquid nitrogen. Brain areas of interest were rapidly dissected using a brain slicer, observing anatomical landmarks (according to Paxinos and Watson, 2005). Samples were snap-frozen (dry ice) and stored at −80°C until use. Quantification of catecholamine levels in the striatum was then performed by high-performance liquid chromatography, combined with electrochemical detection (HPLC/EC) using a Gilson instrument (Gilson, Middleton, WI, USA), fitted with an analytical column (Supleco Supelcosil LC-18 3 mM, Bellefonte, PA, USA; flow rate: 1.0 ml/min). Left and right dorsal striatum were weighted and then incubated with 0.2 N perchloric acid, sonicated (5 min on ice) and centrifuged at 5 000 g. The resulting supernatant was filtered through a Spin-X HPLC column (Costar, Lowell, MA, USA) to remove debris and 150 µl aliquots were injected into the HPLC system, using a mobile phase of 0.7 M aqueous potassium phosphate (pH 3.0) in 10% methanol, 1-heptanesulfonic acid (222 mg/l) and Na-EDTA (40 mg/l). A standard curve using known concentrations of all catecholamines was run each day. Catecholamines concentration in each side were calculated using the standard curve and normalized to the amount of tissue from which they were extracted.

2.15. *Statistical analysis*

A confidence interval of 95 % was assumed for all statistical tests. The assumption of normality was tested for all continuous variables through evaluation of the frequency distribution histogram, the values of skewness and kurtosis and through the Shapiro-Wilk test. For the evaluation of mean differences between samples with one independent variable, One-way ANOVA was used. For evaluation of mean differences between samples with one independent variable and one repeated measures variable, a mixed design ANOVA was carried out. Multiple comparisons were performed with Tukey's post hoc test for pairwise comparison of the independent variable. Results are presented as mean ± SEM. All statistical analysis were performed using Prism GraphPad 8.0.1(GraphPad Software; La Jolla, USA) and results were considered significant for $p \leq 0.05$.

3. Results

3.1. *Generation and characterization of iMSCs*

To address the best approach to obtain iMSCs, we have firstly compared two differentiation protocols. The serum-dependent (SD) protocol was based on a protocol previously described in the literature (Hynes *et al.*, 2014), which included the use of fetal FBS to maintain cell growth. Conversely, the serum-free (SF) protocol was based on a commercially available kit that allows the acquisition of iMSCs using a chemically-defined serum-free medium. Both protocols were able to yield cells with MSC-like morphology, expressing the cell surface markers CD73, CD90 and CD105 to a similar extent to the gold standard BM-MSCs (figure 4.2a – e). Moreover, using a neuronal differentiation assay, both SD and SF iMSCs were able to increase $MAP2^+$ cells to a similar extent to BM-MSCs under SF culture conditions (figure 4.2f), thereby revealing a similar neuroregulatory potential between the two sources. Nevertheless, iMSCs cultured under SF conditions exhibited a higher proliferative capacity than SD conditions (data not shown), as well as a multipotent capacity that better resembles BM-MSCs phenotype (figure 4.2e). Additionally, from a clinical perspective, the use of animal-derived components for MSCs expansion may represent a source of variability, hampering the acquisition of consistent batches of MSCs secretome. Therefore, our subsequent analysis was based on the SF approach to acquire iMSCs from different donors and assess their therapeutic paracrine potential.

Figure 4.3 depicts a complete characterization of iMSCs from three different donors and compared to one donor of BM-MSCs (figure 4.4), according to ISCT guidelines (Dominici *et al.*, 2006). Regarding positive MSC markers, all donors from both sources exhibited most of cell population positive for CD73 and C90 (BM-MSCs Donor 1, 2 and 3 - 100%, 99,9%, 98,7%, respectively; iMSCs donor 1, 2 and 3 – 98,6%, 95,8% and 96,4%, respectively). On the other hand, all cells were negative for hematopoietic markers – CD34, CD45, HLA-DR, as well as for TRA-1-60, a pluripotent cell surface marker. In addition to confirming MSCs identity at the phenotypic level, we have assessed multipotency by differentiating MSCs from both sources into adipogenic, osteogenic and chondrogenic lineage. Although iMSCs from all donors were able to differentiate into all cell types, iMSCs from donor 2 (NRC-4J) display a higher number of cells positive for FAPB4 in comparison to other iMSCs' donors. On the other hand, no differences were observed at the osteogenic lineage, as all iMSCs donors stained positive for osteocalcin at the same extent as BM-MSCs. Regarding chondrogenic differentiation, all iMSCs donors present a positive expression of aggrecan, though the structure of the chondrogenic pellet is not as organized as the ones obtained after

differentiation of BM-MSCs. Altogether, these results confirm the reproducibility of the differentiation protocol to obtain MSC-like cells from different donors.

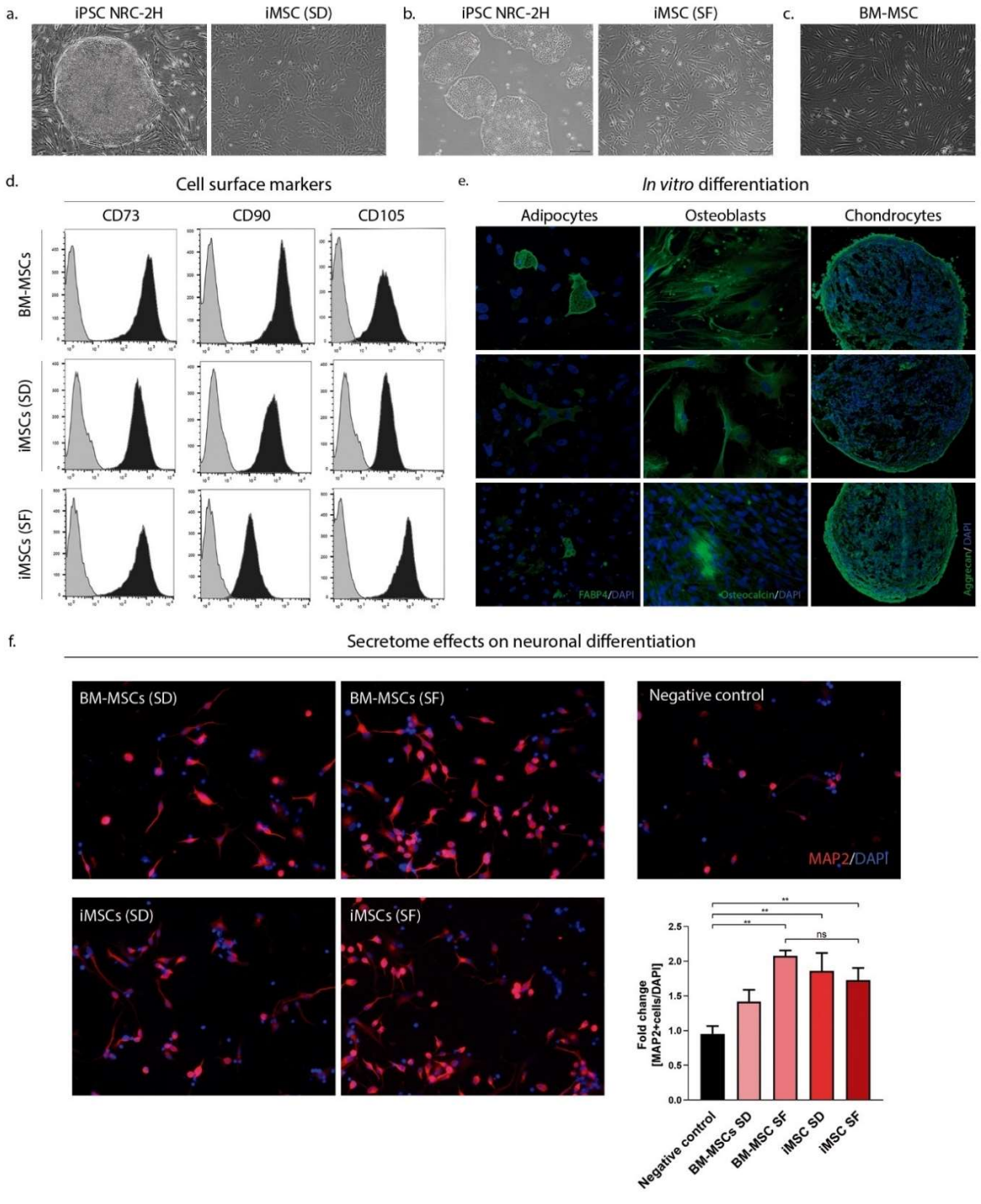

Figure 4.2 – Comparison of serum-dependent (SD) and serum-free (SF) iMSCs generation protocols. a) iPSCs (NRC-2H) colony on top of a MEF-feeder layer (left) and SD-generated iMSCs (right); **b)** iPSCs (NRC-2H) on feeder-fee culture conditions (left)) and SF-generated iMSCs (right); **c)** BM-MSCs cultured under SD conditions; **d)** phenotypic characterization of BM-MSCs and iMSCs on SD and SF culture conditions showing positive expression (black) of MSCs cell surface markers – CD73, CD90, CD105 against unstained control (gray); **e)** functional characterization of BM-MSCs and iMSCs on SD and SF

culture conditions showing their *in vitro* differentiation into adipocytes, osteoblasts and chondrocytes based on the expression of FABP4, Osteocalcin and Aggrecan, respectively; **f)** effect of culture conditions and MSCs source on the neurodifferentiation potential of their secretome, showing representative images and quantification of MAP2 expression on the differentiated neural progenitor cells following incubation with each experimental condition. Data is expressed as mean ± SEM of fold change over negative control (n=4-8 of two independent experiments, **p<0.01).

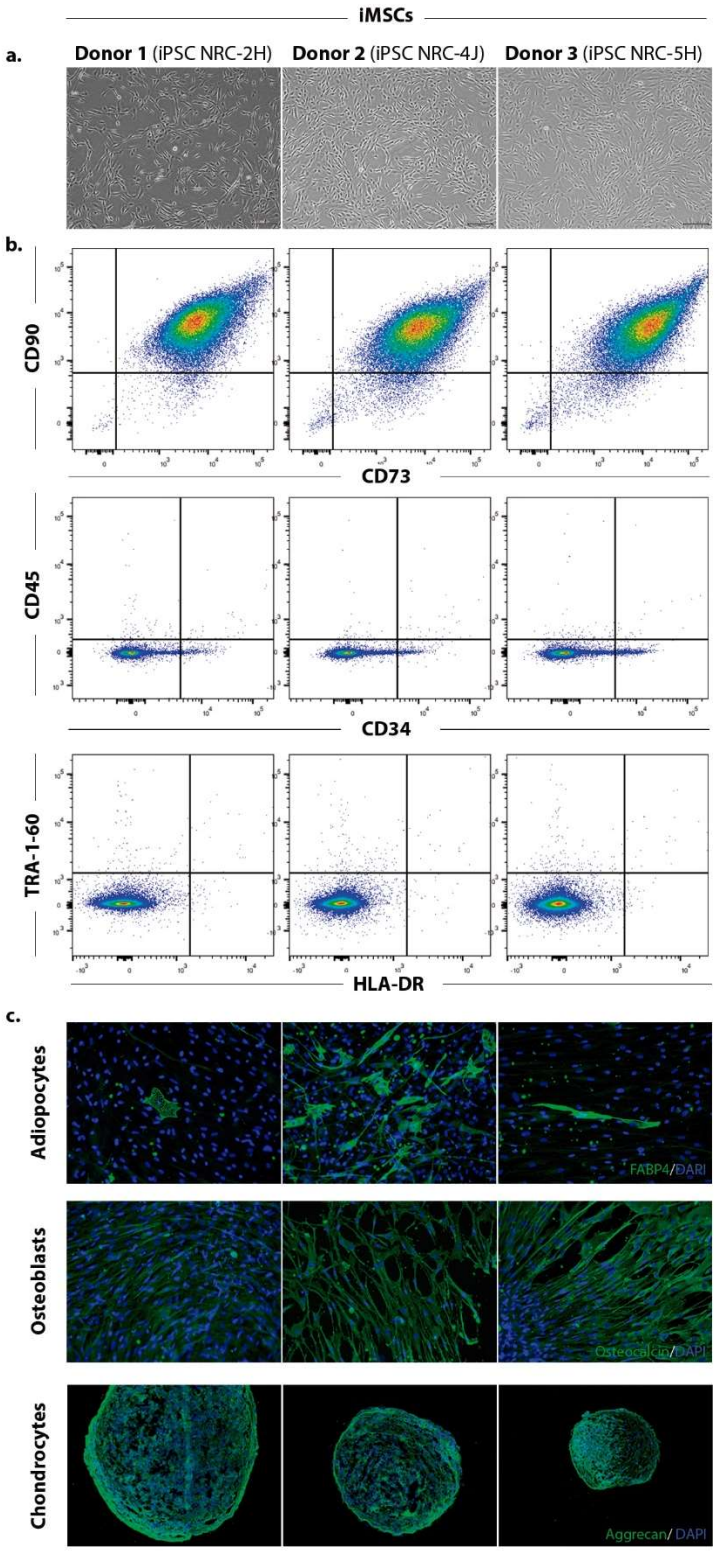

Figure 4.3 – Characterization of iMSCs from three different donors cultured on serum-free conditions. a) representative images of iMSCs morphology; **b)** phenotypic characterization performed by flow cytometry analysis of positive MSC cell surface markers (CD73 and CD90), negative MSCs cell surface markers (CD34, CD45, HLA-DR) and pluripotency marker (TRA-1-60); **c)** functional characterization showing their *in vitro* differentiation into adipocytes, osteoblasts and chondrocytes based on the expression of FABP4, Osteocalcin and Aggrecan, respectively.

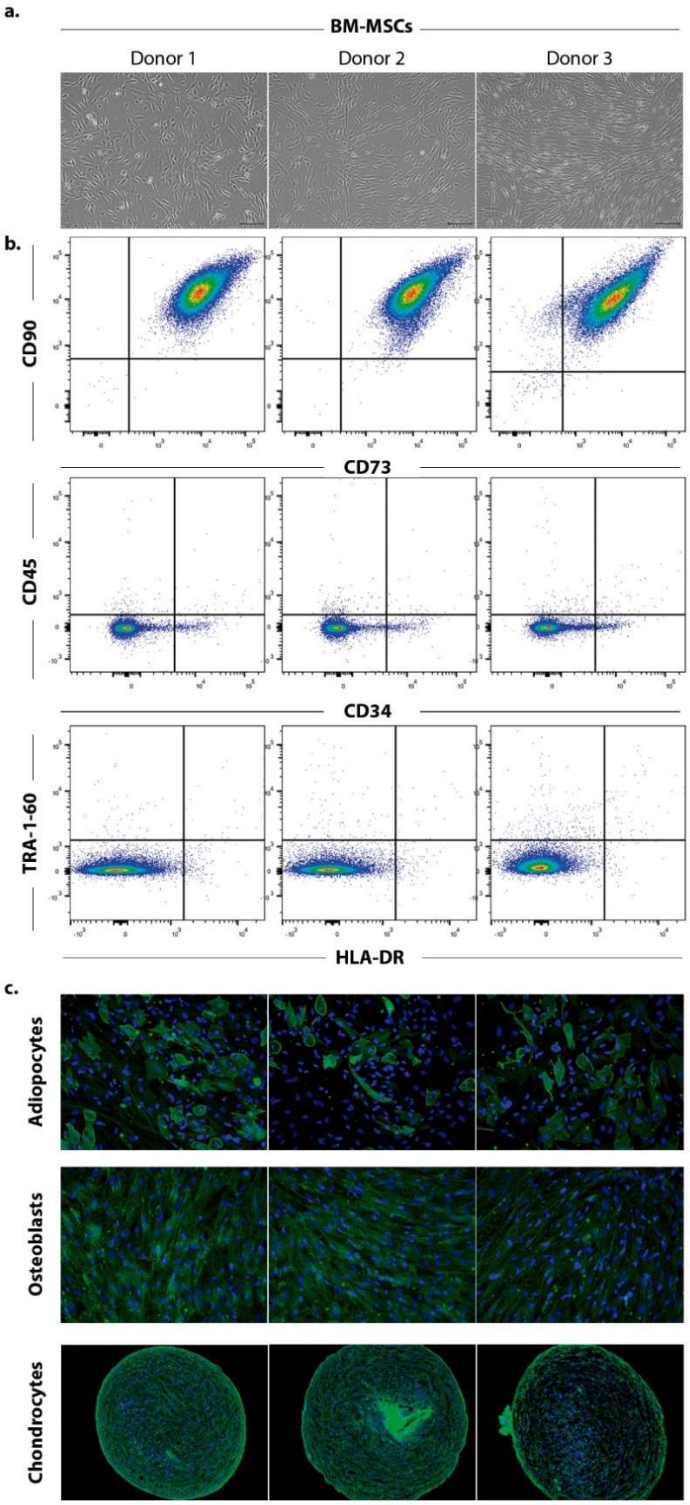

Figure 4.4 – Characterization of BM-MSCs from three different donors cultured on serum-free conditions. a) representative images of BM-MSCs morphology; **b)** phenotypic characterization performed by flow cytometry analysis of positive MSC cell surface markers (CD73 and CD90), negative MSCs cell surface markers (CD34, CD45, HLA-DR) and pluripotency marker (TRA-1-60); **c)** functional characterization showing their *in vitro* differentiation into adipocytes, osteoblasts and chondrocytes based on the expression of FABP4, Osteocalcin and Aggrecan, respectively.

3.2. *Effects of BM-MSCs and iMSCs secretome on an in vitro PD model*

After establishing iMSCs, we proceeded to the collection of their secretome and assessed their effects on neuroprotection. We have firstly addressed iMSCs secretome neuroprotective potential *in vitro*, adding either BM-MSCs or iMSCs conditioned medium (CM) to a 3D culture model of dopaminergic neurons exposed to 6-OHDA (figure 4.5a).

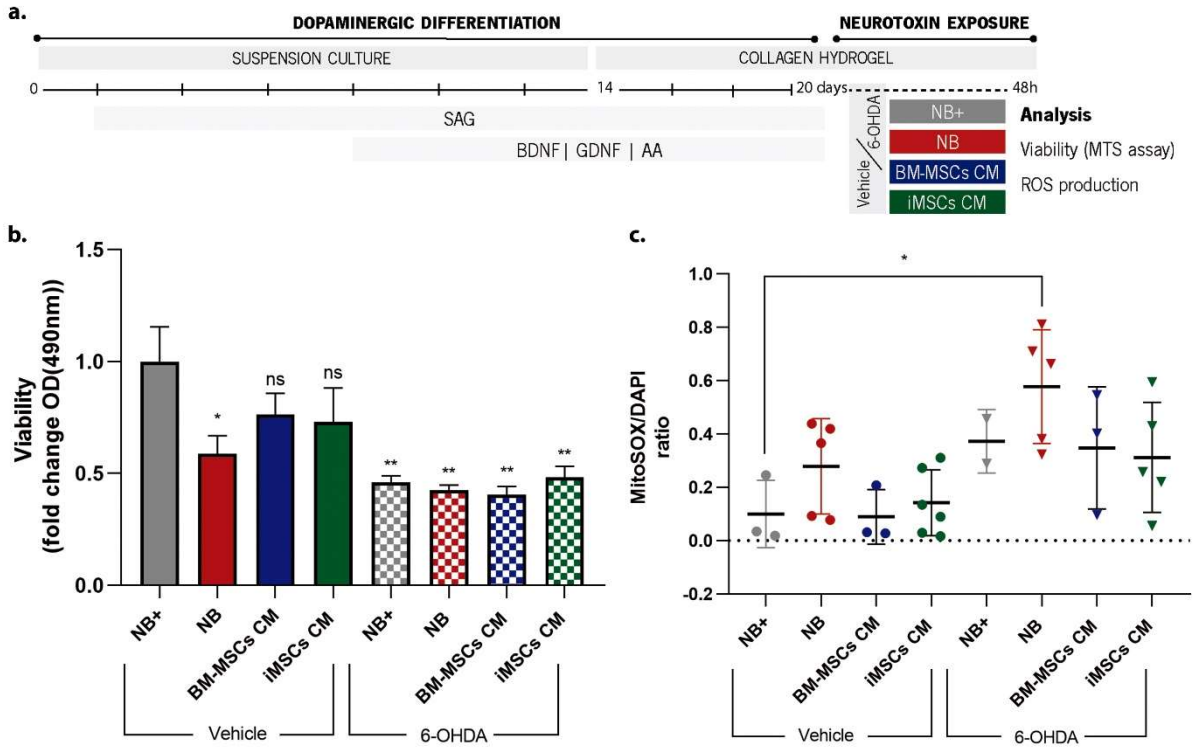

Figure 4.5 – Effects of BM-MSCs and iMSCs secretome on *in vitro* neuroprotection. a) experimental timeline depicting mESC differentiation protocol into dopaminergic neurons, followed by exposure to either vehicle or 6-OHDA [500µM] for 4h and subsequent incubation with either NB+ (a supplemented differentiation medium), NB (a basal medium without any supplementation), BM-MSCs or iMSCs conditioned medium (CM); **b)** effects of 6-OHDA exposure on cell viability measured by MTS assay, results are presented as of fold change over vehicle NB+, n=8-12 of two independent experiments, $F(7, 78) = 4,963$, $p=0,0001$, multiple comparisons are marked by *$p<0.05$, **$p<0.01$, ns = not statistical significant for comparisons with vehicle NB+ group; **c)** effects of 6-OHDA exposure on the production of reactive oxygen species, measured by quantification of MitoSOX, results are depicted as a mean ± SEM ratio between MitoSOX and DAPI fluorescence intensity, $F(5, 21) = 4,025$, $p=0,0102$, *$p<0.05$.

Both secretome sources were able to maintain dopaminergic neurons viability, when the model was not challenged with 6-OHDA, as there is no statistical significant difference between cells cultured under either BM-MSCs or iMSCs secretome and the positive control (NB^+) on the MTS viability assay (figure 4.5b). Nonetheless, neither positive control medium, nor MSCs secretome were able to revert the 50% reduction on cell viability induced by 6-OHDA exposure (figure 4.5b). Still, there is no visible decrease in comparison to the negative control (NB) exposed to 6-OHDA, and there is a slight increase for the group incubated with iMSCs CM. Likewise, the analysis of the production of ROS through quantification of a MitoSOX, which measures the production of superoxide by mitochondria did not reveal a significant reduction of the oxidative stress induced by 6-OHDA exposure (figure 4.5c). Nevertheless, both positive control medium (NB^+) and MSCs CM exposure attenuated the production of ROS in comparison to negative control medium (NB).

Overall, although there is no clear evidence of the neuroprotective effect of MSCs secretome on reversing the effects induced by 6-OHDA exposure in our 3D model of dopaminergic neurons, these results reveal the similarity between both BM-MSCs and iMSCs a sources of secretome.

3.3. *Effects of BM-MSCs and iMSCs secretome on an in vivo PD model*

We have next addressed the effects of MSCs secretome from both sources on an *in vivo* model of PD, in which BM-MSCs CM had been previously shown to attenuate nigrostriatal degeneration and improve animals' motor performance (Mendes-Pinheiro *et al.*, 2019; Teixeira *et al.*, 2017). Moreover, due to the increasingly relevance of nonmotor symptoms on PD clinical picture, we have also addressed the impact of secretome administration on anhedonic and anxious-like behavior following 6-OHDA lesion. To establish an *in vivo* model of PD, 8µg of 6-OHDA were injected at the MFB, which selectively destroys dopaminergic neurons in the nigrostriatal pathway. In this way, we were able to mimic the dopaminergic degeneration observed in PD in one side, while the other was used as a control of the lesion.

3.3.1. *Motor behavior*

Three weeks after performing lesion surgeries, animals were subjected to behavioral characterization at the motor level, including rotatod, to test motor coordination and balance, staircase test, to address fine motor movement control and apomorphine-induced rotations to evaluate the imbalance in dopamine release between the denervated and the non-denervated striata (figure 4.6a). From the total 62 animals to which 6-OHDA was administered, 50 animals presented intense turning behavior after apomorphine administration, as revealed by the increased number of contralateral rotations of 6-OHDA injected animals

(figure 4.6b), thereby confirming the successful depletion of dopamine on the lesioned side. Moreover, as observed in the first timepoint of graphs c and d of figure 4.6, 6-OHDA lesion induced a significant decrease on the time animals are able to spend on the rotating beam (*i.e.* latency to fall) and on their ability to reach and eat the pellets placed on the staircase apparatus (*i.e.* successful reaches).

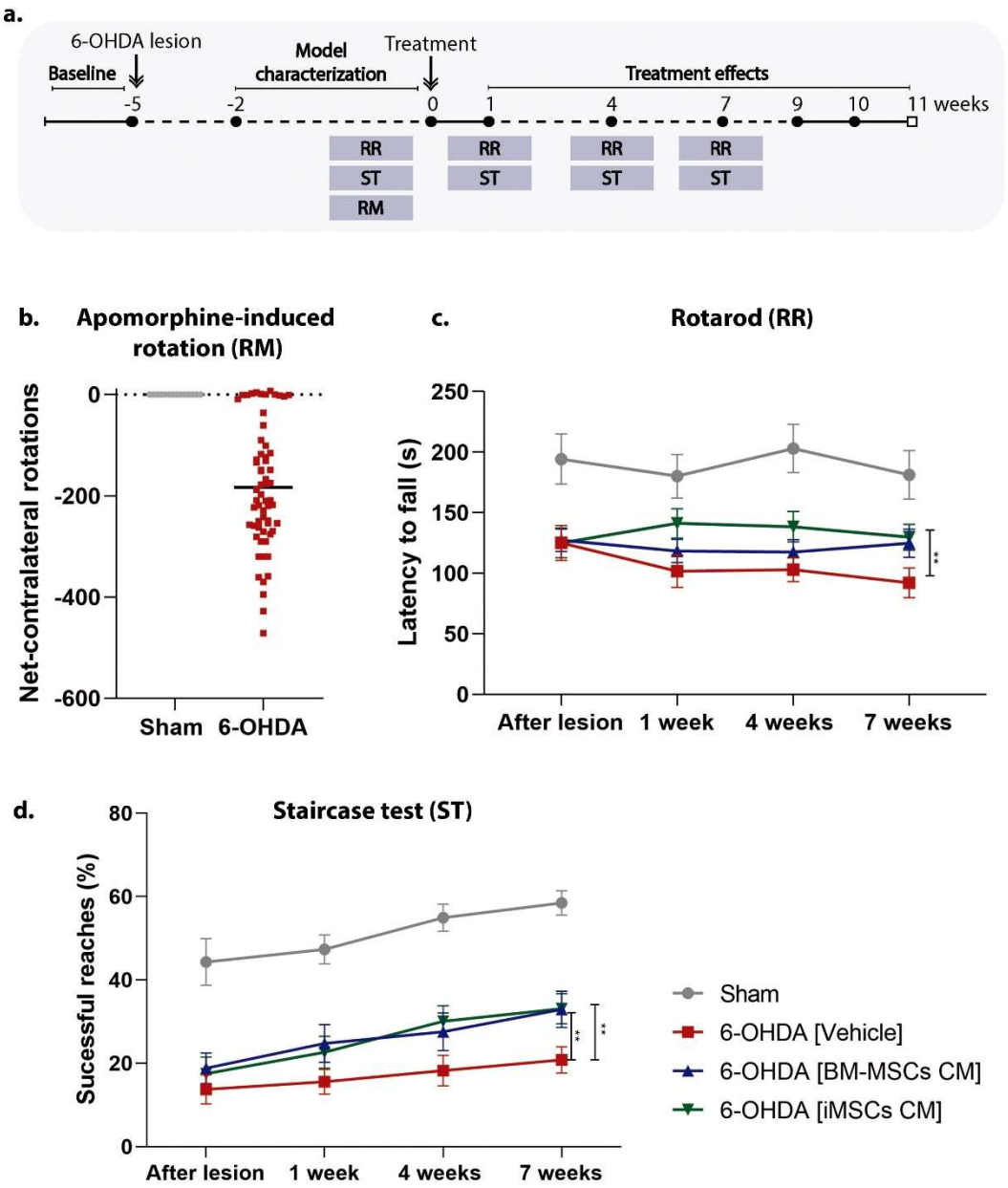

Figure 4.6 – Motor behavioral analysis of 6-OHDA lesioned animals after administration of BM-MSCs and iMSCs secretome. a) timeline of the *in vivo* experiment depicting the timepoints of motor behavioral analysis: *baseline* - before 6-OHDA lesion surgeries, *model characterization* - 3 weeks after lesion surgeries, included rotarod (RR), staircase test (ST) and apomorphine-induced rotations (RM), *treatment effects* - 1, 4 and 7 weeks after treatment surgeries (week 0). Animals were sacrificed 11 weeks after treatment and 16 weeks after lesion surgeries, **b)** apomorphine-induced rotations as a measure

of dopaminergic depletion induced by 6-OHDA lesion and compared to sham animals; **c)** motor coordination and balance assessed by rotarod test (n=5-16;/group, mean ± SEM, **p<0.01 for animals treated with iMSCs secretome vs non-treated animals); **c)** fine motor movements assessed by staircase test and depicted as (%) of successful reaches (n= 12-14/group, mean ± SEM, *p<0.05 for animals treated either with BM-MSCs or iMSCs secretome vs non-treated animals).

After performing the characterization of the *in vivo* model, lesioned animals were divided into three treatment groups: vehicle (n=19, injected with Neurobasal A medium), BM-MSC CM (n=21, injected with BM-MSC secretome) and iMSC CM (n=21, injected with iMSC secretome). Treatment was administered at the striatum and at the SNc of lesioned animals and their effects were evaluated throughout the subsequent 11 weeks (figure 4.5a). Regarding motor coordination (figure 4.6c), iMSC CM-treated animals present a significantly better performance in comparison with non-treated animals ($p<0.05$). This improvement was already visible 1 week after treatment administration and sustained until 7 weeks after treatment. On the other hand, BM-MSC CM-treated animals had a more moderate improvement, only at 7 weeks after treatment. The analysis of fine motor movements revealed a similar success rate between both treated groups, which was statistically significant in comparison to non-treated animals (figure 4.6d). These improvements were visible from the beginning of the post-treatment assessment, highlighting the neuroprotective potential of iMSCs secretome.

In conclusion, these results reveal the ability of iMSCs secretome to improve motor phenotype of 6-OHDA lesioned animals in a similar extent to BM-MSCs, thereby allowing the use of iMSCs as source of cells for the collection of secretome with neuroprotective or regenerative ability.

3.3.2. *Nonmotor behavior*

Whereas motor behavioral deficits are widely reported in unilateral 6-OHDA MFB-lesioned model, nonmotor alterations are less frequently addressed and are greatly inconsistent, as a result of the dissimilarities between protocols that can greatly influence the reported outcomes (Magnard *et al.*, 2016).

We have firstly addressed the impact of 6-OHDA lesion on anhedonia in the animal model, employing the widely reported sucrose consumption test (SCT) three weeks after lesion establishment and comparing to the baseline levels of preference for each animal, assessed before lesion (figure 4.7a). As previously reported by our group (Carvalho *et al.*, 2013), 6-OHDA lesion induced a decreased preference for sucrose consumption (figure 4.7b), suggesting the presence of depressive-like phenotype in lesioned animals. Nevertheless, because the remaining behavioral tests could only be performed once, the impact of 6-OHDA lesion on anxious-like behavior and on a refined test of anhedonia, the Sweet Drive test, was only performed at the same time as the assessment of treatment effects (figure 4.7a).

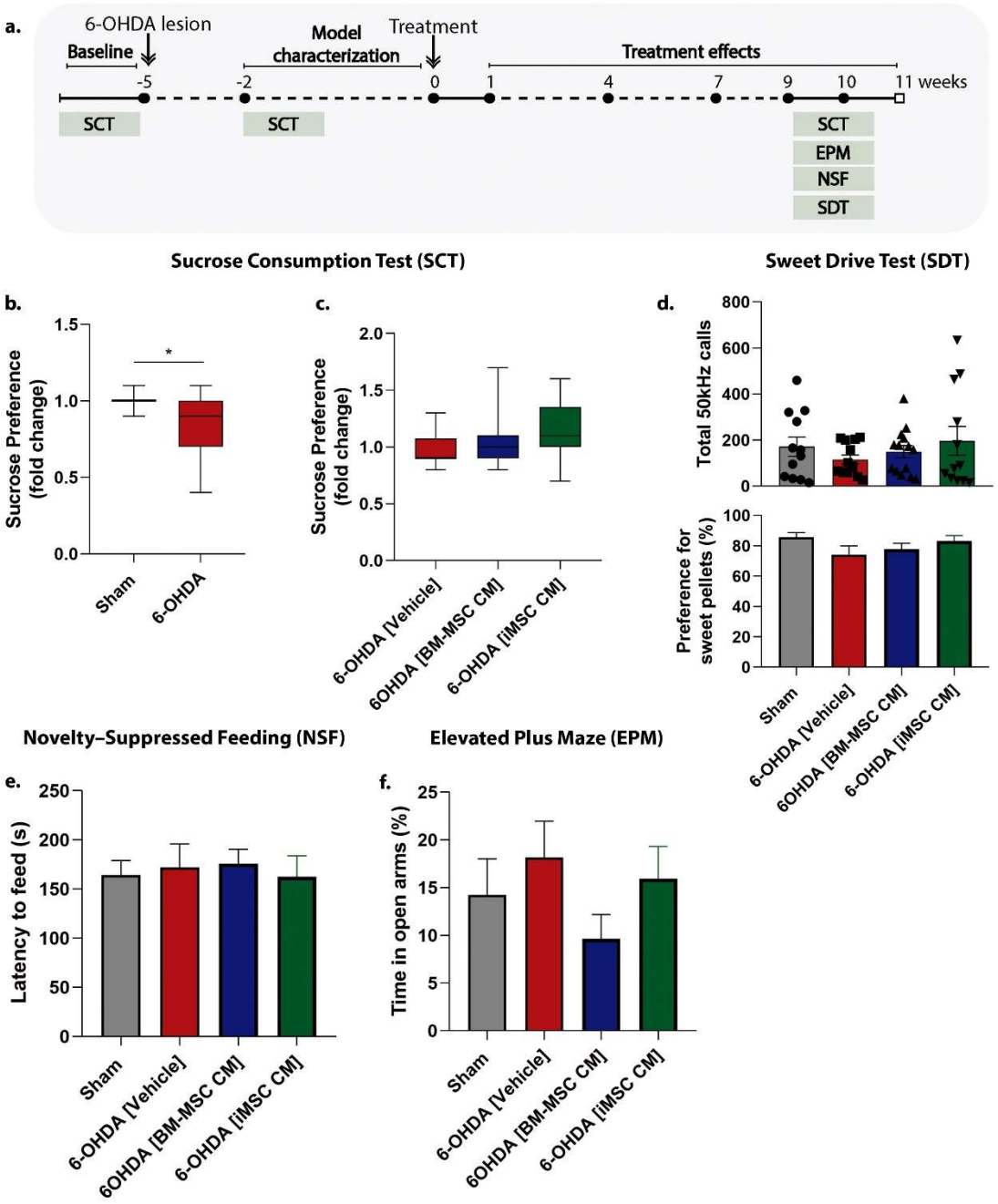

Figure 4.7 – Nonmotor behavioral analysis of 6-OHDA lesioned animals after administration of BM-MSCs and iMSCs secretome. a) timeline of the *in vivo* experiment depicting the timepoints of nonmotor behavioral analysis: *baseline* - before 6-OHDA lesion surgeries, *model characterization* - 3 weeks after lesion surgeries, included sucrose consumption test (SCT), *treatment effects* - non-motor behavior was analyzed 9 weeks after treatment surgeries by performing sucrose consumption (SCT) and SweetDrive (SDT) tests to measure anhedonia and elevated plus maze (EPM) and novelty suppressed feeding (NSF) tests to assess anxiety-like behavior. Animals were sacrificed 11 weeks after treatment and 16 weeks after lesion surgeries. **b)** sucrose consumption test depicting fold change of preference after lesion over baseline (results are presented as min to max boxplot), revealing a statistically significant difference in Mann-Whitney test U= 138.5, p=0.0312; **c)** fold change of preference 7 weeks after treatment over values after lesion (results are presented as min to max boxplot), with no statistically

significant difference between groups, H_2= 3,960, p=0.1380; **d)** preference for sweet pellets and 50kHz ultrasonic vocalizations (USVs) as measures of SweetDrive test; **e)** latency to feed as a measure of the Novelty suppressed feeding test; **f)** time spent in open arms on the elevated plus maze test.

Regarding anxious-like behavior, neither the NSF nor the EPM test revealed differences between lesioned and non-lesioned animals (figure 4.7e and f). Accordingly, the administration of either BM-MSCs or iMSCs CM after 6-OHDA lesion, did not produce alterations in both tests. On the other hand, the reduced sucrose preference evidenced in SCT after 6-OHDA lesion was partially reverted by secretome administration, although without reaching statistical significance (figure 4.7c). A similar tendency was observed in the SDT, which comprises a multi-parametric analysis of anhedonia, integrating measurements of food preference in a non-aversive environment with recordings of 50 kHz ultrasonic vocalizations (USVs) that have been described to be associated with positive and pleasurable experiences (Mateus-Pinheiro *et al.*, 2014; Portfors, 2007). During this behavioral paradigm, non-treated 6-OHDA animals present a decreased preference for sweet pellets over regular food pellets, which correlates with a decreased number of 50kHz vocalizations. Treatment administration, particularly iMSCs secretome partially reverts this phenotype, increasing both preference for sweet food and the number of 50kHz USVs. Notwithstanding, these effects are not statistically significant, possibly as a result of the high level of intra-group variability.

Altogether, these results point toward increased anhedonia as a result of 6-OHDA lesion, with no indication of alterations on anxious-like behavior. Nevertheless, these alterations are not as pronounced as motor deficits and therefore, may hinder potential effects induced by MSCs secretome administration on depressive-like behavior.

3.3.3. *Histological and neurochemical analysis*

At the end of the *in vivo* experiment, animals were divided in two tissue processing groups: whole brain fixing for subsequent sectioning and immunohistochemistry or macrodissection of specific brain regions for neurochemical analysis.

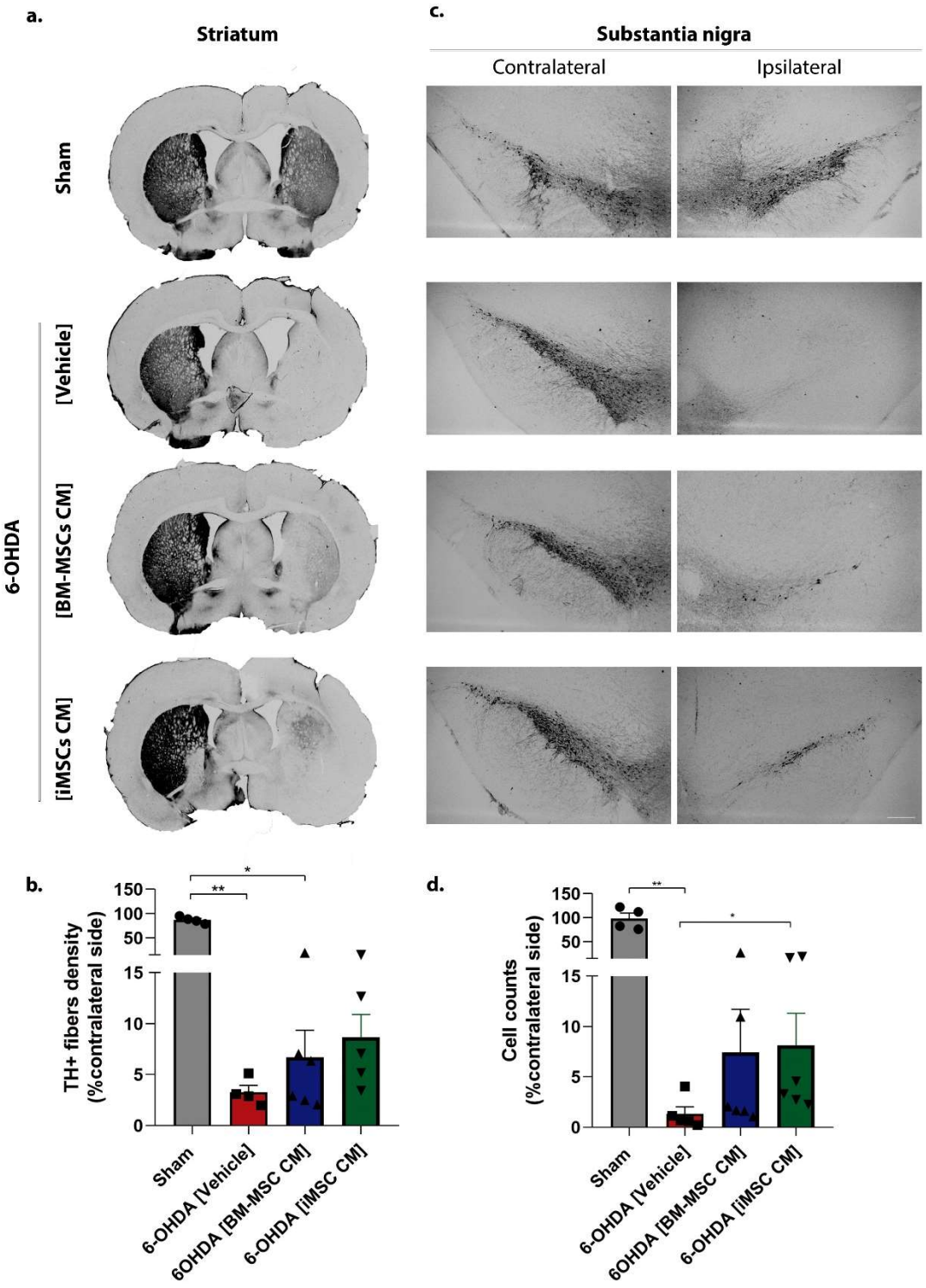

Figure 4.8 – Histological analysis of the striatum and substantia nigra. a) representative images of the tyrosine hydroxylase (TH) staining on the striatum; **b)** quantification of TH fibers density on the striatum, depicted as percentage over non-lesioned side (n=4-6/group); data is presented as mean ± SEM. H_2= 11.78, p=0.008, *p<0.05, **p<0.01; **c)** representative images of the TH staining on the ipsilateral and contralateral substantia nigra of the different experimental groups. Scale bar=2mm; **d)** quantification of TH^+ cells on the SNc, depicted as percentage over non-lesioned side (n=4-6/group); data is presented as mean ± SEM. H_2= 13.54, p=0.0036, *p<0.05, **p<0.01.

Analysis of TH staining revealed a marked decrease (>90%) of the density of fibers and cell number on the striatum and SNc, respectively, on 6-OHDA lesioned animals compared to sham animals (figure 4.8). Treatment with either BM-MSCs CM or iMSC CM induced an increase on the TH^+ fibers density in the striatum (figure 4.8b), whereas only iMSCs CM administration significantly reduced cell loss in the SNc in comparison to lesioned, non-treated animals (figure 4.8d).

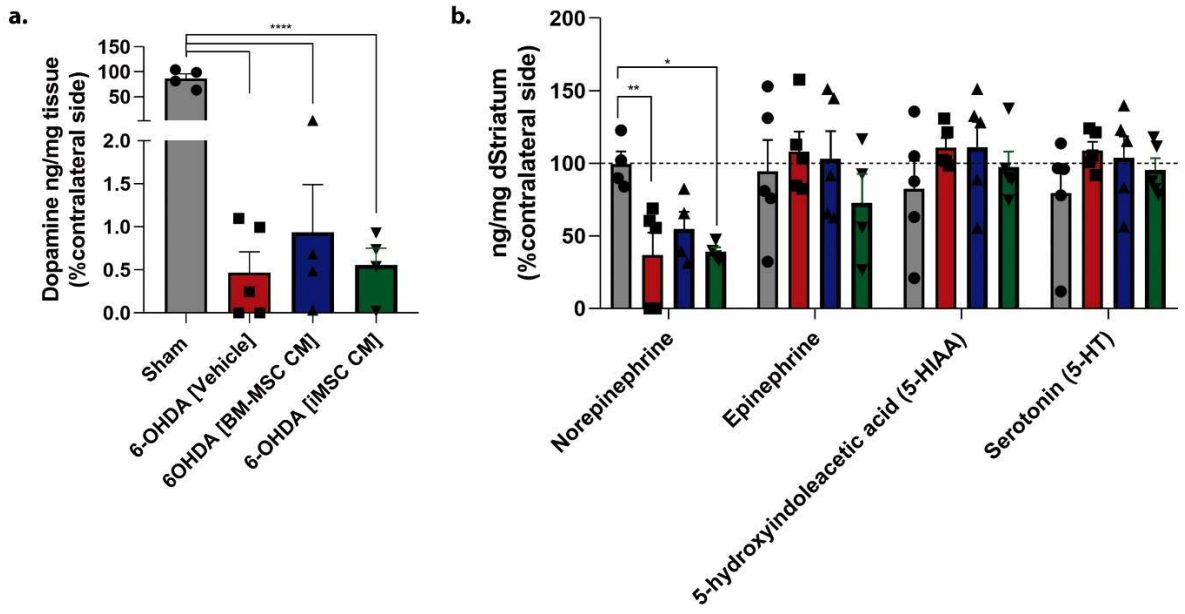

Figure 4.9 – Neurochemical analysis of catecholamines release on the striatum. a) quantification of dopamine release on the striatum performed by high-performance liquid chromatography, combined with electrochemical detection. F (3, 13) = 97.14, p<0.0001 **b)** quantification of other catecholamines release, depicting significant reduction of norepinephrine release on 6-OHDA lesioned animals. F (3, 13) = 6,288, p=0.0072. Data is presented as mean ± SEM, n=4-5/group.

Regarding neurochemical analysis of catecholamines present on the striatum, 6-OHDA lesion induced a marked decrease of dopamine levels that was not reverted by administration of BM-MSCs CM or iMSCs CM (figure 4.9a). Moreover, analysis of the levels of other catecholamines indicated a significant decrease of norepinephrine levels on the striatum of lesioned animals either treated or non-treated (figure 4.9b).

Taken together, both histological and neurochemical analysis reveal the severity of the nigrostriatal degeneration induced by 6-OHDA lesion, which is partially attenuated at the SNc by the administration of iMSCs secretome.

3.4. *Assessment of BM-MSCs and iMSCs secretome profile*

To address which molecules were implicated in the previously described effects, we have subsequently performed an analysis of the secretome content from both sources, using an antibody array that contains

a set of proteins with neuroregulatory effects (figure 4.10a and b). By pooling together the intensity values from the conditioned medium of the three donors of each source, we were able to perform a relative quantification of secretion levels for each protein and address source-dependent differences (figure 4.10c). From all the proteins analyzed on the array, only GCSF and IL-10 were not found on the secretome of both sources. On the other hand, a panel of growth factors, such as BDNF, beta-NGF, GDNF, HB-EGF, TGF-beta, IGF-1, VEGF-A, as well as cytokines, including IL-1 alpha and beta, MCP-1, MIP-1alpha, MMP-2 and -3, TNF alpha and IFNg were present in similar amounts in both sources. Surprisingly, the levels of IL-6 and IL-8 were significantly increased in iMSCs CM.

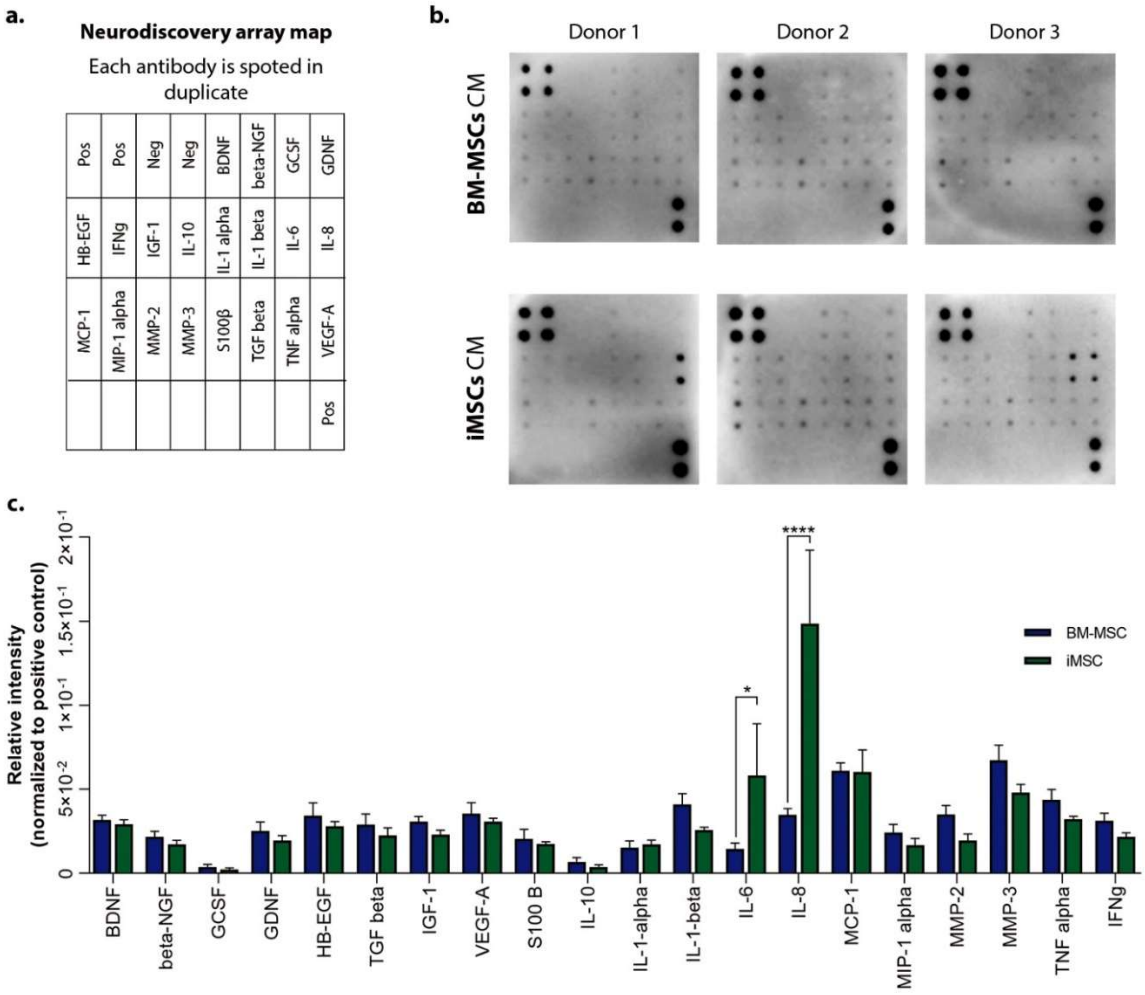

Figure 4.10 – Profile of neuroregulatory proteins present in the conditioned medium of BM-MSCs and iMSCs. **a)** Human Neuro Discovery membrane array map identifying the position of each antibody on the membrane; **b)** membrane arrays depicting the proteins detected on the conditioned medium of each donor from BM-MSCs and iMSCs; **c)** quantification of array spot intensity for each source after pooling the values from the three donors. Data is presented as mean ± SEM of relative intensity for each protein, normalized to positive control intensity. *p<0.05, ****p<0.0001 for Sidak's multiple comparisons test between BM-MSCs and iMSCs CM.

This analysis revealed a similar neuroregulatory potential on the secretome from both sources, with increased secretion levels of two cytokines (IL-6 and IL-8) by iMSCs that do not seem to have negatively impacted their effects *in vivo.*

4. Discussion

The therapeutic potential of MSCs secretome has been widely reported in preclinical models of PD (Marques *et al.*, 2018). Nonetheless, the translation of this cell-free therapeutic approach into a clinical setting requires ameliorations on the standardization on the process of secretome collection. The selection of the appropriate MSCs source is one of issues that can dramatically influence the accessibility and effectiveness of this product. Indeed, tissue-derived MSCs, such as BM-MSCs, on which most reports are based, carry methodological and experimental limitations that hamper their extensive expansion for the collection of large batches of their secreted factors. Due to their unlimited self renewal capacity and ability to differentiate into any cell type, iPSCs have been put forward as an alternative source for obtaining a virtually unlimited number of MSCs. The aim of the present study was to address whether iMSCs secretome presents a similar therapeutic potential for PD, thereby providing an alternative source to the use of BM-MSCs secretome in future PD therapeutic applications.

4.1. *iPSCs can be used as source of MSCs with improved proliferative capacity*

We have firstly established iMSCs from three different iPSC lines from three healthy donors, using a serum-free differentiation protocol (figure 4.3). Besides providing a chemically-defined medium, which allows for a better standardization of MSCs culture conditions, serum-free iMSCs presented a higher proliferative rate (data not shown) and their secretome was able to induce similar levels of neuronal differentiation as serum-free cultured BM-MSCs (figure 4.2). Therefore, serum-free differentiation protocol was selected and yielded consistent amounts of iMSCs, with a high proliferative rate in comparison to BM-MSCs. Indeed, iPSCs have been demonstrated to lose particular age-associated features during iPSC induction, such as increase in telomere length and mitochondrial fitness, as well as loss of senescence markers (Miller *et al.*, 2013), which may explain iMSCs rejuvenated gene signature, regardless of the donor age or cell source used (Hawkins *et al.*, 2018; Spitzhorn *et al.*, 2019). Besides differences in iMSCs proliferative rate, some dissimilarities have also been reported for iMSCs multipotent capacity. Similarly to our observations, iMSCs have been reported to display less adipogenic and chondrogenic differentiation capacity and thence have been suggested to be more closely related to vascular progenitor cells (Xu *et al.*, 2019). Therefore, future studies should be performed to better understand whether these differences

are due to incomplete differentiation of iPSCs into iMSCs or if the expression of typical MSC markers such as CD73, CD90, and CD105 are insufficient to distinguish MSCs from other mesodermal progenitors in iPSC derived cultures.

4.2. *iMSCs secretome attenuates motor deficits and nigrostriatal degeneration in an unilateral 6-OHDA model of PD*

Regardless of identity dissimilarities between BM-MSCs and iMSCs, no differences were observed in the neuroprotective potential of the secretome from both sources, in the *in vivo* model. Previous studies from our group have evidenced the potential of BM-MSCs secretome-based strategy, in contrast to their transplantation, in attenuating motor deficits in an unilateral 6-OHDA lesion rat model (Mendes-Pinheiro *et al.*, 2019). In the present study, we have re-validated this effect for BM-MSCs CM and importantly, further demonstrated a similar effect for iMSCs CM, showing that both treatments are able to significantly increase rats' ability to reach, retrieve and eat food pellets in the staircase test (figure 4.6). Additionally, we have used the established *in vivo* model to address the impact of 6-OHDA nigrostriatal lesion and subsequent secretome treatment on nonmotor phenotype, namely on anhedonia and anxious-like behavior.

In our experimental protocol, only sucrose preference in the SCT was significantly decreased following 6-OHDA lesion, with a strong tendency to be reverted by iMSCs secretome administration (figure 4.7). These results are in accordance with previous reports, demonstrating increased depressive-like behavior in MFB-6-OHDA lesioned rats (Carvalho *et al.*, 2013; Kamińska *et al.*, 2017). Nevertheless, using similar experimental models, other authors have reported no alterations in sucrose preference in 6-OHDA lesioned animals (Delaville *et al.*, 2012). These inconsistencies may arise from differences in the experimental protocol used and reveal the need to establish more refined behavioral paradigms to assess anhedonia in PD animal models. Therefore, in addition to the well-established SCT, we have performed a newly developed test, the SweetDrive test that measures anhedonic behavior in a multiparametric way (Mateus-Pinheiro *et al.*, 2014). Although there was no significant difference between lesioned and non-lesioned animals, there is a tendency for decreased sweet food consumption in lesioned non-treated animals in comparison to non-lesioned and secretome treated animals (figure 4.7). The same variation pattern is observed in the number of 50 kHz USVs, an additional parameter of this test, associated to pleasurable experiences (Portfors, 2007). The lack of statistical significance in the SDT may arise from the high variability within groups, due to distinct preference and number of USVs for each animal. This variability was eliminated in the SCT, since test repetition is not associated to habituation and thus,

preference values were compared regarding animals' fold change preference over baseline, for lesion effects and over lesion, for treatment effects. Despite the impossibility of performing the same type of analysis in SDT, further USVs analysis may reveal distinct patterns between treated and non-treated animals. Indeed, other USVs parameters, such as type and duration, have been found to be altered in 6-OHDA lesioned animals (Ciucci *et al.*, 2009; Grant *et al.*, 2015), thereby demonstrating the complexity of this poorly understood phenotypic outcome, in which motor and emotional components may be implicated and indistinguishable.

In line with the results at the motor level, histological and neurochemical analysis disclosed a significant degeneration at the nigrostriatal pathway and striatal dopamine depletion, respectively, as a consequence of 6-OHDA lesion (figure 4.8 and 4.9). Significant treatment effects were only evident for iMSCs CM in reducing the cell loss at the SNc. The lack of significant effect for BM-MSCs CM, contrary to previous results from our group (Mendes-Pinheiro *et al.*, 2019; Teixeira *et al.*, 2017), may occur as a result of the timepoint at which this post-mortem analysis was performed. In the present study, animal's were sacrificed 16 weeks after lesion induction, whereas in previous studies animals' brains were collected 13 weeks after lesion. This delayed analysis, due to the implementation of non-motor tests, might have accounted for a more pronounced neuronal death that could not be compensated by the a single injection of MSCs secretome. Indeed, at 13 weeks after lesion, non-treated animals presented a 90% decrease of TH fibers density in the striatum (Mendes-Pinheiro *et al.*, 2019), whereas in the present study, 16 weeks after lesion, more than 95% of the TH fibers had been lost.

Lesion severity may also underlie the lack of significant recovery of striatal dopamine depletion following MSCs secretome treatment administration (figure 4.9). Moreover, measurements of neurotransmitters release are subject to a higher degree of variability and thus, an increased number of animals should be analyzed. Notwithstanding, besides marked dopamine depletion, although in a lesser extent, norepinephrine (NA) striatal levels are also significantly decreased in lesioned animals. Indeed, 6-OHDA is thought to be uptaken by noradrenergic fibers projecting from the locus coeruleus to the striatum (Kamińska *et al.*, 2017). This has led some authors to use desipramine, a selective NA reuptake inhibitor, upon 6-OHDA lesion induction to reduce damage of noradrenergic neurons and selectively address the involvement of dopaminergic degeneration in the established model (Schwarting *et al.*, 1996). Nevertheless, neurodegeneration of the locus coeruleus is well-documented in PD and has been linked to a myriad of nonmotor symptoms in PD patients, including depression (Gratwicke *et al.*, 2015; Szabadi,

2013). Therefore, further analysis should determine the exact neuronal circuitry affected by 6-OHDA and understand its implications in motor and nonmotor function.

4.3. *iMSCs secretome sustains mESC-derived dopaminergic neurons in culture, but fail to protect them from 6-OHDA induced toxicity*

Whereas administration of iMSCs secretome in the *in vivo* model induced improvements on motor performance, as well as protection of the nigrostriatal pathway in 6-OHDA lesioned animals, there was no significant effect on cell viability and ROS production with their application in an *in vitro* model mimicking dopaminergic degeneration (figure 4.5). Conversely, the secreted factors present in MSCs secretome from both sources were able to sustain these mESC-derived dopaminergic neurons in culture.

Although further analysis should be performed to specifically address the impact of MSCs secretome administration on dopaminergic neurons morphology after 6-OHDA exposure *in vitro,* there are some possible hypothesis to explain the differences on the effects in both models. First, in the *in vivo* model we have administered 100x concentrated MSCs CM, due to animals' size and complexity, while *in vitro* 6-OHDA exposed dopaminergic neurons were incubated with non-concentrated MSCs CM, wherein the amount of secreted factors may have been insufficient to rescue dopaminergic neurons viability. Therefore, future studies should be performed using similar concentrations of MSCs CM in both models to address this hypothesis.

Alternatively, this differential neuroprotective outcome may suggest that the *in vivo* effects arise from an indirect effect of MSCs secretome on dopaminergic neurons. Indeed, besides severe degeneration of the nigrostriatal system, the 6-OHDA animal model has been shown to display neuroinflammation (Fricke *et al.*, 2016), as well as compromised blood-brain barrier (BBB) integrity (Olmedo-Díaz *et al.*, 2017). Accordingly, MSCs secretome has been demonstrated to modulate astrocyte and microglia activity (Baez-Jurado *et al.*, 2019; Campos *et al.*, 2020), along with evidences on MSC secreted vesicles effects on restoring the integrity of the BBB (Chen *et al.*, 2019). A more detailed analysis on the effect of MSCs secretome on glial cells activity and angiogenesis is therefore required to understand the implications of this non-neuronal cell types on dopaminergic neurons protection from 6-OHDA induced oxidative stress.

4.4. *iMSCs CM contains similar profile of neuroregulatory molecules as BM-MSCs CM*

To better dissect the molecular players mediating neuroprotection in the *in vivo* model, a targeted proteomic analysis of the conditioned medium from both sources was performed using a membrane-based antibody array. This analysis revealed a similar secretory profile between both MSCs sources,

except for the levels of IL-6 and IL-8 (figure 4.10). Besides their activity as pro-inflammatory cytokines, IL-6 and IL-8 have been shown to display pleiotropic effects in the central nervous system, including neuronal protection and regeneration (Jung *et al.*, 2011; Semple *et al.*, 2010; Xia *et al.*, 2015)

Rather than addressing the potential role of each identified molecule, it is important to acknowledge that these signaling molecules present in MSCs secretome, most likely act as a whole, activating a myriad of signaling pathways involved on neuroprotection. One of such pathways is the Akt signaling pathway, which is activated by most of the growth factors and cytokines identified on the array and regulates diverse functions, including glucose metabolism, proliferation, cell growth, transcription and cell survival (Rai *et al.*, 2019). Importantly, deficits in Akt signaling pathway have been linked to loss of dopaminergic neurons in PD (Timmons *et al.*, 2009), whereas their activation has been suggested to mediate neuroprotection of a multitude of compounds tested in PD animal models (Rai *et al.*, 2019). Therefore, the balance of these growth factors and cytokines in the secretome from both sources may provide a toolkit for preventing the degenerative events that take place in PD.

5. Conclusion

In conclusion, our study was the first to address the neuroprotective potential of iMSCs secretome in the context of PD, paving the way for the use of this emerging MSC source for subsequent clinical testing. In view of that, we have produced iMSCs using chemically-defined, serum-free MSC expansion medium and performed a direct comparison between BM-MSCs and iMSCs secretome. We could demonstrate a similar composition of neuroregulatory molecules that is translated in similar neuroprotective capacities *in vivo*.

Acknowledgments

Financial support from MultiPark, Crafoord Foundation Sweden, and Portuguese Foundation for Science and Technology (FCT): IF Development Grant to AJ Salgado, IF starting grant to L. Pinto, PhD scholarships attributed to A. Marote (PDE/BDE/113598/2015) and B. Mendes-Pinheiro (SFRH/BD/120124/2016) and Post-Doctoral Fellowship to F.G. Teixeira (SFRH/BPD/118408/2016). This work was funded by FEDER, through the Competitiveness Internationalization Operational Programme (POCI), and by National funds, through the Foundation for Science and Technology (FCT), under the scope of the projects POCI-01-0145-FEDER-007038; POCI-01-0145-FEDER-029751 and POCI-01-0145-FEDER-032619. This work has also been developed under the scope of the project NORTE-01-0145-FEDER-000023, supported by the Northern Portugal Regional Operational Programme (NORTE 2020), under the Portugal 2020 Partnership Agreement, through the European Regional Development Fund (FEDER).

References

Aarsland D, Påhlhagen S, Ballard CG, Ehrt U, & Svenningsson P. (2012). Depression in Parkinson disease—epidemiology, mechanisms and management. *Nature Reviews Neurology, 8*(1), 35-47. doi:10.1038/nrneurol.2011.189

Athauda D, & Foltynie T. (2015). The ongoing pursuit of neuroprotective therapies in Parkinson disease. *Nature Reviews Neurology, 11*(1), 25-40. doi:10.1038/nrneurol.2014.226

Baez-Jurado E, Hidalgo-Lanussa O, Barrera-Bailón B, Sahebkar A, Ashraf GM, Echeverria V, & Barreto GE. (2019). Secretome of Mesenchymal Stem Cells and Its Potential Protective Effects on Brain Pathologies. *Molecular Neurobiology, 56*(10), 6902-6927. doi:10.1007/s12035-019-1570-x

Barker RA, Drouin-Ouellet J, & Parmar M. (2015). Cell-based therapies for Parkinson disease—past insights and future potential. *Nature reviews. Neurology, 11*(9), 492-503. doi:10.1038/nrneurol.2015.123

Berg D, Postuma RB, Adler CH, Bloem BR, Chan P, Dubois B, Gasser T, Goetz CG, Halliday G, Joseph L, Lang AE, Liepelt-Scarfone I, Litvan I, Marek K, Obeso J, Oertel W, Olanow CW, Poewe W, Stern M, & Deuschl G. (2015). MDS research criteria for prodromal Parkinson's disease. *Movement Disorders, 30*(12), 1600-1611. doi:10.1002/mds.26431

Bessa J, Mesquita A, Oliveira M, Pêgo J, Cerqueira J, Palha J, Almeida O, & Sousa N. (2009). A trans-dimensional approach to the behavioral aspects of depression. *Front Behav Neurosci, 3*(1). doi:10.3389/neuro.08.001.2009

Campos J, Guerra-Gomes S, Serra SC, Baltazar G, Oliveira JF, Teixeira FG, & Salgado AJ. (2020). Astrocyte signaling impacts the effects of human bone marrow mesenchymal stem cells secretome application into the hippocampus: A proliferation and morphometrical analysis on astrocytic cell populations. *Brain Res, 1732*, 146700. doi:https://doi.org/10.1016/j.brainres.2020.146700

Caplan AI, & Dennis JE. (2006). Mesenchymal stem cells as trophic mediators. *Journal of Cellular Biochemistry, 98*(5), 1076-1084. doi:10.1002/jcb.20886

Carvalho MM, Campos FL, Coimbra B, Pêgo JM, Rodrigues C, Lima R, Rodrigues AJ, Sousa N, & Salgado AJ. (2013). Behavioral characterization of the 6-hydroxidopamine model of Parkinson's disease and pharmacological rescuing of non-motor deficits. *Molecular Neurodegeneration, 8*, 14-14. doi:10.1186/1750-1326-8-14

Chen S-Y, Lin M-C, Tsai J-S, He P-L, Luo W-T, Herschman H, & Li H-J. (2019). EP(4) Antagonist-Elicited Extracellular Vesicles from Mesenchymal Stem Cells Rescue Cognition/Learning Deficiencies by Restoring Brain Cellular Functions. *Stem Cells Translational Medicine, 8*(7), 707-723. doi:10.1002/sctm.18-0284

Ciucci MR, Ahrens AM, Ma ST, Kane JR, Windham EB, Woodlee MT, & Schallert T. (2009). Reduction of dopamine synaptic activity: degradation of 50-kHz ultrasonic vocalization in rats. *Behavioral neuroscience, 123*(2), 328-336. doi:10.1037/a0014593

Dauer W, & Przedborski S. (2003). Parkinson's disease: mechanisms and models. *Neuron., 39*(6), 889-909.

Delaville C, Chetrit J, Abdallah K, Morin S, Cardoit L, De Deurwaerdère P, & Benazzouz A. (2012). Emerging dysfunctions consequent to combined monoaminergic depletions in Parkinsonism. *Neurobiology of Disease, 45*(2), 763-773. doi:10.1016/j.nbd.2011.10.023

Dominici M, Le Blanc K, Mueller I, Slaper-Cortenbach I, Marini F, Krause D, Deans R, Keating A, Prockop D, & Horwitz E. (2006). Minimal criteria for defining multipotent mesenchymal stromal cells. The International Society for Cellular Therapy position statement. *Cytotherapy., 8*(4), 315-317. doi: 310.1080/14653240600855905.

Dorsey ER, Elbaz A, Nichols E, Abd-Allah F, Abdelalim A, Adsuar JC, Ansha MG, Brayne C, Choi J-YJ, Collado-Mateo D, Dahodwala N, Do HP, Edessa D, Endres M, Fereshtehnejad S-M, Foreman KJ, Gankpe FG, Gupta R, Hankey GJ, Hay SI, Hegazy MI, Hibstu DT, Kasaeian A, Khader Y, Khalil I, Khang Y-H, Kim YJ, Kokubo Y, Logroscino G, Massano J, Mohamed Ibrahim N, Mohammed MA, Mohammadi A, Moradi-Lakeh M, Naghavi M, Nguyen BT, Nirayo YL, Ogbo FA, Owolabi MO, Pereira DM, Postma MJ, Qorbani M, Rahman MA, Roba KT, Safari H, Safiri S, Satpathy M, Sawhney M, Shafieesabet A, Shiferaw MS, Smith M, Szoeke CEI, Tabarés-Seisdedos R, Truong NT, Ukwaja KN, Venketasubramanian N, Villafaina S, weldegwergs Kg, Westerman R, Wijeratne T, Winkler AS, Xuan BT, Yonemoto N, Feigin VL, Vos T, & Murray CJL. (2018). Global, regional, and national burden of Parkinson's disease, 1990–2016: a systematic analysis for the Global Burden of Disease Study 2016. *The Lancet Neurology, 17*(11), 939-953. doi:10.1016/s1474-4422(18)30295-3

Fan X-L, Zhang Y, Li X, & Fu Q-L. (2020). Mechanisms underlying the protective effects of mesenchymal stem cell-based therapy. *Cell Mol Life Sci*, 10.1007/s00018-00020-03454-00016. doi:10.1007/s00018-020-03454-6

Fitzsimmons REB, Mazurek MS, Soos A, & Simmons CA. (2018). Mesenchymal Stromal/Stem Cells in Regenerative Medicine and Tissue Engineering. *Stem Cells Int, 2018*, 8031718-8031718. doi:10.1155/2018/8031718

Fricke IB, Viel T, Worlitzer MM, Collmann FM, Vrachimis A, Faust A, Wachsmuth L, Faber C, Dollé F, Kuhlmann MT, Schäfers K, Hermann S, Schwamborn JC, & Jacobs AH. (2016). 6-hydroxydopamine-induced Parkinson's disease-like degeneration generates acute microgliosis and astrogliosis in the nigrostriatal system but no bioluminescence imaging-detectable alteration in adult neurogenesis. *The European journal of neuroscience, 43*(10), 1352-1365. doi:10.1111/ejn.13232

Grant LM, Barnett DG, Doll EJ, Leverson G, & Ciucci M. (2015). Relationships among rat ultrasonic vocalizations, behavioral measures of striatal dopamine loss, and striatal tyrosine hydroxylase immunoreactivity at acute and chronic time points following unilateral 6-hydroxydopamine-induced dopamine depletion. *Behavioural brain research, 291*, 361-371. doi:10.1016/j.bbr.2015.05.042

Gratwicke J, Jahanshahi M, & Foltynie T. (2015). Parkinson's disease dementia: a neural networks perspective. *Brain : a journal of neurology, 138*(Pt 6), 1454-1476. doi:10.1093/brain/awv104

Hawkins KE, Corcelli M, Dowding K, Ranzoni AM, Vlahova F, Hau K-L, Hunjan A, Peebles D, Gressens P, Hagberg H, de Coppi P, Hristova M, & Guillot PV. (2018). Embryonic Stem Cell-Derived Mesenchymal Stem Cells (MSCs) Have a Superior Neuroprotective Capacity Over Fetal MSCs in the Hypoxic-Ischemic Mouse Brain. *Stem Cells Translational Medicine, 7*(5), 439-449. doi:10.1002/sctm.17-0260

Hynes K, Menicanin D, Mrozik K, Gronthos S, & Bartold PM. (2014). Generation of functional mesenchymal stem cells from different induced pluripotent stem cell lines. *Stem Cells Dev, 23*(10), 1084-1096. doi:10.1089/scd.2013.0111

Jung JE, Kim GS, & Chan PH. (2011). Neuroprotection by interleukin-6 is mediated by signal transducer and activator of transcription 3 and antioxidative signaling in ischemic stroke. *Stroke, 42*(12), 3574-3579. doi:10.1161/strokeaha.111.626648

Kamińska K, Lenda T, Konieczny J, Czarnecka A, & Lorenc-Koci E. (2017). Depressive-like neurochemical and behavioral markers of Parkinson's disease after 6-OHDA administered unilaterally to the rat medial forebrain bundle. *Pharmacological Reports, 69*(5), 985-994. doi:https://doi.org/10.1016/j.pharep.2017.05.016

Lian Q, Zhang Y, Zhang J, Zhang HK, Wu X, Lam FF, Kang S, Xia JC, Lai WH, Au KW, Chow YY, Siu CW, Lee CN, & Tse HF. (2010). Functional mesenchymal stem cells derived from human induced pluripotent stem cells attenuate limb ischemia in mice. *Circulation, 121*(9), 1113-1123.

Magnard R, Vachez Y, Carcenac C, Krack P, David O, Savasta M, Boulet S, & Carnicella S. (2016). What can rodent models tell us about apathy and associated neuropsychiatric symptoms in Parkinson's disease? *Translational psychiatry, 6*(3), e753-e753. doi:10.1038/tp.2016.17

Marques CR, Marote A, Mendes-Pinheiro B, Teixeira FG, & Salgado AJ. (2018). Cell secretome based approaches in Parkinson's disease regenerative medicine. *Expert Opinion on Biological Therapy, 18*(12), 1235-1245. doi:10.1080/14712598.2018.1546840

Mateus-Pinheiro A, Patrício P, Alves ND, Machado-Santos AR, Morais M, Bessa JM, Sousa N, & Pinto L. (2014). The Sweet Drive Test: refining phenotypic characterization of anhedonic behavior in rodents. *Front Behav Neurosci, 8*, 74-74. doi:10.3389/fnbeh.2014.00074

Mendes-Pinheiro B, Anjo SI, Manadas B, Da Silva JD, Marote A, Behie LA, Teixeira FG, & Salgado AJ. (2019). Bone Marrow Mesenchymal Stem Cells' Secretome Exerts Neuroprotective Effects in a Parkinson's Disease Rat Model. *Frontiers in bioengineering and biotechnology, 7*, 294-294. doi:10.3389/fbioe.2019.00294

Michel Patrick P, Hirsch Etienne C, & Hunot S. (2016). Understanding Dopaminergic Cell Death Pathways in Parkinson Disease. *Neuron, 90*(4), 675-691. doi:10.1016/j.neuron.2016.03.038

Miller Justine D, Ganat Yosif M, Kishinevsky S, Bowman Robert L, Liu B, Tu Edmund Y, Mandal PK, Vera E, Shim J-w, Kriks S, Taldone T, Fusaki N, Tomishima Mark J, Krainc D, Milner Teresa A, Rossi Derrick J, & Studer L. (2013). Human iPSC-Based Modeling of Late-Onset Disease via Progerin-Induced Aging. *Cell Stem Cell, 13*(6), 691-705. doi:10.1016/j.stem.2013.11.006

Olmedo-Díaz S, Estévez-Silva H, Orädd G, Af Bjerkén S, Marcellino D, & Virel A. (2017). An altered blood-brain barrier contributes to brain iron accumulation and neuroinflammation in the 6-OHDA rat model of Parkinson's disease. *Neuroscience, 362*, 141-151. doi:10.1016/j.neuroscience.2017.08.023

Pires AO, Teixeira FG, Mendes-Pinheiro B, Serra SC, Sousa N, & Salgado AJ. (2017). Old and new challenges in Parkinson's disease therapeutics. *Prog Neurobiol, 156*, 69-89. doi:https://doi.org/10.1016/j.pneurobio.2017.04.006

Poewe W, Seppi K, Tanner CM, Halliday GM, Brundin P, Volkmann J, Schrag A-E, & Lang AE. (2017). Parkinson disease. *Nature Reviews Disease Primers, 3*(1), 17013. doi:10.1038/nrdp.2017.13

Pont-Sunyer C, Hotter A, Gaig C, Seppi K, Compta Y, Katzenschlager R, Mas N, Hofeneder D, Brücke T, Bayés A, Wenzel K, Infante J, Zach H, Pirker W, Posada IJ, Álvarez R, Ispierto L, De Fàbregues O, Callén A, Palasí A, Aguilar M, Martí MJ, Valldeoriola F, Salamero M, Poewe W, & Tolosa E. (2015). The Onset of Nonmotor Symptoms in Parkinson's disease (The ONSET PDStudy). *Movement Disorders, 30*(2), 229-237. doi:10.1002/mds.26077

Portfors CV. (2007). Types and functions of ultrasonic vocalizations in laboratory rats and mice. *Journal of the American Association for Laboratory Animal Science : JAALAS, 46*(1), 28-34.

Postuma RB, Berg D, Stern M, Poewe W, Olanow CW, Oertel W, Obeso J, Marek K, Litvan I, Lang AE, Halliday G, Goetz CG, Gasser T, Dubois B, Chan P, Bloem BR, Adler CH, & Deuschl G. (2015). MDS clinical diagnostic criteria for Parkinson's disease. *Movement Disorders, 30*(12), 1591-1601. doi:10.1002/mds.26424

Rai SN, Dilnashin H, Birla H, Singh SS, Zahra W, Rathore AS, Singh BK, & Singh SP. (2019). The Role of PI3K/Akt and ERK in Neurodegenerative Disorders. *Neurotoxicity research, 35*(3), 775-795. doi:10.1007/s12640-019-0003-y

Sabapathy V, & Kumar S. (2016). hiPSC-derived iMSCs: NextGen MSCs as an advanced therapeutically active cell resource for regenerative medicine. *Journal of Cellular and Molecular Medicine, 21*(10), 128-139.

Salgado AJ, Sousa JC, Costa BM, Pires AO, Mateus-Pinheiro A, Teixeira FG, Pinto L, & Sousa N. (2015). Mesenchymal stem cells secretome as a modulator of the neurogenic niche: basic insights and therapeutic opportunities. *Front Cell Neurosci, 9*(249). doi:10.3389/fncel.2015.00249

Schwarting RK, & Huston JP. (1996). Unilateral 6-hydroxydopamine lesions of meso-striatal dopamine neurons and their physiological sequelae. *Prog Neurobiol, 49*(3), 215-266. doi:10.1016/s0301-0082(96)00015-9

Semple BD, Kossmann T, & Morganti-Kossmann MC. (2010). Role of chemokines in CNS health and pathology: a focus on the CCL2/CCR2 and CXCL8/CXCR2 networks. *Journal of cerebral blood flow and metabolism : official journal of the International Society of Cerebral Blood Flow and Metabolism, 30*(3), 459-473. doi:10.1038/jcbfm.2009.240

Shi Y, Inoue H, Wu JC, & Yamanaka S. (2016). Induced pluripotent stem cell technology: a decade of progress. *Nature Reviews Drug Discovery, 16*, 115. doi:10.1038/nrd.2016.245

Spitzhorn L-S, Megges M, Wruck W, Rahman MS, Otte J, Degistirici Ö, Meisel R, Sorg RV, Oreffo ROC, & Adjaye J. (2019). Human iPSC-derived MSCs (iMSCs) from aged individuals acquire a rejuvenation signature. *Stem Cell Res Ther, 10*(1), 100. doi:10.1186/s13287-019-1209-x

Szabadi E. (2013). Functional neuroanatomy of the central noradrenergic system. *Journal of psychopharmacology (Oxford, England), 27*(8), 659-693. doi:10.1177/0269881113490326

Takahashi K, Tanabe K, Ohnuki M, Narita M, Ichisaka T, Tomoda K, & Yamanaka S. (2007). Induction of pluripotent stem cells from adult human fibroblasts by defined factors. *Cell., 131*(5), 861-872.

Teixeira F, Panchalingam KM, Assunção-Silva R, Serra SC, Mendes-Pinheiro B, Patrício P, Jung S, Anjo SI, Manadas B, Pinto L, Sousa N, Behie LA, & Salgado AJ. (2016). Modulation of the Mesenchymal Stem Cell Secretome Using Computer-Controlled Bioreactors: Impact on Neuronal Cell Proliferation, Survival and Differentiation. *Scientific Reports, 6*, 27791. doi:10.1038/srep27791

Teixeira FG, Carvalho MM, Panchalingam KM, Rodrigues AJ, Mendes-Pinheiro B, Anjo S, Manadas B, Behie LA, Sousa N, & Salgado AJ. (2017). Impact of the Secretome of Human Mesenchymal Stem Cells on Brain Structure and Animal Behavior in a Rat Model of Parkinson's Disease. *Stem Cells Transl Med., 6*(2), 634-646. doi: 610.5966/sctm.2016-0071. Epub 2016 Sep 5922.

Teixeira FG, Carvalho MM, Sousa N, & Salgado AJ. (2013). Mesenchymal stem cells secretome: a new paradigm for central nervous system regeneration? *Cellular and Molecular Life Sciences, 70*(20), 3871-3882.

Timmons S, Coakley MF, Moloney AM, & O' Neill C. (2009). Akt signal transduction dysfunction in Parkinson's disease. *Neuroscience letters, 467*(1), 30-35. doi:10.1016/j.neulet.2009.09.055

Tysnes OB, & Storstein A. (2017). Epidemiology of Parkinson's disease. *J Neural Transm (Vienna). 124*(8), 901-905. doi: 910.1007/s00702-00017-01686-y. Epub 02017 Feb 00701.

Volkman R, & Offen D. (2017). Concise Review: Mesenchymal Stem Cells in Neurodegenerative Diseases. *Stem Cells, 35*(8), 1867-1880. doi:10.1002/stem.2651

Xia W, Peng G-Y, Sheng J-T, Zhu F-F, Guo J-F, & Chen W-Q. (2015). Neuroprotective effect of interleukin-6 regulation of voltage-gated Na(+) channels of cortical neurons is time- and dose-dependent. *Neural regeneration research, 10*(4), 610-617. doi:10.4103/1673-5374.155436

Xu M, Shaw G, Murphy M, & Barry F. (2019). Induced Pluripotent Stem Cell-Derived Mesenchymal Stromal Cells Are Functionally and Genetically Different From Bone Marrow-Derived Mesenchymal Stromal Cells. *Stem cells (Dayton, Ohio), 37*(6), 754-765. doi:10.1002/stem.2993

Zhang Y, Liang X, Liao S, Wang W, Wang J, Li X, Ding Y, Liang Y, Gao F, Yang M, Fu Q, Xu A, Chai YH, He J, Tse HF, & Lian Q. (2015). Potent Paracrine Effects of human induced Pluripotent Stem Cell-derived Mesenchymal Stem Cells Attenuate Doxorubicin-induced Cardiomyopathy. *Scientific Reports, 5*, 112-135.

CHAPTER 5

GENERAL DISCUSSION AND CONCLUSIONS

Stem cells potential for addressing Parkinson's disease complexity

Neurological disorders, such as Parkinson's disease (PD), are the leading cause of disability worldwide (Dorsey *et al.*, 2018). In particular, PD prevalence has grown exponentially in the past decades, pointing out the need to design novel therapeutic strategies able to modify disease progression and consequently, prevent its associated disability. Nevertheless, PD complexity and multifactorial nature hinders the development of therapies that effectively prevent, halt or reverse PD-associated neurodegeneration. Besides classical motor symptoms - bradykinesia, rigidity and rest tremor - PD patients may display a myriad of nonmotor symptoms, including depression, sleep disturbances and constipation, that take place even before clinical diagnosis (Berg *et al.*, 2015). Widespread α-synuclein aggregation, as well as neuronal loss, not only at the substantia nigra *pars compacta* (SNc), but also in other dopaminergic and non-dopaminergic areas, are main neuropathological hallmarks of the disease. Both genetic and environmental factors have been proposed as triggers of oxidative stress, impaired proteostasis and mitochondrial dysfunction, which are the main cellular alterations thought to underlie neurodegeneration and α-synuclein aggregation (Michel *et al.*, 2016). Notwithstanding, currently available therapies only target the symptoms, by replenishing dopaminergic input in the striatum, without addressing neurodegenerative events that occur in the disease.

Stem cells, characterized by their ability to continuously self-renew and differentiate into specialized cells, hold great potential for addressing PD complexity and designing novel disease-modifying strategies. Pluripotent stem cells, with the capacity to give rise to all cell types of the body, are particularly relevant, as they can be differentiated into inaccessible cell types, like neuronal cells. In 2007, the revolutionary discovery of induced pluripotent stem cells (iPSCs), obtained through reprogramming of somatic cell sources, avoided the ethical concerns associated to the so far used human embryonic stem cells (ESCs) and offered unprecedent opportunities for generating patient-specific cell types for human disease modeling and regenerative medicine applications (Takahashi *et al.*, 2007).

Multipotent stem cells are lineage committed stem cells, able to give rise to all cells of a certain embryonic layer. In their niches, these adult stem cells are also crucial mediators of signal transduction, being able to receive cues from the microenvironment and respond accordingly, by producing the appropriate factors to maintain tissue homeostasis (Tewary *et al.*, 2018). These paracrine signaling properties have been put forward as a potential underlying mechanism for the therapeutic effects of mesenchymal stem cells (MSCs), a population of multipotent stem cells that can be isolated from adult tissues, such as bone marrow and adipose tissue.

In this thesis, we have generated stem cell-based tools that may contribute for a better understanding of PD pathogenesis, as well as provide a source of therapeutic factors with neuroprotective potential (figure 5.1). In this chapter, we will discuss the potential applications of the generated stem cell-based tools, with a special focus on the main aim of this thesis, which was the use of iPSCs-derived MSCs as an alternative source to tissue-derived MSCs for the collection of secretome with neuroprotective potential.

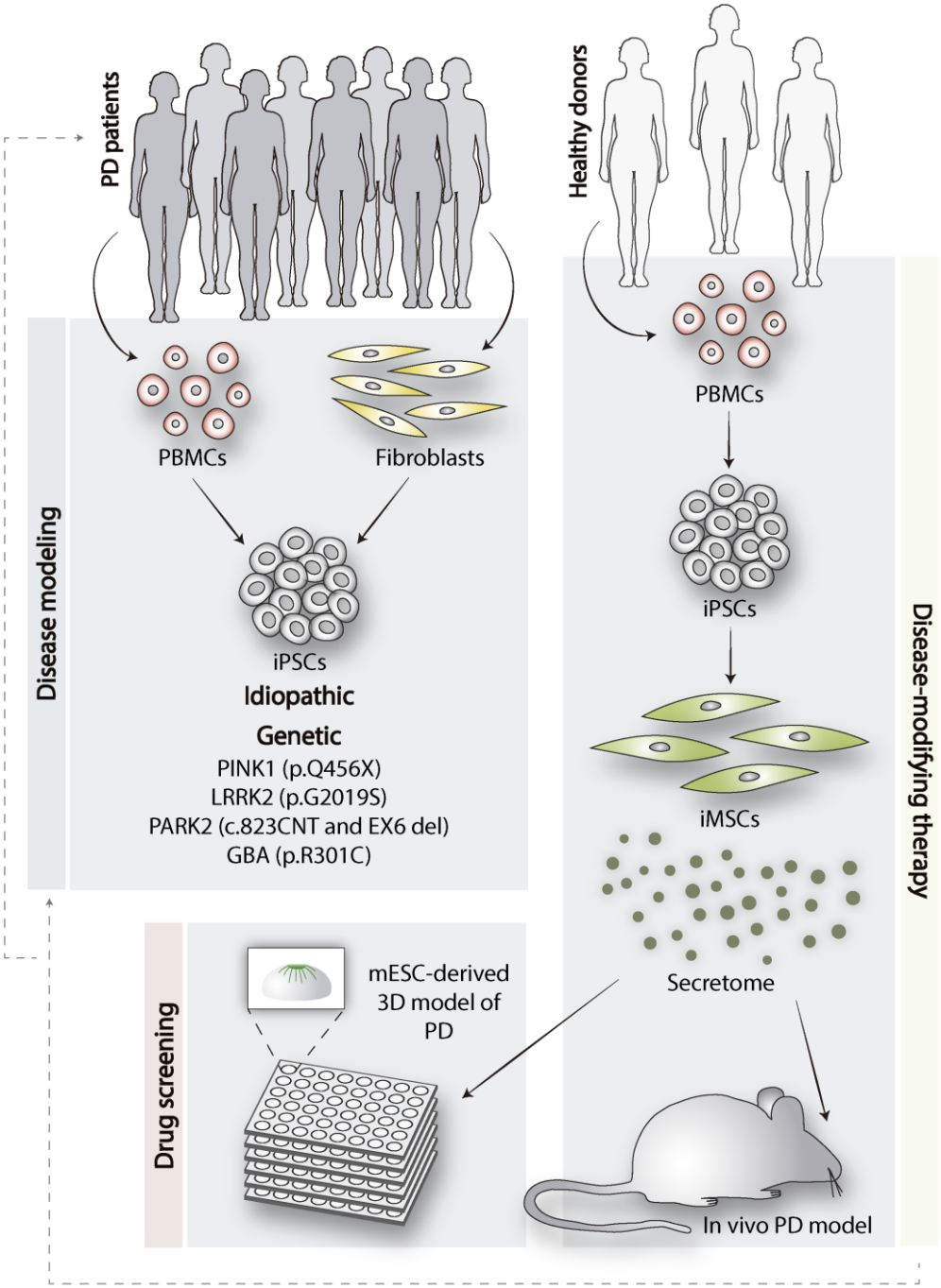

Figure 5.1 – Summary of stem cell-based tools generated in this thesis and their potential applications. *PBMCs – peripheral blood mononuclear cells; iPSCs – induced pluripotent stem cells; iMSCs – induced mesenchymal stem cells; mESC – mouse embryonic stem cells.*

iPSCs as source of patient-specific cells for disease modeling

In chapter 2, we describe the generation of human iPSCs using the non-integrating Sendai virus technology to reprogram peripheral blood mononuclear cells (PBMCs) and fibroblasts (figure 5.1). Eight out of the eleven generated iPSCs lines were derived from PD patients, both idiopathic and carrying genetic mutations in PD-associated genes, namely LRRK2, PINK1, *parkin*, GBA. Importantly, new mutation variants were described for *parkin* and GBA genes, which may not only provide new information regarding their impact on cellular dysfunction, but also contribute for a better characterization of PD genetic basis. Therefore, these iPSCs lines offer unique opportunities for providing large amounts of patient and disease-relevant cells for personalized disease modeling strategies.

Mouse embryonic stem-cell based 3D model for drug screening

In chapter 3, mouse embryonic stem cells (mESCs) were used to develop a 3D model of PD. For that, mESCs were initially differentiated into dopaminergic neurons, subsequently cultured on a collagen hydrogel and finally, exposed to 6-OHDA to induce oxidative stress-mediated cell death. This model displays phenotypic features of dopaminergic neurons degeneration, including decreased cell viability, increased oxidative stress, as well as morphological alterations, thereby providing a cost-effective platform for drug screening of potential neuroprotective drugs. Notwithstanding, future ameliorations can be performed on this model, not only to better dissect the mechanisms underlying 6-OHDA induced cell death, but also in view of delivering additional molecular and functional readouts.

Firstly, in order to provide an additional identity marker of dopaminergic neurons, as well as to understand 6-OHDA mechanism of action, dopamine transporter (DAT) expression should be analyzed in these dopaminergic cultures. 6-OHDA is an hydroxylated analogue of dopamine that is thought to be selectively toxic for dopaminergic neurons, via DAT uptake and subsequent intracellular auto-oxidation and mitochondrial function impairment (Blum *et al.*, 2001). Nevertheless, other studies have suggested that 6-OHDA induced cell damage occurs as a result of its extracellular autoxidation and consequent intracellular access of 6-OHDA oxidation products (Hanrott *et al.*, 2006; Varešlija *et al.*, 2020). Therefore, the assessment of DAT expression in mESC-derived dopaminergic neurons and a better understanding of the signaling cascades mediating 6-OHDA induced cell death, may provide additional molecular readouts to assess the therapeutic potential of neuroprotective therapies tested in this model.

Another phenotypic measure should include electrophysiological recordings to address the functionality of the established dopaminergic neurons, as well as the impact of 6-OHDA exposure on their firing rate.

Indeed, very few *in vitro* studies have addressed the effects of 6-OHDA on dopaminergic neurons electrophysiological properties, showing rapid dose-dependent changes of cell membrane properties on midbrain slices exposed to 6-OHDA (Berretta *et al.*, 2005). Because our culture system is established on multi-well plates, high-throughput electrophysiological recordings based on microelectrode arrays could provide a quick functional assessment of the impact of neuroprotective strategies.

Therefore, this 3D model of dopaminergic neurons holds great potential for being used as a platform for large-scale drug screenings of neuroprotective drugs. Despite the advantages of using human stem cell-based models on preclinical studies, the protocols for differentiating dopaminergic neurons from hiPSCs are time- and money- consuming, thereby preventing their use in large scale. On the other hand, mESCs-derived dopaminergic neurons were obtained after 14 days of differentiation, without the use of expensive morphogens, like FGF8. Hence, this model may be used in preliminary preclinical screenings to rapidly select drugs with therapeutic potential, which can be thereafter validated, in a smaller scale, using human stem cell-based models.

Induced mesenchymal stem cell- derived secretome as a potential disease-modifying therapy

In chapter 4, and in keeping with the main aim of this thesis, we describe the generation of MSCs from iPSCs. Importantly, we further demonstrate a similar paracrine potential between these induced MSCs (iMSCs) and the gold standard tissue-derived MSCs, bone-marrow derived MSCs (BM-MSCs), in attenuating 6-OHDA induced nigrostriatal degeneration and the resultant motor deficits.

<u>iMSCs as a source</u>

The use of iMSCs as a source of secreted factors with therapeutic potential presents several methodological and technical advantages over tissue-derived MSCs, making this potential disease-modifying therapy better suited for a widespread clinical application (figure 5.2). Firstly, iMSCs are derived from iPSCs, which are generated from minimal invasive somatic cell sources (PBMCs or skin fibroblasts), thereby avoiding the need to perform invasive isolation procedures associated to tissue-derived MSCs, like bone marrow biopsy for isolating BM-MSCs. After being established in culture, iPSCs can be cryopreserved and thus, become readily available for expansion and subsequent *in vitro* differentiation. Moreover, iMSCs present a higher proliferative capacity than their tissue-derived counterparts (Frobel *et al.*, 2014), allowing a superior expansion for the collection of a larger amount of secretome from the same donor. Indeed, besides accessibility, standardization is a major advantage of using iPSCs as a source of MSCs for secretome-based therapeutic approaches. Tissue-derived MSCs' number, quality and

proliferative capacity are dependent on donor's age, thereby compromising the reproducibility of this therapeutic approach. On the other hand, establishing MSCs from iPSCs may provide a master bank of high-quality iMSCs with known therapeutic paracrine potential.

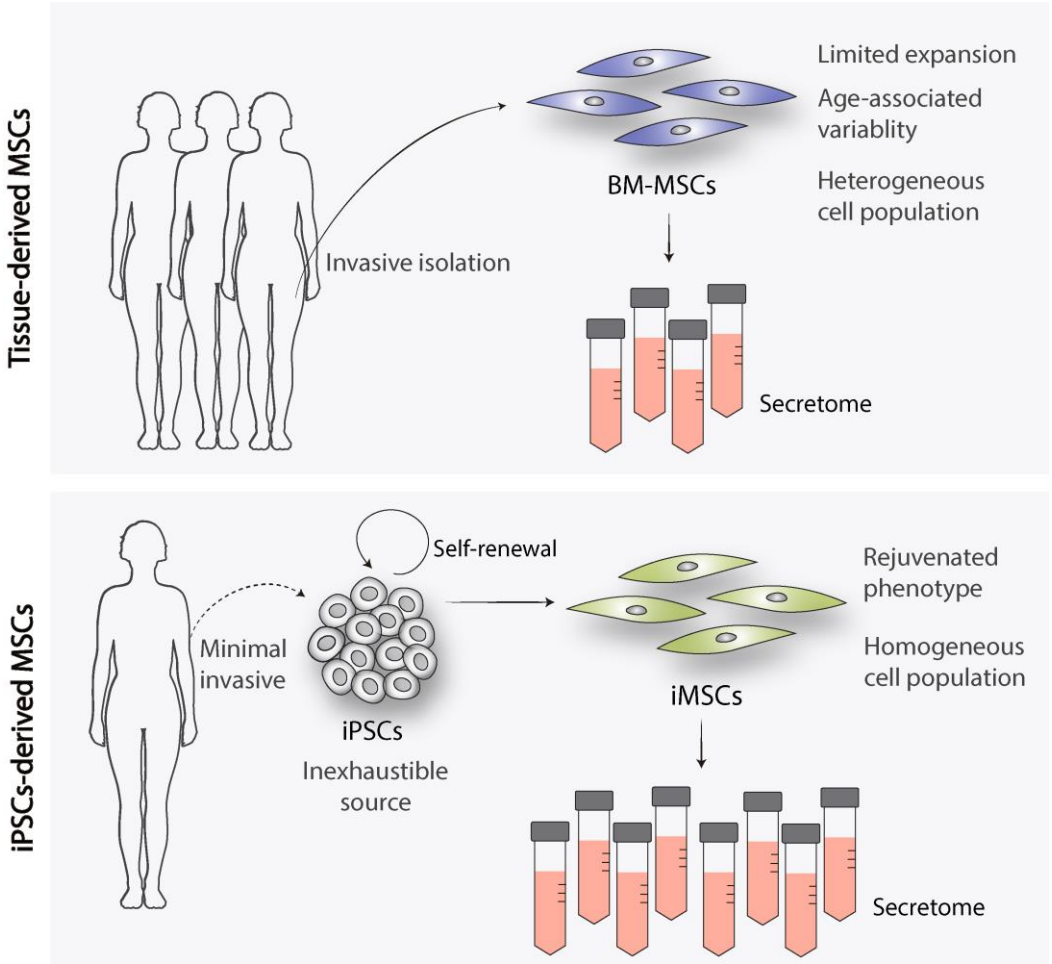

Figure 5.2 – Comparison between the use of tissue and induced pluripotent stem cells- derived mesenchymal stem cells as sources for secretome collection. The limitations and advantages are described at each step of the process.

Nevertheless, to fully recognize iMSCs therapeutic potential, some caveats on their generation and characterization should be addressed. Firstly, a vast number of iMSCs generation protocols have been reported, using different serum supplementation, growth factors, coating materials and small molecule inhibitors (Abdal Dayem *et al.*, 2019), which may yield distinct cellular phenotypes, with distinct therapeutic potential. Therefore, a unifying protocol should be established for producing *bona fide* iMSCs, in compliance with Good Manufacturing Practices to ensure reproducibility, efficacy and safety of their use.

Another potential source of variability is the somatic cell of iPSC origin used for MSCs generation, which has been shown to lead to a differentiation bias towards their starting population (Hargus *et al.*, 2014). Consequently, iPSCs obtained from mesodermal-derived somatic sources, such as PBMCs used in our work, may have a better differentiation efficiency towards MSCs. Indeed, most studies have used tissue-derived MSCs as somatic cell sources for reprogramming into iPSCs and further re-differentiated into iMSCs (Fernandez-Rebollo *et al.*, 2020; Frobel *et al.*, 2014; Sabapathy *et al.*, 2016). Although this strategy eliminates possible donor variability between both sources, it is based on the use of invasive tissue-derived MSCs sources and may present a stronger bias towards differentiation into MSCs. Therefore, future studies should address the influence of different somatic cells of iPSC origin on iMSCs phenotype and therapeutic potential.

Finally, a major hurdle in the uniformization of iMSCs generation is the lack of clear criteria for defining their identity. Similarly to other MSCs, iMSCs are characterized according to the minimal criteria established by the International Society for Cellular Therapy in 2006 (Dominici *et al.*, 2006). Nevertheless, additional markers should be used to provide a better quality control of cultured MSCs, as well as distinguish between MSCs from different sources. For instance, Camilleri and colleagues (Camilleri *et al.*, 2016) have recently reported new cell surface biomarkers for adipose-derived MSCs characterization based on RNA sequencing and subsequent validation by flow cytometry. The identification of additional iMSCs markers would therefore yield a more homogeneous cell population.

MSCs secretome as a PD therapy

Despite these constraints in MSCs culture standardization, their therapeutic potential has been widely accepted. Particularly in PD, the use of tissue-derived MSCs secretome has been put forward as a promising therapeutic approach with neuroprotective potential (Cova *et al.*, 2010; Marques *et al.*, 2018; Mendes-Pinheiro *et al.*, 2019; Teixeira *et al.*, 2017; Teixeira *et al.*, 2020). Previous studies have evidenced diverging effects and content between the secretome collected from different tissue-specific MSCs (Assuncao-Silva *et al.*, 2018; Pires *et al.*, 2016; Pires *et al.*, 2014), suggesting the need to select the most appropriate MSCs source for a specific secretome application. In the present work, the use of secretome either from BM-MSCs or iMSCs induced similar neuroprotective effects in a preclinical model of PD, thereby validating the use of iMSCs as a worthwhile source for future secretome-based clinical applications.

The cocktail of growth factors, cytokines and extracellular matrix remodeling proteins present in MSCs secretome have been suggested to consist of a senescence-associated secretory phenotype (SASP), which

is implicated in their paracrine regenerative effects (Lunyak *et al.*, 2017). Indeed, continuous expansion of MSCs *in vitro* results in replicative senescence, characterized by decreased proliferation rates, cellular enlargement, loss of differentiation potential, but still with high metabolic activity (Campisi *et al.*, 2007; Wiley *et al.*, 2016). Whereas iPSCs do not present signs of replicative senescence, iMSCs have been shown to present a similar senescence-associated metabolomic phenotype to tissue-derived MSCs during culture expansion (Fernandez-Rebollo *et al.*, 2020). Accordingly, in our targeted proteomic analysis, both BM-MSCs and iMSCs presented a similar secretory profile, except for IL-6 and IL-8 levels. A better characterization of iMSCs secretome composition and its variation according to culture conditions, such as number of passages, media composition, as well as dynamic expansion (e.g. in bioreactors), is therefore required to fully reveal their therapeutic potential.

Notwithstanding further characterization of MSCs secretome composition, accumulating evidence has demonstrated their potential disease-modifying effects in PD preclinical models. As presented in this thesis (chapter 4) and in previous studies from our group (Mendes-Pinheiro *et al.*, 2019; Teixeira *et al.*, 2017), MSCs secretome administration has consistently protected SNc dopaminergic neurons from 6-OHDA induced cell death, reinforcing their potential role in reducing neurodegeneration in PD patients.

Besides these neuroprotective effects, MSCs secretome has been shown to 1) degrade α-synuclein aggregates and prevent their transsynaptic transmission (Oh *et al.*, 2016; Oh *et al.*, 2017); 2) modulate microglial activation (Danielyan *et al.*, 2011; Kim *et al.*, 2009; Mccoy *et al.*, 2008; Suzuki *et al.*, 2015); and 3) induce the formation of new neurons to reinnervate degenerated areas (Cova *et al.*, 2010; Schwerk *et al.*, 2015a; Schwerk *et al.*, 2015b). MSCs secretome effect on angiogenesis is another possible mechanism underlying its regenerative effects (Kehl *et al.*, 2019), which has not been explored in the context of PD. Indeed, compromised blood-brain barrier integrity has been reported in the striatum of PD patients (Gray *et al.*, 2015) and thus, future studies are required to address the role of MSCs secretome in this PD pathological feature.

Therefore, the complex mixture of bioactive factors present in MSCs secretome may not only have a direct impact on dopaminergic neurons survival, but also in other potential mechanisms underlying PD pathogenesis, providing a multitargeted approach for halting PD-associated neurodegeneration. In the present preclinical study, MSCs secretome was administered in a severely degenerated nigrostriatal system, possibly mimicking an advanced stage of PD neurodegeneration. Although we were able to observe significant motor improvements over non-treated animals, future studies in less severe degeneration models, may contribute for an increased motor recovery, thereby addressing the impact of

this potential disease-modifying therapy on earlier stages of the disease. Besides the assessment of the appropriate therapeutic window, further analyses are also required for developing novel and less invasive delivery routes, as well as for establishing the appropriate dosage regimens of MSCs secretome administration.

Nonetheless, the experimental models in which MSCs secretome has demonstrated therapeutic effects do not fully recapitulate the pathological features underlying PD. Indeed, this is a major obstacle in the development of disease-modifying therapies that reveals the lack of complete understanding of PD etiology. The possibility of acquiring patient- and disease- specific iPSCs provides a unique opportunity for dissecting the molecular mechanisms underlying PD pathogenesis and thereafter, consider the generation of animal models with improved construct validity. Moreover, a better characterization of PD at the clinical and pathological level, namely regarding the manifestation and anatomical correlates of nonmotor symptoms may also contribute for the establishment of animal models with better face validity. Overall, the development of PD therapeutic strategies with disease-modifying potential requires unifying research efforts at the clinical and experimental level to address this multifactorial neurodegenerative disease.

References

Abdal Dayem A, Lee SB, Kim K, Lim KM, Jeon T-I, Seok J, Cho, & Ssang G. (2019). Production of Mesenchymal Stem Cells Through Stem Cell Reprogramming. *International journal of molecular sciences, 20*(8), 1922. doi:10.3390/ijms20081922

Assuncao-Silva RC, Mendes-Pinheiro B, Patricio P, Behie LA, Teixeira FG, Pinto L, & Salgado AJ. (2018). Exploiting the impact of the secretome of MSCs isolated from different tissue sources on neuronal differentiation and axonal growth. *Biochimie., 155:83-91.*(doi), 10.1016/j.biochi.2018.1007.1026. Epub 2018 Aug 1012.

Berg D, Postuma RB, Adler CH, Bloem BR, Chan P, Dubois B, Gasser T, Goetz CG, Halliday G, Joseph L, Lang AE, Liepelt-Scarfone I, Litvan I, Marek K, Obeso J, Oertel W, Olanow CW, Poewe W, Stern M, & Deuschl G. (2015). MDS research criteria for prodromal Parkinson's disease. *Movement Disorders, 30*(12), 1600-1611. doi:10.1002/mds.26431

Berretta N, Freestone PS, Guatteo E, de Castro D, Geracitano R, Bernardi G, Mercuri NB, & Lipski J. (2005). Acute effects of 6-hydroxydopamine on dopaminergic neurons of the rat substantia nigra pars compacta in vitro. *Neurotoxicology, 26*(5), 869-881. doi:10.1016/j.neuro.2005.01.014

Blum D, Torch S, Lambeng N, Nissou M, Benabid AL, Sadoul R, & Verna JM. (2001). Molecular pathways involved in the neurotoxicity of 6-OHDA, dopamine and MPTP: contribution to the apoptotic theory in Parkinson's disease. *Prog Neurobiol., 65*(2), 135-172.

Camilleri ET, Gustafson MP, Dudakovic A, Riester SM, Garces CG, Paradise CR, Takai H, Karperien M, Cool S, Sampen HJ, Larson AN, Qu W, Smith J, Dietz AB, & van Wijnen AJ. (2016). Identification and validation of multiple cell surface markers of clinical-grade adipose-derived mesenchymal stromal cells as novel release criteria for good manufacturing practice-compliant production. *Stem Cell Res Ther., 7*(1), 107. doi: 110.1186/s13287-13016-10370-13288.

Campisi J, & d'Adda di Fagagna F. (2007). Cellular senescence: when bad things happen to good cells. *Nature Reviews Molecular Cell Biology, 8*(9), 729-740. doi:10.1038/nrm2233

Cova L, Armentero MT, Zennaro E, Calzarossa C, Bossolasco P, Busca G, Lambertenghi Deliliers G, Polli E, Nappi G, Silani V, & Blandini F. (2010). Multiple neurogenic and neurorescue effects of human mesenchymal stem cell after transplantation in an experimental model of Parkinson's disease. *Brain Res., 1311:12-27.*(doi), 10.1016/j.brainres.2009.1011.1041. Epub 2009 Nov 1026.

Danielyan L, Schäfer R, von Ameln-Mayerhofer A, Bernhard F, Verleysdonk S, Buadze M, Lourhmati A, Klopfer T, Schaumann F, Schmid B, Koehle C, Proksch B, Weissert R, Reichardt HM, van den Brandt J, Buniatian GH, Schwab M, Gleiter CH, & Frey WH, 2nd. (2011). Therapeutic efficacy of intranasally delivered mesenchymal stem cells in a rat model of Parkinson disease. *Rejuvenation research, 14*(1), 3-16. doi:10.1089/rej.2010.1130

Dominici M, Le Blanc K, Mueller I, Slaper-Cortenbach I, Marini F, Krause D, Deans R, Keating A, Prockop D, & Horwitz E. (2006). Minimal criteria for defining multipotent mesenchymal stromal cells. The International Society for Cellular Therapy position statement. *Cytotherapy., 8*(4), 315-317. doi: 310.1080/14653240600855905.

Dorsey ER, & Bloem BR. (2018). The Parkinson Pandemic—A Call to Action. *JAMA Neurology, 75*(1), 9-10. doi:10.1001/jamaneurol.2017.3299

Fernandez-Rebollo E, Franzen J, Goetzke R, Hollmann J, Ostrowska A, Oliverio M, Sieben T, Rath B, Kornfeld J-W, & Wagner W. (2020). Senescence-Associated Metabolomic Phenotype in Primary and iPSC-Derived Mesenchymal Stromal Cells. *Stem Cell Reports, 14*(2), 201-209. doi:https://doi.org/10.1016/j.stemcr.2019.12.012

Frobel J, Hemeda H, Lenz M, Abagnale G, Joussen S, Denecke B, Sarić T, Zenke M, & Wagner W. (2014). Epigenetic rejuvenation of mesenchymal stromal cells derived from induced pluripotent stem cells. *Stem Cell Reports, 3*(3), 414-422. doi:10.1016/j.stemcr.2014.07.003

Gray MT, & Woulfe JM. (2015). Striatal blood-brain barrier permeability in Parkinson's disease. *Journal of cerebral blood flow and metabolism : official journal of the International Society of Cerebral Blood Flow and Metabolism, 35*(5), 747-750. doi:10.1038/jcbfm.2015.32

Hanrott K, Gudmunsen L, O'Neill MJ, & Wonnacott S. (2006). 6-hydroxydopamine-induced apoptosis is mediated via extracellular auto-oxidation and caspase 3-dependent activation of protein kinase Cdelta. *The Journal of biological chemistry, 281*(9), 5373-5382. doi:10.1074/jbc.M511560200

Hargus G, Ehrlich M, Arauzo-Bravo MJ, Hemmer K, Hallmann AL, Reinhardt P, Kim KP, Adachi K, Santourlidis S, Ghanjati F, Fauser M, Ossig C, Storch A, Kim JB, Schwamborn JC, Sterneckert J, Scholer HR, Kuhlmann T, & Zaehres H. (2014). Origin-dependent neural cell identities in

differentiated human iPSCs in vitro and after transplantation into the mouse brain. *Cell Rep., 8*(6), 1697-1703. doi: 1610.1016/j.celrep.2014.1608.1014. Epub 2014 Sep 1615.

Kehl D, Generali M, Mallone A, Heller M, Uldry A-C, Cheng P, Gantenbein B, Hoerstrup SP, & Weber B. (2019). Proteomic analysis of human mesenchymal stromal cell secretomes: a systematic comparison of the angiogenic potential. *npj Regenerative Medicine, 4*(1), 8. doi:10.1038/s41536-019-0070-y

Kim Y-J, Park H-J, Lee G, Bang OY, Ahn YH, Joe E, Kim HO, & Lee PH. (2009). Neuroprotective effects of human mesenchymal stem cells on dopaminergic neurons through anti-inflammatory action. *Glia, 57*(1), 13-23. doi:10.1002/glia.20731

Lunyak VV, Amaro-Ortiz A, & Gaur M. (2017). Mesenchymal Stem Cells Secretory Responses: Senescence Messaging Secretome and Immunomodulation Perspective. *Frontiers in genetics, 8*, 220-220. doi:10.3389/fgene.2017.00220

Marques CR, Marote A, Mendes-Pinheiro B, Teixeira FG, & Salgado AJ. (2018). Cell secretome based approaches in Parkinson's disease regenerative medicine. *Expert Opinion on Biological Therapy, 18*(12), 1235-1245. doi:10.1080/14712598.2018.1546840

McCoy MK, Martinez TN, Ruhn KA, Wrage PC, Keefer EW, Botterman BR, Tansey KE, & Tansey MG. (2008). Autologous transplants of Adipose-Derived Adult Stromal (ADAS) cells afford dopaminergic neuroprotection in a model of Parkinson's disease. *Experimental Neurology, 210*(1), 14-29. doi:10.1016/j.expneurol.2007.10.011

Mendes-Pinheiro B, Anjo SI, Manadas B, Da Silva JD, Marote A, Behie LA, Teixeira FG, & Salgado AJ. (2019). Bone Marrow Mesenchymal Stem Cells' Secretome Exerts Neuroprotective Effects in a Parkinson's Disease Rat Model. *Frontiers in bioengineering and biotechnology, 7*, 294-294. doi:10.3389/fbioe.2019.00294

Michel Patrick P, Hirsch Etienne C, & Hunot S. (2016). Understanding Dopaminergic Cell Death Pathways in Parkinson Disease. *Neuron, 90*(4), 675-691. doi:10.1016/j.neuron.2016.03.038

Oh SH, Kim HN, Park HJ, Shin JY, Bae EJ, Sunwoo MK, Lee SJ, & Lee PH. (2016). Mesenchymal Stem Cells Inhibit Transmission of alpha-Synuclein by Modulating Clathrin-Mediated Endocytosis in a Parkinsonian Model. *Cell Rep., 14*(4), 835-849. doi: 810.1016/j.celrep.2015.1012.1075. Epub 2016 Jan 1014.

Oh SH, Kim HN, Park HJ, Shin JY, Kim DY, & Lee PH. (2017). The Cleavage Effect of Mesenchymal Stem Cell and Its Derived Matrix Metalloproteinase-2 on Extracellular α-Synuclein Aggregates in Parkinsonian Models. *Stem Cells Translational Medicine, 6*(3), 949-961. doi:10.5966/sctm.2016-0111

Pires AO, Mendes-Pinheiro B, Teixeira FG, Anjo SI, Ribeiro-Samy S, Gomes ED, Serra SC, Silva NA, Manadas B, Sousa N, & Salgado AJ. (2016). Unveiling the Differences of Secretome of Human Bone Marrow Mesenchymal Stem Cells, Adipose Tissue-Derived Stem Cells, and Human Umbilical Cord Perivascular Cells: A Proteomic Analysis. *Stem Cells Dev, 25*(14), 1073-1083. doi:10.1089/scd.2016.0048

Pires AO, Neves-Carvalho A, Sousa N, & Salgado AJ. (2014). The Secretome of Bone Marrow and Wharton Jelly Derived Mesenchymal Stem Cells Induces Differentiation and Neurite Outgrowth in SH-SY5Y Cells. *Stem Cells Int, 2014*, 438352. doi:10.1155/2014/438352

Sabapathy V, & Kumar S. (2016). hiPSC-derived iMSCs: NextGen MSCs as an advanced therapeutically active cell resource for regenerative medicine. *J Cell Mol Med, 21*(10), 12839.

Schwerk A, Altschüler J, Roch M, Gossen M, Winter C, Berg J, Kurtz A, Akyüz L, & Steiner B. (2015a). Adipose-derived human mesenchymal stem cells induce long-term neurogenic and anti-inflammatory effects and improve cognitive but not motor performance in a rat model of Parkinson's disease. *Regenerative medicine, 10*(4), 431-446. doi:10.2217/rme.15.17

Schwerk A, Altschüler J, Roch M, Gossen M, Winter C, Berg J, Kurtz A, & Steiner B. (2015b). Human adipose-derived mesenchymal stromal cells increase endogenous neurogenesis in the rat subventricular zone acutely after 6-hydroxydopamine lesioning. *Cytotherapy, 17*(2), 199-214. doi:10.1016/j.jcyt.2014.09.005

Suzuki S, Kawamata J, Iwahara N, Matsumura A, Hisahara S, Matsushita T, Sasaki M, Honmou O, & Shimohama S. (2015). Intravenous mesenchymal stem cell administration exhibits therapeutic effects against 6-hydroxydopamine-induced dopaminergic neurodegeneration and glial activation in rats. *Neuroscience letters, 584*, 276-281. doi:10.1016/j.neulet.2014.10.039

Takahashi K, Tanabe K, Ohnuki M, Narita M, Ichisaka T, Tomoda K, & Yamanaka S. (2007). Induction of pluripotent stem cells from adult human fibroblasts by defined factors. *Cell., 131*(5), 861-872.

Teixeira FG, Carvalho MM, Panchalingam KM, Rodrigues AJ, Mendes-Pinheiro B, Anjo S, Manadas B, Behie LA, Sousa N, & Salgado AJ. (2017). Impact of the Secretome of Human Mesenchymal Stem Cells on Brain Structure and Animal Behavior in a Rat Model of Parkinson's Disease. *Stem Cells Transl Med., 6*(2), 634-646. doi: 610.5966/sctm.2016-0071. Epub 2016 Sep 5922.

Teixeira FG, Vilaça-Faria H, Domingues AV, Campos J, & Salgado AJ. (2020). Preclinical Comparison of Stem Cells Secretome and Levodopa Application in a 6-Hydroxydopamine Rat Model of Parkinson's Disease. *Cells., 9*(2), 315. doi: 310.3390/cells9020315.

Tewary M, Shakiba N, & Zandstra PW. (2018). Stem cell bioengineering: building from stem cell biology. *Nature Reviews Genetics, 19*(10), 595-614. doi:10.1038/s41576-018-0040-z

Varešlija D, Tipton KF, Davey GP, & McDonald AG. (2020). 6-Hydroxydopamine: a far from simple neurotoxin. *Journal of neural transmission (Vienna, Austria : 1996), 127*(2), 213-230. doi:10.1007/s00702-019-02133-6

Wiley CD, & Campisi J. (2016). From Ancient Pathways to Aging Cells—Connecting Metabolism and Cellular Senescence. *Cell Metabolism, 23*(6), 1013-1021. doi:https://doi.org/10.1016/j.cmet.2016.05.010

ANNEXES

ANNEX I

Stem Cell Research 27 (2018) 78–81

Contents lists available at ScienceDirect

Stem Cell Research

journal homepage: www.elsevier.com/locate/scr

Lab Resource: Stem Cell Line

Generation of a human induced pluripotent stem cell line (CSC-42) from a patient with sporadic form of Parkinson's disease

Ekaterina Savchenko [a,b,c], Ana Marote [d,e], Kaspar Russ [a,b,c], Anna Collin [f], Stefano Goldwurm [g], Laurent Roybon [a,b,c,*], Yuriy Pomeshchik [a,b,c]

[a] Stem Cell Laboratory for CNS Disease Modeling, Wallenberg Neuroscience Center, Department of Experimental Medical Science, BMC A10, Lund University, Lund, Sweden
[b] Strategic Research Area MultiPark, Lund University, Lund, Sweden
[c] Lund Stem Cell Center, Lund University, Lund, Sweden
[d] Life and Health Sciences Research Institute (ICVS), School of Health Sciences, University of Minho, Braga, Portugal
[e] ICVS/3B's, PT Government Associate Laboratory, Braga, Guimarães, Portugal
[f] Department of Clinical Genetics and Pathology, Office for Medical Services, Division of Laboratory Medicine, Lund, Sweden
[g] Parkinson Institute, ASST PINI-CTO, Milan, Italy

ARTICLE INFO

Article history:
Received 15 October 2017
Received in revised form 13 December 2017
Accepted 3 January 2018
Available online 4 January 2018

ABSTRACT

Skin fibroblasts were collected from a 44-year-old patient with sporadic case of Parkinson's disease (PD). The non-integrating Sendai virus vector encoding OCT3/4, SOX2, c-MYC and KLF4 was used to reprogram fibroblasts into induced pluripotent stem cells (iPSCs). Generated iPSCs had normal karyotypes, expressed common stem cell markers, and were capable of differentiating into all three germ layers. Generated line could be used for PD modeling to understand the mechanisms that influence the disorder.

Resource table

Unique stem cell line identifier	ULUNDi004-A
Alternative name(s) of stem cell line	CSC-42L
Institution	Stem Cell Laboratory for CNS Disease Modeling, Department of Experimental Medical Science, Lund University
Contact information of distributor	Laurent Roybon, Laurent.Roybon@med.lu.se
Type of cell line	IPSC
Origin	Human
Additional origin info	Age of patient at onset: 38 Sex of patient: female Ethnicity: N/A
Cell Source	Skin fibroblasts
Clonality	Clonal
Method of reprogramming	Sendai virus mediated delivery of OCT3/4, SOX2, c-MYC and KLF4
Genetic Modification	No modification
Type of Modification	No modification
Associated disease	Parkinson's disease
Gene/locus	N/A
Method of modification	No modification
Name of transgene or resistance	No transgene or resistance
Inducible/constitutive system	Not inducible
Date archived/stock date	N/A
Cell line repository/bank	N/A
Ethical approval	Parkinson Institute Biobank (part of the Telethon Genetic Biobank Network http://biobanknetwork.telethon.it/): approved by Ethics Committee "Milano Area C" (http://comitatoeticoareac.ospedaleniguarda.it/) on the 26/06/2015, Numero Registro dei pareri: 370-062015. Reprogramming: 202,100-3211 (delivered by Swedish work environment Arbetsmiljöverket).

Resource utility

The sporadic Parkinson's disease (PD) is the second most frequent degenerative disorder of the human nervous system (Braak and Del Tredici, 2009). Generated induced pluripotent stem cell (iPSC) line can be utilized for in vitro disease modeling to study the mechanisms underlying Parkinson's disease (PD).

Resource details

Fibroblasts from a 44-year-old female patient with sporadic form of PD were reprogrammed through introduction of OCT3/4, SOX2, c-MYC and KLF4 factors. Delivery of the pluripotency-inducing factors was

* Corresponding author at: Stem Cell Laboratory for CNS Disease Modeling, Wallenberg Neuroscience Center, Department of Experimental Medical Science, BMC A10, Lund University, Lund, Sweden.
E-mail address: laurent.roybon@med.lu.se (L. Roybon).

https://doi.org/10.1016/j.scr.2018.01.002

achieved using CytoTune™-iPS 2.0 Sendai Reprogramming Kit. At day 28, colonies were manually picked and expanded clonally. Three clones (CSC-42I, CSC-42K, CSC-42L) were further selected based on the morphology of the colonies, for characterization using the methods we previously described in Holmqvist et al., 2016. Here, we present the characterization of clone CSC-42L. Pluripotency of generated cells was confirmed by immunocytochemistry using staining for OCT4, NANOG, TRA1–81 and SSEA4 markers (Fig. 1A) as well as by demonstration of alkaline phosphatase (ALP) activity in cultured cells (Fig. 1B). Flow cytometry analysis revealed that >99% of the iPSCs were positive for SSEA4 (Fig. 1C; non-stained iPSCs are shown in grey). The clearance of the virus was confirmed by staining against Sendai after 7 passages (Fig. 1D). G-banding analysis showed a normal karyotype (Fig. 1E). The genetic fingerprinting showed genetic identity of CSC-42 L line to parental fibroblasts. In addition, CSC-42 L iPSCs cultured on non-adherent surfaces were able to form embryoid bodies (EBs) and subsequently differentiate into all three embryonic germ layers, in vitro, as detected by the presence of lineage specific markers such as ecto dermal

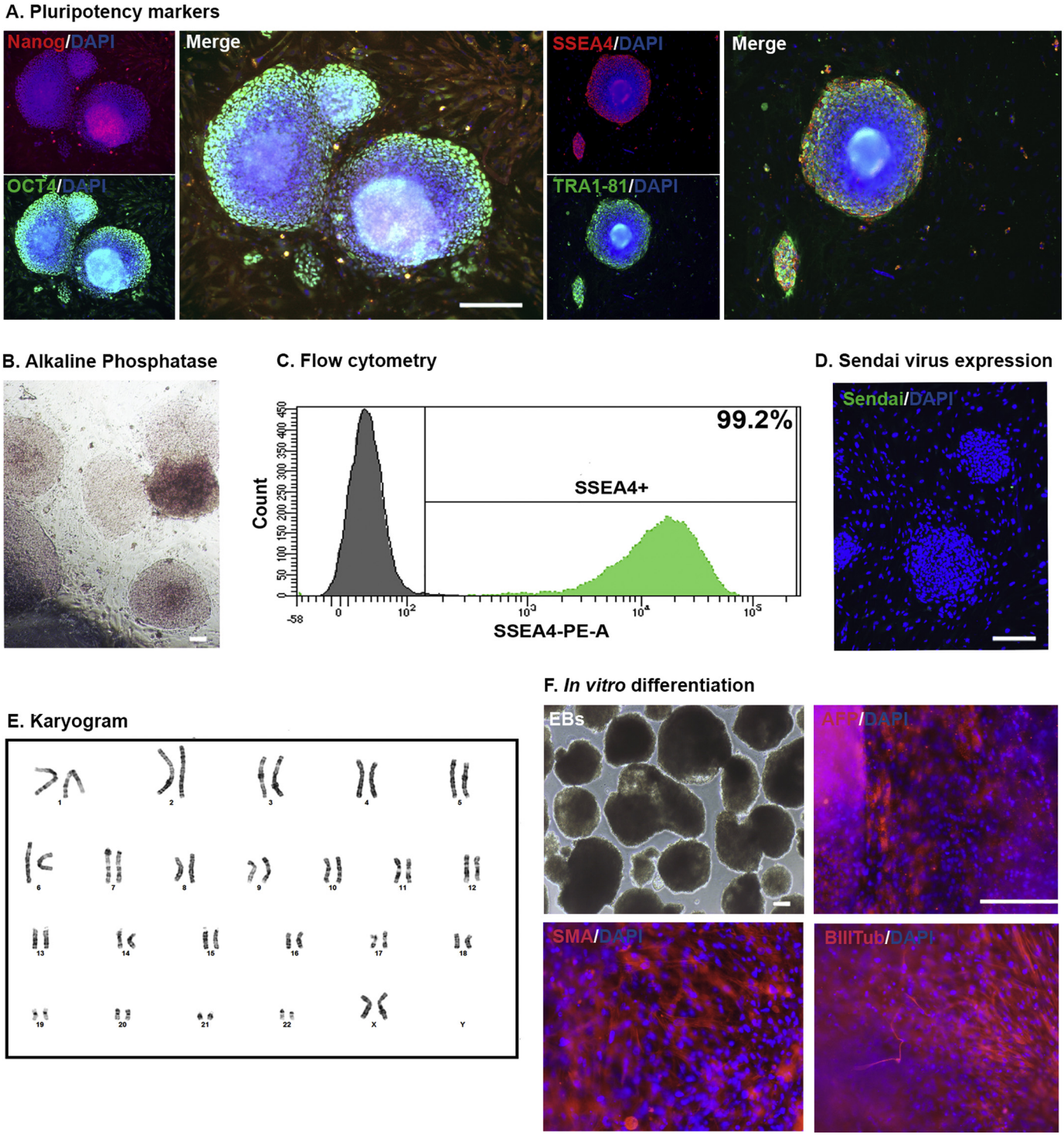

Fig. 1. Characterisation of the iPSC line CSC-42.

marker beta-III-tubulin (BIIITub), the mesodermal marker smooth muscle actin (SMA) and the endodermal marker alpha-fetoprotein (AFP) (Fig. 1F). Mycoplasma infection was prevented by routine addition of plasmocin in cell culture media.

Materials and methods

Fibroblast culture

The skin biopsy sample was collected from a 44-year-old patient with a confirmed sporadic form of PD, after obtaining informed consent. After collection, fibroblasts were cultured in Dulbecco's modified eagle's medium (DMEM) containing 10% fetal bovine serum and 1% Penicillin-Streptomycin and passaged with 0.05% trypsin.

iPSC generation

Human fibroblasts were reprogrammed to iPSCs through introduction of OCT3/4, SOX2, c-MYC and KLF4. For this purpose, cells were plated on a 12-well plate at a density of 75,000 cells per well. After two days of incubation cells were transduced with Sendai virus containing four reprogramming factors mentioned above using CytoTune™-iPS 2.0 Sendai reprogramming kit (ThermoFisher Scientific). After transduction, cell media was changed every second day. At day 7, the cells were collected and re-plated onto irradiated mouse embryonic fibroblasts (MEF) feeder cells in DMEM media containing 10% fetal bovine serum and 1% Penicillin-Streptomycin. On the day after and until the day 28, the cells were cultured in WiCell medium containing advanced DMEM/F12 (ThermoFisher Scientific), 20% Knock-Out Serum Replacement (v/v, ThermoFisher Scientific), 2 mM l-glutamine (ThermoFisher Scientific), 1% non-essential amino acids (NEAA, v/v, Millipore), 0.1 mM β-mercaptoethanol (Sigma-Aldrich), and 20 ng/ml FGF2 supplemented daily (ThermoFisher Scientific). On day 28, single colonies were picked and seeded on a MEF-coated 24-well plate. A week after, three separate clones were randomly selected for further expansion. Once a week cells were cryopreserved or re-plated on the appropriate cell culture surface for further analysis.

Immunocytochemistry

For immunocytochemistry, iPSC cells were fixed with 4% paraformaldehyde (PFA), permeabilized and blocked with solution containing 0.1% TritonX-10 (Sigma) and 10% donkey serum in PBS for 1 h at room temperature (RT). Then, the cells were incubated overnight at +4 °C with the primary antibodies (Table 2) diluted in the blocking solution. Next day, the cells were washed with PBS and incubated for 1 h at RT in the dark with secondary antibodies diluted in PBS. DAPI (Life Technologies) was used to counterstain nuclei (1:10,000). The staining was visualized using a fluorescence microscope LRI - Olympus IX-73. Scale bars are 200 μm (Table 1).

Alkaline phosphatase activity

Alkaline phosphatase staining was done using Alkaline Phosphatase Staining Kit according to the manufacturer's instructions (Stemgent, MA).

Embryoid body (EB) formation

For in vitro embryoid body formation, iPSCs were plated on low-attachment 24-well plates in WiCell medium supplemented with 20 ng/ml FGF2 allowing them to grow for 2 weeks as EBs. After that, EBs were collected, dissociated and plated onto 96-well plate in DMEM media containing 10% fetal bovine serum and 1% Penicillin-Streptomycin for 2 more weeks. Then the cells were harvested, fixed and stained for markers against three germ layers (Table 2).

Karyotype analysis

Karyotype analysis was performed at 300–400 band resolution in average after 10 passages using G-banding technique at the Department of Clinical Genetics and Pathology in Lund.

DNA fingerprinting

Genomic DNA was extracted from fibroblasts and iPSCs using conventional lysis buffer composed of 100 mM Tris (pH 8.0), 200 mM NaCl, 5 mM EDTA and 0.2% SDS in distilled autoclaved water supplemented with 1.5 mg/ml Proteinase K. DNA fingerprinting was performed by IdentiCell STR profiling service at the Department of Molecular Medicine, Aarhus University Hospital, Skejby, Denmark.

Mycoplasma detection

Absence of mycoplasma contamination was confirmed by the real-time PCR method at GATC Biotech AG (European Genome and Diagnostics Centre, Konstanz, Germany).

Table 1
Characterization and validation.

Classification	Test	Result	Data
Morphology	Photography	Visual record of the line: Normal	Not shown but available with author
Phenotype	Immunocytochemisty	Positive staining for pluripotency markers: OCT4, NANOG, TRA1-81 and SSEA4	Fig. 1 panel A
	Alkaline phosphatase activity	Visible activity	Fig. 1 panel B
	Flow cytometry	99.2% SSEA4	Fig. 1 panel C
Genotype	Karyotype (G-banding) and resolution	46,XX (300–400 bands resolution in average)	Fig. 1 panel E
Identity	STR analysis	10 sites analyzed, all matched with parent fibroblast cell line	Available with author
Mutation analysis (IF APPLICABLE)	N/A	N/A	N/A
Microbiology and virology	Mycoplasma	Mycoplasma testing by RT-PCR. Negative.	Not shown but available with author
Differentiation potential	Embryoid body formation	Positive staining for smooth muscle actin, beta-III-tubulin and alpha-fetoprotein after spontaneous differentiation of embryoid bodies	Fig. 1 panel F
Donor screening (OPTIONAL)	HIV 1 + 2 Hepatitis B, Hepatitis C	N/A	N/A
Genotype additional info (OPTIONAL)	Blood group genotyping	N/A	N/A
	HLA tissue typing	N/A	N/A

Table 2
Reagents details.

Antibodies used for immunocytochemistry			
	Antibody	Dilution	Company Cat # and RRID
Pluripotency Markers	Mouse anti-OCT4	1:200	Millipore Cat# MAB4401, RRID:AB_2167852
	PE-conjugated mouse anti-human NANOG	1:200	BD Biosciences Cat# 560483, RRID:AB_1645522
	Mouse anti-TRA-1-81	1:200	Thermo Fisher Scientific Cat# 41-1100, RRID:AB_2533495
	PE-conjugated mouse anti-SSEA4	1:200	Thermo Fisher Scientific Cat# A14766, RRID:AB_2534281
Sendai	Chicken anti-Sendai virus	1:1000	Abcam Cat# ab33988, RRID:AB_777877
Differentiation Markers	Mouse anti-AFP	1:200	Sigma-Aldrich Cat# A8452, RRID:AB_258392
	Mouse anti-SMA	1:200	Sigma-Aldrich Cat# A2547, RRID:AB_476701
	Mouse anti-beta-III tubulin	1:200	Sigma-Aldrich Cat# T8660, RRID:AB_477590
Secondary antibodies	Donkey anti-mouse Alexa Fluor® 488	1:400	Molecular Probes Cat# A-21202, RRID:AB_141607
	Donkey anti-chicken Alexa Fluor® 488	1:400	Jackson ImmunoResearch Labs Cat# 703-545-155, RRID:AB_2340375
	Donkey anti-mouse Alexa Fluor® 555	1:400	Thermo Fisher Scientific Cat# A-31570, RRID:AB_2536180

Acknowledgements

We thank AnnaKarin Oldén and Marianne Juhlin, for their technical support. We are also thankful to the 'Cell Line and DNA Biobank from Patients affected by Genetic Diseases' (Istituto G. Gaslini, Genova, Italy) and the 'Parkinson Institute Biobank, members of the Telethon Network of Genetic Biobanks (http://biobanknetwork.telethon.it; project no. GTB12001) funded by Telethon Italy, for providing fibroblasts samples. This work was supported by the Strategic Research Environment MultiPark at Lund University, the strong research environment BAGADILICO (349-2007-8626), the Swedish Parkinson Foundation (Parkinsonfonden; grant 899/16), the Swedish Research Council (grant 2015-03684 to LR), Finnish Cultural Foundation (grant 00161167 to YP) and the Portuguese Foundation for Science and Technology for the doctoral fellowship - PDE/BDE/113598/2015 to AM.

Appendix A. Supplementary data

Supplementary data to this article can be found online at https://doi.org/10.1016/j.scr.2018.01.002.

References

Braak, H., Del Tredici, K., 2009. Neuroanatomy and pathology of sporadic Parkinson's disease. Adv. Anat. Embryol. Cell Biol. 201, 1–119.

Holmqvist, S., Lehtonen, S., Chumarina, M., Puttonen, K.A., Azevedo, C., Lebedeva, O., Ruponen, M., Oksanen, M., Djelloul, M., Collin, A., et al., 2016. Creation of a library of induced pluripotent stem cells from parkinsonian patients. NPJ Parkinsons Dis 2, 16009.

ANNEX II

Stem Cell Research 27 (2018) 82–85

Contents lists available at ScienceDirect

Stem Cell Research

journal homepage: www.elsevier.com/locate/scr

Lab resource: Stem Cell Line

Generation of an integration-free induced pluripotent stem cell line (CSC-43) from a patient with sporadic Parkinson's disease

Ana Marote [a,b], Yuriy Pomeshchik [c,d,e], Stefano Goldwurm [f], Anna Collin [g], Nuno J. Lamas [a,b,i], Luísa Pinto [a,b,h], António J. Salgado [a,b], Laurent Roybon [c,d,e,*]

[a] Life and Health Sciences Research Institute (ICVS), School of Medicine, University of Minho, Braga, Portugal
[b] ICVS/3B's, PT Government Associate Laboratory, Braga/Guimarães, Portugal
[c] Stem Cell Laboratory for CNS Disease Modeling, Wallenberg Neuroscience Center, Department of Experimental Medical Science, BMC A10, Lund University, Lund, Sweden
[d] Strategic Research Area MultiPark, Lund University, Lund, Sweden
[e] Lund Stem Cell Center, Lund University, Lund, Sweden
[f] Parkinson Institute, ASST PINI-CTO, Milan, Italy
[g] Department of Clinical Genetics and Pathology, Office for Medical Services, Division of Laboratory Medicine, Lund, Sweden
[h] BnML, Behavioral and Molecular Lab, Braga, Portugal
[i] Anatomic Pathology Department, Braga Hospital, Braga, Portugal

ARTICLE INFO

Article history:
Received 15 October 2017
Received in revised form 13 December 2017
Accepted 3 January 2018
Available online 4 January 2018

ABSTRACT

An induced pluripotent stem cell (iPSC) line was generated from a 36-year-old patient with sporadic Parkinson's disease (PD). Skin fibroblasts were reprogrammed using the non-integrating Sendai virus technology to deliver OCT3/4, SOX2, c-MYC and KLF4 factors. The generated cell line (CSC-43) exhibits expression of common pluripotency markers, *in vitro* differentiation into three germ layers and normal karyotype. This iPSC line can be used to study the mechanisms underlying the development of PD.

Resource table

Unique stem cell line identifier	ULUNDi005-A
Alternative name(s) of stem cell line	CSC-43 J
Institution	Stem Cell Laboratory for CNS Disease Modeling, Department of Experimental Medical Science, Lund University
Contact information of distributor	Laurent Roybon, Laurent.Roybon@med.lu.se
Type of cell line	iPSC
Origin	Human
Additional origin info	Age of patient at onset: 31 Sex of patient: male Ethnicity: N/A
Cell Source	Skin fibroblasts
Clonality	Clonal
Method of reprogramming	Sendai virus mediated delivery of OCT3/4, SOX2, c-MYC and KLF4
Genetic Modification	No modification
Type of Modification	No modification
Associated disease	Parkinson's disease
Gene/locus	N/A
Method of modification	No modification
Name of transgene or resistance	No transgene or resistance
Inducible/constitutive system	Not inducible
Date archived/stock date	N/A
Cell line repository/bank	N/A
Ethical approval	Parkinson Institute Biobank (part of the Telethon Genetic Biobank Network http://biobanknetwork.telethon.it/): approved by Ethics Committee "Milano Area C" (http://comitatoeticoareac.ospedaleniguarda.it/) on the 26/06/2015, Numero Registro dei pareri: 370–062015. Reprogramming: 202,100–3211 (delivered by Swedish work environment Arbetsmiljöverket).

Resource utility

This iPSC line can be used to explore the development of sporadic Parkinson's disease *in vitro*.

* Corresponding author.
E-mail address: laurent.roybon@med.lu.se (L. Roybon).

https://doi.org/10.1016/j.scr.2018.01.007

Resource details

Dopaminergic neurons obtained from the differentiation of sporadic Parkinson's disease (PD) patient derived - induced pluripotent stem cells (iPSCs) have been shown to express a pathogenic phenotype, including morphological alterations and accumulation of autophagic vacuoles (Sánchez-Danés et al., 2012). Here we report the generation of an induced pluripotent stem cell line (CSC-43) from a patient with early-onset PD with no identified genetic cause, which can be used to understand the molecular basis of this neurodegenerative disease.

To generate CSC-43 iPSC line, skin fibroblasts collected by punch skin biopsy from a 36-year-old PD patient were reprogrammed using a non-integrating Sendai virus technology. Briefly, fibroblasts were seeded (75,000 cells/well) on a 12-well plate, two days before transduction. The CytoTune™-iPS 2.0 Sendai Reprogramming Kit was then used to deliver the four reprogramming factors, OCT3/4, SOX2, c-MYC and KLF4. At day 7 post-transduction, the cells were re-seeded onto mouse embryonic fibroblasts (MEF)-feeder layer and expanded until colonies presented an embryonic stem cell (ES)-like morphology. At day 28, 12 colonies were picked and expanded as individual clones for 7 days.

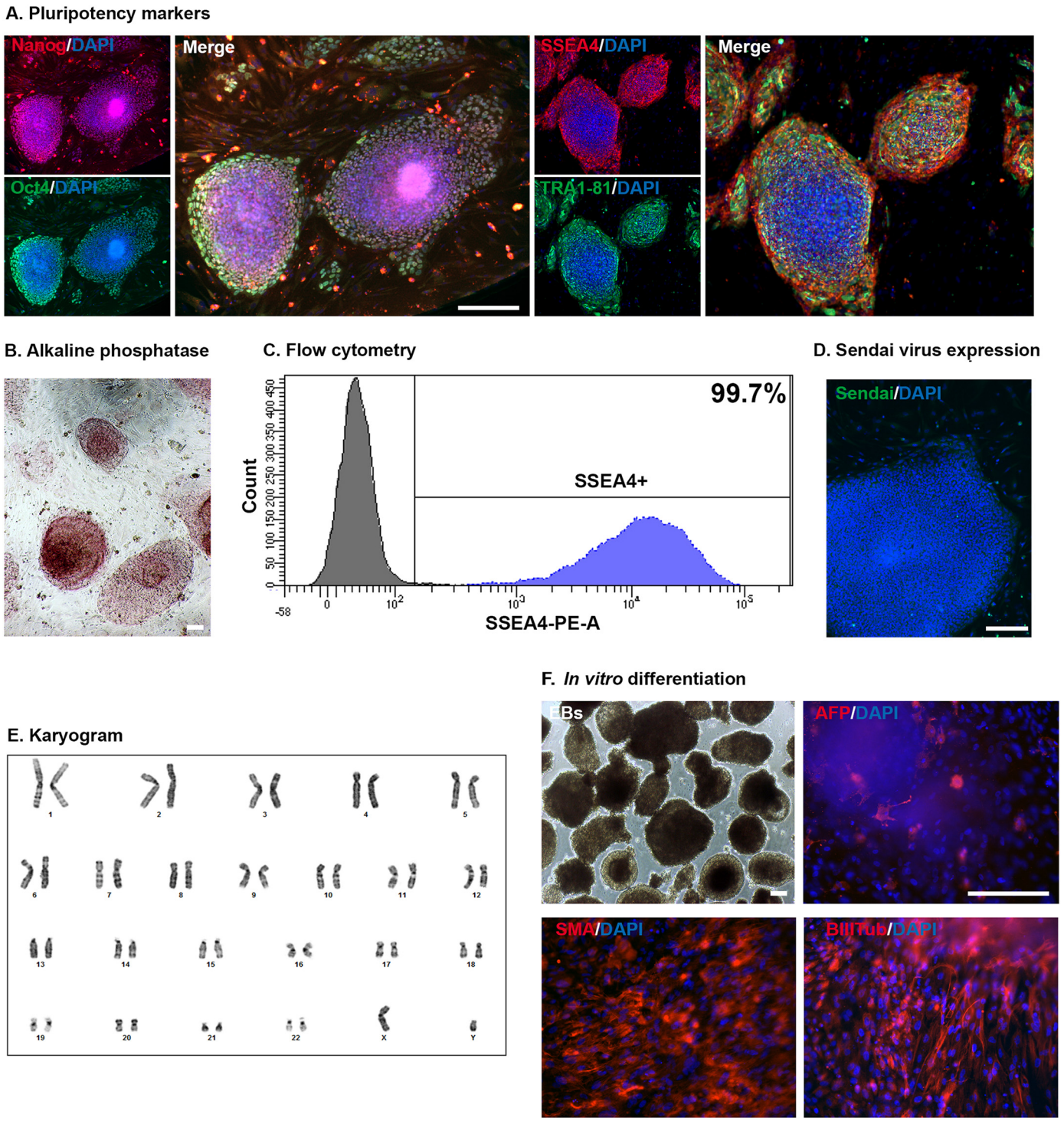

Fig. 1. Characterization of the iPSC line CSC 43J.

Three clones (CSC-43D, CSC-43I and CSC-43J) were further selected for expansion and karyotype analysis. All clones were characterized using the methods we previously described (Holmqvist et al., 2016). We report, herein the characterization of clone CSC-43J.

The generated clone, CSC-43J, expressed the common nuclear and cell surface pluripotency markers, OCT4/Nanog and TRA1-81/SSEA4 (Fig. 1A) and showed alkaline phosphatase (ALP) activity (Fig.1B). Flow cytometry analysis showed >99% of the iPSCs positive for SSEA4 (Fig. 1C; non-stained iPSCs are shown in grey). Additional immunocytochemistry analysis revealed elimination of the Sendai virus at passage 8 (Fig. 1D). Fig. 1E depicts a normal male karyogram identified in CSC-43J clone. Embryoid bodies (EBs) generated from CSC-43J iPSC present three-germ layer differentiation capacity as shown by the *in vitro* expression of alpha-fetoprotein (AFP), an endodermal marker, smooth muscle actin (SMA), a mesodermal marker, and beta-III tubulin (BIIITub), an ectodermal marker (Fig. 1F). The identity of the generated iPSC line was confirmed by DNA fingerprint, showing genetic correspondence to parental fibroblasts. Mycoplasma infection was prevented by routine addition of plasmocin in cell culture media, at early passages.

Materials and methods

Fibroblast culture

Dermal fibroblasts were collected by punch skin biopsy from a patient diagnosed with PD, after obtaining informed consent. The fibroblasts were maintained in fibroblast growth medium, composed of DMEM media (ThermoFisher Scientific) with 10% fetal bovine serum and 1% Penicillin-Streptomycin and passaged with 0.05% trypsin.

iPSC generation and expansion

For reprogramming, 75,000 cells were seeded on a 12-well plate and maintained in fibroblast growth medium. Two days after (day 0), the cells were transduced using the three vector preparations (MOI = 5, 5, 3) included in the CytoTune™-iPS 2.0 Sendai Reprogramming Kit (ThermoFisher Scientific). On the following day and on every other day, the medium was replaced with fresh fibroblast growth medium. At day 7, the cells were re-seeded onto irradiated mouse embryonic fibroblasts (MEFs) feeder cells with fibroblast growth medium. On the day after and until colony picking, the cells were cultured in WiCell medium composed of advanced DMEM/F12 (ThermoFisher Scientific), 20% Knock-Out Serum Replacement (v/v, ThermoFisher Scientific), 2 mM L-glutamine (ThermoFisher Scientific), 1% non-essential amino acids (NEAA, v/v, Millipore) and 0.1 mM β-mercaptoethanol, supplemented with 20 ng/ml FGF2 (ThermoFisher Scientific). On day 28, individual colonies were picked and re-seeded on a 24-well plate containing fresh MEFs. One week after, three clones were selected and further expanded on 6-well plates. The cells were passaged once a week and seeded on the appropriate cell culture surface for characterization assays at the indicated passage numbers (Table 1).

Immunocytochemistry

The iPSCs cultures were fixed with 4% paraformaldehyde for 15 min at room temperature (RT), permeabilized and blocked for 1 h at RT with PBS containing 10% donkey serum and 0.1% TritonX-100 (Sigma) and incubated overnight at + 4 °C with the primary antibodies (Table 2) diluted in the blocking buffer. The secondary antibodies were thereafter added for 1 h at RT in the dark, followed by nuclei counterstain with DAPI (1:10,000 (Life Technologies)) and image acquisition on inverted epifluorescence microscope LRI - Olympus IX-73. Scale bars are 200μm.

Alkaline phosphatase activity

Alkaline phosphatase staining was performed using Alkaline Phosphatase Staining Kit (Stemgent, MA).

In vitro differentiation by embryoid body (EB) formation

Human iPSC were grown for 2 weeks as embryoid bodies (EBs) in low-attachment 24-well plates (Corning) in WiCell medium supplemented with 20 ng/ml FGF2. The EBs were then seeded on a 0.1% gelatin-coated 96-well plate (Greiner Bio-One) in DMEM media containing 10% fetal bovine serum and 1% Penicillin-Streptomycin for subsequent spontaneous differentiation, with media changes every 2–3 days. After 2 weeks, the cells were fixed and stained for three germ-layer markers as described in Table 2.

Karyotype analysis

The G-banding analysis was performed at 300–400 band resolution in average after 11 passages, at the Department of Clinical Genetics and Pathology in Lund.

DNA fingerprinting

Genomic DNA from fibroblasts and hiPSCs was extracted using conventional lysis buffer composed of 100 mM Tris (pH 8.0), 200 mM NaCl, 5 mM EDTA and 0.2% SDS in distilled autoclaved water supplemented

Table 1
Characterization and validation.

Classification	Test	Result	Data
Morphology	Photography	Visual record of the line: Normal	Not shown but available with the author
Phenotype	Immunocytochemisty	Positive staining for pluripotency markers: OCT4, NANOG, TRA1-81 and SSEA4	Fig. 1 panel A
	Alkaline phosphatase activity	Visible activity	Fig. 1 panel B
	Flow cytometry	99.7% SSEA4	Fig. 1 panel C
Genotype	Karyotype (G-banding) and resolution	46,XY (300–400 bands resolution in average)	Fig. 1 panel E
Identity	STR analysis	10 sites analyzed, all matched with parent fibroblast cell line	Available with the author
Mutation analysis (if applicable)	N/A	N/A	N/A
Microbiology and virology	Mycoplasma	Mycoplasma testing by RT-PCR. Negative.	Not shown but available with author
Differentiation potential	Embryoid body formation	Staining of smooth muscle actin, beta-III-tubulin and alpha-fetoprotein after spontaneous differentiation of embryoid bodies	Fig. 1 panel F
Donor screening (optional)	HIV 1 + 2 Hepatitis B, Hepatitis C	N/A	N/A
Genotype additional info (optional)	Blood group genotyping	N/A	N/A
	HLA tissue typing	N/A	N/A

Table 2
Reagents details.

Antibodies used for immunocytochemistry			
	Antibody	Dilution	Company Cat # and RRID
Pluripotency markers	Mouse anti-Oct4	1:200	Millipore Cat# MAB4401, RRID:AB_2167852
	PE-conjugated mouse anti-human Nanog	1:200	BD Biosciences Cat# 560483, RRID:AB_1645522
	Mouse anti- TRA-1-81	1:200	Thermo Fisher Scientific Cat# 41-1100, RRID:AB_2533495
	PE-conjugated mouse anti-SSEA4	1:200	Thermo Fisher Scientific Cat# A14766, RRID:AB_2534281
Sendai	Chicken anti-Sendai virus	1:1000	Abcam Cat# ab33988, RRID:AB_777877
Differentiation Markers	Mouse anti-AFP	1:200	Sigma-Aldrich Cat# A8452, RRID:AB_258392
	Mouse anti-SMA	1:200	Sigma-Aldrich Cat# A2547, RRID:AB_476701
	Mouse anti-BIII tubulin	1:200	Sigma-Aldrich Cat# T8660, RRID:AB_477590
Secondary antibodies	Donkey anti-mouse Alexa Fluor® 488	1:400	Molecular Probes Cat# A-21202, RRID:AB_141607
	Donkey anti-chicken Alexa Fluor® 488	1:400	Jackson ImmunoResearch Labs Cat# 703-545-155, RRID:AB_2340375
	Donkey anti-mouse Alexa Fluor® 555	1:400	Thermo Fisher Scientific Cat# A-31570, RRID:AB_2536180

with 1.5 mg/ml Proteinase K. Fingerprinting analyses were outsourced to the IdentiCell STR profiling service (Department of Molecular Medicine, Aarhus University Hospital, Skejby, Denmark).

Mycoplasma detection

Absence of mycoplasma contamination was confirmed by the real-time PCR method at GATC Biotech AG (European Genome and Diagnostics Centre, Konstanz, Germany).

Acknowledgements

We are greatly thankful to AnnaKarin Oldén and Marianne Juhlin, for their technical assistance and to the 'Cell Line and DNA Biobank from Patients affected by Genetic Diseases' (Istituto G. Gaslini, Genova, Italy) and the Parkinson Institute Biobank, members of the Telethon Network of Genetic Biobanks (http://biobanknetwork.telethon.it; project no. GTB12001) funded by Telethon Italy, for providing fibroblasts samples. This work was supported by the Strategic Research Environment MultiPark at Lund University, the strong research environment BAGADILICO (grant 349-2007-8626), the Swedish Parkinson Foundation (Parkinsonfonden, grant 889/16), the Swedish Research Council (grant 2015-03684 to LR) and Finnish Cultural Foundation (grant 00161167 to YP). We also acknowledge the Portuguese Foundation for Science and Technology for the doctoral fellowship - PDE/BDE/113598/2015 to AM and IF Starting and Development Grants to LP and AJS (IF/00111/2013 and IF/01079/2014), respectively.

Appendix A. Supplementary data

Supplementary data to this article can be found online at https://doi.org/10.1016/j.scr.2018.01.007.

References

Holmqvist, S., Lehtonen, S., Chumarina, M., Puttonen, K.A., Azevedo, C., Lebedeva, O., Ruponen, M., Oksanen, M., Djelloul, M., Collin, A., et al., 2016. Creation of a library of induced pluripotent stem cells from Parkinsonian patients. NPJ Parkinsons Dis. 2 (16009).

Sánchez-Danés, A., Richaud-Patin, Y., Carballo-Carbajal, I., Jiménez-Delgado, S., Caig, C., Mora, S., Di Guglielmo, C., Ezquerra, M., Patel, B., Giralt, A., Canals, J.M., Memo, M., Alberch, J., López-Barneo, J., Vila, M., Cuervo, A.M., Tolosa, E., Consiglio, A., Raya, A., 2012. Disease-specific phenotypes in dopamine neurons from human iPS-based models of genetic and sporadic Parkinson's disease. EMBO Mol. Med. 4, 380–395.

ANNEX III

Stem Cell Research 27 (2018) 61–64

Contents lists available at ScienceDirect

Stem Cell Research

journal homepage: www.elsevier.com/locate/scr

Lab Resource: Stem Cell Line

Generation of a human induced pluripotent stem cell line (CSC-40) from a Parkinson's disease patient with a *PINK1* p.Q456X mutation

Kaspar Russ [a,b,c], Ana Marote [d,e], Ekaterina Savchenko [a,b,c], Anna Collin [f], Stefano Goldwurm [g], Yuriy Pomeshchik [a,b,c], Laurent Roybon [a,b,c,*]

[a] Stem Cell Laboratory for CNS Disease Modeling, Wallenberg Neuroscience Center, Department of Experimental Medical Science, BMC A10, Lund University, Lund, Sweden
[b] Strategic Research Area MultiPark, Lund University, Lund, Sweden
[c] Lund Stem Cell Center, Lund University, Lund, Sweden
[d] Life and Health Sciences Research Institute (ICVS), School of Health Sciences, University of Minho, Braga, Portugal
[e] ICVS/3B's, PT Government Associate Laboratory, Braga, Guimarães, Portugal
[f] Department of Clinical Genetics and Pathology, Office for Medical Services, Division of Laboratory Medicine, Lund, Sweden
[g] Parkinson Institute, ASST PINI-CTO, Milan, Italy

ARTICLE INFO

Article history:
Received 15 October 2017
Received in revised form 13 December 2017
Accepted 3 January 2018
Available online 4 January 2018

ABSTRACT

Parkinson's disease (PD) is a neurodegenerative disease with unknown etiology. Here we show the generation of an induced pluripotent stem cell (iPSC) line, named CSC-40, from dermal fibroblasts obtained from a 59-year-old male patient with a homozygous p.Q456X mutation in the PTEN-induced putative kinase 1 *(PINK/PARK6)* gene and a confirmed diagnosis of PD, which could be used to model familial PD. A non-integrating Sendai virus-based delivery of the reprogramming factors OCT3/4, SOX2, c-MYC and KLF4 was employed. The CSC-40 cell line showed normal karyotyping and fingerprinting following transduction as well as sustained expression of several pluripotency markers and the ability to differentiate into all three germ layers.

Resource table

Unique stem cell line identifier	ULUNDi001-A
Alternative name(s) of stem cell line	CSC-40F
Institution	Stem Cell Laboratory for CNS Disease Modeling, Department of Experimental Medical Science, Lund University
Contact information of distributor	Laurent Roybon; Laurent.Roybon@med.lu.se
Type of cell line	iPSC
Origin	Human
Additional origin info	Age of patient at onset: 36 Sex of patient: male Ethnicity: N/A
Cell Source	Skin fibroblasts
Clonality	Clonal
Method of reprogramming	Sendai virus transduction with OCT3/4, SOX2, c-MYC, and KLF4
Genetic Modification	No modification
Type of Modification	No modification
Associated disease	Parkinson's disease
Gene/locus	*PINK1* (MIM # 608309) located on the chromosome 1p36.12 Genotype: c.1366C–T transition in exon 7 (p.Q456X substitution)
Method of modification	No modification
Name of transgene or resistance	No transgene or resistance
Inducible/constitutive system	Not inducible
Date archived/stock date	N/A
Cell line repository/bank	N/A
Ethical approval	Parkinson Institute Biobank (part of the Telethon Genetic Biobank Network http://biobanknetwork.telethon.it/): approved by Ethics Committee "Milano Area C" (http://comitatoeticoareac.ospedaleniguarda.it/) on the 26/06/2015, Numero Registro dei pareri: 370–062015. Reprogramming: 202,100–3211 (delivered by Swedish work environment Arbetsmiljöverket).

Resource utility

The mutation in the *PINK1* gene, encoding the phosphatase and tensin homolog (PTEN)-induced kinase 1 (PINK1) protein, was

* Corresponding author.
E-mail address: laurent.roybon@med.lu.se (L. Roybon).

https://doi.org/10.1016/j.scr.2018.01.001

identified in early-onset recessive Parkinson's disease (PD) in 2001 (Valente et al., 2001). The CSC-40 induced pluripotent stem cell (iPSC) line, with a mutation in the *PINK1* gene, allows investigations of familial PD cells for disease modeling and potential therapeutic explorations.

Resource details

The PINK1 protein together with PARKIN can initiate the ubiquitination and removal of the damaged mitochondrion (Geisler et al., 2010). Mutation in *PINK1* is linked to early-onset recessive PD

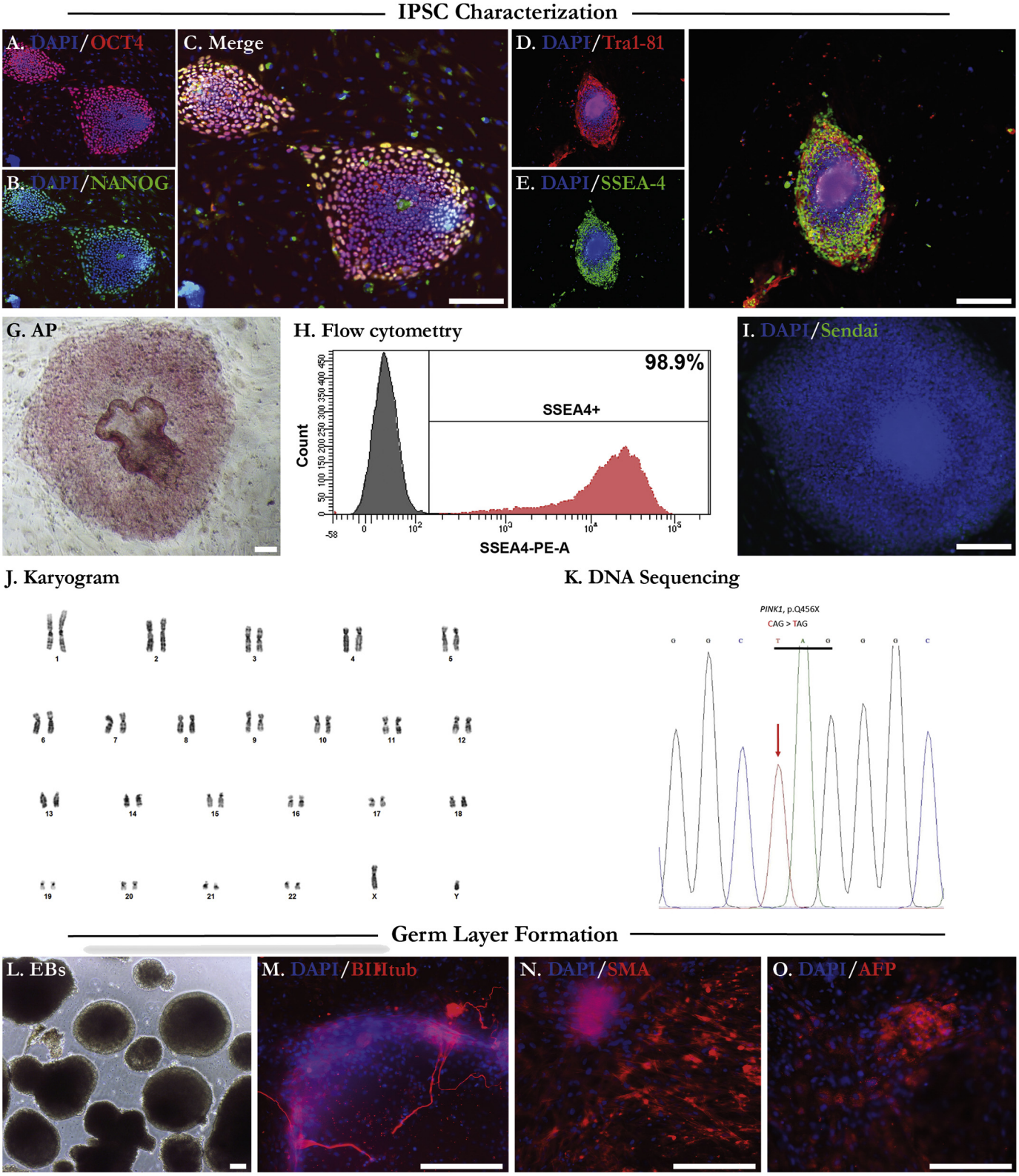

Fig. 1. Characterization of the iPSC line CSC-40F.

(Valente et al., 2001). Here we report the generation of a novel iPSC line, named CSC-40, from dermal fibroblasts obtained from a 59-year-old male PD patient with a homozygous p.Q456X mutation in *PINK1*.

Reprograming of patient fibroblasts was done using non-integration Sendai virus to deliver the reprograming factors OCT3/4, SOX2, c-MYC and KLF4 to the cells. Three clones (CSC-40F, CSC-40I and CSC-40G) were selected based on the morphology of the colonies, and characterized as previously described (Holmqvist et al., 2016). Here, we report the characterization of the clone CSC-40F.

The generated CSC-40F line stained positive for the common nuclear and cell surface pluripotency markers, OCT4, NANOG, TRA1-81 and SSEA4 (Fig. 1A–F). Flow cytometry analysis showed that >98% of the iPSCs were positive for SSEA4 (Fig. 1H; non-stained iPSCs are shown in grey). An alkaline phosphatase staining further confirmed the pluripotency of CSC-40F iPSC line (Fig. 1G). The CSC-40F line was clear of Sendai virus by passage 7 (Fig. 1I) and showed normal karyotyping (Fig. 1J). Genetic integrity was confirmed by fingerprint analysis of isolated DNA from both patient fibroblasts and CSC-40F iPSC line, while the presence of the homozygous p.Q456X mutation was detected by DNA sequencing (Fig. 1K). Finally, CSC-40F iPSC line was cultured as embryoid bodies (EBs) and then plated onto a 96-well plate to demonstrate its ability to differentiate into each of the three germ layers, in vitro. Immunocytochemistry revealed the expression of ectodermal marker beta-III-tubulin (BIIItub), the mesodermal marker smooth muscle actin (SMA), and the endodermal marker alpha-fetoprotein (AFP; Fig. 1L–O). Plasmocin was used during the reprogramming and early passages as prophylactic dose to prevent Mycoplasma (Table 1).

Materials and methods

Collection and reprogramming of patient's fibroblasts

Induced PSCs were generated from human dermal fibroblasts, harvested using a skin punch biopsy, from patient with a confirmed clinical diagnosis of PD. Patient fibroblasts were cultured and expanded in Dulbecco's modified eagle's medium (DMEM) supplemented with 10% fetal bovine serum and 1% Penicillin-Streptomycin (v/v, all ThermoFisher Scientific) at 37 °C and 5% CO_2 for several passages before being cryopreserved and stored at −150 °C.

For reprogramming, fibroblasts were thawed and plated on a 0.1% gelatin-coated 12-well plate at a concentration of 75,000 per well. Two days after, the cells were transduced with OCT3/4, SOX2, c-MYC and KLF4 reprogramming factors using CytoTune™-iPS 2.0 Sendai reprogramming kit according to manufacturer's instructions (ThermoFisher Scientific). Fibroblast growth media was changed every other day for 7 days following transduction. At day 7, the fibroblasts were passaged using 0.05% trypsin-EDTA (Sigma-Aldrich) and plated onto irradiated mouse embryonic fibroblasts feeder cells (CF-1 MEF, GlobalStem) with WiCell media composed of advanced DMEM/F12 (Thermo Fisher Scientific), 20% Knock-Out Serum Replacement (v/v, ThermoFisher Scientific), 2 mM L-glutamine (Thermo Fisher Scientific), 1% non-essential amino acids (NEAA, v/v, Millipore), 0.1 mM β-mercaptoethanol (Sigma-Aldrich) and 20 ng/ml FGF2 (ThermoFisher Scientific). At day 28, single colonies were manually picked and re-seeded separately onto a fibroblast feeder cell-coated 12-well plate. Individual clones were passaged using dispase (ThermoFisher Scientific) weekly with media changed daily. Cells were then frozen in WiCell media and freezing media (20% DMSO + FBS 80%) 1:1 with 10 μM Rock inhibitor (Sigma-Aldrich) and stored at −150 °C.

Alkaline phosphatase activity

Alkaline phosphatase staining was completed using the Alkaline Phosphatase Staining Kit according to manufacturer's protocol (Stemgent, MA).

Karyotyping

The G-banding analysis was performed at 300–400 band resolution in average after 14 passages at the Department of Clinical Genetics and Pathology in Lund.

Mutation sequencing and fingerprint analysis

The mutation p.Q456X in *PINK1*, was confirmed by direct DNA sequencing (Macrogen Europe, Amsterdam, The Netherlands) following DNA isolation using a lysis buffer (100 mM Tris (pH 8.0), 200 mM NaCl, 5 mM EDTA, and 0.2% SDS in distilled and autoclaved water supplemented with 1.5 mg/ml Proteinase K). Primers used for amplification and directed sequencing of *PINK* around the mutation site are listed in the Table 2. To confirm the genetic integrity of the DNA between patient fibroblasts and iPSCs, DNA was isolated and sent to IdentiCell STR profiling service (Department of Molecular Medicine, Aarhus University Hospital, Denmark).

In vitro differentiation

For spontaneous differentiation, iPSCs were grown as EBs for 2 weeks on ultra low-attachment 24-well plates (Corning) with WiCell media. At the end of 2 weeks, EBs were dissociated and plated onto adherent 96-well plates (Greiner Bio-One) coated with 0.1% gelatin (Millipore) in DMEM supplemented with 10% fetal bovine serum and

Table 1
Characterization and validation.

Classification	Test	Result	Data
Morphology	Photography	Visual record of the line: normal	Not shown but available with author
Phenotype	Immunocytochemistry	Positive staining for pluripotency markers OCT4, NANOG, TRA1–81, SSEA4.	Fig. 1 panel A-F
	Flow cytometry	98.9% SSEA4	Fig. 1 panel H
	Alkaline phosphatase activity	Visible activity	Fig. 1 panel G
Genotype	Karyotype (G-banding) and resolution	46,XY, (300–400 bands resolution in average)	Fig. 1 panel J
Identity	STR analysis	10 sites analyzed, all matched with fibroblasts from the original donor	Available with author
Mutation analysis	Sequencing	homozygous p.Q456X mutation in *PINK1*	Fig. 1 panel K
Microbiology and virology	Mycoplasma	Mycoplasma testing by RT-PCR. Negative.	Not shown but available with author
Differentiation potential	Embryoid body formation	Positive staining for smooth muscle actin, beta-III-tubulin and alpha-fetoprotein after spontaneous differentiation of embryoid bodies	Fig. 1 panel L-O
Donor screening (OPTIONAL)	HIV 1 + 2 Hepatitis B, Hepatitis C	N/A	N/A
Genotype additional info (OPTIONAL)	Blood group genotyping	N/A	N/A
	HLA tissue typing	N/A	N/A

Table 2
Reagents details.

Antibodies used for immunocytochemistry			
	Antibody	Dilution	Company Cat # and RRID
Pluripotency Markers	Mouse anti-OCT4	1:200	Millipore Cat# MAB4401, RRID:AB_2167852
	PE-conjugated mouse anti-human NANOG	1:200	BD Biosciences Cat# 560483, RRID:AB_1645522
	Mouse anti- TRA-1-81	1:200	Thermo Fisher Scientific Cat# 41–1100, RRID:AB_2533495
	PE-conjugated mouse anti-SSEA4	1:200	Thermo Fisher Scientific Cat# A14766, RRID:AB_2534281
Sendai	Chicken anti-Sendai virus	1:1000	Abcam Cat# ab33988, RRID:AB_777877
Differentiation Markers	Mouse anti-AFP	1:200	Sigma-Aldrich Cat# A8452, RRID:AB_258392
	Mouse anti-SMA	1:200	Sigma-Aldrich Cat# A2547, RRID:AB_476701
	Mouse anti-beta-III tubulin	1:200	Sigma-Aldrich Cat# T8660, RRID:AB_477590
Secondary antibodies	Donkey anti-mouse Alexa Fluor® 488	1:400	Molecular Probes Cat# A-21202, RRID:AB_141607
	Donkey anti-chicken Alexa Fluor® 488	1:400	Jackson ImmunoResearch Labs Cat# 703-545-155, RRID:AB_2340375
	Donkey anti-mouse Alexa Fluor® 555	1:400	Thermo Fisher Scientific Cat# A-31570, RRID:AB_2536180

Primers		
	Target	Forward/Reverse primer (5′–3′)
Mutation sequencing	*PINK1*	TGGATCAGGTGATGTGCAGGA/ AGGATCTGTCACTGTGGCTCT

1% Penicillin-Streptomycin. iPSCs were cultured for 2 additional weeks with media changed every 2 days before being stained with antibodies against BIIItub, SMA, and AFP.

Immunocytochemistry

For immunocytochemical analysis, iPSCs were fixed with 4% PFA for 10 min at RT followed by standard immunocytochemical procedures. Blocking was done in 10% donkey serum in PBS with 0.1% Triton-X100 (Sigma-Aldrich) for 1 h at RT. Primary antibodies, listed in the Table 2, were then added to the cells and incubated overnight at 4 °C. Next the secondary antibodies, listed in the Table 2, were added and incubated for 1 h at RT in the dark. Additionally, nuclei were stained by DAPI (1:10,000; Life Technologies). All fluorescent photomicrographs were taken using an inverted epifluorescence microscope (LRI - Olympus IX-73). Scale bars are 200μm.

Mycoplasma detection

Absence of mycoplasma contamination was confirmed by the real-time PCR method at GATC Biotech AG (European Genome and Diagnostics Centre, Konstanz, Germany).

Acknowledgements

We thank AnnaKarin Oldén and Marianne Juhlin, for their technical support. We are also thankful to the 'Cell Line and DNA Biobank from Patients affected by Genetic Diseases' (Istituto G. Gaslini, Genova, Italy) and the Parkinson Institute Biobank, members of the Telethon Network of Genetic Biobanks (http://biobanknetwork.telethon.it; project no. GTB12001) funded by Telethon Italy, for providing fibroblasts samples. This work was supported by the Strategic Research Environment MultiPark at Lund University, and the strong research environment BAGADILICO (grant 349-2007-8626), the Swedish Parkinson Foundation (Parkinsonoden; grant 889/16), the Swedish Research Council (grant 2015-03684 to LR), Finnish Cultural Foundation (grant 00161167 to YP) and the Portuguese Foundation for Science and Technology for the doctoral fellowship - PDE/BDE/113598/2015 to AM.

Appendix A. Supplementary data

Supplementary data to this article can be found online at https://doi.org/10.1016/j.scr.2018.01.001.

References

Geisler, S., Holmström, K.M., Skujat, D., Fiesel, F.C., Rothfuss, O.C., Kahle, P.J., Springer, W., 2010. PINK1/Parkin-mediated mitophagy is dependent on VDAC1 and p62/SQSTM1. Nat. Cell Biol. 12, 119–131.

Holmqvist, S., Lehtonen, S., Chumarina, M., Puttonen, K.A., Azevedo, C., Lebedeva, O., Ruponen, M., Oksanen, M., Djelloul, M., Collin, A., et al., 2016. Creation of a library of induced pluripotent stem cells from Parkinsonian patients. NPJ Parkinsons Dis. 2 (16009).

Valente, E.M., Bentivoglio, A.R., Dixon, P.H., Ferraris, A., Ialongo, T., Frontali, M., Albanese, A., Wood, N.W., 2001. Localization of a novel locus for autosomal recessive early-onset parkinsonism, PARK6, on human chromosome 1p35-p36. Am. J. Hum. Genet. 68, 895–900.

ANNEX IV

Stem Cell Research 28 (2018) 44–47

Contents lists available at ScienceDirect

Stem Cell Research

journal homepage: www.elsevier.com/locate/scr

Lab Resource: Stem Cell Line

Generation of an induced pluripotent stem cell line (CSC-41) from a Parkinson's disease patient carrying a p.G2019S mutation in the *LRRK2* gene

Ana Marote [a,b], Yuriy Pomeshchik [c,d,e], Anna Collin [f], Stefano Goldwurm [g], Nuno J. Lamas [a,b,i], Luísa Pinto [a,b,h], António J. Salgado [a,b], Laurent Roybon [c,d,e,*]

[a] Life and Health Sciences Research Institute (ICVS), School of Medicine, University of Minho, Braga, Portugal
[b] ICVS/3B's, PT Government Associate Laboratory, Braga, Guimarães, Portugal
[c] Stem Cell Laboratory for CNS Disease Modeling, Wallenberg Neuroscience Center, Department of Experimental Medical Science, BMC A10, Lund University, Lund, Sweden
[d] Strategic Research Area MultiPark, Lund University, Lund, Sweden
[e] Lund Stem Cell Center, Lund University, Lund, Sweden
[f] Department of Clinical Genetics and Pathology, Office for Medical Services, Division of Laboratory Medicine, Lund, Sweden
[g] Parkinson Institute, ASST PINI-CTO, Milan, Italy
[h] BnML, Behavioral and Molecular Laboratory, Braga, Portugal
[i] Anatomic Pathology Department, Braga Hospital, Braga, Portugal

ARTICLE INFO

Article history:
Received 15 October 2017
Received in revised form 3 January 2018
Accepted 18 January 2018
Available online 2 February 2018

ABSTRACT

The leucine-rich repeat kinase 2 (LRRK2) p.G2019S mutation is the most common genetic cause of Parkinson's disease (PD). An induced pluripotent stem cell (iPSC) line CSC-41 was generated from a 75-year old patient diagnosed with PD caused by a p.G2019S mutation in *LRRK2*. Skin fibroblasts were reprogrammed using a non-integrating Sendai virus-based technology to deliver OCT3/4, SOX2, c-MYC and KLF4 transcription factors. The generated iPSC line exhibits expression of common pluripotency markers, differentiates into the three germ layers and has a normal karyotype. The iPSC line can be used to explore the association between *LRRK2* mutation and PD.

Resource table

Unique stem cell line identifier	ULUNDi002-A
Alternative name(s) of stem cell line	CSC-41C
Institution	Stem Cell Laboratory for CNS Disease Modeling, Department of Experimental Medical Science, Lund University
Contact information of distributor	Laurent Roybon, Laurent.Roybon@med.lu.se
Type of cell line	iPSC
Origin	Human
Additional origin info	Age of patient: 75 Sex of patient: female Ethnicity: N/A
Cell source	Skin fibroblasts
Clonality	Clonal
Method of reprogramming	Sendai virus-mediated delivery of OCT3/4, SOX2, c-MYC and KLF4
Genetic modification	No modification
Type of modification	No modification
Associated disease	Parkinson's disease
Gene/locus	*LRRK2* (MIM # 607060) located on the chromosome 12q12 Genotype: c.6055G–A transition in exon 41 (p.G2019S substitution)
Method of modification	No modification
Name of transgene or resistance	No transgene or resistance
Inducible/constitutive system	Not inducible
Date archived/stock date	N/A
Cell line repository/bank	N/A
Ethical approval	Parkinson Institute Biobank (part of the Telethon Genetic Biobank Network http://biobanknetwork.telethon.it/): approved by Ethics Committee "Milano Area C" (http://comitatoeticoareac.ospedaleniguarda.it/) on the 26/06/2015, Numero Registro dei pareri: 370-062015. Reprogramming: 202100-3211 (delivered by Swedish work environment Arbetsmiljöverket).

* Corresponding author at: Stem Cell Laboratory for CNS Disease Modeling, Wallenberg Neuroscience Center, Department of Experimental Medical Science, BMC A10, Lund University, Lund, Sweden.
E-mail address: laurent.roybon@med.lu.se (L. Roybon).

http://dx.doi.org/10.1016/j.scr.2018.01.022

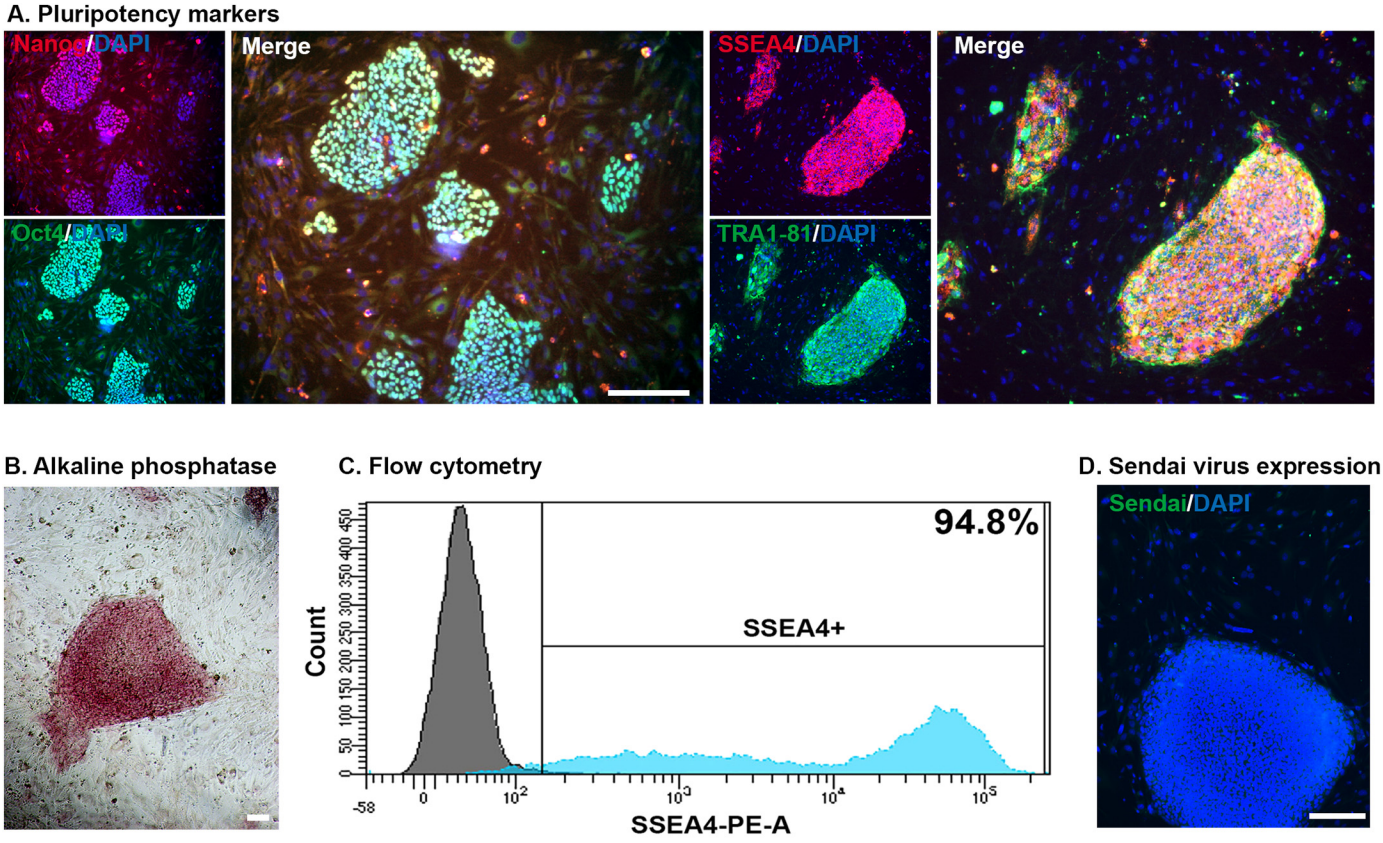

Fig. 1. Characterization of the iPSC line CSC 41C.

Resource utility

The *LRRK2* mutation p.G2019S is the most common genetic cause of Parkinson's disease (PD). The line CSC-41 was generated from a patient with PD carrying a p.G2019S mutation in *LRRK2* encoding for the leucine-rich repeated kinase 2 (LRRK2) protein. This induced pluripotent stem cell (iPSC) line can be used as a model to explore the link between mutant *LRRK2* and PD pathology.

Resource details

Mutations in *LRRK2* result in autosomal-dominant familial PD and have also been identified in sporadic PD cases with no family history of the disease. LRRK2 is encoded by the *LRRK2* gene, and is a protein with GTPase and kinase activity. The most frequent *LRRK2* mutation among PD patients, is a glycine-to-serine substitution at amino acid 2019 (p.G2019S) which causes increased kinase activity and has been reported to have implications in oxidative stress response and neuronal plasticity (Reinhardt et al., 2013). Here we report the generation of an induced pluripotent stem cell line (CSC-41) from a patient with PD carrying a p.G2019S *LRRK2* mutation. CSC-41 iPSC line can be used to better understand the molecular mechanisms underlying p.G2019S *LRRK2* associated PD.

To generate this line, skin fibroblasts collected by punch skin biopsy from a 75-year-old PD patient were reprogrammed using a non-integrating Sendai virus-based technology. Briefly, fibroblasts were seeded (75,000 cells/well) on a 12-well plate, two days before transduction. The CytoTune™-iPS 2.0 Sendai Reprogramming Kit was then used to deliver the four reprogramming factors (OCT3/4, SOX2, c-MYC and KLF4). At day 7 post-transduction, the cells were re-seeded onto irradiated mouse embryonic fibroblasts (MEF)-feeder layer and expanded until colonies presented an embryonic stem cell-like morphology. At day 28, 12 colonies were picked and expanded as individual clones for 7 days. Three clones (CSC-41C, CSC-41I, CSC-41K) were further selected, based on their morphology, for expansion and karyotype analysis. All clones were characterized using the methods we previously described (Holmqvist et al., 2016). Here, we present the characterization of clone CSC-41C.

Briefly, the generated clone, CSC-41C, expressed the common nuclear and cell surface pluripotency markers, OCT4/NANOG and TRA1-81/SSEA4 (Fig. 1A), and exhibited alkaline phosphatase (ALP) activity (Fig. 1B). According to flow cytometry analysis, >94% of the iPSCs were positive for SSEA4 (Fig. 1C; non-stained iPSCs are shown in grey). Additional immunocytochemistry analysis revealed elimination of the Sendai virus at passage 11 (Fig. 1D). Fig. 1E depicts a normal female karyogram of the CSC-41C clone. The identity of the generated iPSC line was confirmed by DNA fingerprint, showing genetic correspondence to parental fibroblasts. The mutation p.G2019S was confirmed by DNA sequencing (Fig. 1F). Embryoid bodies (EBs) generated from CSC-41C iPSCs differentiate into the three-germ layer, *in vitro*. Differentiated cells express endodermal marker alpha-fetoprotein (AFP), mesodermal marker smooth muscle actin (SMA), and ectodermal marker beta-III-tubulin (BIIITub) (Fig. 1G). During the generation of the iPSC clones, plasmocin was used to prevent Mycoplasma contamination.

Materials and methods

Fibroblast culture

Dermal fibroblasts were collected by punch skin biopsy from a patient diagnosed with PD, after obtaining informed consent. The fibroblasts were maintained in fibroblast growth medium, composed of DMEM media (ThermoFisher Scientific) with 10% fetal bovine serum and 1% Penicillin-Streptomycin and passaged with 0.05% trypsin.

iPSC generation and expansion

For reprogramming, 75,000 cells were seeded on a 12-well plate and maintained in fibroblast growth medium. Two days after (day 0), the cells were transduced using the three vector preparations (MOI = 5, 5, 3) included in the CytoTune™-iPS 2.0 Sendai Reprogramming Kit (ThermoFisher Scientific). On the following day and on every other day, the medium was replaced with fresh fibroblast growth medium. At day 7, the cells were re-seeded onto irradiated mouse embryonic fibroblasts (MEF) feeder cells with fibroblast growth medium. On the day after and until colony picking, the cells were cultured in WiCell medium composed of advanced DMEM/F12 (ThermoFisher Scientific), 20% Knock-Out Serum Replacement (v/v, ThermoFisher Scientific), 2 mM L-glutamine (Thermo Fisher Scientific), 1% non-essential amino acids (NEAA, v/v, Millipore) and 0.1 mM β-mercaptoethanol (Sigma-Aldrich), supplemented with 20 ng/ml FGF2 (ThermoFisher Scientific). On day 28, individual colonies were picked and re-seeded on a 24-well plate containing fresh MEFs. One week after, three clones were selected and further expanded on 6-well plates. The cells were passaged once a week and seeded on the appropriate cell culture surface for characterization assays at the indicated passage numbers (Table 1).

Immunocytochemistry

The iPSC cultures were fixed with 4% paraformaldehyde for 15 min at room temperature (RT), permeabilized and blocked for 1 h at RT with PBS containing 10% donkey serum and 0.1% TritonX-10 (Sigma)

Table 1
Characterization and validation.

Classification	Test	Result	Data
Morphology	Photography	Visual record of the line: Normal	Not shown but available with author
Phenotype	Immunocytochemistry	Positive staining for pluripotency markers: OCT4, NANOG, TRA1–81 and SSEA4	Fig. 1 panel A
	Alkaline phosphatase activity	Visible activity	Fig. 1 panel B
	Flow cytometry	98.7% SSEA4	Fig. 1 panel C
Genotype	Karyotype (G-banding) and resolution	46,XX, (300–400 bands resolution in average)	Fig. 1 panel E
Identity	STR analysis	10 sites analyzed, all matched with parent fibroblast cell line	Available with author
Mutation analysis (IF APPLICABLE)	Sequencing	Heterozygous p.G2019S mutation in *LRRK2*	Fig. 1 panel F
Microbiology and virology	Mycoplasma	Mycoplasma testing by RT-PCR. Negative.	Not shown but available with author
Differentiation potential	Embryoid body formation	Positive staining for smooth muscle actin, beta-III-tubulin and alpha-fetoprotein after spontaneous differentiation of embryoid bodies	Fig. 1 panel G
Donor screening (OPTIONAL)	HIV 1 + 2 Hepatitis B, Hepatitis C	N/A	N/A
Genotype additional info (OPTIONAL)	Blood group genotyping	N/A	N/A
	HLA tissue typing	N/A	N/A

Table 2
Reagents details.

Antibodies used for immunocytochemistry			
	Antibody	Dilution	Company Cat # and RRID
Pluripotency markers	Mouse anti-OCT4	1:200	Millipore Cat# MAB4401, RRID:AB_2167852
	PE-conjugated mouse anti-human Nanog	1:200	BD Biosciences Cat# 560483, RRID:AB_1645522
	Mouse anti-TRA-1-81	1:200	Thermo Fisher Scientific Cat# 41-1100, RRID:AB_2533495
	PE-conjugated mouse anti-SSEA4	1:200	Thermo Fisher Scientific Cat# A14766, RRID:AB_2534281
Sendai	Chicken anti-Sendai virus	1:1000	Abcam Cat# ab33988, RRID:AB_777877
Differentiation markers	Mouse anti-AFP	1:200	Sigma-Aldrich Cat# A8452, RRID:AB_258392
	Mouse anti-SMA	1:200	Sigma-Aldrich Cat# A2547, RRID:AB_476701
	Mouse anti-beta-III tubulin	1:200	Sigma-Aldrich Cat# T8660, RRID:AB_477590
Secondary antibodies	Donkey anti-mouse Alexa Fluor® 488	1:400	Molecular Probes Cat# A-21202, RRID:AB_141607
	Donkey anti-chicken Alexa Fluor® 488	1:400	Jackson ImmunoResearch Labs Cat# 703-545-155, RRID:AB_2340375
	Donkey anti-mouse Alexa Fluor® 555	1:400	Thermo Fisher Scientific Cat# A-31570, RRID:AB_2536180

Primers		
	Target	Forward/reverse primer (5′-3′)
Mutation sequencing	*LRRK2*	TTTTGATGCTTGACATAGTGGAC/CACATCTGAGGTCAGTGGTTATC

and incubated overnight at +4 °C with the primary antibodies (Table 2) diluted in the blocking buffer. The secondary antibodies were thereafter added for 1 h at RT in the dark, followed by nuclei counterstain with DAPI (1:10,000 (Life Technologies)) and image acquisition on inverted epifluorescence microscope LRI - Olympus IX-73. Scale bars are 200 μm.

Alkaline phosphatase activity

Alkaline phosphatase staining was performed using Alkaline Phosphatase Staining Kit (Stemgent, MA).

In vitro differentiation by embryoid body (EB) formation

Human iPSCs were grown for 2 weeks as embryoid bodies (EBs) in low-attachment 24-well plates (Corning) in WiCell medium supplemented with 20 ng/ml FGF2. The EBs were then seeded on a 0.1% gelatin-coated 96-well plate (Greiner Bio-One) in DMEM media containing 10% fetal bovine serum and 1% Penicillin-Streptomycin for subsequent spontaneous differentiation, with media changes every 2–3 days. After 2 weeks, the cells were fixed and stained for three germ-layer markers as described in the Table 2.

Karyotype analysis

The G-banding analysis was performed after 14 passages at 300–400 band resolution in average, at the Department of Clinical Genetics and Pathology in Lund.

Mutation sequencing

Genomic DNA from fibroblasts and iPSCs was extracted using conventional lysis buffer composed of 100 mM Tris (pH 8.0), 200 mM NaCl, 5 mM EDTA and 0.2% SDS in distilled autoclaved water supplemented with 1.5 mg/ml Proteinase K. The mutation, p.G2019S in *LRRK2*, was confirmed by direct DNA sequencing (Macrogen Europe, Amsterdam, The Netherlands). Primers used for amplification and directed sequencing of *LRRK2* around the mutation sites are listed in the Table 2.

DNA fingerprinting

Genomic DNA from fibroblasts and iPSCs was isolated as described above and fingerprinting analyses were outsourced to the IdentiCell STR profiling service (Department of Molecular Medicine, Aarhus University Hospital, Skejby, Denmark).

Mycoplasma detection

Absence of mycoplasma contamination was confirmed by the real-time PCR method at GATC Biotech AG (European Genome and Diagnostics Centre, Konstanz, Germany).

Acknowledgements

We are greatly thankful to AnnaKarin Oldén and Marianne Juhlin, for their technical assistance and to the 'Cell Line and DNA Biobank from Patients affected by Genetic Diseases' (Istituto G. Gaslini, Genova, Italy) and the Parkinson Institute Biobank, members of the Telethon Network of Genetic Biobanks (http://biobanknetwork.telethon.it; project no. GTB12001) funded by Telethon Italy, for providing fibroblasts samples. This work was supported by the Strategic Research Environment MultiPark at Lund University, the strong research environment BAGADILICO (grant 349-2007-8626), the Swedish Parkinson Foundation (Parkinsonfonden, grant 889/16), the Swedish Research Council (grant 2015-03684 to LR) and Finnish Cultural Foundation (grant 00161167 to YP). We also acknowledge the Portuguese Foundation for Science and Technology for the doctoral fellowship - PDE/BDE/113598/2015 to AM and IF Starting and Development Grants to LP and AJS (IF/00111/2013 and IF/01079/2014), respectively.

Appendix A. Supplementary data

Supplementary data to this article can be found online at https://doi.org/10.1016/j.scr.2018.01.022.

References

Holmqvist, S., Lehtonen, S., Chumarina, M., Puttonen, K.A., Azevedo, C., Lebedeva, O., Ruponen, M., Oksanen, M., Djelloul, M., Collin, A., et al., 2016. Creation of a library of induced pluripotent stem cells from parkinsonian patients. NPJ Parkinsons Dis. 2, 16009.

Reinhardt, P., Schmid, B., Burbulla, L.F., Schondorf, D.C., Wagner, L., Glatza, M., Hoing, S., Hargus, G., Heck, S.A., Dhingra, A., et al., 2013. Genetic correction of a LRRK2 mutation in human iPSCs links parkinsonian neurodegeneration to ERK-dependent changes in gene expression. Cell Stem Cell 12, 354–367.

ANNEX V

Stem Cell Research 27 (2018) 90–94

Contents lists available at ScienceDirect

Stem Cell Research

journal homepage: www.elsevier.com/locate/scr

Lab Resource: Stem Cell Line

Generation of an induced pluripotent stem cell line (CSC-44) from a Parkinson's disease patient carrying a compound heterozygous mutation (c.823C>T and EX6 del) in the *PARK2* gene

Ana Marote [a,b], Yuriy Pomeshchik [c,d,e], Stefano Goldwurm [f], Anna Collin [g], Nuno J. Lamas [a,b,i], Luísa Pinto [a,b,h], António J. Salgado [a,b], Laurent Roybon [c,d,e,*]

[a] *Life and Health Sciences Research Institute (ICVS), School of Medicine, University of Minho, Braga, Portugal*
[b] *ICVS/3B's, PT Government Associate Laboratory, Braga/Guimarães, Portugal*
[c] *Stem Cell Laboratory for CNS Disease Modeling, Wallenberg Neuroscience Center, Department of Experimental Medical Science, BMC A10, Lund University, Lund, Sweden*
[d] *Strategic Research Area MultiPark, Lund University, Lund, Sweden*
[e] *Lund Stem Cell Center, Lund University, Lund, Sweden*
[f] *Parkinson Institute, ASST PINI-CTO, Milan, Italy*
[g] *Department of Clinical Genetics and Pathology, Office for Medical Services, Division of Laboratory Medicine, Lund, Sweden*
[h] *BnML, Behavioral and Molecular Lab, Braga, Portugal*
[i] *Anatomic Pathology Department, Braga Hospital, Braga, Portugal*

ARTICLE INFO

Article history:
Received 15 October 2017
Received in revised form 13 December 2017
Accepted 3 January 2018
Available online 4 January 2018

ABSTRACT

Mutations in the *PARK2* gene, which encodes PARKIN, are the most frequent cause of autosomal recessive Parkinson's disease (PD). We report the generation of an induced pluripotent stem cell (iPSC) line from a 78-year-old patient carrying a compound heterozygous mutation (c.823C>T and EX6del) in the *PARK2* gene. Skin fibroblasts were reprogrammed using the non-integrating Sendai virus technology to deliver OCT3/4, SOX2, c-MYC and KLF4 factors. The generated cell line CSC-44 exhibits expression of common pluripotency markers, *in vitro* differentiation into the three germ layers and normal karyotype. This iPSC line can be used to explore the association between *PARK2* mutations and PD.

Resource table.

Unique stem cell line identifier	ULUNDi006-A
Alternative name(s) of stem cell line	CSC-44I
Institution	Stem Cell Laboratory for CNS Disease Modeling, Department of Experimental Medical Science, Lund University
Contact information of distributor	Laurent Roybon, Laurent.Roybon@med.lu.se
Type of cell line	iPSC
Origin	Human
Additional origin info	Age of patient at onset: 33 Sex of patient: female Ethnicity: N/A
Cell source	Skin fibroblasts
Clonality	Clonal
Method of reprogramming	Sendai virus mediated delivery of OCT3/4, SOX2, c-MYC and KLF4
Genetic modification	No modification
Type of modification	No modification
Associated disease	Parkinson's disease
Gene/locus	*PARK2* (MIM #602544) on chromosome 6q26 Genotype: compound heterozygous mutation: c.823C>T in exon 7 and deletion of exon 6
Method of modification	No modification
Name of transgene or resistance	No transgene or resistance
Inducible/constitutive system	Not inducible
Date archived/stock date	N/A
Cell line repository/bank	N/A
Ethical approval	Parkinson Institute Biobank (part of the Telethon Genetic Biobank Network http://biobanknetwork.telethon.it/): approved by Ethics Committee "Milano Area C" (http://comitatoeticoareac.ospedaleniguarda.it/) on the 26/06/2015, Numero Registro dei pareri: 370-062015. Reprogramming: 202100-3211 (delivered by Swedish work environment Arbetsmiljöverket).

* Corresponding author at: Stem Cell Laboratory for CNS Disease Modeling, Wallenberg Neuroscience Center, Department of Experimental Medical Science, BMC A10, Lund University, Lund, Sweden.
E-mail address: laurent.roybon@med.lu.se (L. Roybon).

https://doi.org/10.1016/j.scr.2018.01.006

Resource utility

Mutations in the *PARK2* gene are the second most common known cause of Parkinson's disease (PD). CSC-44 iPSC line was generated from a PD patient with a compound heterozygous mutation in *PARK2*. This iPSC line can be used as a model to explore the link between mutant *PARK2* and PD pathology.

Resource details

Mutations in *PARK2* result in autosomal-recessive familial PD and are the second most common known cause of this neurodegenerative disease. *PARK2* encodes for PARKIN, a E3 ubiquitin ligase that plays a role in targeting proteins for degradation and maintaining mitochondrial function (Nuytemans et al., 2010). Among the identified *PARK2* mutations, both deletions and insertions of one or more exons and missense mutations have been described. Here, we report the generation of an induced pluripotent stem cell line (CSC-44) from a patient with PD caused by a compound heterozygous *PARK2* mutation: point mutation c.823C>T in exon 7 and deletion of exon 6. The c.823C>T mutation in *PARK2* gene predicts an arginine to tryptophan substitution at amino acid residue 275 (p.R275W), which is located within the RING1 domain of *PARK2*. This mutation disrupts the charge distribution and leads to local rearrangements in the RING1-IBR interface, which hampers ubiquitin ligase activity and confers a toxic gain of function to PARKIN, leading to its aggregation (Fiesel et al., 2015; Oczkowska et al., 2013). Even though this point mutation has been well characterized and associated with other mutations in compound heterozygotes, its association with the deletion of exon 6 has not been described. Given the importance of compound heterozygous mutations on *PARK2* gene, CSC-44 iPSC line can be used to better understand the impact of both alterations on cellular function.

To generate this line, skin fibroblasts collected by punch skin biopsy from a 78-year-old PD patient were reprogrammed using a non-integrating Sendai virus technology. Briefly, fibroblasts were seeded (75,000 cells/well) on a 12-well plate, two days before transduction. The CytoTune™-iPS 2.0 Sendai Reprogramming Kit was then used to deliver the four reprogramming factors (OCT3/4, SOX2, c-MYC and KLF4). At day 7 post-transduction, the cells were re-seeded onto mouse embryonic fibroblasts (MEF)-feeder layer and expanded until colonies presented an embryonic stem cell (ES)-like morphology. At day 28, 12 colonies were picked and expanded as individual clones for 7 days. Three clones (CSC-44G, CSC-44I, CSC-44J) were further selected for expansion and karyotype analysis. All clones were characterized using the methods we previously described (Holmqvist et al., 2016). Here, we present the characterization of clone CSC-44I.

The generated clone, CSC-44I, expressed the common nuclear and cell surface pluripotency markers, OCT4/NANOG and TRA1-81/SSEA4 (Fig. 1A) and showed alkaline phosphatase (ALP) activity (Fig. 1B). Flow cytometry analysis demonstrated that >98% of the iPSCs were positive for SSEA4 (Fig. 1C). Additional immunocytochemistry analysis revealed elimination of the Sendai virus at passage 7 (Fig. 1D). Fig. 1E presents a normal female karyogram identified in CSC-44I clone. The identity of the generated iPSC line was confirmed by DNA fingerprint, showing genetic correspondence to parental fibroblasts. DNA sequencing analysis of CSC-44I iPSCs confirmed the presence of mutations in the *PARK2* gene (Fig. 1F). Embryoid bodies (EBs) generated from CSC-44I iPSCs present three-germ layer differentiation capacity as shown by the *in vitro* expression of alpha-fetoprotein (AFP), an endodermal marker, smooth muscle actin (SMA), a mesodermal marker, and beta-III-tubulin (BIIITub), an ectodermal marker (Fig. 1G). Mycoplasma infection was prevented by routine addition of plasmocin in cell culture media at early passages.

Materials and methods

Fibroblast culture

Dermal fibroblasts were collected by punch skin biopsy from a patient diagnosed with PD, after obtaining informed consent. The fibroblasts were maintained in fibroblast growth medium, composed of DMEM media (ThermoFisher Scientific) with 10% fetal bovine serum and 1% Penicillin-Streptomycin and passaged with 0.05% trypsin.

iPSC generation and expansion

For reprogramming, 75,000 cells were seeded on a 12-well plate and maintained in fibroblast growth medium. Two days after (day 0), the cells were transduced using the three vector preparations (MOI = 5, 5, 3) included in the CytoTune™-iPS 2.0 Sendai Reprogramming Kit (ThermoFisher Scientific). On the following day and on every other day, the medium was replaced with fresh fibroblast growth medium. At day 7, the cells were re-seeded onto irradiated mouse embryonic fibroblasts (MEFs) feeder cells with fibroblast growth medium. On the day after and until colony picking, the cells were cultured in WiCell medium composed of advanced DMEM/F12 (ThermoFisher Scientific), 20% Knock-Out Serum Replacement (v/v, ThermoFisher Scientific), 2 mM L-glutamine (ThermoFisher Scientific), 1% non-essential amino acids (NEAA, v/v, Millipore) and 0.1 mM β-mercaptoethanol (Sigma-Aldrich), supplemented with 20 ng/ml FGF2 (ThermoFisher Scientific). On day 28, individual colonies were picked and re-seeded on a 24-well plate containing fresh MEFs. One week after, three clones were selected based on the morphology of the colonies, and further expanded on 6-well plates. The cells were passaged once a week and seeded on the appropriate cell culture surface for characterization assays at the indicated passage numbers (Table 1).

Immunocytochemistry

The iPSCs cultures were fixed with 4% paraformaldehyde for 15 min at room temperature (RT), permeabilized and blocked for 1 h at RT with PBS containing 10% donkey serum and 0.1% TritonX-100 (Sigma) and incubated overnight at +4 °C with the primary antibodies (Table 2) diluted in the blocking buffer. The secondary antibodies were thereafter added for 1 h at RT in the dark, followed by nuclei counterstain with DAPI (1:10,000 (Life Technologies)) and image acquisition on inverted epifluorescence microscope LRI - Olympus IX-73. Scale bars are 200 μm.

Alkaline phosphatase activity

Alkaline phosphatase staining was performed using Alkaline Phosphatase Staining Kit (Stemgent, MA).

In vitro differentiation by embryoid body (EB) formation

Human iPSCs were grown for 2 weeks as embryoid bodies (EBs) in low-attachment 24-well plates (Corning) in WiCell medium supplemented with 20 ng/ml FGF2. The EBs were then seeded on a 0.1% gelatin-coated 96-well plate (Greiner Bio-One) in DMEM media containing 10% fetal bovine serum and 1% Penicillin-Streptomycin for subsequent spontaneous differentiation, with media changes every 2–3 days. After 2 weeks, the cells were fixed and stained for three germ-layer markers as described in Table 2.

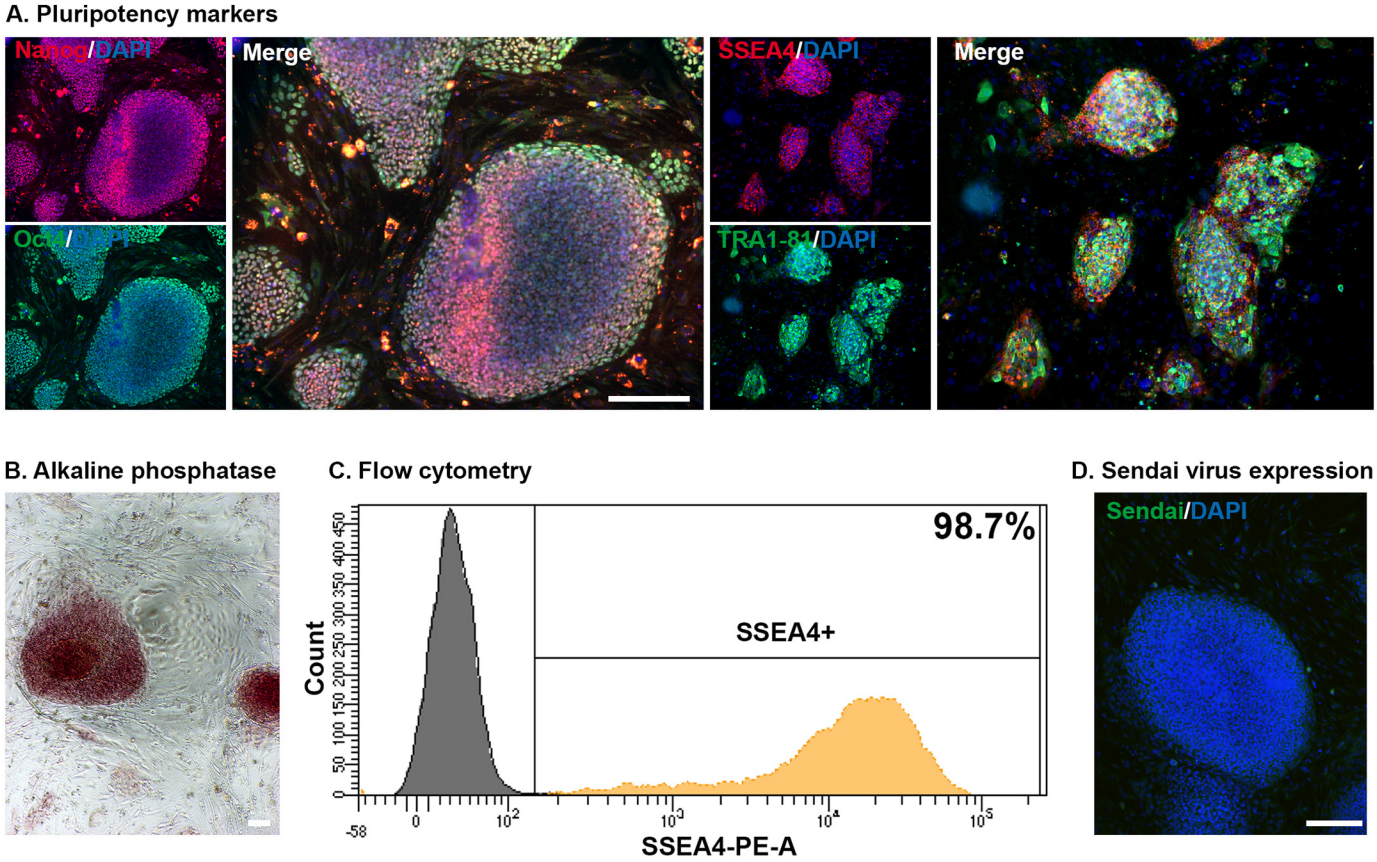

Fig. 1. Characterization of the iPSC line CSC-44I.

Table 1
Characterization and validation.

Classification	Test	Result	Data
Morphology	Photography	Visual record of the line: normal	Not shown but available with author
Phenotype	Immunocytochemisty	Positive staining for pluripotency markers: OCT4, NANOG, TRA1-81 and SSEA4	Fig. 1 panel A
	Alkaline phosphatase activity	Visible activity	Fig. 1 panel B
	Flow cytometry	94.8% SSEA4	Fig. 1 panel C
Karyotype	G-banding	46,XX, (300–400 bands resolution in average)	Fig. 1 panel E
Identity	STR analysis	10 sites analyzed, all matched with parent fibroblast cell line	Available with author
Mutation analysis (IF APPLICABLE)	Sequencing	Compound heterozygous mutation in the *PARK2* gene (c.823C>T and EX6del)	Fig. 1 panel F
Microbiology and virology	Mycoplasma	Mycoplasma testing by RT-PCR. Negative.	Not shown but available with author
Differentiation potential	Embryoid body formation	Staining of smooth muscle actin, beta-III-tubulin and alpha-fetoprotein after spontaneous differentiation of embryoid bodies	Fig. 1 panel G
Donor screening (OPTIONAL)	HIV 1 + 2 Hepatitis B, Hepatitis C	N/A	N/A
Genotype additional info (OPTIONAL)	Blood group genotyping	N/A	N/A
	HLA tissue typing	N/A	N/A

Karyotype analysis

The G-banding analysis was performed at 300–400 band resolution in average after 9 passages, at the Department of Clinical Genetics and Pathology in Lund.

Mutation sequencing

Genomic DNA from fibroblasts and iPSCs was extracted using conventional lysis buffer composed of 100 mM Tris (pH 8.0), 200 mM NaCl, 5 mM EDTA and 0.2% SDS in distilled autoclaved water supplemented with 1.5 mg/ml Proteinase K. The mutation in the *PARK2* gene was confirmed by direct DNA sequencing (Macrogen Europe, Amsterdam, The Netherlands). Primers used for amplification and directed sequencing of *PARK2* around the mutation sites are listed in Table 2.

DNA fingerprinting

Genomic DNA from fibroblasts and iPSCs was isolated as described above and fingerprinting analyses was outsourced to the IdentiCell STR profiling service (Department of Molecular Medicine, Aarhus University Hospital, Skejby, Denmark).

Mycoplasma detection

Absence of mycoplasma contamination was confirmed by the real-time PCR method at GATC Biotech AG (European Genome and Diagnostics Centre, Konstanz, Germany).

Acknowledgements

We are greatly thankful to AnnaKarin Oldén and Marianne Juhlin, for their technical assistance and to the 'Cell Line and DNA Biobank from Patients affected by Genetic Diseases' (Istituto G. Gaslini, Genova, Italy) and the 'Parkinson Institute Biobank, members of the Telethon Network of Genetic Biobanks (http://biobanknetwork.telethon.it; project no. GTB12001) funded by Telethon Italy, for providing fibroblasts samples. This work was supported by the Strategic Research Environment MultiPark at Lund University and the strong research environment BAGADILICO (grant 349-2007-8626), the Swedish Parkinson Foundation (Parkinsonfonden; grant 889/16), the Swedish Research Council (grant 2015-03684 to LR) and Finnish Cultural Foundation (grant 00161167 to YP). We also acknowledge the Portuguese Foundation for Science and Technology for the doctoral fellowship - PDE/BDE/113598/2015 to AM and IF Starting and Development Grants to LP and AJS (IF/00111/2013 and IF/01079/2014), respectively.

Table 2
Reagents details.

Antibodies used for immunocytochemistry			
	Antibody	Dilution	Company Cat # and RRID
Pluripotency markers	Mouse anti-Oct4	1:200	Millipore Cat# MAB4401, RRID:AB_2167852
	PE-conjugated mouse anti-human NANOG	1:200	BD Biosciences Cat# 560483, RRID:AB_1645522
	Mouse anti- TRA-1-81	1:200	Thermo Fisher Scientific Cat# 41–1100, RRID:AB_2533495
	PE-conjugated mouse anti-SSEA4	1:200	Thermo Fisher Scientific Cat# A14766, RRID:AB_2534281
Sendai	Chicken anti-Sendai virus	1:1000	Abcam Cat# ab33988, RRID:AB_777877
Differentiation markers	Mouse anti-AFP	1:200	Sigma-Aldrich Cat# A8452, RRID:AB_258392
	Mouse anti-SMA	1:200	Sigma-Aldrich Cat# A2547, RRID:AB_476701
	Mouse anti-beta-III tubulin	1:200	Sigma-Aldrich Cat# T8660, RRID:AB_477590
Secondary antibodies	Donkey anti-mouse Alexa Fluor® 488	1:400	Molecular Probes Cat# A-21202, RRID:AB_141607
	Donkey anti-chicken Alexa Fluor® 488	1:400	Jackson ImmunoResearch Labs Cat# 703–545-155, RRID:AB_2340375
	Donkey anti-mouse Alexa Fluor® 555	1:400	Thermo Fisher Scientific Cat# A-31570, RRID:AB_2536180

Primers		
	Target	Forward/reverse primer (5′–3′)
Mutation sequencing	*PARK2*	AGGATTACAGAAATTGGTCT/TCTGTTCTTCATTAGCATTAGA

Appendix A. Supplementary data

Supplementary data to this article can be found online at https://doi.org/10.1016/j.scr.2018.01.006.

References

Fiesel, F.C., Caulfield, T.R., Moussaud-Lamodière, E.L., Ogaki, K., Dourado, D.F., Flores, S.C., Ross, O.A., Springer, W., 2015. Structural and functional impact of Parkinson disease-associated mutations in the E3 ubiquitin ligase parkin. Hum. Mutat. 36, 774–786.

Holmqvist, S., Lehtonen, S., Chumarina, M., Puttonen, K.A., Azevedo, C., Lebedeva, O., Ruponen, M., Oksanen, M., Djelloul, M., Collin, A., et al., 2016. Creation of a library of induced pluripotent stem cells from Parkinsonian patients. NPJ Parkinsons Dis. 2 (16009).

Nuytemans, K., Theuns, J., Cruts, M., Van Broeckhoven, C., 2010. Genetic etiology of Parkinson disease associated with mutations in the SNCA, PARK2, PINK1, PARK7, and LRRK2 genes: a mutation update. Hum. Mutat. 31, 763–780.

Oczkowska, A., Kozubski, W., Lianeri, M., Dorszewska, J., 2013. Mutations in PRKN and SNCA genes important for the progress of Parkinson's disease. Curr. Genomics 14, 502–517.

ANNEX VI

Stem Cell Research 34 (2019) 101373

Contents lists available at ScienceDirect

Stem Cell Research

journal homepage: www.elsevier.com/locate/scr

Lab Resource: Single Cell Line

Generation of an induced pluripotent stem cell line (CSC-46) from a patient with Parkinson's disease carrying a novel p.R301C mutation in the GBA gene

Nadja Gustavsson[a], Ana Marote[b,c], Yuriy Pomeshchik[d,e], Kaspar Russ[d,e], Carla Azevedo[d,e], Margarita Chumarina[d,e], Stefano Goldwurm[f], Anna Collin[g], Luisa Pinto[b,c], António J. Salgado[b,c], Oxana Klementieva[a], Laurent Roybon[d,e,*], Ekaterina Savchenko[d,e]

[a] Medical Microspectroscopy, Department of Experimental Medical Science, Lund University, Lund, Sweden
[b] Life and Health Sciences Research Institute (ICVS), School of Medicine, University of Minho, Braga, Portugal
[c] ICVS/3B's, PT Government Associate Laboratory, Braga/Guimarães, Portugal
[d] Stem Cell Laboratory for CNS Disease Modeling, Department of Experimental Medical Science, BMC D10, Lund University, Lund, Sweden
[e] Strategic Research Area MultiPark, Lund Stem Cell Center, Lund University, Lund, Sweden
[f] Parkinson Institute, Istituti Clinici di Perfezionamento, Milan, Italy
[g] Department of Clinical Genetics and Pathology, Office for Medical Services, Division of Laboratory Medicine, Lund, Sweden

A B S T R A C T

Mutations in the glucocerebrosidase (GBA) gene have been associated with the development of Parkinson's disease (PD). An induced pluripotent stem cell (iPSC) line was generated from a 60-year old patient diagnosed with PD and carrying a new mutation variant p.R301C in *GBA*. Using non-integrating Sendai virus-based technology, we utilized OCT3/4, SOX2, c-MYC and KLF4 transcription factors to reprogram skin fibroblasts into iPSCs. The generated iPSC line retained the mutation, displayed expression of common pluripotency markers, differentiated into the three germ layers, and exhibited normal karyotype. The iPSC line can be further used for studying PD pathogenesis.

Resource table

Unique stem cell line identifier	ULUNDi007-A
Alternative name(s) of stem cell line	CSC-46 L
Institution	Stem Cell Laboratory for CNS Disease Modeling, Department of Experimental Medical Science, Lund University
Contact information of distributor	Laurent Roybon, Laurent.Roybon@med.lu.se
Type of cell line	iPSCs
Origin	Human
Additional origin info	Age of patient: 60 Sex of patient: Male
Cell Source	Skin fibroblasts
Clonality	Clonal
Method of reprogramming	Sendai virus mediated delivery of OCT3/4, SOX2, c-MYC and KLF4
Genetic Modification	No modification
Type of Modification	N/A
Associated disease	Parkinson's disease
Gene/locus	*GBA* (MIM # 606463) on chromosome 1q22
Method of modification	N/A N/A
Name of transgene or resistance	
Inducible/constitutive system	N/A
Date archived/stock date	N/A
Cell line repository/bank	N/A
Ethical approval	Parkinson Institute Biobank (part of the Telethon Genetic Biobank Network http://biobanknetwork.telethon.it/): approved by Ethics Committee "Milano Area C" (http://comitatoeticoareac.ospedaleniguarda.it/) on the 26/06/2015, Numero Registro dei pareri: 370–062015. Reprogramming: 202100–3211 (delivered by Swedish work environment Arbetsmiljöverket).

Resource utility

GBA mutations are associated with the development of Parkinson's disease (PD). The CSC-46 iPSC line was generated from a PD patient carrying a new mutation variant p.R301C in the GBA gene. This iPSC line can be used to explore the association between PD and *GBA* mutation in disease modeling studies.

* Corresponding author.
E-mail address: Laurent.roybon@med.lu.se (L. Roybon).

https://doi.org/10.1016/j.scr.2018.101373
Received 28 November 2018; Accepted 17 December 2018
Available online 26 December 2018

Resource details

GBA encodes the enzyme glucocerebrosidase (GBA), a lysosomal hydrolase that digests glycolipids and which is deficient in Gaucher's disease, a recessive lysosomal storage disorder. Mutations in *GBA* are linked to an increased risk of developing PD (Sidransky and Lopez, 2012) and PD patients with identified heterozygous *GBA* mutations present with early-onset motor symptoms together with cognitive impairment (Sidransky and Lopez, 2012; Mata et al., 2016). Several mutations have been identified in *GBA*. For example, p.N370S and p.L444P are most frequently described in genetic screening studies (Asselta et al., 2014). Here we report the generation of an iPSC line (clone CSC-46 L) from a PD patient carrying a new mutation variant p.R301C in *GBA*. This line can be used to decipher molecular mechanisms underlying p.R301C *GBA* associated PD.

To generate the CSC-46 iPSC line, skin fibroblasts were collected by punch skin biopsy from a 60-year old male PD patient and reprogrammed using CytoTune™-iPS 2.0 Sendai Reprogramming Kit. Briefly, fibroblasts were seeded on a 12-well plate (75.000 cells/well) and two days later four separate vectors carrying genes OCT-3/4, KLF-4, SOX-2 and c-MYC were delivered to the cells to induce pluripotency. At day 7 post-transduction, the cells were re-seeded onto mouse embryonic fibroblasts (MEF)-feeder layer and expanded until an embryonic stem cell (ES)-like morphology was observed. At day 28, several colonies were collected and expanded as single clones for 7 days. Three clones (CSC-46F, CSC-46 K and CSC-46 L) were selected for further expansion and karyotype analysis. Here, we present the detailed characterization of clone CSC-46 L (Table 1) using the methods we previously described (Holmqvist et al., 2016).

The generated iPSC line CSC-46 L displayed typical colony shape and morphology when grown on mouse fibroblast feeders (Fig. 1A). The colonies expressed the common nuclear and cell surface pluripotency markers, Oct4, Nanog, TRA1–81 and SSEA4 (Fig. 1B) as well as alkaline phosphatase (ALP) activity (Fig. 1C). In addition flow cytometry confirmed that > 92% of the iPSCs were positive for the pluripotent cell marker SSEA4 (Fig. 1D). The elimination of the Sendai virus was demonstrated with immunohistochemistry analysis at passage 7 (Fig. 1E). The generated iPSC line had normal karyotype (Fig. 1F). The presence of the p.R301C mutation in GBA gene was confirmed by DNA sequence analysis (Fig. 1G). Immunocytochemistry for endodermal marker alpha-fetoprotein (AFP), the mesodermal marker smooth muscle actin (SMA), and the ectodermal marker beta-III-tubulin revealed formation of all three germ layers from the embryoid bodies (EBs) generated from the CSC-46 L line (Fig. 1H). DNA fingerprinting showed genetic equivalency to parental fibroblasts, thus confirming the identity of the generated iPSC line. Finally, standardised qPCR test showed absence of mycoplasma contamination in the generated iPSC line.

Materials and methods

Fibroblast culture

Human dermal fibroblasts were obtained by punch skin biopsy from a PD patient carrying *GBA* mutation after written informed consent. Fibroblasts were cultured and expanded in culture medium containing DMEM media (ThermoFisher Scientific), 10% fetal bovine serum and 1% Penicillin-Streptomycin. Cells were passaged with 0.05% trypsin (Invitrogen).

iPSC generation and expansion

For reprogramming, fibroblasts were transduced using the three vector preparations (MOI = 5, 5, 3) included in the CytoTune™-iPS 2.0 Sendai Reprogramming Kit (Thermo Fisher Scientific). The medium was replaced daily for 7 days, after which the cells were re-seeded onto irradiated mouse embryonic fibroblasts (MEF) feeder cells. From the day 8 and until day 28, the cells were cultured in WiCell medium composed of advanced DMEM/F12 (Thermo Fisher Scientific), 20% Knock-Out Serum Replacement (v/v, Thermo Fisher Scientific), 2 mM L-glutamine (Thermo Fisher Scientific), 1% non-essential amino acids (NEAA, v/v, (v/v, Thermo Fisher Scientific) and 0.1 mM β-mercaptoethanol (Sigma-Aldrich), supplemented with 20 ng/mL FGF2 (Thermo Fisher Scientific). On day 28, several single colonies were picked and re-seeded to fresh MEFs, on a 24-well plate. Seven days later, three individual clones were randomly selected and re-plated on a 6-well plate for further expansion. Cells were passaged weekly and re-plated on appropriate cell culture surface for characterization assays (Table 1).

Immunocytochemistry

The cells were fixed with 4% paraformaldehyde (PFA) for 15 min at room temperature (RT) followed by blocking and permeabilization for 1 h at RT with PBS containing 10% donkey serum and 0.1% TritonX-10 (Sigma). Then the cells were incubated overnight at +4 °C with the primary antibodies (Table 2) diluted in the blocking buffer followed by incubation with secondary antibodies in the dark for 1 h at RT. DAPI (1:10000) was used for nuclei counterstaining. Image acquisition were performed on inverted epifluorescence microscope LRI – Olympus IX-73.

Alkaline phosphatase activity

Alkaline phosphatase staining was performed using Alkaline Phosphatase Staining Kit (Stemgent, MA) according to the manufacturer's protocol.

Table 1
Characterization and validation.

Classification	Test	Result	Data
Morphology	Photography	Visual record of the line: Normal morphology	Fig. 1 panel A
Phenotype	Immunocytochemistry	Positive staining for pluripotency markers: Oct4, Nanog, TRA1–81 and SSEA4	Fig. 1 panel B
	Alkaline phosphatase activity	Visible activity	Fig. 1 panel C
	Flow cytometry	92.8% SSEA4	Fig. 1 panel D
Genotype	Karyotype (G-banding) and resolution	Normal karyotype 46,XY (300–400 bands resolution in average)	Fig. 1 panel F
Identity	STR analysis	matched with parental fibroblasts	STR analysis
Mutation analysis (IF APPLICABLE)	Sequencing	Heterozygous p.R301C mutation in *GBA*	Fig. 1 panel G
Microbiology and virology	Mycoplasma	Mycoplasma testing by RT-PCR. Negative.	Not shown but available with author
Differentiation potential	Embryoid body formation	Spontaneous EB formation and positive staining for smooth muscle actin (SMA), beta-III-tubulin (BIIITub) and α-fetoprotein (AFP)	Fig. 1 panel H
Donor screening (OPTIONAL)	HIV 1 + 2 Hepatitis B, Hepatitis C	N/A	N/A
Genotype additional info (OPTIONAL)	Blood group genotyping	N/A	N/A
	HLA tissue typing	N/A	N/A

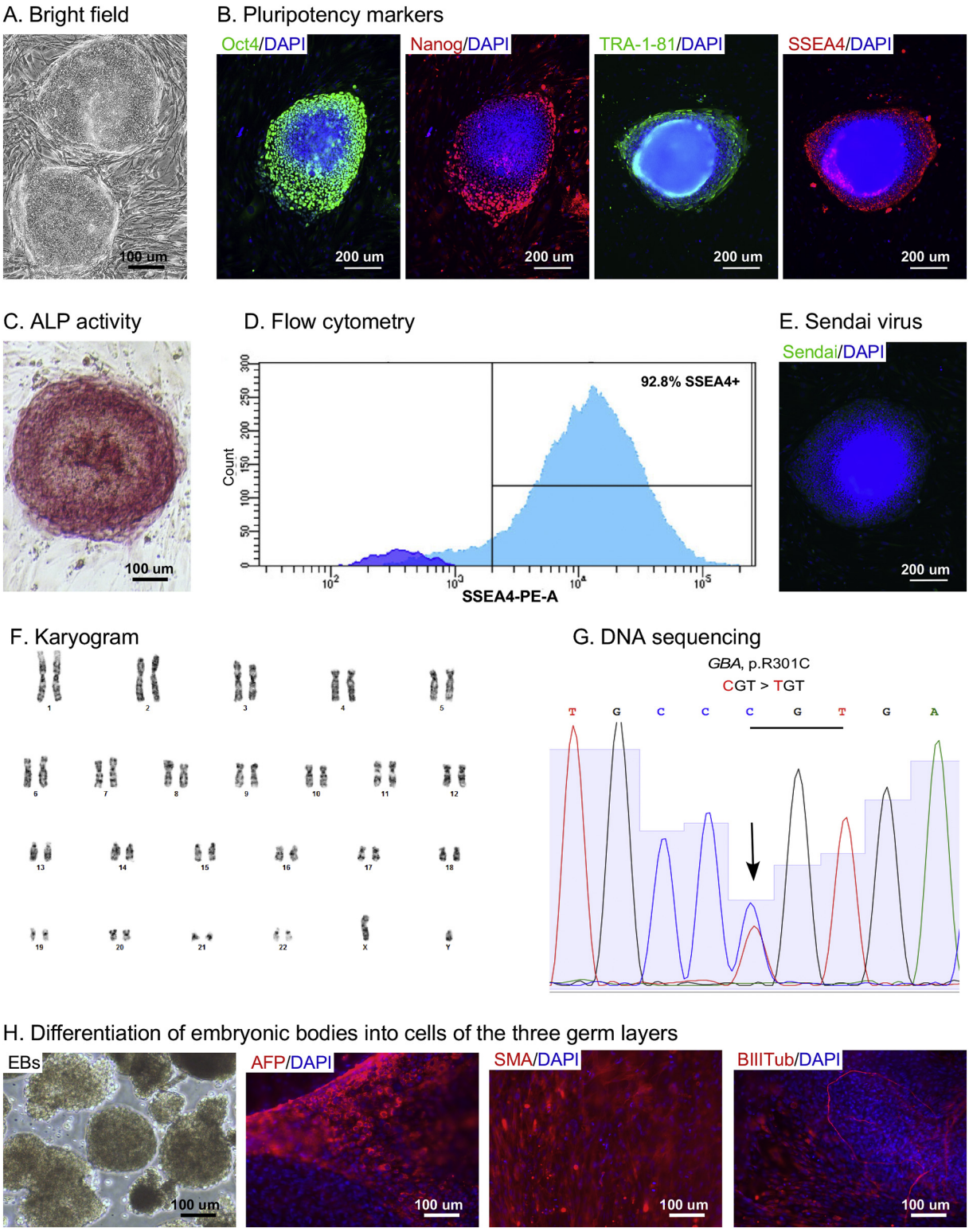

Fig. 1. Characterization of the iPSC line CSC 46L.

In vitro differentiation by embryoid body (EB) formation

iPSCs were plated on low-attachment 24-well plates and grown as embryoid bodies (EBs) for 2 weeks in WiCell medium supplemented with 20 ng/mL FGF2. For subsequent spontaneous differentiation, EBs were seeded on a 0.1% gelatin-coated 96-well plate in DMEM media containing 10% fetal bovine serum and 1% Penicillin-Streptomycin. Media was changed every 2–3 days. After 2 weeks, the cells were fixed and stained for markers against three germ layers (Table 2).

Karyotype analysis

The G-banding analysis was performed at 300–400 band resolution in a clinical diagnostic setting after 11 passages.

Table 2
Reagents details.

Antibodies used for immunocytochemistry/flow-cytometry			
	Antibody	Dilution	Company Cat # and RRID
Pluripotency Markers	Mouse anti-Oct4	1:200	Millipore Cat# MAB4401, RRID:AB_2167852
	PE-conjugated mouse anti-human Nanog	1:200	BD Biosciences Cat# 560483, RRID:AB_1645522
	Mouse anti- TRA-1-81	1:200	Thermo Fisher Scientific Cat# 41-1100, RRID:AB_2533495
	PE-conjugated mouse anti-SSEA4	1:200	Thermo Fisher Scientific Cat# A14766, RRID:AB_2534281
Differentiation Markers	Mouse anti-AFP	1:200	Sigma-Aldrich Cat# A8452, RRID:AB_258392
	Mouse anti-SMA	1:200	Sigma-Aldrich Cat# A2547, RRID:AB_476701
	Mouse anti-beta-III- tubulin	1:200	Sigma-Aldrich Cat# T8660, RRID:AB_477590
Secondary antibodies	Donkey anti-mouse Alexa Fluor® 488	1:400	Molecular Probes Cat# A-21202, RRID:AB_141607
	Donkey anti-chicken Alexa Fluor® 488	1:400	Jackson ImmunoResearch Labs Cat# 703-545-155, RRID:AB_2340375
	Donkey anti-mouse Alexa Fluor® 555	1:400	Thermo Fisher Scientific Cat# A-31570, RRID:AB_2536180

Primers		
	Target	Forward/Reverse primer (5′–3′)
Targeted mutation sequencing	*GBA*	TGGTCCACTTTCTTGGCCG/AGGGGAATGGTGCTCTAGGA

Mutation sequencing

Genomic DNA was extracted from fibroblasts and iPSCs with the use of conventional lysis buffer composed of 100 mM Tris (pH 8.0), 200 mM NaCl, 5 mM EDTA, 1.5 mg/mL Proteinase K, and 0.2% SDS in distilled autoclaved water. Direct DNA sequencing (Macrogen Europe, Amsterdam, The Netherlands) confirmed the presence of the p.R301C mutation in *GBA*. Primers used for amplification and directed sequencing of GBA around the mutation sites are listed in Table 2.

DNA fingerprinting

DNA fingerprinting analysis was performed by the IdentiCell STR profiling service (Department of Molecular Medicine, Aarhus University Hospital, Skejby, Denmark).

Mycoplasma detection

Absence of mycoplasma contamination was confirmed by real-time PCR analysis at GATC Biotech AG (European Genome and Diagnostics Centre, Konstanz, Germany).

Acknowledgements

We thank AnnaKarin Oldén, Anna Hammarberg and Marianne Juhlin, for their technical support. We are also thankful to the 'Cell Line and DNA Biobank from Patients affected by Genetic Diseases' (Istituto G. Gaslini, Genova, Italy) and the 'Parkinson Institute Biobank, members of the Telethon Network of Genetic Biobanks (http://biobanknetwork.telethon.it; project no. GTB12001) funded by Telethon Italy, for providing fibroblast samples. This work was supported by the Strategic Research Environment MultiPark at Lund University, the Swedish Research Council (grant 2015-03684 to LR), Finnish Cultural Foundation (grant 00161167 to YP), Portuguese Foundation for Science and Technology for the doctoral fellowship - PDE/BDE/113598/2015 to AM and IF Starting and Development Grant to LP and AJS (IF/01079/2014 and IF/00111/2013).

References

Asselta, R., Rimoldi, V., Siri, C., Cilia, R., Guella, I., Tesei, S., Soldà, G., Pezzoli, G., Duga, S., Goldwurm, S., 2014. Glucocerebrosidase mutations in primary parkinsonism. Parkinsonism Relat. Disord. 20 (11), 1215–1220.

Holmqvist, S., Lehtonen, S., Chumarina, M., Puttonen, K., Azevedo, C., Lebedeva, O., Ruponen, M., Oksanen, M., Djelloul, M., Collin, A., et al., 2016. Creation of a library of induced pluripotent stem cells from parkinsonian patients. NPJ. Parkinsons Dis. 2, 16009.

Mata, I.F., Leverenz, J.B., Weintraub, D., Trojanowski, J.Q., Chen-Plotkin, A., Van Deerlin, V.M., Ritz, B., Rausch, R., Factor, S.A., Wood-Siverio, C., et al., 2016. GBA variants are associated with a distinct pattern of cognitive deficits in Parkinson disease. Mov. Dis: Offl. J. Mov. Dis. Soc. 31 (1), 95–102.

Sidransky, E., Lopez, G., 2012. The link between the GBA gene and parkinsonism. Lancet. Neurol. 11, 986–998.

ANNEX VII

Autorização n.º 11739/ 2016

António José Braga Osório Gomes Salgado notificou à Comissão Nacional de Protecção de Dados (CNPD) um tratamento de dados pessoais com a finalidade de realizar um Estudo Clínico sem Intervenção, denominado Derivação de células estaminais humanas pluripotentes (hiPSCs) a partir de doentes portadores da doença de Parkinson: do doente para o doente .

Do estudo resulta a criação de um biobanco, sendo respeitados os requisitos do artigo 19.º da Lei n.º 12/2005, de 26 de janeiro.

Existe justificação específica para o tratamento de dados comportamentais, psicológicos ou volitivos, os quais estão diretamente relacionados com a investigação.

O participante é identificado por um código especificamente criado para este estudo, constituído de modo a não permitir a imediata identificação do titular dos dados; designadamente, não são utilizados códigos que coincidam com os números de identificação, iniciais do nome, data de nascimento, número de telefone, ou resultem de uma composição simples desse tipo de dados. A chave da codificação só é conhecida do(s) investigador(es).

É recolhido o consentimento expresso do participante ou do seu representante legal.

A informação é recolhida diretamente do titular e indiretamente de fontes especificadas na notificação.

As eventuais transmissões de informação são efetuadas por referência ao código do participante, sendo, nessa medida, anónimas para o destinatário.

A CNPD já se pronunciou na Deliberação n.º 1704/2015 sobre o enquadramento legal, os fundamentos de legitimidade, os princípios aplicáveis para o correto cumprimento da Lei n.º 67/98, de 26 de outubro, alterada pela Lei n.º 103/2015, de 24 de agosto, doravante LPD, bem como sobre as condições e limites aplicáveis ao tratamento de dados efetuados para a finalidade de investigação clínica.

No caso em apreço, o tratamento objeto da notificação enquadra-se no âmbito daquela deliberação e o responsável declara expressamente que cumpre os limites e

condições aplicáveis por força da LPD e da Lei n.º 21/2014, de 16 de abril, alterada pela Lei n.º 73/2015, de 27 de junho – Lei da Investigação Clínica –, explicitados na Deliberação n.º 1704/2015.

O fundamento de legitimidade é o consentimento do titular.

A informação tratada é recolhida de forma lícita, para finalidade determinada, explícita e legitima e não é excessiva – cf. alíneas a), b) e c) do n.º 1 do artigo 5.º da LPD.

Assim, nos termos das disposições conjugadas do n.º 2 do artigo 7.º, da alínea a) do n.º 1 do artigo 28.º e do artigo 30.º da LPD, bem como do n.º 3 do artigo 1.º e do n.º 9 do artigo 16.º ambos da Lei de Investigação Clínica, com as condições e limites explicitados na Deliberação da CNPD n.º 1704/2015, que aqui se dão por reproduzidos, autoriza-se o presente tratamento de dados pessoais nos seguintes termos:

Responsável – António José Braga Osório Gomes Salgado

Finalidade – Estudo Clínico sem Intervenção, denominado Derivação de células estaminais humanas pluripotentes (hiPSCs) a partir de doentes portadores da doença de Parkinson: do doente para o doente

Categoria de dados pessoais tratados – Código do participante; comportamentais, psicológicos ou volitivos com conexão com a Investigação

Exercício do direito de acesso – Através dos investigadores, presencialmente

Comunicações, interconexões e fluxos transfronteiriços de dados pessoais identificáveis no destinatário – Não existem

Prazo máximo de conservação dos dados – A chave que produziu o código que permite a identificação indireta do titular dos dados deve ser eliminada 5 anos após o fim do estudo.

Da LPD e da Lei de Investigação Clínica, nos termos e condições fixados na presente Autorização e desenvolvidos na Deliberação da CNPD n.º 1704/2015, resultam

obrigações que o responsável tem de cumprir. Destas deve dar conhecimento a todos os que intervenham no tratamento de dados pessoais.

Lisboa, 31-10-2016

A Presidente

Filipa Calvão

Data: 8/11/2016

Nossa referência: CESHB -137/2016

Outra referência: CNPD/11739/2016

Relator: Sara Barroso

Parecer emitido em reunião ordinária de 8 de novembro

Nos termos dos Nº 1 e 6 do Artigo 16º da Lei Nº 21/2014, de 16 de Abril, a Comissão de Ética para a Saúde do Hospital de Braga emite o seguinte parecer sobre o projeto de investigação ***Derivação de células estaminais humanas pluripotentes (hiPSCs) a partir de doentes portadores da doença de Parkinson: do doente para o doente?,*** de que são investigadores responsáveis o Doutor Fábio Teixeira e Doutor António Salgado, do Instituto de Investigação em Ciências da Vida e Saúde (ICVS) e do ICVS/3B's - Laboratório Associado; a Dra. Margarida Rodrigues, do Serviço de Neurologia, do Hospital de Braga, e o Dr. Miguel Gago, do Serviço Neurologia, do Hospital Senhora da Oliveira – Guimarães:

a) Trata-se de um estudo prospetivo que terá como população-alvo todos os doentes portadores da Doença de Parkinson (DP) avaliados em consulta externa de Neurologia no Hospitais de Braga e Guimarães, com início em janeiro de 2017 e conclusão prevista em 2021.
b) O objetivo geral do estudo é a geração de células estaminais pluripotentes (iPSCs) a partir de uma amostra de sangue que será recolhida a partir de pacientes com doença de Parkinson, amostra esta que será utilizada para o estudo e compreensão da patofisiologia da doença;
c) O estudo revela-se pertinente por contribuir para o desenvolvimento de potenciais estratégias terapêuticas. A colheita de sangue está prevista no acompanhamento clínico destes doentes, não implicando, por isso, qualquer incómodo ou risco adicional;
d) O protocolo de investigação é adequado e estão definidos os critérios de divulgação dos resultados;
e) Está demonstrada a aptidão dos membros da equipa de investigação;
f) Estão reunidas as condições humanas e materiais à realização do estudo;

g) O projeto de investigação não implica custos adicionais e não é objeto de qualquer financiamento;

h) A população alvo do projeto será constituída por todos os doentes portadores da doença de Parkinson avaliados em consulta externa de Neurologia no Hospital de Braga/Guimarães;

i) Serão constituídos dois grupos de doentes: Um de doentes cumprindo critérios de DP clinicamente estabelecida; e o outro por doentes não cumprindo estes critérios, mas com critérios para DP prodrómica com pelo menos 80% de certeza, de acordo com tabela II da "*MDS Research Criteria for Prodromal Parkinson's Disease.*"

O diagnóstico de DP prodrómica ou conversão para DP estabelecida será reconsiderado ao final de 1-2 anos. Por sua vez, serão excluídos do estudo doentes com Parkinsonismo devido a outras causas, nomeadamente Parkinsonismo atípico; doentes com Demência de Parkinson ou Demência de Corpos de Lewy; doentes cumprindo apenas critérios de DP provável, e doentes menores de 18 anos de idade.

j) Não existem situações de conflito de interesse por parte dos elementos que integram a equipa de investigação;

k) O acompanhamento clínico dos doentes incluídos não será influenciado pela inclusão dos doentes no estudo;

l) Os dados serão recolhido através da consulta do processo clínico dos doentes. Os dados recolhidos incluem: idade; motivo da consulta; medicação prescrita e duração da toma; estadiamento de Hoehn&Yahr; pontuação de MDS-UPDRS classificada por dois peritos de Neurologia; história recente de cirurgia (i.e., estimulação cerebral profunda), história familiar de Parkinsonismo. A confidencialidade estará salvaguardada pela anonimização dos dados, através da criação de um código a cada participante no estudo;

m) O projeto envolve a dádiva, e/ou colheita, análise laboratorial, e/ou processamento, e/ou preservação, e/ou armazenamento de células de origem humana, estando respeitados os requisitos do artigo 19.o da Lei n.o 12/2005, de 26 de janeiro, conforme Autorização nº 11739/ 2016 da CNPD.

n) O modelo de Consentimento Informado é adequado;

Face ao exposto, o estudo cumpre as normas da Bioética e nada há a opor à sua realização.

Presidente da Comissão de Ética

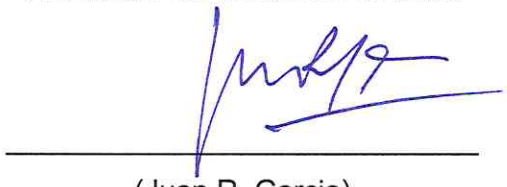

(Juan R. Garcia)